MICROSCOPIC ANATOMY OF *EUKOENENIA SPELAEA* (PALPIGRADI) — A MINIATURIZED EUCHELICERATE

Dissertation der Fakultät für Biologie

der Ludwig-Maximilians-Universität München

Sandra Franz-Guess

Gröbenzell, Deutschland

2019

For my wife

Diese Dissertation wurde angefertigt

unter der Leitung von Herrn Prof. Dr. J. Matthias Starck

im Bereich von Department Biologie II

an der Ludwig-Maximilians-Universität München

Erstgutachter: Prof. Dr. J. Matthias Starck

Zweitgutachter: Prof. Dr. Roland Melzer

Tag der Abgabe: 18.12.2018

Tag der mündlichen Prüfung: 01.03.2019

Erklärung

Ich versichere hiermit an Eides statt, dass meine Dissertation selbständig und ohne unerlaubte Hilfsmittel angefertigt worden ist.

Die vorliegende Dissertation wurde weder ganz, noch teilweise bei einer anderen Prüfungskommission vorgelegt.

Ich habe noch zu keinem früheren Zeitpunkt versucht, eine Dissertation einzureichen oder an einer Doktorprüfung teilzunehmen.

Gröbenzell, den 18.12.2018   Sandra Franz-Guess, M.Sc.

List of additional publications

Publication I

Czaczkes, T. J.; Franz, S.; Witte, V.; Heinze, J. 2015. Perception of collective path use affects path selection in ants. *Animal Behaviour* 99: 15–24.

Publication II

Franz-Guess, S.; Klußmann-Fricke, B. J.; Wirkner, C. S.; Prendini, L.; Starck, J. M. 2016. Morphology of the tracheal system of camel spiders (Chelicerata: Solifugae) based on micro-CT and 3D-reconstruction in exemplar species from three families. *Arthropod Structure & Development* 45: 440–451.

Publication III

Franz-Guess, S.; & Starck, J. M. 2016. Histological and ultrastructural analysis of the respiratory tracheae of *Galeodes granti* (Chelicerata: Solifugae). *Arthropod Structure & Development* 45: 452–461.

Publication IV

Starck, J. M.; Neul, A.; Schmidt, V.; Kolb, T.; Franz-Guess, S.; Balcecean, D.; Pees, M. 2017. Morphology and morphometry of the lung in corn snakes (*Pantherophis guttatus*) infected with three different strains of ferlavirus. *Journal of Comparative Pathology* 156: 419–435.

Publication V

Starck, J. M.; Mehnert, L.; Biging, A.; Bjarsch, J.; Franz-Guess, S.; Kleeberger, D.; Hörnig, M. 2018. Morphological responses to feeding in ticks (*Ixodes ricinus*). *Zoological Letters* 4: 1–19.

Content

Yup… still afraid of spiders.

Summary

Eukoenenia spelaea is a troglobiont palpigrade found in caves of the European Alps. These small animals have a maximum body length of 1.5 mm without the characteristic terminal flagellum. They lack eyes and breathing organs but have unique sensory organs. Detailed morphological studies of Palpigradi date back the late 19th and early 20th century. The placement of Palpigradi within a morphology based phylogeny of Euchelicerata is difficult. Data on microscopic anatomy and comparative morphology is incomplete, they show numerous plesiomorphic features, and they are so small, resulting in reduction, simplification and loss of organ systems. In this study, I analyze the microscopic anatomy of *Eukoenenia spelaea*, present evidence that progenesis is the developmental mechanism resulting in a paedomorphic adult morphology and miniaturized size, and discuss the results in a phylogenetic framework.

I used serial sectioning for light microscopy as well as transmission and scanning electron microscopy to describe the microscopic anatomy. The morphological analysis comprised all organs and external structures. Several new morphological features were described which are unique for *Eukoenenia spelaea*. For other structures I provide evidence that allow for new interpretations in the light of evolutionary morphology. (1) The prosoma is dorsally divided into two prosomal shields, the pro- and metapeltidium. (2) The ventral plate is probably an osmoregulatory organ. (3) The prosternum consists of the fused sternites of segments 2–4. (4) The frontal organ and trichobothria were found to have a morphology which is unique within euchelicerates. (5) The esophagus is enveloped by the supraesophageal ganglion associated with the chelicerae. (6) The heart lacks ostia, a pericard, a nerve, and well developed musculature. (7) The rostrosoma is not associated with chelicerae or pedipalps. (8) The midgut is simple and sac-like, a hindgut is missing. (9) The coxal gland (tubule and glandular section) has no lumen. (10) Females have an unpaired ovary with only few large eggs. (11) The aflagellate sperm has a prominent vacuole.

The morphological results were fed into a phylogenetic analysis. Several autapomorphic characters were recognized to characterize Palpigradi (i.e. the dorsal division of the prosoma into pro- and metapeltidium, the frontal organ, and

the rostrosoma with no association with chelicerae or pedipalps). A phylogenetic sister group relationship was found with Acaromorpha with which they share the morphology of the leg musculature and joints, the opening of the coxal organ on leg 1, the lack of a postcerebral suction pump, a myogenic heart, and vacuolated sperm.

This phylogenetic position suggests that the common ancestor of Palpigradi and Acaromorpha was already small. The small body size of *Eukoenenia spelaea* (and probably all Palpigradi) resulted in reduction or even loss of structures like musculature, and the complete lack of breathing organs and Malpighian tubules. Some organs showed a typical paedomorphotic morphology which was interpreted as the result of progenetic development, e.g. the microscopic anatomy of the heart, the brain, and the midgut. These findings suggest that *E. spelaea* is miniaturized.

1. Introduction

1.1 Palpigradi and Miniaturization

Palpigradi are a small, enigmatic group of arachnids. 96 extant and two known fossil species of Palpigradi have been described and assigned to two taxa, Eukoeneniidae Petrunkevitch, 1955, and Prokoeneniidae Condé, 1996. Eukoeneniidae includes five genera: *Allokoenenia* Silvestri, 1913, with one extant species; *Electrokoenenia* Engel and Huang, 2016, with one fossil species; *Eukoenenia* Börner, 1901, with 75 extant species; *Koeneniodes* Silvestri, 1913, with eight extant species, and *Leptokoenenia* Condé, 1965, with five extant species (e.g. Harvey 2003, Barranco and Mayoral 2007, 2014). Prokoeneniidae includes two genera: *Prokoenenia* Börner, 1901, with six extant species and *Triadokoenenia* Condé, 1991, with one extant species. Another genus, *Paleokoenenia* Rowland and Sissom, 1980, includes the second known fossil species (Harvey 2002).

Palpigradi are small, the largest species reaching a body length of 3 mm. They have no eyes, neither book lungs nor tracheae, but a prominent long terminal flagellum which they hold parallel to the ground while walking and hold erect during short stops (Kováč et al. 2002). Palpigrades are characterized by a unique set of sensory organs (frontal organ, lateral organ) in addition to sense organs known from other arachnids. Palpigrades are distributed in the pantropical region between 48°N and

40°S. However, most species are described from Africa and Europe (Condé 1996, Harvey 2003). While some species live in the upper soil layer, others are troglobiont – especially in Central Europe. One of these cave dwelling species is *Eukoenenia spelaea*. This species is found in caves of the Karst region in the European Alps (Christian et al. 2014), where they inhabit a mixture of mineral sediments (e.g. erosion of cave walls), plant material (e.g. transported through flooding of the cave), and animal excrements (e.g. bat guano) on the cave floor.

Morphological studies of Palpigradi date back to the late 19th and early 20th century, when studies were performed on *Eukoenenia angusta* (Hansen 1901), *Eukoenenia florenciae* (Rucker 1903), *Eukoenenia grassii* (Hansen 1901), *Eukoenenia mirabilis* (Hansen and Sørensen 1897, Wheeler 1900, Hansen 1901, Börner 1904, Buxton 1917, Kästner 1931*a*, Millot 1942, 1943), *Eukoenenia siamensis* (Hansen 1901), *Prokoenenia chilensis* (Hansen 1901), and *Prokoenenia wheeleri* (Hansen 1901, Rucker 1901, Kästner 1931*a*). The main focus of these studies was on the external morphology. Some aspects of the internal morphology were described by Rucker (1901), Börner (1904), Buxton (1917), and Kästner (1931*a*). More recent publications on Palpigradi are predominantly of taxonomic character, with focus on features relevant for classification. These include number and placement of setae, number of lateral organs, morphology of the genital plate, and body measurements. Only three recent studies looked at internal structures: Alberti (1979) analyzed the ultrastructure and development of spermatozoa in *P. wheeleri*, Ludwig and Alberti (1992) documented the ultrastructure of the midgut in *P. wheeleri*, and Smrž et al. (2013) studied the gut content of *Eukoenenia spelaea.*

Because comparative morphological and microscopic anatomy data on this group is incomplete, a valid phylogenetic positioning within arachnids based on morphological characters is difficult. The phylogeny of euchelicerates is much debated. Recent studies based on morphological characters as well as gene sequencing, and fossil records, result in diverging phylogenetic hypotheses of euchelicerate relationships (Fig. 1; Weygoldt and Paulus 1979*a*, Shultz 1990, 2007*a*, Giribet et al. 2002, Regier et al. 2010, Garwood and Dunlop 2014). Arachnida and Tetrapulmonata are the only taxa that are repeatedly confirmed and, thus, can be considered to represent established groups within the euchelicerates.
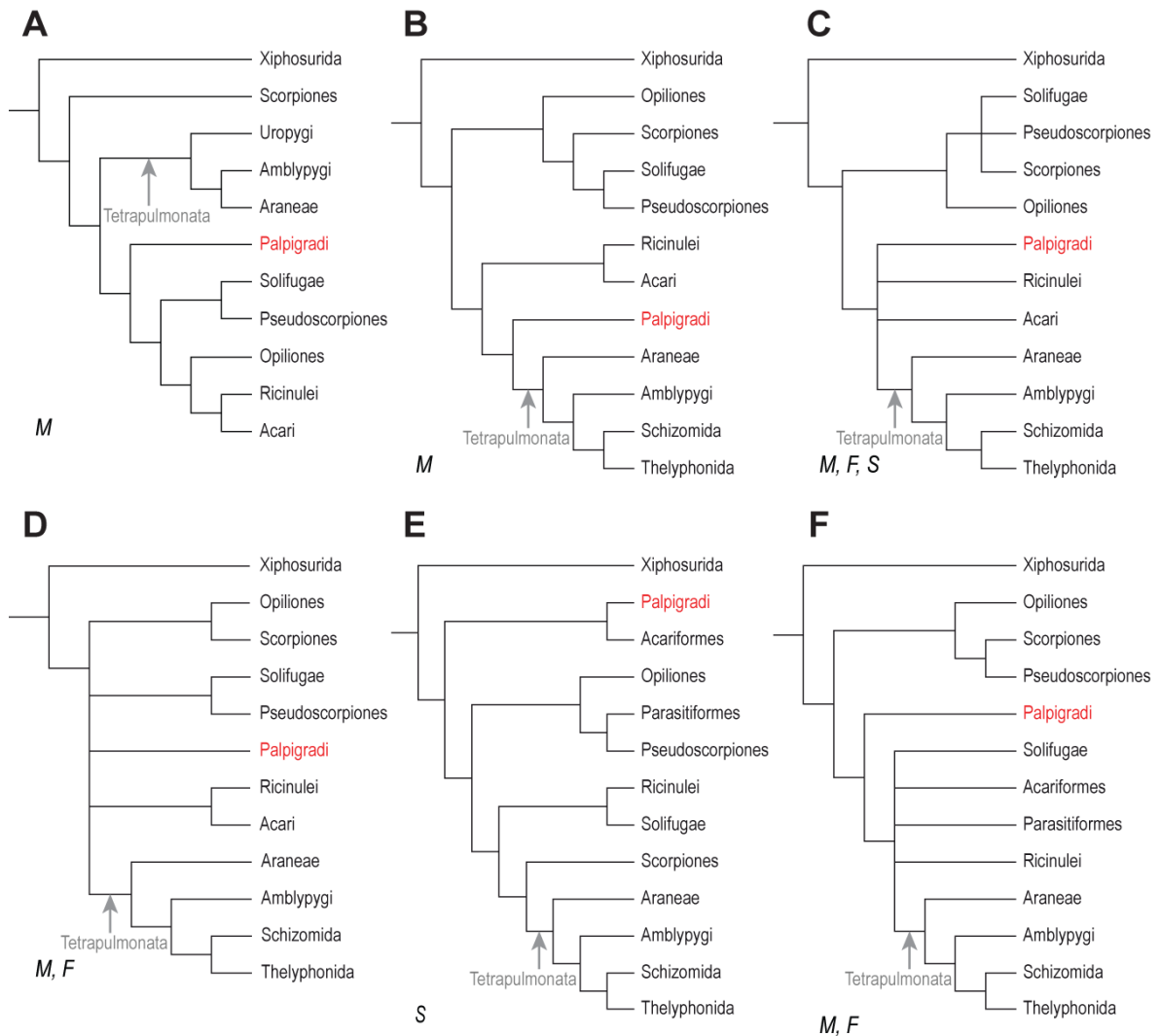
Fig. 1. Different proposed euchelicerate phylogenies. (**A**) Phylogeny based on morphological characters sensu Weygoldt and Paulus (1979*a*). Scorpiones are the sister group to all other arachnids, which are grouped into Tetrapulmonata and Apulmonata. (**B**) Phylogeny based on morphological characters sensu Shultz (1990). Arachnida are divided into two major sister groups. (**C**) Phylogeny based on morphological characters, fossil records, and gene sequencing sensu Giribet et al. (2002). The standing of the Palpigradi is unresolved. (**D**) Phylogeny based on morphological characters of extant and fossil records sensu Shultz (2007*a*). Aside from Tetrapulmonata, the relationships within the euchelicerates are not resolved. (**E**) Phylogeny based on gene sequencing sensu Regier et al. (2010). Palpigradi are positioned at the base and sister group to Acariformes. Scorpiones, a group usually placed at the base of the euchelicerates, is here the sister group of Tetrapulmonata. (**F**) Phylogeny based on morphological characters and fossil records sensu Garwood and Dunlop (2014). While the base is resolved here, the relationships between Solifugae, Acariformes, Parasitiformes, and Ricinulei is unresolved. Abbreviations: F: fossil record analysis; M: morphological character analysis; S: gene sequence analysis.

All other higher order group relationships are yet to be established including the phylogenetic position of Palpigradi. Weygoldt and Paulus (1979*a*; Fig. 1A) considered Palpigradi to be the sister group to all other Apulmonata (Pseudoscorpiones + Solifugae + Opiliones + Ricinulei + Acari). Shultz's (1990) analysis of morphological characters recovered Palpigradi as sister group to Tetrapulmonata (Araneae + Amblypygi + Thelyphonida + Schizomida; Fig. 1B). The

analysis of Giribet et al. (2002) included fossil records as well as gene sequences and recovered palpigrades as sister group to Acari, Ricinulei, and Tetrapulmonata (Fig. 1C). Palpigradi were further recovered in an unresolved position within Arachnida based on morphological characters as well as fossil data by Shultz (2007*a*; Fig. 1D). Palpigradi were later placed in a basal position with Acariformes as sister group after analysis of gene sequences only (Regier et al. 2010; Fig. 1E). Garwood and Dunlop (2014) included fossil data in their morphological data set and placed palpigrades as sister group to Acari, Ricinulei, Solifugae, and Tetrapulmonata (Fig. 1F). Giribet et al. (2014) conducted the first comprehensive phylogenetic analysis of Palpigradi (29 species) based on gene sequences. In the authors' analysis which also included data from Pycnogonida, Xiphosura, Scorpiones, Opiliones, Pseudoscorpiones, Acari, Solifugae, and Thelyphonida, Palpigradi were placed as sister group to Scorpiones and Thelyphonida.

Palpigradi are small when compared to other arachnids, e.g. Amblypygi (up to 45 mm body length), Scorpiones (up to 210 mm body length), Solifugae (up to 70 mm body length), or Thelyphonida (up to 75 mm body length), and one may hypothesize that the group evolved by miniaturization. Among invertebrates, miniaturization as an evolutionary process has been described for mollusks (Landman et al. 1991, Payne and Allen 1991), eucrustaceans (Hartmann 1973), insects (Dybas 1966, Polilov 2015*a*), and arachnids (Williams and McIntyre 1980, Platnick and Forster 1982). However, miniaturization does not only mean small body size. As an evolutionary process, miniaturization implies that the ancestor was larger and that small body size is the result of directional selection. As a result a characteristic morphological pattern may be found, i.e. (allometric) reduction of organ size and structural simplification (e.g. midgut differentiation simplified in insects; Polilov 2015*a*). This can ultimately result in a complete loss of a structure or organ (e.g. lack of a heart in insects; Polilov 2015*a*). A possible evolutionary mechanism for such morphological changes can be ontogenetic truncation (i.e. paedomorphosis: remaining in a sub adult state, e.g. Acari: Atyeo et al. 1984). Paedomorphosis can occur by progenesis and neoteny (Gould 1977). Progenesis is the accelerated maturation with respect to the somatic development of the organism. Neoteny describes the retardation of the shape with regards to the developmental stage of the organism (Gould 1977, Alberch 1980, McNamara 1986,

1988). In both cases of paedomorphosis, larval structures are retained in the adult, however, reduction in body size can only be found associated with progenesis. In addition, selection on reduced body size can also result in morphological novelties as well as an increase in morphological variability (e.g. modified eye morphology in arachnids; Williams and MeIntyre 1980, Hanken and Wake 1993).

1.2   Aims of the thesis

Conducting a detailed analysis of the microscopic anatomy of *Eukoenenia spelaea*, I aimed at aiding in the resolution of the phylogenetic standing of Palpigradi within Euchelicerata as well as diagnose morphological features which might indicate miniaturization in these small animals. Thus, the main focus of this thesis was to study the external and internal anatomy of *E. spelaea* as well as the ultrastructure of its organs. With the collected data, I aimed at answering the following questions:

- Where can *E. spelaea*/Palpigradi be placed within the Euchelicerata? What sister group relationship can be established?
- Does *E. spelaea* display morphological characters consistent with miniaturization?

The morphological characters found in this study were compared with morphological characters of other euchelicerates to establish possible autapomorphies of *Eukoenenia spelaea*. In addition, possible synapomorphies with other euchelicerate groups were discussed. These results were used to test an existing phylogeny of Euchelicerata based on morphological characters and to establish whether the ancestor of Palpigradi was large in body size (prerequisite for miniaturization). The morphological characters of *E. spelaea* were then analyzed for morphological indicators of miniaturization such as reduction and simplification of organs or structures in the form of paedomorphic morphology as well as novel structures and morphological variability. These findings were discussed in the context of the established phylogeny to elucidate a possible miniaturization event in Palpigradi.

2. Materials and Methods

2.1 Sampling and sourcing of specimens

Twenty-two specimens of *Eukoenenia spelaea* Peyerimhoff (1902) were collected in the Ardovská Cave (Fig. 2; Slovak Aggtelek Karst, 48° 31′ 18.613″ N, 20° 25′ 13.798″ E) in April, July, and October 2016 and in August 2018. Species determination was done by Ľubomír Kováč.

The cave is not accessible to tourists, thus, it is undisturbed and free of artificial lighting, except for the occasional visit from scientists. The temperature within Ardovská Cave ranges from +7.9 to +10.8 °C and the humidity is approx. 97 % (Kováč et al. 2002, 2014). The cave consists of numerous narrow passages as well as few larger caverns. It is characterized by the presence of stalactites and stalagmites of various sizes (Fig. 3A). The habitat of *Eukoenenia spelaea* are small patches of sediment consisting of mineral sediments, pieces of charcoal (brought in by scientists for an experimental setup on cave fauna), marten excrements, and bat guano (Fig. 3B).

The body length of the collected specimens without the flagellum was 1.23 mm ± 0.13 mm for adult females and 1.03 mm ± 0.13 mm for adult males. Nine animals (six females and three males) were fixed using paraformaldehyde (PFA 5 % in 0.1 mol l^{-1} phosphate buffered saline, pH 7.4). These animals were used for light microscopic (LM) histology and scanning electron microscopy (SEM). Ten animals (all females) were fixed using glutardialdehyde (GDA 2.5 % in 0.2 mol l^{-1} phosphate buffered saline, pH 7.4). These samples were used for transmission electron microscopy (TEM). Three specimens were fixed using a modified Karnovsky's fixative (GDA 2.5 % and PFA 1.5 % in 0.1 mol l^{-1} phosphate buffered saline, pH 7.4). All animal material (including unsectioned specimens) is stored at the Zoological State Collection in Munich, Germany (project numbers ZSMS20190030 – ZSMS20190051).
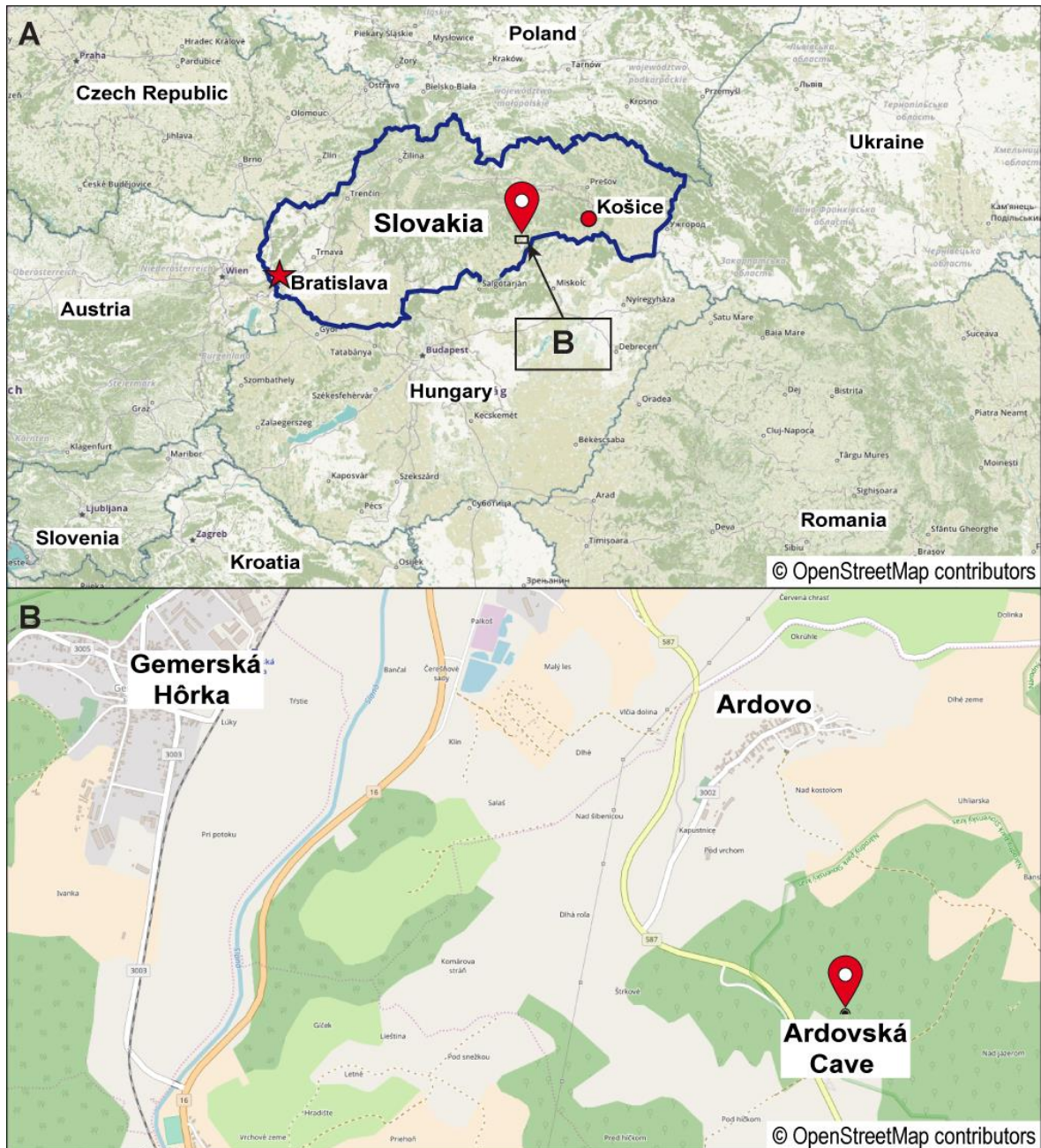
Fig. 2. Sampling location. (**A**) Slovakia is a small country, located in the heart of Eastern Europe. Most of Slovakia is mountainous and numerous Karst caves can be found. The collection site is located approx. 90 km west of Košice. (**B**) Ardovská Cave lies in a small wooded area off route 587, close to the village of Ardovo. The map was created by OpenStreetMap® (http://www.openstreetmap.org/copyright/en; accessed December 6, 2017).
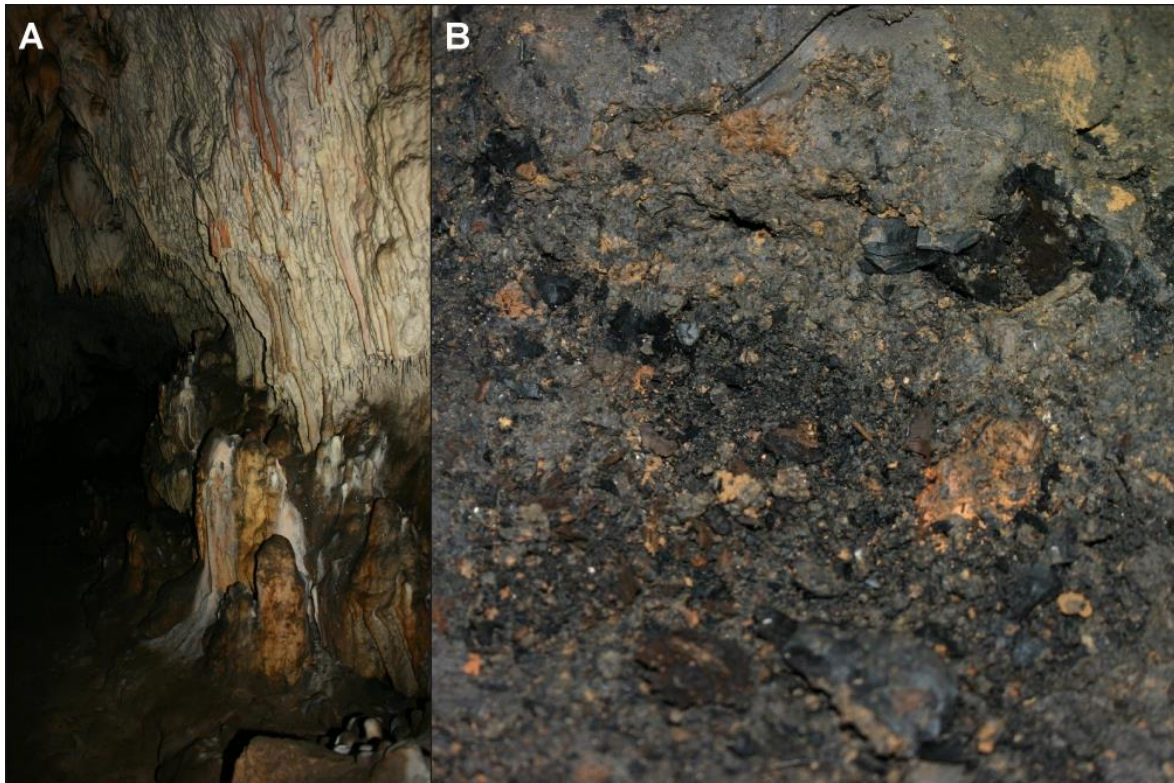
Fig. 3. Cave interior. (**A**) In some areas of the caves, stalactites and stalagmites build pillars. The cave is also characterized by narrow passageways. (**B**) Habitat of *Eukoenenia spelaea* at Ardovská Cave, Slovakia. The sediment consists of mineral sediments, pieces of charcoal, marten excrements, and bat guano.

2.2 Scanning electron microscopy

Scanning electron microscopy (SEM) was used to document the external anatomy of the animals. Fixed specimens were dehydrated through a graded series of acetone. The samples were then dried using the critical point drying method. The samples were mounted and later sputter coated for 200 s with gold. Images were captured using a LEO 1430VP SEM (LEO Elektronenmikroskopie GmbH, Oberkochen, Germany) and the software SmartSEM (version 5.07, Carl Zeiss AG, Oberkochen, Germany).

2.3 Histology

The specimens were washed four times in phosphate buffered saline (0.1 mol l^{-1}) over a period of 20 minutes, post fixed in 1 % osmium tetroxide for two hours and washed again (four times, 20 minutes each) in phosphate buffered saline to remove excess osmium tetroxide. Samples were dehydrated through graded series of acetone (30–100 %) and then embedded in Glycidether 100 (Carl Roth GmbH + Co.
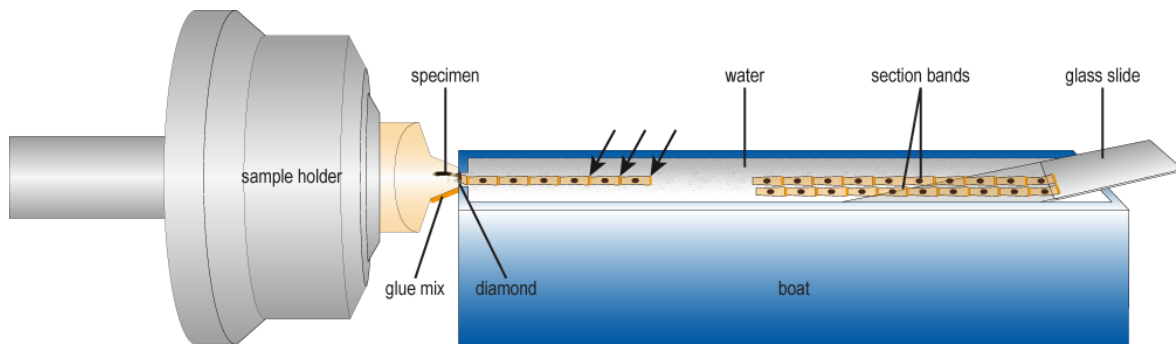
Fig. 4. Setup for semithin serial sectioning. The layer of glue mix on the ventral side of the specimen block ensures, that the following section is firmly attached to the previous section (arrows). Once several bands are attached to the glass slide, the slide is removed from the boat and dried.

KG, Karlsruhe, Germany). Histological semithin sections were cut at 1.5 µm, 1 µm and 500 nm thickness using an RMC MTXL ultra-microtome (Boeckeler Instruments, Inc., Tucson, Arizona, USA) equipped with a histo Jumbo diamond knife (DiATOME Ltd, Biel, Switzerland). In order to obtain serial sections, the ventral side of the trimmed specimen block was covered with a thin layer of ethyl acetate/ methyl cyclohexane glue (Pattex Kraftkleber Classic, Henkel AG & Co. KGaA, Düsseldorf, Germany) mixed with xylene in a 1:1 mixing ratio. The section bands were then collected in water, attached to a glass slide (Fig. 4) and dried. The sections were stained using Rüdeberg staining solution (Rüdeberg 1967). Light microscopic images were taken with an automated Olympus BX61VS microscope and DotSlide software (Olympus, Hamburg, Germany) or an Olympus BX51TF microscope (Olympus, Hamburg, Germany) equipped with a microscope camera (UCMOS camera, ToupTek Photonics, Hangzhou, P. R. China). Image capturing was processed via ToupView (ToupTek Photonics, Hangzhou, P. R. China). Image analysis was done using OlyVIA (version 2.9, Build 13735, Olympus Soft Imaging Solutions GmbH, Münster, Germany).

2.4   Transmission electron microscopy

For transmission electron microscopy (TEM), ultrathin sections were cut at 50 nm thickness using an RMC MTXL ultra-microtome (Boeckeler Instruments, Inc., Tucson, Arizona, USA). Sections were collected on copper triple slot grids and contrasted using uranyl acetate and lead citrate following standard protocols (Reynolds 1963). For transmission electron microscopy, a Morgagni 268 electron microscope (FEI Company, Hillsboro, OR, USA) and MegaView III CCD - iTEM-SIS
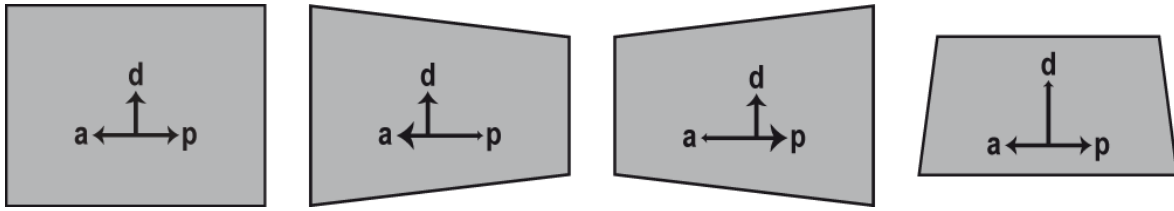
Fig. 5. To aid in understanding of the orientation of a section or image, different arrows were used to indicate the orientation. If all arrowheads and arrow lengths are identical, the section is straight. In case a section is oblique, large arrowheads on short directional arrows indicate that this side of the animal is closer to the viewer, small arrowheads on long directional arrows indicate that this side of the animal is further away from the viewer.

software (Olympus, Soft Imaging System GmbH, Münster, Germany) for image capture was used.

2.5   Image processing

All light microscopic (LM) and transmission electron microscopic (TEM) images were processed using ImageJ (version 1.50d, NIH, USA) and Adobe Photoshop CC 2014 (Adobe Systems Incorporated, San Jose, CA, USA). Image processing included background subtraction (LM), removal of non-relevant embedding material (TEM), and contrast enhancement. Assembly of images was done using Image Composite Editor (version 2.0.3.0, Microsoft Corporation, Redmond, WA, USA). Addition of labels and scale bars were done using Adobe Illustrator CC 2014 (Adobe Systems Incorporated, San Jose, CA, USA). To aid recognition of organs in LM and TEM images, a color overlay was applied. The color code of the LM images corresponds with the color coding used in the schematic drawings.

In cases where the cutting plane was oblique, I place directional arrows in the lower left corner of an image to indicate the orientation of the section. Small arrowheads on long directional arrows indicate an orientation away from the viewer, large arrowheads on short directional arrows indicate an orientation towards the viewer (Fig. 5).

2.6   Phylogenetic analysis

The phylogenetic analysis is based on the work of Shultz (2007*a*). He analyzed 59 euchelicerate taxa (41 extant, 18 fossil) coded for 202 binary and unordered multistate morphological characters. The author's matrix was supplemented with the data collected in this study (Tabs. 6, 7, A1, A2). *Eukoenenia spelaea* was regarded as a separate taxon to allow independent analysis of its characters. The analysis

was set up identical to Shultz (2007*a*), i.e. using Tree Analysis using New Technologies (TNT), however, the newer version 1.5 was used (Goloboff et al. 2008, Goloboff and Catalano 2016). The non-arachnid euchelicerate taxa were chosen as outgroup. "Traditional" tree searches with 1000 replicates using TBR branch swapping were performed. Bootstrap percentages (Felsenstein 1985) and Bremer support (Bremer 1994) were calculated in TNT. Absolute bootstrap percentages were determined by 1000 pseudo-replicates, which were analyzed by ten random-addition replicates using TBR branch swapping, each. Absolut Bremer support was determined by measurement of the difference between the unconstrained and constrained minimal-length trees. Implied weights analysis (Goloboff 1993) was performed to examine homoplasy effects. Following the phylogenetic analysis of Shultz (2007*a*), implied weights analyses with constant of concavity (k) values of 1–6 were conducted using "traditional" search based on 1000 replicates using TBR branch swapping. Lower k-values are weighted more strongly against homoplastic characters while higher k-values are weighted less.

The analysis of only extant taxa was performed in the same way as described above, however, characters specific to fossil taxa (characters 49, 98, 99, 100, 113, 114, 125, 161) were removed prior to analysis. In the interest of easy recognition of relationships between groups within the displayed trees, the single taxa were omitted and only the major euchelicerate groups depicted. The analyses, however, were conducted with the full matrix.

In addition to the analyses described above, an updated matrix was analyzed in the same manner (extant and fossil, extant only). The character changes applied to the matrix and the respective updated character coding are listed in tables 6 and 7. The newly described fossil *Chimerarachne yingi* was included in the analysis of extant and fossil taxa. This taxon was added due to the fact that it is the only araneid with a flagellum known today. The coding sequence in table A2 is based on the publication of Wang et al. (2018) and was included into the matrix. Additional changes to character states were conducted for Acariformes, Palpigradi, Schizomida, Solifugae, *Mastigoproctus* (Thelyphonida; Grams et al. 2018), and *Palaeocharinus* (Trigonotarbida; Dunlop et al. 2009). All changes are listed in table 7.

2.7 Terminology

In the interest of allowing comparisons across all arthropod groups, I have sought to keep terminology as neutral as possible. The numbering of the body segments starts with 1 for the first segment (the "ocular" segment) and not with zero as used by several authors (Millot 1949*a*, van der Hammen 1989, Shultz 2007*b*, Dunlop and Lamsdell 2017). For the pedipalps and legs, the most proximal article is termed "coxa" following a largely practiced nomenclature. The following articles are numbered (Tab. 9).

3. Results

Individuals of *Eukoenenia spelaea* are small delicate animals with an elongate body shape, a long terminal flagellum (Figs. 6, 7), and a light, almost translucent body. The body length of the analyzed individuals varied between 0.90 mm and 1.35 mm. The entire body is covered by a dense pubescence (Pub; Fig. 12) and numerous large, spiked sensory setae (SS; Figs. 6, 7, 12; Tabs. 1–4). The pubescence consists of a multitude of small cuticular protuberances ranging in length between 5 µm and 8 µm. The number and position of setae was the same in all individuals, except for the setae associated with the genitalia (Tab. 3). I observed a slight sexual dimorphism in the shape of the genitalia, body length (females 1.23 ± 0.13 mm, males 1.03 ± 0.13 mm), the extent of the sclerite duplicature of the opisthosoma, and the musculature of the prosoma and opisthosoma (see below).

3.1 External morphology

The tagmatisation of *Eukoenenia spelaea* (Fig. 8) follows the typical euchelicerate body plan with a prosoma (seven segments) and an opisthosoma (11 segments). The prosoma carries the extremities, i.e. the chelicerae, the pedipalps and four pairs of legs (Ch, PP, L1–4; Fig. 6). The opisthosoma is subdivided into an anterior mesosoma (seven segments) and a posterior metasoma (four segments). The metasoma carries a terminal flagellum with 15 articles. The flagellum has approximately the length of the entire body.

3.1.1 Prosoma dorsum

The seven segments of the prosoma are partially merged forming topographically distinct sclerites; however, the borders between sclerites differ on the dorsal and the ventral the side of the prosoma (Figs. 6–8). Dorsally, the prosoma is covered by the three sclerites that have traditionally been considered tergites and termed pro-, meso- and metapeltidium. The propeltidium presumably is the common dorsal sclerite (tergite) of segments 1–6 with a posterior overhang. The posterior end of the propeltidium tapers off and partially covers the mesopeltidium as well as the most anterior part of the metapeltidium (PrPlt, PaPlt, MtPlt; Figs. 6A, C, 8A, B). The mesopeltidium is represented by a pair of small, poorly sclerotized dorsolateral sclerites in the region of leg 3, and partially covers the anterior part of the metapeltidium. I will show below that the mesopeltidium does not represent a tergite, but is a sclerotization of the dorsolateral pleural membrane, and I, therefore, suggest the term "parapeltidium" which I will use from here on. The metapeltidium is an unpaired sclerite (tergite of segment 7 as discussed below), roughly triangular shaped with the pointed end towards anterior, and a broad base towards posterior. It extends from the region between leg 2 and 3, i.e. at the beginning of the overhang of the propeltidium, to the end of the prosoma (Figs. 6A, C, 8A, B). Each prosomal segment carries a fixed number of setae in the same topographic positions. The number and position of setae do not vary among individuals. (Tab. 1).

3.1.2 Prosomal sternum

The ventral side of the prosoma has four sclerites, representing the sternites of segments 2–7 (Fig. 6D). The large anterior sternite represents the fused sternites of segments 2–4, the prosternum (Figs. 6D, 8C, see discussion 4.1.2). Traditionally, this element has been termed deuto-tritosternum, however I provide evidence (see discussion 4.1.2) that it contains 3 prosomal segments. At its anterior margin, it has a medial indentation which embraces the ventral plate (see below; Fig. 6D). The ventral sclerites following posterior to the prosternum lie between the legs 2–4 and represent the segmental sternites of prosomal segments 5–7 (Figs. 6D, 8C). They cover the entire region between the coxae. All prosomal sternites are free of setae, with the exception of the prosternum which carries six setae (Tab. 1).
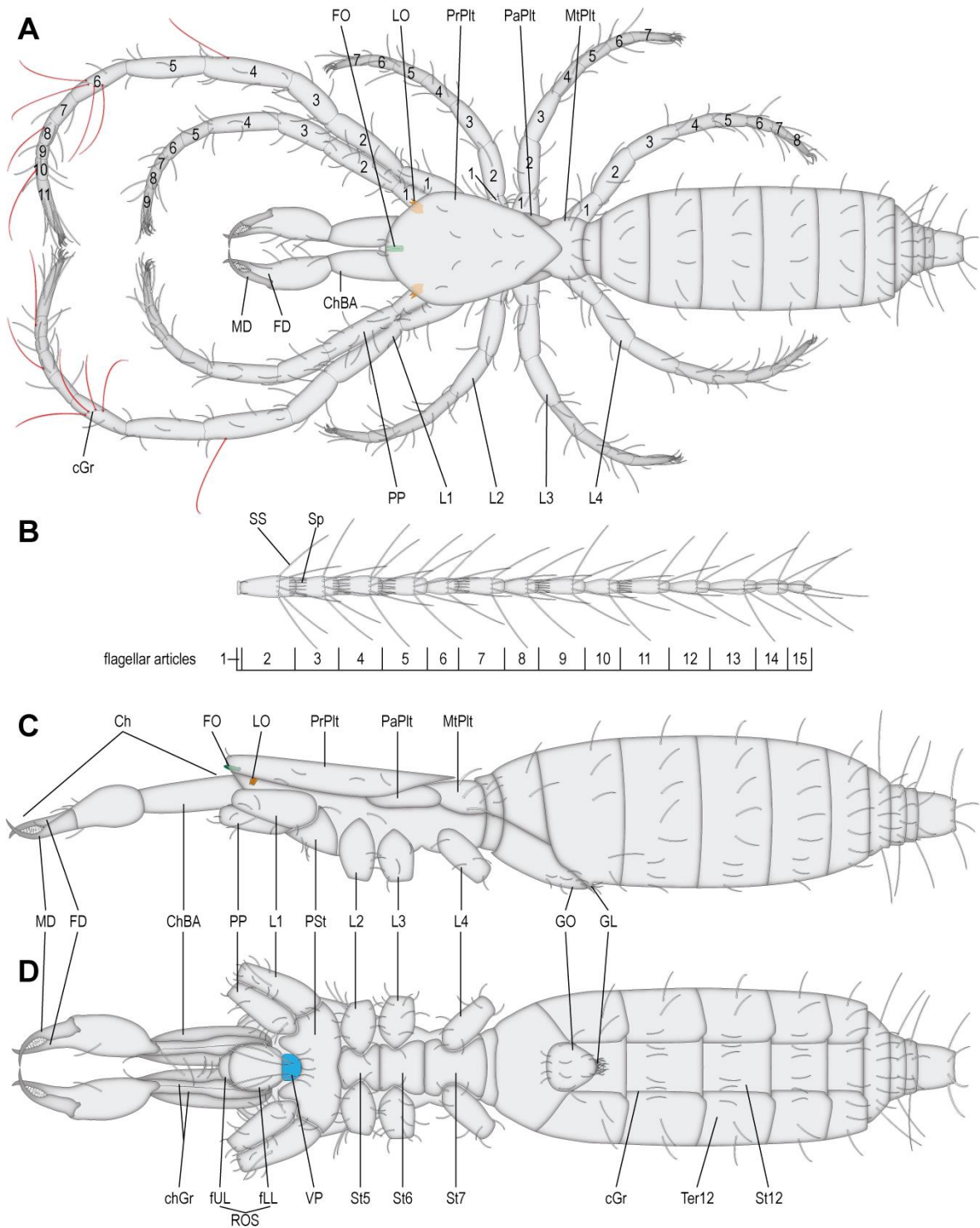
Fig. 6. *Eukoenenia spelaea*, schematic drawing. (**A**) Dorsally, the prosoma is divided into a pro-, para- (see discussion 4.1.1), and metapeltidium. The opisthosoma tapers off in segment 15. The chelicerae consist of three articles. Arabic numbers indicate leg articles, article 1 is the coxa. The frontal organ (green) and the lateral organ (orange) are largely covered by the propeltidium. Trichobothria are highlighted in red. (**B**) The flagellum. Long setae are less numerous than spikes and located more proximal on the articles. (**C**) Lateral view of a female. The frontal organ is nested underneath the anterior end of the propeltidium. (**D**) Ventral view of a female. The prosternum (see discussion 4.1.2) is a fusion of the sternites associated with the chelicerae, pedipalps and the 1st leg. The previously undescribed ventral plate (blue), is located between the rostrosoma and prosternum. Only large spiked setae are depicted. Abbreviations: Ch: Chelicerae; ChBA: cheliceral basal article; cGr: cuticular groove; chGr: cheliceral groove; FD: fixed digit; fLL: functional lower lip; FO: frontal organ; fUL: functional upper lip; GL: genital lobe; GO: genital operculum; L1–4: leg 1–4; LO: lateral organ; MD: movable digit; MtPlt: metapeltidium; PaPlt: parapeltidium; PP: pedipalp; PrPlt: propeltidium; PSt: prosternum; ROS: Rostrosoma; SS: sensory seta; Sp: spike; St: sternite; Ter: tergite; VP: ventral plate.

15
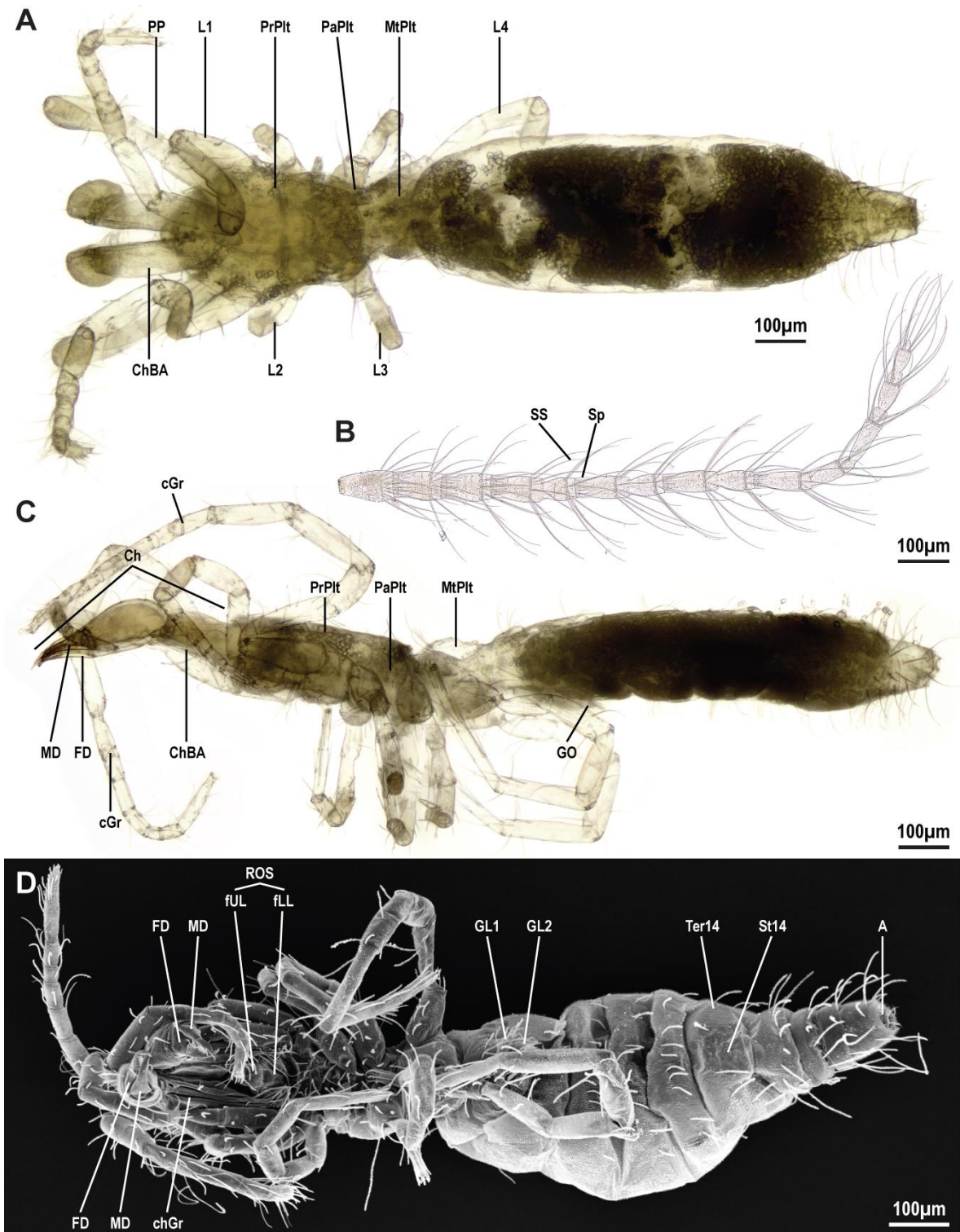
Fig. 7. *Eukoenenia spelaea*, overview images. (**A**) Dorsal view of a female, light microscopy. (**B**) Lateral view of a flagellum, light microscopy. (**C**) Lateral view of a female, light microscopy. Sternites cannot be clearly seen due to the drying process. (**D**) Ventral view of a male, scanning electron micrograph. Abbreviations: A: anus; cGr: cuticular groove; Ch: Chelicerae; ChBA: cheliceral basal article; chGr: cheliceral groove; FD: fixed digit; fLL: functional lower lip; fUL: functional upper lip; GL: genital lobe; GO: genital operculum; L1–4: leg 1–4; MD: movable digit; MtPlt: metapeltidium; PaPlt: parapeltidium; PP: pedipalp; PrPlt: propeltidium; ROS: Rostrosoma; SS: sensory seta; Sp: spike; St: sternite; Ter: tergite.
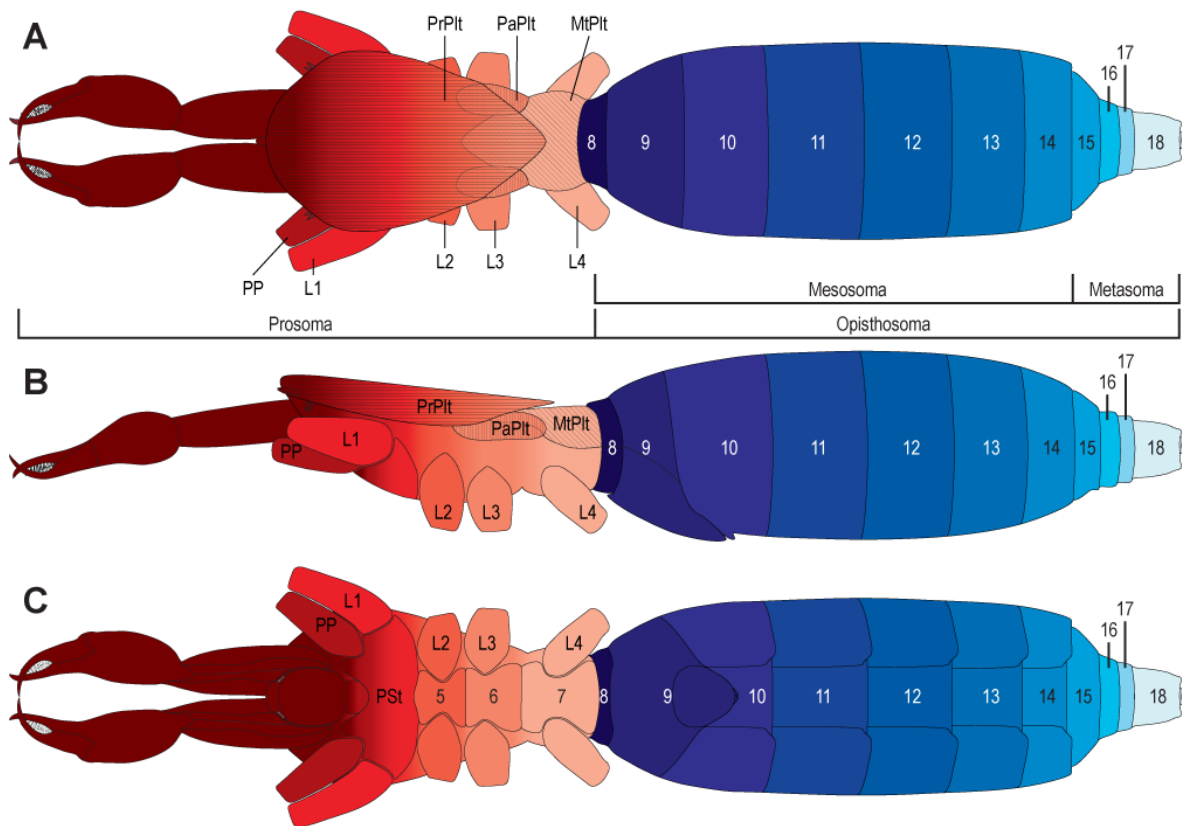
Fig. 8. *Eukoenenia spelaea*, segmentation. Prosomal structures are marked in shades of red, opisthosomal structures are marked in blues. Every hue marks a segment. (**A**) Dorsal view. The propeltidium (horizontal lines) extends to the level between the 3rd and 4th leg, however, it is only attached to the body from the anterior end of the prosoma to the level of the 2nd leg. The parapeltidium (vertical lines) is located at the level of the 3rd leg. The metapeltidium (diagonal lines) extends anteriorly to the level between leg 2 and 3. Opisthosomal segments are clearly defined by the tergites and sclerites. Segments 15– 18 have sclerotized rings instead of tergite and sternite, and are therefore termed here as metasoma. (**B**) Lateral view. Laterally, prosomal segments are difficult to discern as there are no visible cuticular structures indicating borders. Opisthosomal segments are clearly defined by the sclerites. (**C**) Ventral view. The first articles of the extremities as well as the presence of sternites define the prosomal segments ventrally. The rostrosoma cannot clearly be associated with a prosomal segment. The fused sternites from the cheliceral segment, pedipalpal segment and the segment of the 1st leg build the prosternum. Opisthosomal segments are clearly defined by the sternites and sclerites. Numbers indicate segments. Abbreviations: L1–4: leg 1–4; MtPlt: metapeltidium; PaPlt: parapeltidium; PP: pedipalp; PrPlt: propeltidium; PSt: prosternum.

Tab. 1. *Eukoenenia spelaea*, number of setae located on the prosoma. The mesopeltidium is termed here "parapeltidium" (see discussion 4.1.1). The fused sternite of segments 2–4 is termed here "prosternum" (see discussion 4.1.2).

	Number
Propeltidium	8
Parapeltidium	-
Metapeltidium	6
Prosternum	6
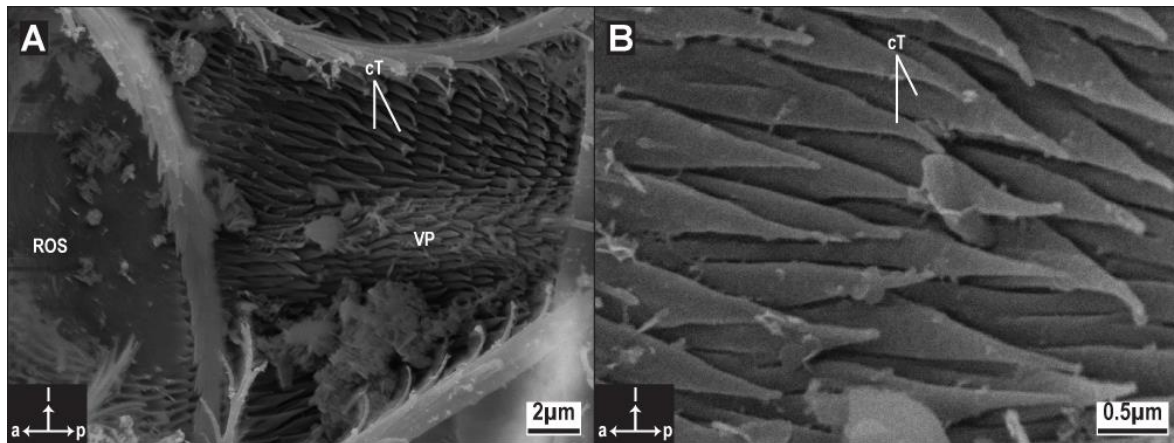
Fig. 9. *Eukoenenia spelaea*, scanning electron micrographs of the ventral plate. (**A**) Ventral view of the ventral plate. The cuticular teeth are arranged in even rows pointing posteriorly. (**B**) Close-up image of the cuticular teeth. The teeth are elongated and taper off at the tip. Abbreviations: a: anterior; cT: cuticular teeth; l: left; p: posterior; ROS: rostrosoma; VP: ventral plate.

3.1.3 Ventral plate

In ventral view, the large lower lip covers the mouth opening and bases of the chelicerae (Fig. 6D). Directly behind the posterior end of the lower lip and in front of the anterior end of the prosternum is a large ventral plate with a unique morphology (VP; Figs. 6, 9). The plate is covered with cuticular teeth which face posterior. These teeth have a uniform appearance. They are approx. 2 µm long, 0.4 µm thick at the base and taper off at the tip (cT; Fig. 9B).

3.1.4 Rostrosoma

The rostrosoma is a prominent tubular structure that forms a preoral cavity, carries the mouth opening and (parts) of the pharynx. It originates as a cuticular tube, ventromedial between the bases of the chelicerae and protrudes towards anterior, where it is nestled between the basal articles of the chelicerae (ROS; Fig. 6D). Anteriorly, the rostrosoma has a functional upper and a functional lower lip (Fig. 10). The functional upper lip forms lateral side walls overhanging the lower lip. These lateral side walls emerge from the point where upper and lower lip separate from the cuticular tube and extend to the anterior end of the lower lip (fLL, fUL; Fig. 10F) where both sides merge forming an anterior overhang in front of the lower lip.

This anterior overhang of the functional upper lip is covered with a coarse pubescence on the outside and fine-toothed transversal ridges on the inside (tR; Figs. 10B, D–F). Five small setae insert on the ventral margin of the functional upper
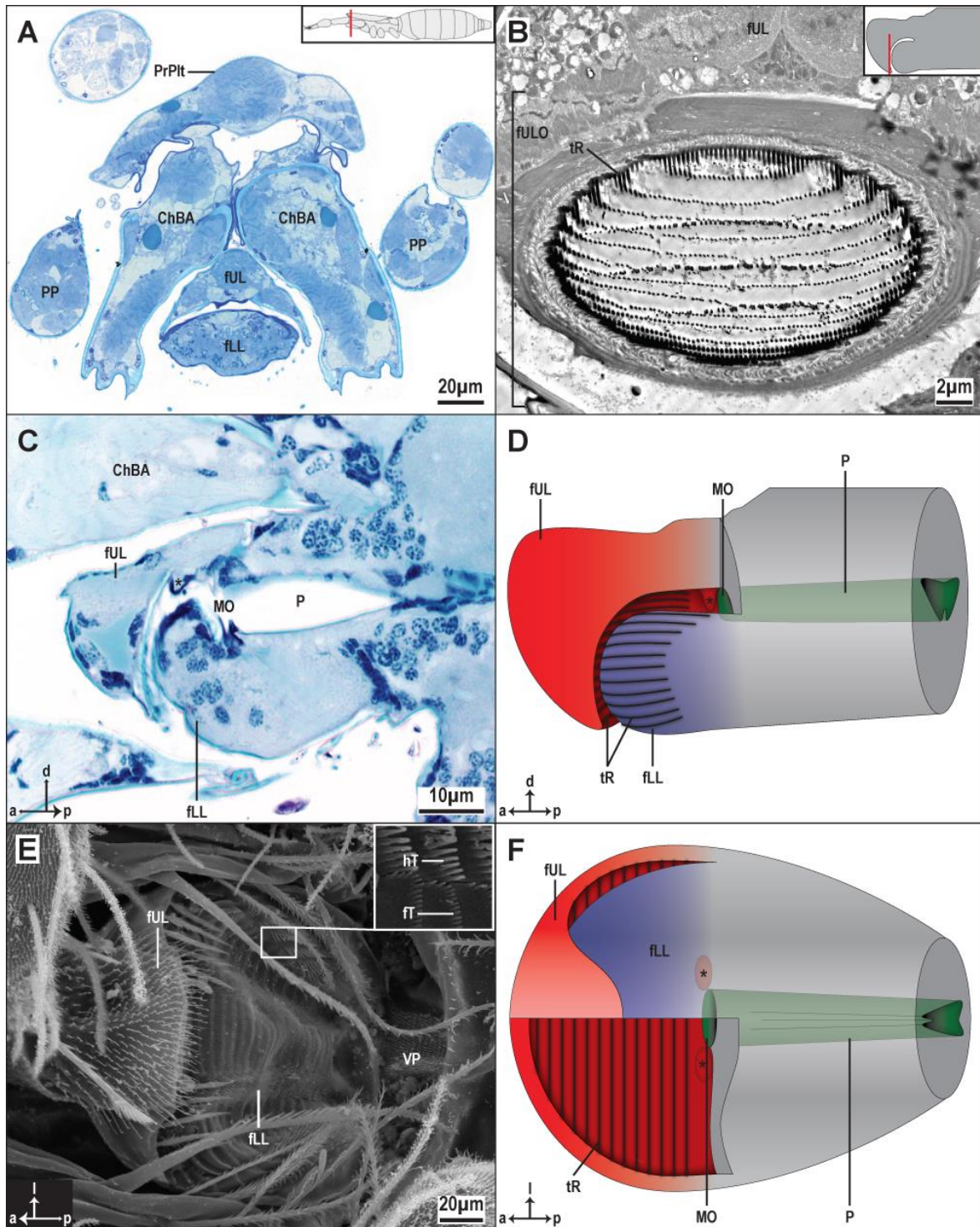
Fig. 10. *Eukoenenia spelaea*, rostrosoma. (**A**) Light micrograph of a cross-section through the rostrosoma anterior to the mouth opening (inset). The rostrosoma is nestled between the cheliceral basal articles. (**B**) Transmission electron micrograph of cross-section of the anterior overhang of the functional upper lip (inset). The toothed ridges are spaced regularly. (**C**) Light micrograph of a longitudinal section of the rostrosoma. The mouth opening lies posteriorly of the lateral protrusions (asterisk) of the functional upper lip. (**D**) Lateral view of the rostrosoma, schematic drawing. Parts of the functional upper lip (red) have been removed to display the mouth opening. The grey area indicates that functional upper and lower lip have fused. (**E**) Ventral view of the rostrosoma, scanning electron micrograph. The functional lower lip is covered in finely toothed ridges and hook-like teeth (inset). (**F**) Ventral view of the rostrosoma, schematic drawing. Parts of the functional upper and lower lip have been removed to display the close association of the lateral protrusions with the mouth opening. Abbreviations: a: anterior; ChBA: cheliceral basal article; d: dorsal; fLL: functional lower lip; fT: fine tooth; fUL: functional upper lip; fULO: functional lip overhang; hT: hook-like tooth; l: left; MO: mouth opening; P: pharynx; p: posterior; PP: pedipalp; PrPlt: propeltidium; tR: toothed ridge; asterisk: lateral protrusions of functional upper lip; VP: ventral plate.

19

lip (Fig. 10E). The lower lip extends into the anterior overhang of the functional upper lip where its cuticle forms fine-toothed, transversal ridges. These transversal ridges possibly act as counterpart to the transversal ridges on the inner side of the upper lip (tR; Fig. 10D). On its ventral side, the lower lip is covered by fine-toothed, transversal ridges. Each of these ridges intercalates laterally with two sections of elongated, hook-like teeth (fT, hT; Fig. 10E). Immediately anterior to the mouth opening, i.e. where both lips fuse into the tube-like structure, two sclerotized medial knobs from the ventral side of the upper lip are in close contact with the dorsal side of the lower lip (*,Figs. 10C, D, F); the cavity anterior to these knobs is the preoral cavity. The mouth opening is a small opening where upper and lower lip merge into a cuticular tube. The pharynx with its associated musculature is housed in the tubular part of the rostrosoma.

3.1.5 Sensory organs on the prosoma

The prosoma carries several sensory organs, i.e. the frontal organ, the lateral organ, numerous sensory setae, and trichobothria. The frontal organ is located dorsally on the apex of the prosoma and is partially covered by the propeltidium (FO; Figs. 6A, C). The unpaired frontal organ has a base with two modified setae. Each seta is approx. 25 µm long and has a diameter of approx. 5 µm. The cuticular surface of the frontal organ has a honeycomb pattern (Fig. 11A). This pattern is formed by cuticular ridges which enclose cuticular pits.
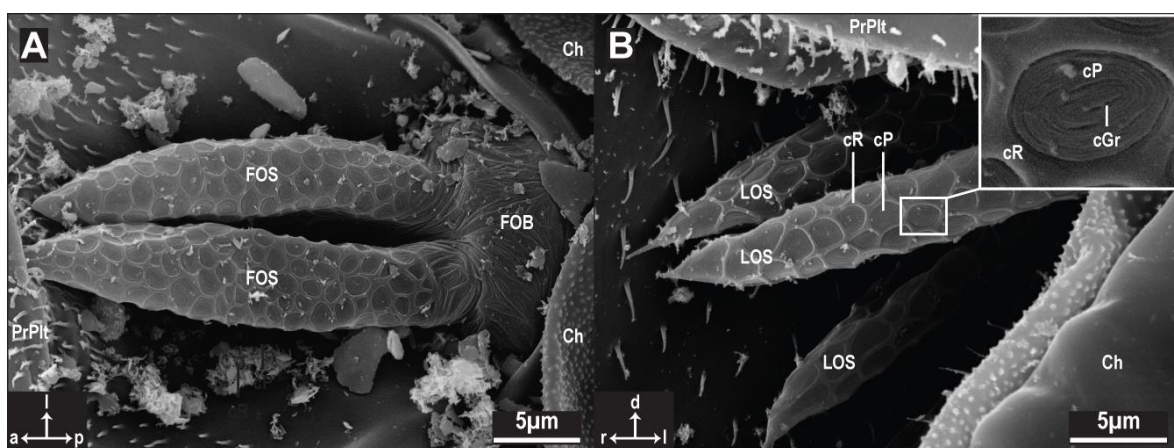
Fig. 11. *Eukoenenia spelaea*, scanning electron micrographs of the frontal organ and lateral organ. (**A**) Ventral view of the frontal organ. It consists of a base and two modified setae. The cuticular structure of the base is irregular. The setae have a honeycomb pattern. (**B**) Ventral view of the lateral organ. It consists of four modified setae. There is a striking similarity of the vesicles' honeycomb pattern compared with the frontal organ. The cuticular ridges form pits with grooved openings in the cuticle (inset). Identical structures are found on the frontal organ. Abbreviations: a: anterior; Ch: chelicera; cGr: cuticular groove; cP: cuticular pit; cR: cuticular ridge; d: dorsal; FOB: frontal organ base; FOS: frontal organ seta: LOS: lateral organ seta; p: posterior; PrPlt: propeltidium.

The topographic position of the lateral organs is dorsolateral under the propeltidium, on the level of the base of the pedipalps (LO; Figs. 6A, C). However, an explicit association with a prosomal segment is not possible because prosomal segments 1–6 are fused dorsally. The lateral organs consist of four modified setae each. These setae are similar in shape and size to the setae of the frontal organ (approx. 25 μm long and 4.5 μm in diameter; Fig. 11B). Their cuticular surface also carries a honeycomb pattern like the frontal organ. The pits, which are formed by the cuticular ridges, display cuticular grooves.

The entire animal is covered with numerous sensory setae. The topographic pattern of sensory setae was the same in all studied individuals (Fig. 6; Tab. 1–4). The spiked setae can reach up to 120 μm in length. Each sensory seta is nested within a circular socket (diameter approx. 2 μm) in the cuticle and is flexible (Fig. 12). The diameter of the sensory setae decreases gradually from base (approx. 1.2 μm) to tip (approx. 0.8 μm).

Like other euchelicerates, *Eukoenenia spelaea* has specialized sensory setae, the trichobothria. They are located on the first pair of legs. The topographic distribution of trichobothria on the leg is as follows: article 4 carries one, article 6 carries four, and articles 8 and 10 carry one trichobothrium each (Fig. 6A). The single trichobothria of articles 4, 8, and 10 are oriented toward dorsolateral and distal, i.e. away from the body median line. On article 6, the four trichobothria are arranged
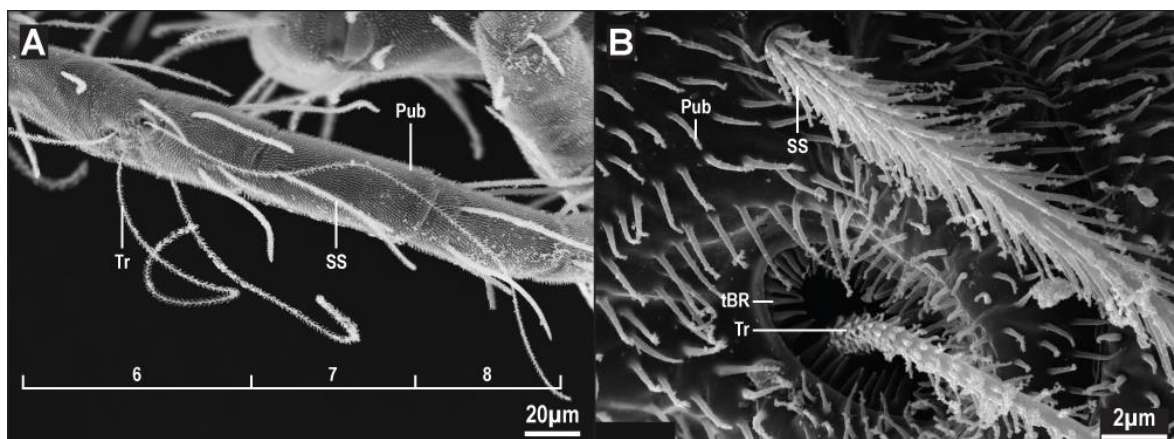
Fig. 12. *Eukoenenia spelaea*, scanning electron micrographs of the different hair types. (**A**) Articles 6–8 of leg 1. The entire animal is covered by an even pubescence. There are noticeable differences in length and thickness between sensory setae and trichobothria. (**B**) Close-up of the bases of sensory seta and trichobothrium. The sensory seta is thicker and its spikes are longer than in the trichobothrium. However, the cuticular socket of the sensory seta is an approx. 3-fold smaller than that of the trichobothrium. The protuberances of the pubescence have no sockets. Abbreviations: Pub: pubescence; SS: sensory seta; tBR: toothed bothrial rim; Tr: trichobothrium.

along the cuticular groove of the article (see 3.1.7). Out of these four, the first two trichobothria are located dorsal and distal to the cuticular groove. The other two trichobothria are located to the left and right of the first two trichobothria and are proximal to the cuticular groove. Both dorsolateral trichobothria are located proximally to the cuticular groove on article 6, however, both dorsal trichobothria are located distal to this groove. The setal part of the trichobothria roots in a cuticular cup-shaped socket (bothrium, diameter approx. 6 µm) with a toothed rim (tBR, Tr; Fig. 12). The cuticular teeth surrounding the socket are approx. 1 µm long and 0.2 µm thick at the base (Fig. 12B). The maximum deflection of the seta before touching the cuticular teeth of the socket is 25–30°. The seta is longer (approx. 250 µm) and thinner (diameter consistently approx. 0.8 µm) than other sensory setae.

3.1.6   Chelicerae

The chelicerae are proportionally large, and are oriented straight towards anterior. They have three articles, i.e. the basal article, the fixed finger, and the movable digit which together form a chela (FD, MD; Figs. 6A, 13A). The basal article has approximately the same length as the chela. The propeltidium overlaps the proximal parts of the basal article anteriorly. The basal article is covered in pubescence. On the ventral side of the basal article are two grooves which span the entire length of the article. The lateral walls of the grooves are knobbed, whereas the inner ridge is smooth like the rest of the ventral side of the basal article (arrows; Fig. 13B). The medial face of the basal articles is concave providing space for the rostrosoma (Figs. 6D, 10A).

The main body of the fixed digit is covered in pubescence, however, the medial faces of the chelicerae are free of cuticle protuberances (*; Fig. 13A). A total of 12 setae are located on each chelicera: six on the basal article and six on the fixed digit. The movable digit is free of setae (Figs. 6, 13; Tab. 2). The teethed sections of the digits carry eight serrated teeth each (sT; Figs. 13A, C, D). The distance between the teeth is approx. 1–1.5 µm, between the serrations, the distance is approx. 0.05–0.1 µm. The tips of the digits are elongated and almost as long as the toothed section of the digits. The tips cross each other (Figs. 6, 13C).
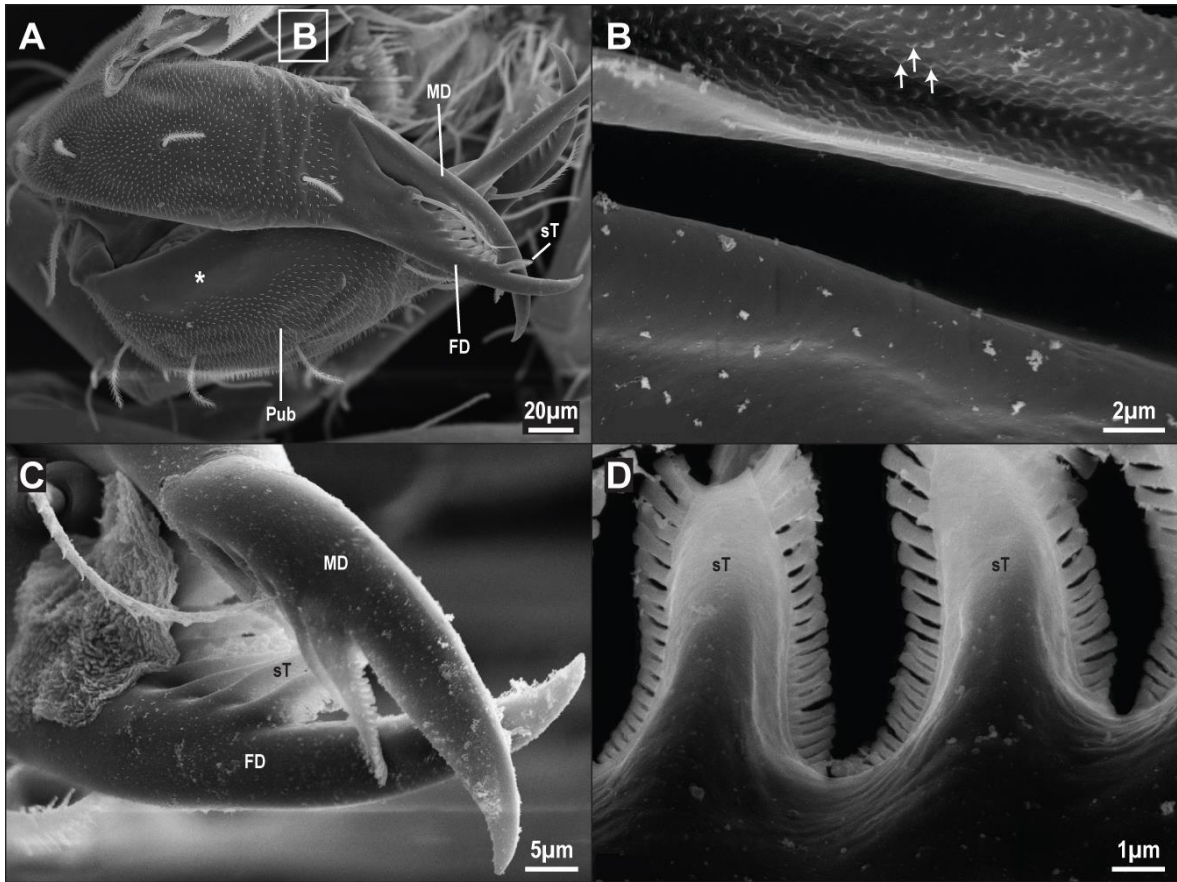
Fig. 13. *Eukoenenia spelaea*, scanning electron micrographs of the chelicerae. (**A**) Dorsal view of the fixed and movable digits. The inward oriented part of the main body of the fixed digit is free of pubescence (asterisk). The basal article displays cuticular grooves (see B). (**B**) The ridges of the lateral basal article grooves are knobbed (arrows), the central ridge is smooth. (**C**) The tips of the cheliceral digits are crossed. (**D**) Close-up image of the teethed section of the cheliceral digits. The teeth are serrated. Abbreviations: d: distal; FD: fixed digit; l: left; MD: movable digit; p: proximal; Pub: pubescence; sT: serrated tooth.

3.1.7 Pedipalps and legs

The pedipalps and the following extremities are leg-like, have a terminal claw and carry numerous setae (Tab. 2). The pedipalps are located in segment 3, closely neighboring leg 1. Both extremities insert on sockets of the prosternum that are bent to the anterior so that the pedipalps and leg 1 are oriented towards anterior. The pedipalps are divided into nine articles. Leg 1 is the longest pair of extremities and shaped like a palp. It articulates to the posterolateral part of the prosternum in segment 4, and consists of 11 articles. Like in the pedipalps, the coxa is elongated. Article 6 of leg 1 shows a cuticular groove which spans the entire article diagonally (Figs. 6A, 7C). Legs 2 and 3 are located on segments 5 and 6, respectively. They are both oriented towards lateral and consist of seven articles. The coxa of both legs is short and appears broader than in the other legs. Leg 4, is located in segment 7.

23

It is oriented toward posterior and consists of eight articles. The coxa is elongated and borders the sternite.

3.1.8 Opisthosoma

The opisthosoma is divided into a mesosoma (segments 8–14) and a metasoma (segments 15–18), consisting of a total of 11 segments (Figs. 6, 8). Segment borders are described by the anterior and the posterior margins of the tergites and sternites, respectively (Fig. 6). Mesosoma and metasoma are distinguished by their covering sclerites, i.e. segments of the mesosoma carry dorsal and ventral sclerites, and in the metasoma sclerites are fused forming cuticular rings around the segments. In the mesosoma, segment 8 is short and has a smaller diameter than the following six segments. In segments 9–17, the dorsal sclerites form posterior overhangs that reach over the anterior section of the following segment. In females, these overhangs are thicker than in males (SD; Figs. 14A, B). In females, the base of the overhang is up to 20 µm wide while the distal part tapers off gradually

Tab. 2. *Eukoenenia spelaea*, number of setae located on each article of the extremities, excluding trichobothria on leg 1 (see 3.2.8.4).

	Coxa/ basal article	Art. 2/ fixed digit	Art. 3/ movable digit	Art. 4	Art. 5	Art. 6	Art. 7	Art. 8	Art. 9	Art. 10	Art. 11
Chelicera	6	6	-	n.a.	n.a.	n.a.	n.a.	n.a.	n.a.	n.a.	n.a.
Pedipalp	17	9	7	10	3	6	1	6	20	n.a.	n.a.
Leg 1	15	13	9	9	9	9	4	5	4	6	22
Leg 2	13	3	5	5	5	4	11	n.a.	n.a.	n.a.	n.a.
Leg 3	13	3	5	5	5	4	11	n.a.	n.a.	n.a.	n.a.
Leg 4	10	3	3	5	4	4	4	7	n.a.	n.a.	n.a.

Tab. 3. *Eukoenenia spelaea*, number of setae located on opisthosomal segments (S) 8–18. The number of setae on the genital plates are listed separately.

	S8	S9	S10	S11	S12	S13	S14	S15	S16	S17	S18
Tergite	-	8	12	12	12	12	14	12	10	8	8
Sternite	-	4	-	4	4	4	2	4	4	n.a.	n.a.
Genitalia ♀	n.a.	22	n.a.	n.a.	n.a.	n.a.	n.a.	n.a.	n.a.	n.a.	n.a.
Genitalia ♂	n.a.	32	n.a.	n.a.	n.a.	n.a.	n.a.	n.a.	n.a.	n.a.	n.a.

(Fig. 14A). In males, however, the base of the overhang is 5 µm wide and the distal part is evenly thin (diameter max. 1 µm; Fig. 14B). The segments of the metasoma, 15–18, evenly decrease in diameter (Fig. 8). Attached to the last segment is an additional sclerotized ring, which carries the flagellum (Fig. 16). The anus is located ventrally of the flagellar base on the last metasomal segment. The number of setae found on each segment, excluding the sex-specific number of setae on the genital plate, were consistent in all individuals (Tab. 4).

3.1.9   Opisthosomal sclerites

The tergites of the mesosomal segments expand far laterally (Figs. 6C, D). In segments 8 and 9, the tergites expand over the dorsal and lateral side of the opisthosoma. In segments 10–14, the tergites reach to the ventral side of the opisthosoma (Fig. 14C) and the sternite of these segments is reduced to a small medial sclerite. The segments of the metasoma, 15–18, carry a circular cuticular sclerite around the entire segment with no distinction between tergite and sternite (Figs. 6, 8).

On the ventral side of the mesosoma, the sternites differ between segments. The sternites are more distinct in males than in females. In both sexes, the cuticle of the sternites of segments 8–14 forms folds, which are particularly well developed on the lateral side of the sternite (Figs. 14C–E). The sternite of segment 8 covers the entire ventral side of the animal's body (Figs. 6C, D). The sternite of segment 9 also covers the entire ventral side. It does, however, carry the genital plate which gives it a unique morphology (see below; Fig. 15) and is firmly attached to the body. In segment 10, the sternite is restricted to the middle part of the ventral side (Fig. 6D). The anterior part of this sternite is also involved in building the genital plate, the rest of the sternite is shaped evenly. Sternites of segments 11–14 have the same shape as the posterior part of the sternite of segment 10. Each sternite between segments 10 to 14 is firmly attached to the body anteriorly and turns into an epidermal fold posteriorly. A groove emerges at the border of the fold of the tergite and the corresponding fold of the sternite. This groove is vaguely perceptible at the lateral overhang of the tergite (Fig. 6D).
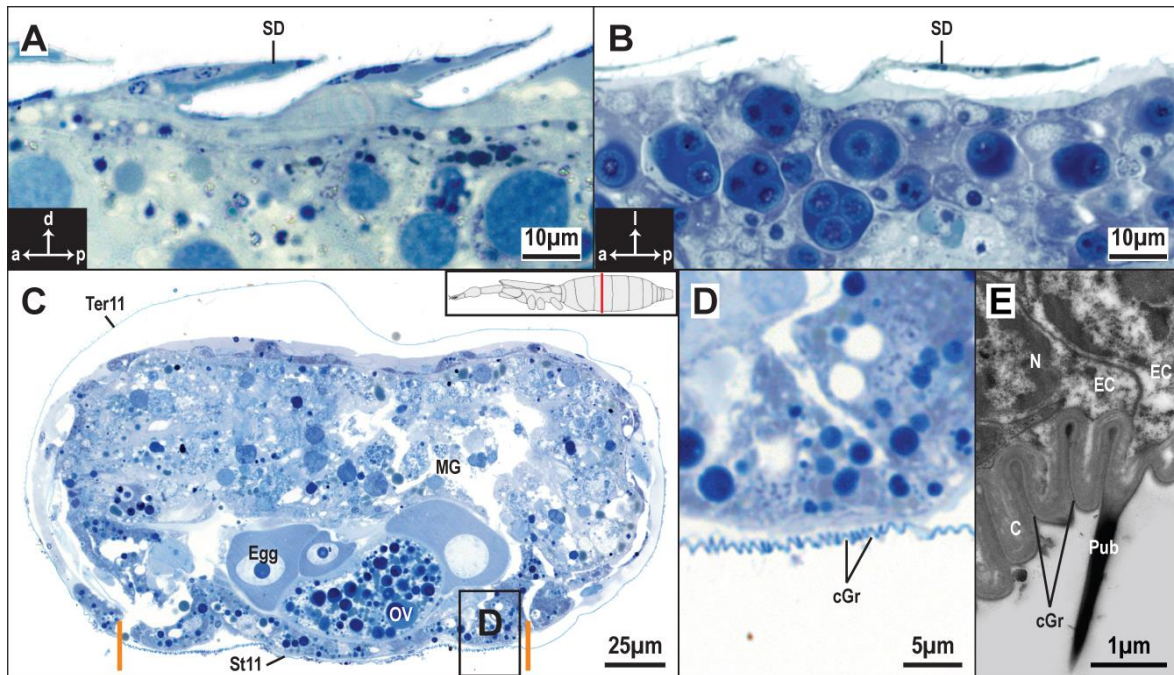
Fig. 14. *Eukoenenia spelaea*, structure of the cuticle. (**A**) Female, light micrograph of a sagittal section of the opisthosoma. Two segments are shown with their dorsal sclerites. The sclerites overlap broadly. The base of the sclerite duplicature is between 10 μm and 20 μm wide. The distal part of the duplicature is thicker in females than in males (see B). (**B**) Light micrograph of longitudinal section of the opisthosoma cuticle of a male. The base of the duplicature is approx. 5 μm wide. The distal part of the duplicature is max. 1 μm in thickness. (**C**) Light micrograph of a cross-section through segment 11 (inset). The ventral sclerite carries cuticular grooves laterally. Orange lines indicate the border of tergite and sternite. (**D**) High power light micrograph of the lateral region of the sternite from C. The cuticular grooves are clearly visible. (**E**) Transmission electron micrograph of cross-section of the same region as D. The cuticle in this area is thin compared to the neighboring areas. Abbreviations: a: anterior; C: cuticle; cGr: cuticular grooves; d: dorsal; EC: epidermal cell; l: left; MG: midgut; N: nucleus; OV: ovary; p: posterior; Pub: pubescence; SD: sclerite duplicature; St11: sternite of segment 11; Ter11: tergite of segment 11.

3.1.10 Genital segment

In females, the genital opening and the paired genital lobes originate anteriorly in segment 10 (GL, GO; Figs. 6C, D, 15A–C). These are almost entirely covered by the genital operculum which is formed by the sternite of segment 9. At its posterior end, the genital operculum shows an elongated extension, the sides of which arch upward to create a tube-like structure. The genital operculum carries 16 setae, the genital lobes carry three setae each (Figs. 15A–C; Tab. 3).

In males, three pairs of genital lobes mark the genital plate. Two pairs of genital lobes emerge from the central and the posterior part of segment 9. They are followed by one pair of genital lobes which originates at the anterior border of segment 10. The first pair of genital lobes originates from the center of segment 9. Each lobe has a broad base and two finger-like processes. At the tip of each process are two
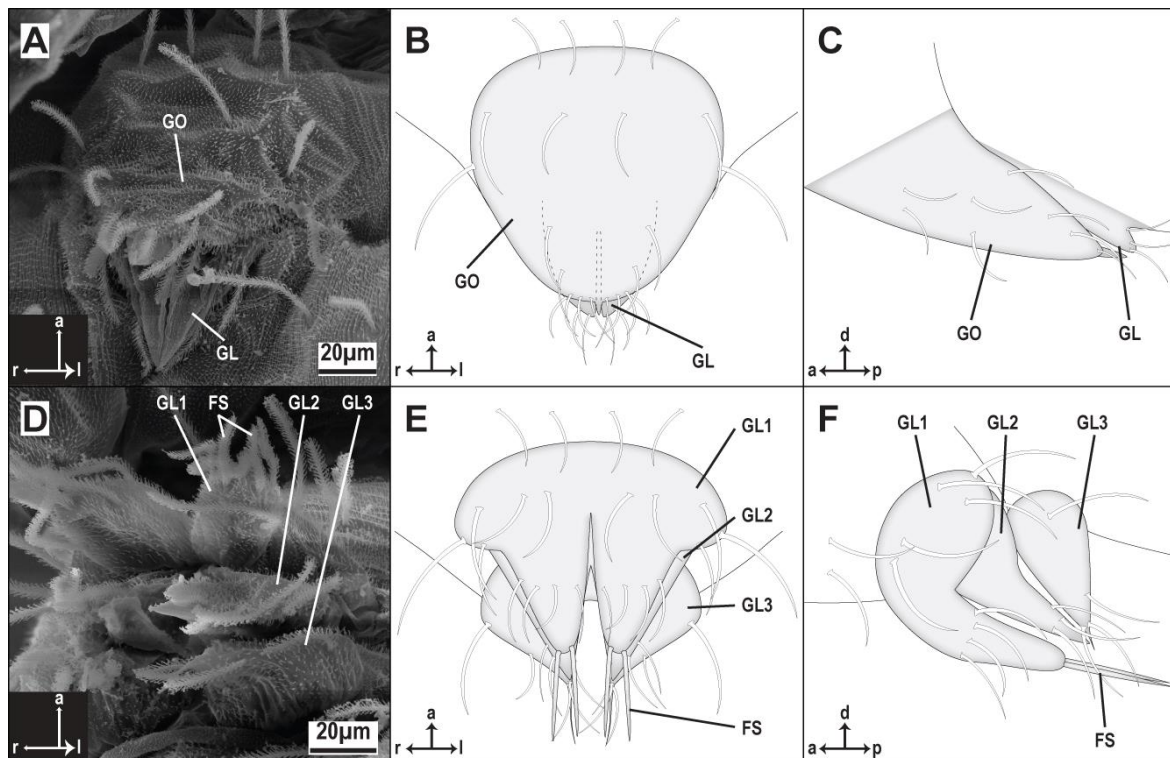
Fig. 15. *Eukoenenia spelaea*, genital structures. (**A**) Scanning electron micrograph of female genitalia in slightly oblique dorsal view. The genital operculum covers the genital lobes. (**B**) Schematic drawing of female genitalia in dorsal view. The extension of the genital operculum is elongated. (**C**) Schematic drawing of female genitalia in lateral view. The finger-like genital lobes originate at the junction of segments 9 and 10. (**D**) Scanning electron micrograph of male genitalia in dorsolateral view. The number of setae is larger in comparison to the female genitalia. (**E**) Schematic drawing of male genitalia in dorsal view. The base of the first pair of genital lobes is broadest compared to genital lobes 2 and 3. At the base, all genital lobes are closely together, at their tips, the lobes are spread farther apart. (**F**) Schematic drawing of male genitalia in lateral view. The first pair of genital lobes has a rounded tip, whereas lobes 2 and 3 are pointed. The paired fusules originate on genital lobe 1. These fusules extend posterior past genital lobe 3. Abbreviations: a: anterior; FS: fusules; GL: genital lobe; GO: genital operculum; l: left; r: right.

adjoining fusules (FS, GL1; Figs. 15D–F). The second pair of genital lobes, originates from the posterior part of segment 9, is located just posterior to the first pair of genital lobes and has triangular-shaped lobes (GL2; Figs. 15D–F). The third pair of genital lobes is similar in shape to the second pair, but ends in two needle-like processes (GL3; Figs. 15D–F). The tips of the lobes are in contact with the tips of the preceding lobes. A total of 32 setae are located on the genital lobes: 18 on the first pair, six on the second pair, and eight on the third pair (Figs. 15D–F; Tab. 3).

3.1.11 Flagellum

The flagellum is a long terminal attachment to the metasoma which is covered in flexible setae and inflexible spikes. It is an extremely delicate and fragile structure.

Only one intact flagellum was obtained from all analyzed specimens. It consists of 15 articles and has a total length of 1.40 mm (Fig. 6B). The flagellar base article is a sclerotized ring and is connected with segment 18 with a membranous fold which displays a knobbed surface (mF; Fig. 16). This base article carries four short setae (approx. 20 µm each) in a square arrangement. The other articles are similar to each other in shape but vary in size, the number of setae, and the number of spikes. The general number of setae and spikes decreases from proximal to distal (Tab. 4).

The setae are located posteriorly on each article. The spikes are located towards the apical end. The surface of the spikes is, in contrast to that of the setae, smooth. The length of a spike (approx. 30 µm) is about one sixth the length of a seta (approx. 200 µm; Fig. 6B, 7B).
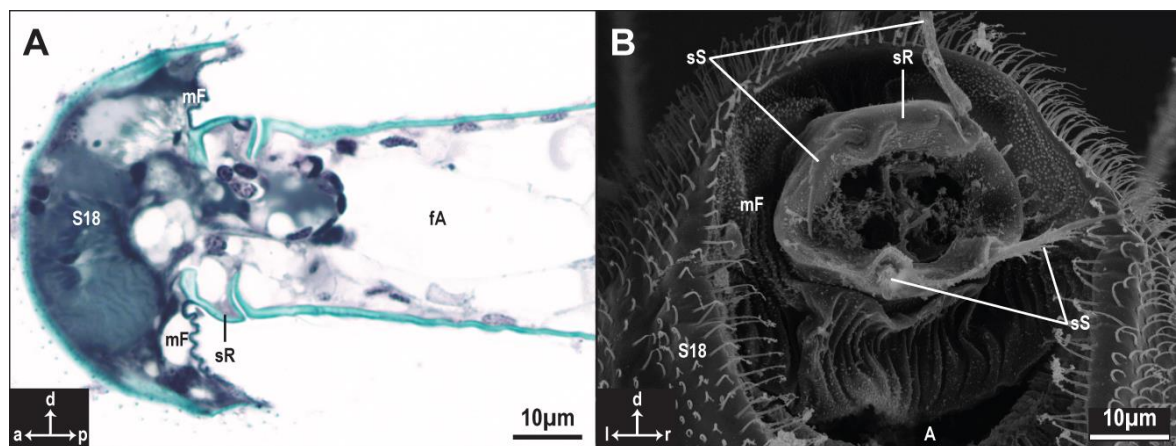
Fig. 16. *Eukoenenia spelaea*, structure of the terminal ring. (**A**) Light micrograph of longitudinal section through the terminal structures. The sclerotized ring is articulated with segment 18 and the following flagellar article. (**B**) Scanning electron micrograph of the sclerotized ring, viewed from posterior. The membranous fold between segment 18 and flagellar base lacks pubescence but shows a knobbed structure. The four short setae are arranged in a square. Abbreviations: a: anterior; A: anus; d: dorsal; fA: flagellar article; mF: membranous fold; l: left; p: posterior; r: right; S18: segment 18; sR: sclerotized ring; sS: short seta.

Tab. 4 *Eukoenenia spelaea*, number of setae and spikes located on each article of the flagellum.

	Art. 1	Art. 2	Art. 3	Art. 4	Art. 5	Art. 6	Art. 7	Art. 8	Art. 9	Art. 10	Art. 11	Art. 12	Art. 13	Art. 14
Setae	11	10	10	10	8	8	8	8	8	7	7	7	7	6
Spikes	14	14	14	-	13	-	13	-	12	-	-	-	-	-

3.2 Internal morphology

3.2.1 Epidermis

The epidermis of *Eukoenenia spelaea* is a typical single-layered squamous epithelium with elongated, heterochromatin-rich nuclei. The thickness of the epidermis varies throughout the body. In the tightly packed prosoma, the squamous cells can become very thin with a height of less than 1 µm. In these regions, the heterochromatin-rich nuclei of the epidermal cells appear flattened as well (Fig. 17A). The cytoplasm carries the cell organelles and glycogen granules.

The epidermal cells of the ventral plate, posterior to the rostrosoma, are highly modified. In light microscopy they appear as an evenly stained mass between the subesophageal ganglion and the body cuticle (sEC; Fig. 17B). These modified epidermal cells occupy the entire region of the ventral plate (Figs. 6C, 17B, D). Transmission electron microscopy reveals cellular polarity with the nuclei and mitochondria located basally (M, N; Fig. 17D). The basal part of the cells shows membranous invaginations, i.e. a basal labyrinth and displays glycogen granules. The apical border of the cells consists of numerous microvilli (MV; Fig. 17C). These microvilli extend into the cuticle, tightly connecting the epidermal cells with the overlaying cuticle. Cuticular pores associated with the microvilli were not found. The apical part of the specialized epidermal cells is almost completely free of glycogen granules. The cuticle in the region of the specialized epidermal cells displays smooth cuticular teeth. These cuticular teeth, which make up the ventral plate are part of the exocuticle and are covered by electron-dense epicuticle (EpC, ExC, VP; Fig. 17C).

3.2.2 Cuticle

The cuticle of *Eukoenenia spelaea*, like that of other arthropods, consists of two layers: the procuticle and the epicuticle (EpC, ProC; Fig. 18). The thickness of the procuticle is about 0.2 µm in the region of the epidermal fold of the opisthosoma (Fig. 14E) and 1.5 µm in the region of the prosomal sternites (Fig. 18E). The procuticle of the prosomal sternites and the ventral plate is stratified into an endo- and an exocuticle (EnC, ExC; Figs. 17D, 18E). The exocuticle is approx. 0.3 µm thick. Pore canals of different shape and size are found within the procuticle (PC; Fig. 18). The processes of the pubescence are built from procuticle and appear to

lack an epicuticle (Fig. 18C). In contrast to the procuticle, the epicuticle is uniform in thickness (0.01 µm) but differs in its electron density. While overall the epicuticle is electron-dense, it is electron-translucent in the esophagus (Fig. 39D), the frontal (Fig. 29B), and the lateral organ, as well as some regions of the opisthosoma (Figs. 18F).
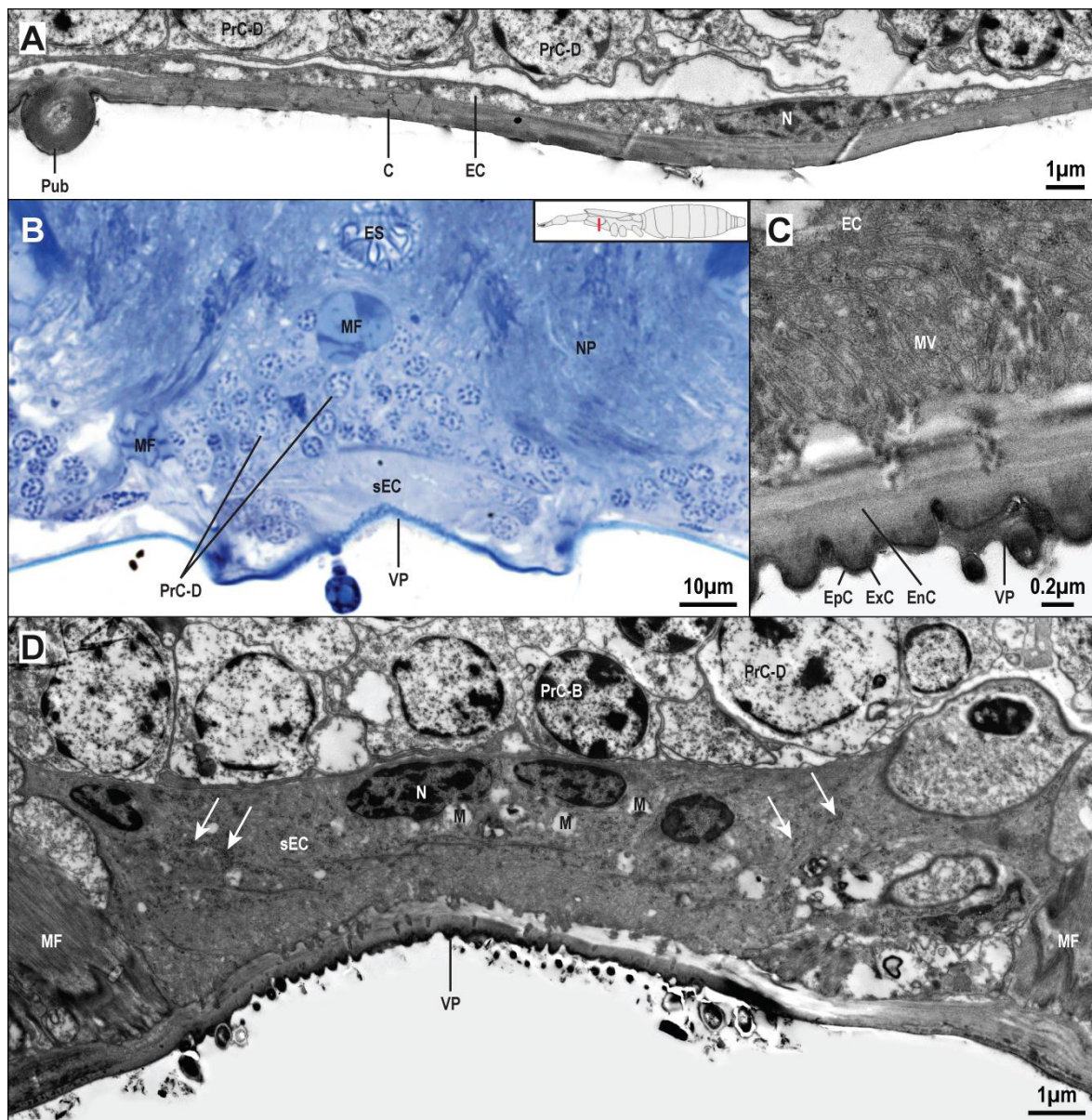
Fig. 17. *Eukoenenia spelaea*, epidermis. (**A**) Transmission electron micrograph of the cuticle and epidermis on the ventral side of the prosoma. The epidermal cell form a squamous epithelium with flattened nuclei. (**B**) Light micrograph of the ventral part of a cross-section through the prosoma at the level of the pedipalp. The epidermal cells under the ventral plate are specialized. (**C**) Transmission electron micrograph of the epidermis cells under the ventral plate showing microvilli that extend into the cuticle. (**D**) Transmission electron micrograph of the epidermis under the ventral plate. The nuclei and mitochondria are located basally in the cells, whereas the apical part carries microvilli. The basal part of the cells displays glycogen granules (arrows). Abbreviations: C: cuticle; EC: epidermal cell; EnC: endocuticle; EpC: epicuticle; ES: esophagus; ExC: exocuticle; M: mitochondria; MF: muscle fiber; MV: microvilli; N: nucleus; NP: neuropil; Pub: pubescence; sEC: specialized epidermal cell; VP: ventral plate.
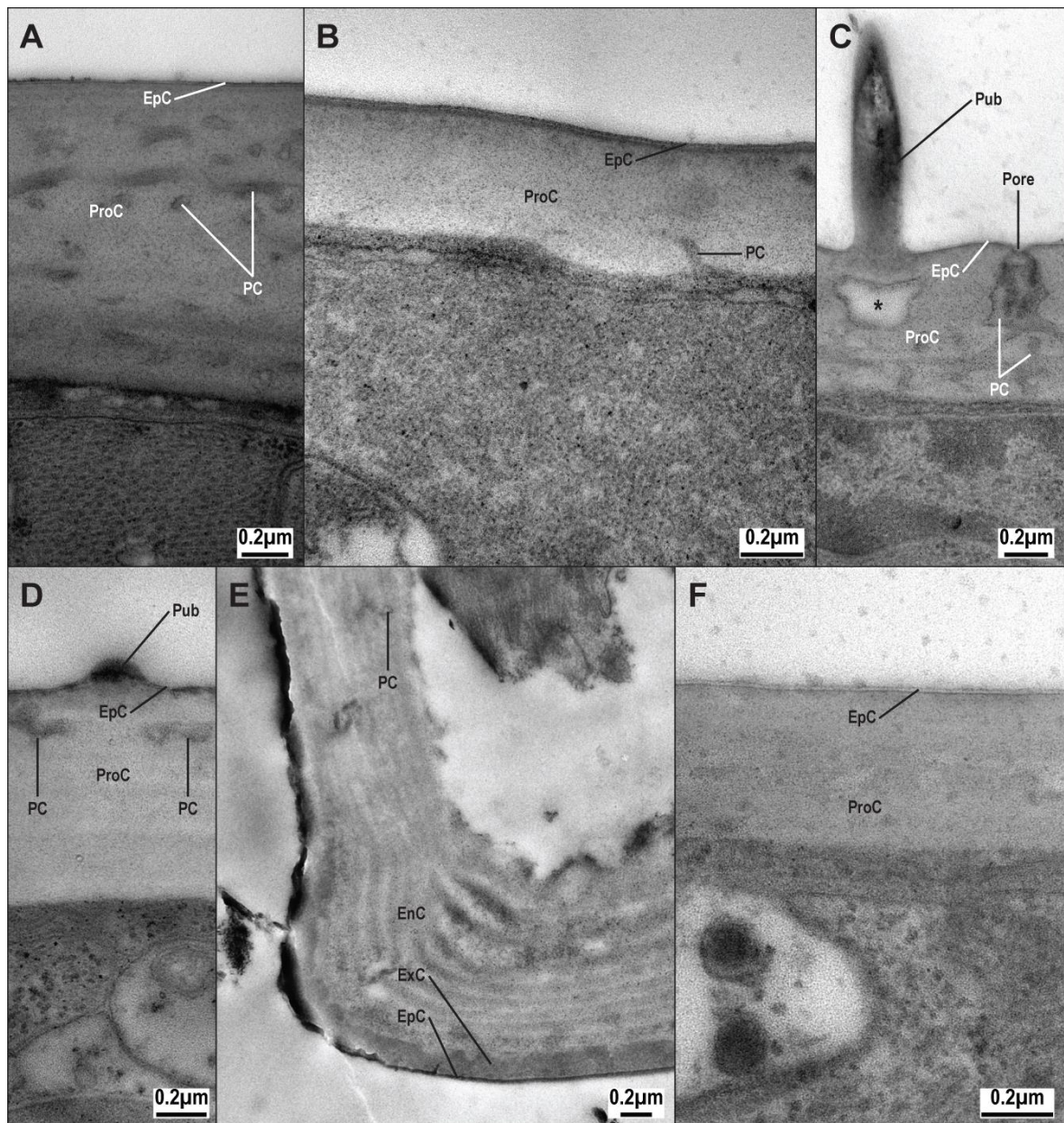
Fig. 18. *Eukoenenia spelaea*, transmission electron micrographs of the cuticle. (**A**) Cross-section of the basal article of the chelicera. The procuticle is rich in thin pore canals. (**B**) Cross-section of the rostrosoma. The electron-translucent procuticle appears single layered and has only few pore canals. The epicuticle appears electron-dense. (**C**) Cross-section of the propeltidium. The pore canals in the procuticle widen towards the surface of the cuticle and show electron-dense areas. The area below a process of the pubescence is electron-translucent and appears like a pocket (asterisk). The pubescence consists of electron-dense procuticle. (**D**) Cuticle of a leg. The procuticle shows few pore canals. The electron-dense epicuticle appears frayed. (**E**) Cuticle of prosomal sternite associated with leg 2. The layering of the procuticle in endo- and exocuticle is clearly visible. The endocuticle is multi-layered as well. The exocuticle is electron-denser than the endocuticle (**F**) Cuticle of the opisthosoma. The procuticle is approx. 0.4 μm thin. The epicuticle is electron-translucent. Abbreviations: EnC: endocuticle; EpC: epicuticle; ExC: exocuticle; PC: pore canal; ProC: procuticle; Pub: pubescence.

3.2.3 Endosternite

The endosternite lies in the center of the prosoma. It extends from the level of the 1st leg to the level of the 4th leg. The two lateral arms of the endosternite form a horizontal V in an anterior-posterior axis, with the opening towards anterior (EBr; Fig. 23A). In the level of the 2nd leg, the anterior transverse bridge connects both lateral arms of the endosternite (EaB; Fig. 23B). The lateral arms continue towards posterior to the posterior transverse bridge in the level of the 3rd leg (EpB; Fig. 23). The anterior and the posterior bridges are connected by a medial central bridge (EcB; Fig. 23A). Posterior to the level of the 3rd leg, the endosternite narrows and makes a concave bend towards ventral (EU; Fig. 23B). It then broadens into a stylized W in an anterior-posterior axis, with the opening towards posterior, before terminating in the last prosoma segment (EpS; Fig. 23A).

The endosternite is cellular (ESt; Fig. 19A). The endosternal cells are surrounded by an approx. 1.5 µm thick layer of extra-cellular granular matrix, similar to cartilage (Fig. 19D). This granular matrix is the point of attachment for a large number of muscles (see 3.2.5.3). These muscles are attached to the ECM with hemidesmosomes (arrows; Figs. 19B, D). The endosternite cells have a central heterochromatin-rich nucleus which is surrounded by the cytoplasmic compartment containing all other cellular organelles. The cytoplasm stains light in light microscopy and is electron-translucent in transmission electron microscopy (Figs. 19A, B). The rough endoplasmic reticulum does not form flattened cisternae but large tubular compartments filled with fine granules (Figs. 19B, C). Few glycogen granules and free ribosomes are also found in the cytoplasm.
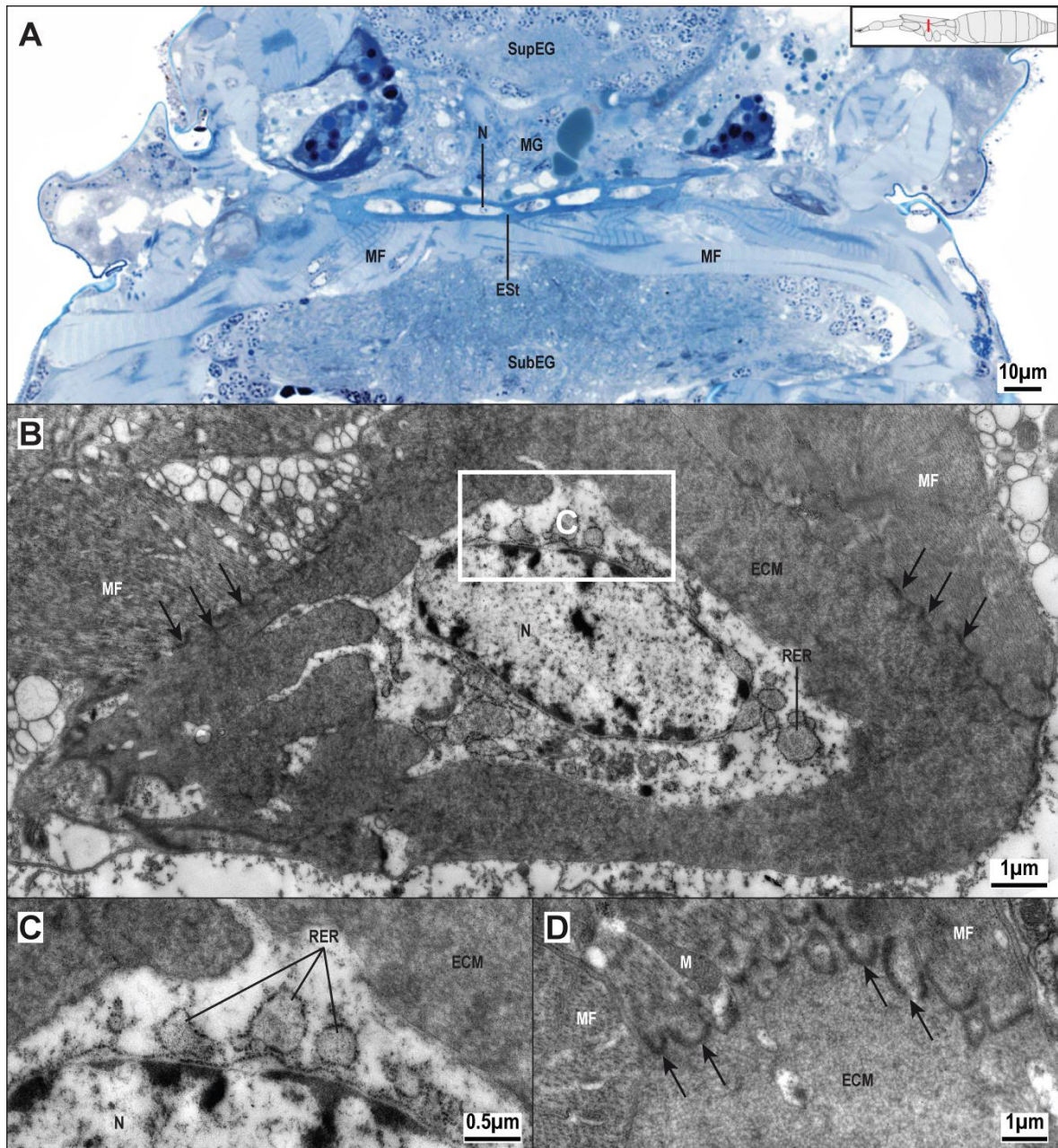
Fig. 19. *Eukoenenia spelaea*, endosternite. (**A**) Light micrograph of a cross-section of middle position at the level of the 2nd leg. The endosternite is cellular with its cells having a central nucleus, peripheral cytoplasm and substantial extracellular matrix around the cells. (**B**) Transmission electron micrograph of the endosternite. Cytoplasmic extensions of the endosternite cells extend into the ECM. Musculature attaches to the ECM by hemidesmosomes (arrows). (**C**) High power transmission electron micrograph of the rough endoplasmic reticulum surrounding the nucleus from B. The RER forms large tubular compartments instead of flattened cisternae. (**D**) Transmission electron micrograph of the endosternite's ECM. The muscles are attached with hemidesmosomes (arrows). The ECM has a granular character. Abbreviations: ECM: extra cellular matrix; ESt: endosternite; M: mitochondrion; MF: muscle fiber; MG: midgut; N: nucleus; RER: rough endoplasmic reticulum; SubEG: subesophageal ganglion; SupEG: supraesophageal ganglion.

33

3.2.4 Muscle ultrastructure

The somatic musculature of *Eukoenenia spelaea* is transversely striated and each fiber consists of several myofibrils (MF, MyF; Figs. 20A, B). The visceral musculature is the same muscle type but muscle fibers are small usually containing only a single myofibril (Fig. 20D). In the somatic muscles, the Z-line, A-band and I-band are clearly visible in longitudinal section (A, J, Z; Fig. 20B). Laterally, the sarcolemma displays indentations which correspond with the Z-line (S, arrowheads; Fig. 20B). These indentations represent probably the T-tubular system. The sarcoplasmic reticulum is well developed (SR; Fig. 20C). Both components, the T-tubular system and the sarcoplasmic reticulum, form diads throughout the muscle
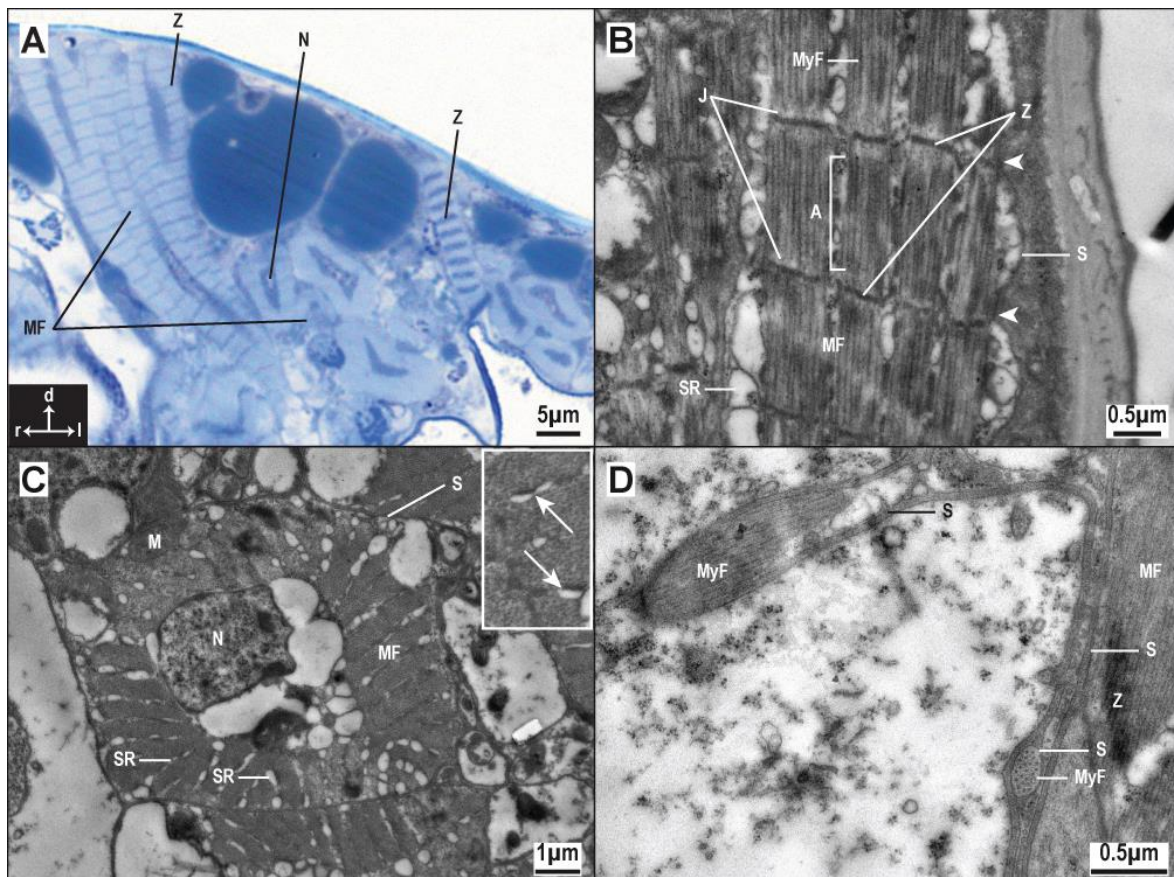
Fig. 20. *Eukoenenia spelaea*, musculature. (**A**) Cross-section of prosoma, light microscopy. Striated muscles fibers (C1 and L1) are arranged in a bundle, the nuclei are located centrally. The Z-lines are clearly visible. (**B**) Prosomal muscle fiber, transmission electron micrograph. The Z-lines as well as the A-band and I-band are also clearly visible. H-Zone and M-line are not discernible within the A-band. The lateral indentations of the sarcolemma (arrowheads) possibly belong to the T-tubular system. (**C**) Prosomal muscle fiber, transmission electron micrograph. The sarcoplasmic reticulum (SR) displays narrow as well as widened areas. The nucleus is located in the center. The T-tubular system together with the SR form diads throughout the muscle (inset, arrows). (**D**) Visceral muscle of the midgut, transmission electron micrograph. The muscles are delicate in comparison with the somatic muscles. Abbreviations: A: A-band, d: dorsal; J: I-band; l: left; M: mitochondrion; MF: muscle fiber; MyF: myofibril; N: nucleus; r: right, S: sarcolemma; SR: sarcoplasmic reticulum; Z: Z-line.

fiber. The nuclei of the striated muscle fibers are located centrally and surrounded by a perinuclear cytoplasmic compartment that contains all cellular organelles. Mitochondria, however, are located throughout the muscle fibers (M; Fig. 20C). The prosoma has prominent musculature associated with the endosternite and the body wall as well as musculature in the legs (Figs. 21–23; Tab. 5). The musculature of the opisthosoma is less prominently developed than in the prosoma (Figs. 21, 22).

3.2.5 Musculature of the prosoma

The description of the musculature of the prosoma follows major topographic relationships, i.e. muscles of the extremities, muscles of the body wall, and muscles associated with the endosternite. This formal distinction is for descriptive purpose and does not intend any functional interpretation. Detailed descriptions with points of origin and insertion for each muscle are given in table 5. Possible antagonists are described according to the topography of their origin and insertion points.

Tab. 5. *Eukoenenia spelaea*, list of musculature. Each muscle or muscle branch is listed with its points of origin and insertion. When two or more points of origin are listed, two or more branches originate and fuse into one strand. When two or more points of insertion are listed, the muscle branches. Within extremities, the term "proximal" is used to describe the location of origin/insertion of a muscle oriented toward the body, "distal" is used for the location away from the body. This terminology is used for the entire extremities as well as their separate articles. Muscles associated with the box-truss axial muscle system (Shultz 2001, 2007b) are marked grey. Abbreviations: C1–13: cheliceral muscle; D1–2: dorsal muscle; DV1–5: dorsoventral muscle; E1–20: endosternite muscle; F1–3: flagellar muscle; Gf: genital muscle female; Gm1–4: genital muscle male; JI1–4: intersegmental muscle 1; JII1–6: intersegmental muscle 2; JIII1–6: intersegmental muscle 3; JIV1–6: intersegmental muscle 4; JV1–6: intersegmental muscle 5; JVI1–5: intersegmental muscle 6; JVII1–4: intersegmental muscle 7; JVIII1–3: intersegmental muscle 8; JIX1–2: intersegmental muscle 9; LI1–14t: leg 1 muscle/tendon; LII1–9: leg 2 muscle; LIII1–10t: leg 3 muscle; LIV1–14: leg 4 muscle; P1–13: prosomal muscle; PP1–10t: pedipalps muscle/tendon; TI1–2: transversal muscle 1; TII1–2: transversal muscle 2; TIII1–2: transversal muscle 3; TIV1–2: transversal muscle 4; TV1–2: transversal muscle 5; TVI1: transversal muscle 6; V: ventral muscle.

Muscle	Origin	Insertion	Fig.
	Extremities: Cheliceral muscles		
C1	propeltidium, dorsolateral above the prosternum, lateral to C4, *extrinsic muscle*	ventrolateral at the base of the chelicera, where chelicera articulates with prosoma	21B, 22A
C2	anteroventral, between insertion of C1 and C3, where chelicera articulates with prosoma	posterolateral in cheliceral basal article, just posterior to C7	21A, 22A
C3	propeltidium, anterodorsal and medial, splits in two strands that extend to each chelicera, *extrinsic muscle*	ventrolateral and proximal, where chelicera articulates with prosoma	21B, 22A
C4	propeltidium, dorsolateral at posterior end, *extrinsic muscle*	dorsomedial and proximal, where chelicera articulates with prosoma, adjacent to C5	21B, 22A

Tab. 5 continued

Muscle	Origin	Insertion	Fig.
C5	cheliceral basal article, dorsomedial and proximal, where chelicera articulates with prosoma	ventrolateral and immediately proximal to the joint connecting cheliceral base with chela	21A, 22A
C6	lateral and proximal in cheliceral basal article, where chelicera articulates with prosoma	ventrolateral and proximal, where cheliceral base articulates with chela, opposite C5	21A, 22A
C7	ventrolateral and proximal in cheliceral basal article, where chelicera articulates with prosoma	same as C5	21A, 22A
C8	dorsal and distal in cheliceral basal article, starts as two strands which join ventral	same as C5	21A, 22A
C9	ventrolateral from cheliceral base, immediately proximal to the joint connecting cheliceral base and chela	as tendon, in the center of the dorsoventral axis, immediately proximal to the joint connecting fixed digit and movable digit	21A
C10	ventrolateral and immediately proximal to the joint connecting cheliceral base and chela	same as C9	21A, 22A
C11	dorsolateral and immediately proximal to the joint connecting cheliceral base and chela	same as C9	21A
C12	dorsolateral and immediately proximal to the joint connecting cheliceral base and chela	same as C9	21A, 22A
C13	dorsal, immediately proximal to the joint connecting cheliceral base and chela	same as C9	21A, 22A
	Muscles of the pedipalp		
PP1	propeltidium, posterodorsal to C3, posterolateral to C4, *extrinsic muscle*	dorsomedial and proximal on coxa	21B, 22A
PP2	medioproximal, immediately distal to where coxa articulates with prosoma	dorsomedial, immediately distal to the joint connecting coxa and article 2	21A, 22C
PP3	posteroventral, immediately distal to the joint connecting coxa and article 2, splits in two branches just prior to end	posterior, immediately distal to the joint connecting article 2 and 3	21A, 22C
		anterior, immediately distal to the joint connecting article 2 and 3	21A, 22C
PP4	dorsal, in the center of the anterior-posterior axis, and distal in article 2, splits in four branches in the center of the anterior-posterior axis in article 3	posterodorsal, immediately distal to the joint connecting article 3 and 4	21A, 22C
		anterodorsal, immediately distal to the joint connecting article 3 and 5	21A, 22C
		as tendon ventral and in the center of the anterior-posterior axis, immediately distal to the joint connecting article 3 and 4	21A, 22C
		ventral and in the center of the anterior-posterior axis, immediately distal to the joint connecting article 4 and 5	21A, 22C
PP5	dorsal, in the center of the anterior-posterior axis, and distal in article 4	ventral and in the center of the anterior-posterior axis, immediately proximal to the joint connecting article 6 and 7	21A, 22C
PP6t	as tendon ventral, immediately distal to the joint connecting article 4 and 5	dorsal and in the center of the anterior-posterior axis, immediately distal to the joint connecting article 5 and 6	21A, 22C

36

Tab. 5 continued

Muscle	Origin	Insertion	Fig.
PP7t	as tendon ventral, immediately distal to the joint connecting article 5 and 6	ventral and in the center of the anterior-posterior axis, immediately distal to the joint connecting article 6 and 7	21A, 22C
PP8t	as tendon ventral and in the center of the anterior-posterior axis, immediately distal to the joint connecting article 6 and 7	ventral and in the center of the anterior-posterior axis, immediately distal to the joint connecting article 7 and 8	21A, 22C
PP9t	as tendon ventral and in the center of the anterior-posterior axis, immediately distal to the joint connecting article 7 and 8	ventral and in the center of the anterior-posterior axis, immediately distal to the joint connecting article 8 and 9	21A, 22C
PP10t	as tendon ventral and in the center of the anterior-posterior axis, immediately distal to the joint connecting article 8 and 9	ventral and in the center of the anterior-posterior axis at tarsal claw	21A, 22C
	Leg 1		
LI1	propeltidium, dorsolateral and between C1 and PP1, *extrinsic muscle*	dorsomedial and proximal on coxa	21B, 22A
LI2	lateral on anterior transverse bridge of endosternite in segment 5, *extrinsic muscle*	in the center of the proximal-distal axis and anterior in coxa	21A, 22B
LI3	laterodistal, immediately distal to where coxa articulates with prosoma	posteroventral and proximal in article 2	21A, 22C
LI4	dorsal and in the center of the anterior-posterior axis, immediately distal to the joint connecting coxa and article 2, splits in two branches in the center of the anterior-posterior axis in article 2	posterior, immediately distal to the joint connecting article 2 and 3	21A, 22C
		anterior, immediately distal to the joint connecting article 3 and 4	21A, 22C
LI5	posterior, immediately distal to the joint connecting article 3 and 4	posterior, immediately distal to the joint connecting article 4 and 5	21A, 22C
LI6	dorsal and in the center of the anterior-posterior axis, immediately distal to the joint connecting article 2 and 3	as tendon anteroventral, immediately distal to the joint connecting article 5 and 6	21A, 22C
	posterodorsal and proximal in article 3		
	anterodorsal and proximal in article 3		
LI7	posterolateral, immediately distal to the joint connecting article 4 and 5	posteroventral, immediately distal to the joint connecting article 5 and 6	21A, 22C
		as tendon ventral and in the center of the anterior-posterior axis, immediately distal to the joint connecting article 5 and 6	21A, 22C
LI8	dorsal and in the center of the anterior-posterior axis in article 5	ventral and in the center of the anterior-posterior axis, immediately proximal to the joint connecting article 6 and 7	21A, 22C
LI9t	as tendon ventral and in the center of the anterior-posterior axis, immediately proximal to the joint connecting article 5 and 6	as tendon ventral and in the center of the anterior-posterior axis, immediately distal to the joint connecting article 6 and 7	21A, 22C
LI10t	as tendon ventral and in the center of the anterior-posterior axis, immediately proximal to the joint connecting article 6 and 7	as tendon anteroventral, immediately distal to the joint connecting article 7 and 8	21A, 22C

Tab. 5 continued

Muscle	Origin	Insertion	Fig.
LI11t	as tendon anteroventral, immediately distal to the joint connecting article 7 and 8	as tendon anteroventral, immediately distal to the joint connecting article 8 and 9	21A, 22C
LI12t	as tendon anteroventral, immediately distal to the joint connecting article 8 and 9	as tendon ventral and in the center of the anterior-posterior axis, immediately distal to the joint connecting article 9 and 10	21A, 22C
LI13t	as tendon ventral and in the center of the anterior-posterior axis, immediately distal to the joint connecting article 9 and 10	as tendon ventral and in the center of the anterior-posterior axis, immediately distal to the joint connecting article 10 and 11	21A, 22C
LI14t	as tendon ventral and in the center of the anterior-posterior axis, immediately distal to the joint connecting article 10 and 11	in the center of the anterior-posterior axis at tarsal claw	21A, 22C
	Leg 2		
LII1	propeltidium, dorsolateral, posterior to P6, splits in two branches medial, *extrinsic muscle*	dorsal and in the center of the anterior-posterior axis on coxa, thicker	21B, 22B
		lateral at pleural membrane between leg 2 and leg 3, thinner	21B, 22B
LII2	medial on anterior transverse bridge and central bridge of endosternite in the region of leg 2 and 3, splits in two branches medial, *extrinsic muscle*	posterior, immediately proximal to the joint connecting coxa and article 2, thinner	21A, 22B
		posterior in coxa, thicker	21A, 22B
LII3	in the center of the anterior-posterior axis, immediately distal to where coxa articulates with prosoma	dorsal and in the center of the anterior-posterior axis, immediately distal to the joint connecting coxa and article 2	21A, 22C
	in the center of the proximal-distal axis and anterior in coxa		
LII4	anterodorsal, immediately distal to the joint connecting coxa and article 2	anterodorsal and proximal in article 2	21A, 22C
LII5	ventral and in the center of the anterior-posterior axis, immediately distal to the joint connecting coxa and article 2, splits in two branches in the center of the anterior-posterior axis in article 3	posterior, immediately distal to the joint connecting article 3 and 4	21A, 22C
		posterodorsal and proximal in article 5	21A, 22C
LII6	dorsal and in the center of the anterior-posterior axis, immediately distal to the joint connecting article 2 and 3	posterodorsal and proximal in article 4	21A, 22C
LII7	dorsal, in the center of the anterior-posterior axis and distal in article 3	ventral and in the center of the anterior-posterior axis, immediately proximal to the joint connecting article 5 and 6	21A, 22C
LII8	posterodorsal, immediately distal to the joint connecting article 4 and 5	ventral and in the center of the anterior-posterior axis, immediately distal to the joint connecting article 5 and 6	21A, 22C
LII9	dorsal, in the center of the anterior-posterior axis and distal in article 5	in the center of the anterior-posterior axis at tarsal claw	21A, 22C
	Leg 3		
LIII1	propeltidium, dorsomedial, above anterior bridge of endosternite in the region of leg 3, *extrinsic muscle*	posterodorsal and in center of the proximal-distal axis in coxa	21A, 22B

Tab. 5 continued

Muscle	Origin	Insertion	Fig.
LIII2	at central bridge, medial at posterior bridge, and at upturned U section of endosternite in the region of leg 3 and 4, splits in two branches medial, *extrinsic muscle*	posterior, immediately proximal to the joint connecting coxa and article 2, thinner	21A, 22B
		posterior in coxa, thicker	21A, 22B
LIII3	in the center of the anterior-posterior axis, immediately distal to where coxa articulates with prosoma	dorsal and in the center of the anterior-posterior axis, immediately distal to the joint connecting coxa and article 2	21A, 22C
	in the center of the proximal-distal axis and anterior in coxa		
LIII4	posterodorsal, immediately distal to the joint connecting coxa and article 2	posterodorsal and proximal in article 3	21A, 22C
LIII5	ventral and in the center of the anterior-posterior axis, immediately distal to the joint connecting coxa and article 2	ventral and in the center of the anterior-posterior axis, immediately distal to the joint connecting article 3 and 4	21A, 22C
LIII6	anterodorsal and distal in article 2	posterodorsal, immediately proximal to the joint connecting article 3 and 4	21A, 22C
LIII7	anteroventral and distal in article 2	anteroventral, immediately proximal to the joint connecting article 3 and 4	21A, 22C
LIII8	dorsal, in the center of the anterior-posterior axis, and distal in article 3	ventral and in the center of the anterior-posterior axis, immediately proximal to the joint connecting article 5 and 6	21A, 22C
LIII9	anterodorsal and distal in article 4	anterior, immediately proximal to the joint connecting article 5 and 6	21A, 22C
LIII10	dorsal, in the center of the anterior-posterior axis, and distal in article 5	in the center of the anterior-posterior axis at tarsal claw	21A, 22C
Leg 4			
LIV1	ventrolateral at posterior section of endosternite in the region of leg 4, splits in two branches just after origin, *extrinsic muscle*	lateral at pleural membrane between first articles of leg 3 and 4	21A, 22B
		posterior in coxa, adjacent to LIV3	21A, 22B
LIV2	ventrolateral and posterior to LIV1 at endosternite in the region of leg 4, *extrinsic muscle*	in the center of the anterior-posterior axis between LIV4 and LIV5, fuses with LIV4 and LIV5	21A, 22B
LIV3	ventromedial of LIV2 at endosternite in the region of leg 4, *extrinsic muscle*	posterior in coxa, adjacent to LIV1	21A, 22B
LIV4	anterodorsal, immediately distal to where coxa articulates with prosoma	dorsal and in the center of the anterior-posterior axis, immediately distal to the joint connecting coxa and article 2	21A, 22C
LIV5	ventral and in the center of the anterior-posterior axis, immediately distal to where coxa articulates with prosoma	ventral, in the center of the anterior-posterior, and proximal axis in article 2	21A, 22C
LIV6	dorsal and in the center of the anterior-posterior axis, immediately distal to the joint connecting coxa and article 2	anterodorsal, immediately proximal to the joint connecting article 2 and 3	21A, 22C
LIV7	posteroventral and distal in article 2	posterior in article 3	21A, 22C
LIV8	anteroventral and distal in article 2	anterodorsal, immediately proximal to the joint connecting article 3 and 4	21A, 22C

Tab. 5 continued

Muscle		Origin	Insertion	Fig.
LIV9		posteroventral and distal in article 3	posterior, immediately proximal to the joint connecting article 4 and 5	21A, 22C
		posterior and proximal in article 4		
LIV10		ventral, in the center of the anterior-posterior axis, and distal in article 3	anterior, immediately proximal to the joint connecting article 4 and 5	21A, 22C
LIV11		posteroventral, immediately distal to the joint connecting article 4 and 5	posterior, immediately distal to the joint connecting article 5 and 6	21A, 22C
LIV12		dorsal, in the center of the anterior-posterior axis, and distal in article 4	dorsal and in the center of the anterior-posterior axis, immediately proximal to the joint connecting article 5 and 6	21A, 22C
LIV13		anterior, immediately distal to the joint connecting article 4 and 5	anterior, immediately distal to the joint connecting article 5 and 6	21A, 22C
LIV14		anteroventral and distal in article 5	ventral and in the center of the anterior-posterior axis at tarsal claw	21A, 22C
Prosomal body wall:				
P1	unpaired	anteromedial in functional upper lip of rostrosoma	dorsomedial in functional upper lip of rostrosoma, just anterior to mouth opening	21B, 22A
P2	paired	anterolateral in functional upper lip of rostrosoma	dorsolateral in functional upper lip of rostrosoma, just anterior to mouth opening	21B, 22A
P3	unpaired	dorsal on pharynx	dorsomedial at intercheliceral sclerite	21B, 22A
P4	paired	lateral on pharynx	ventrolateral in rostrosoma	21B, 22A
P5	paired	propeltidium, ventrolateral and anterior, in the region of the chelicerae	propeltidium, anterolateral, in the region of the chelicerae	21B, 22B
P6	paired	propeltidium, dorsolateral, in the region of leg 1, between C1 and LII1	lateral at pleural membrane between coxa of leg 1 and 2, dorsal to E7	21B, 22A
P7	paired	propeltidium, dorsolateral, in the region of leg 2, between LII1 and P8	lateral at pleural membrane and in the center of the anterior-posterior axis in the region of leg 3	21B, 22A
P8	paired	propeltidium, dorsolateral, in the region of leg 2, posterior to P7	lateral at pleural membrane and in the center of the anterior-posterior axis in the region of leg 3, anteroventral to P7	21B, 22A
P9	paired	parapeltidium, dorsolateral and posterior in the region of leg 3, between both branches of P11	parapeltidium, dorsal in the region of leg 2	21B, 22A
P10	paired	propeltidium, dorsolateral and posterior in the region of leg 2, outside of P11	anterolateral at pleural membrane in the region of leg 4	21B, 22A
P11	paired	FEMALE: propeltidium, dorsomedial in the region of leg 1, splits in two branches posterior	metapeltidium, dorsal and in the center of the anterior-posterior axis in the region of leg 3, thicker	21C, 22A
			posterolateral at pleural membrane in the region of leg 3, posterodorsal to LIII1, thinner	21C, 22A
	paired	MALE: propeltidium, dorsomedial in the region of leg 2, splits in two branches medial	metapeltidium, dorsal and in the center of the anterior-posterior axis in the region of leg 3, thicker	21B, 22B
			posterolateral at pleural membrane in the region of leg 3, posterodorsal to LIII1, thinner	21B, 22B

Tab. 5 continued

Muscle		Origin	Insertion	Fig.
P12	unpaired	FEMALE: metapeltidium, medial and in the center of the anterior-posterior axis in the region of leg 3	metapeltidium, medial and in the center of the anterior-posterior axis in the region of leg 4	21C, 22A
	paired	MALE: metapeltidium, dorsomedial and in the center of the anterior-posterior axis in the region of leg 3	dorsolateral at tergite and in the center of the anterior-posterior axis in segment 8	21B, 22B
P13	paired	metapeltidium, posterolateral in the region of leg 3	metapeltidium, lateral and in the center of the anterior-posterior axis in the region of leg 4	21B, 22A
		Endosternite:		
E1	paired	ventral at branch of endosternite in the region of pedipalp and leg 1, splits in two branches just after origin	ventromedial at intersegmental membrane and in the center of the anterior-posterior axis in the region of the pedipalp, lateral to ventral plate	23
			prosternum, ventromedial and in the center of the anterior-posterior axis in the region of leg 1, posterior to first branch	23
E2	paired	anterior at branch of endosternite in the region of pedipalp and leg 1	ventrolateral at pleural membrane adjacent to coxa of pedipalp	23
E3	paired	anterodorsal at branch of endosternite in the region of leg 1, just posterior to E1, splits into three branches just after origin	propeltidium, dorsolateral in the region of leg 1	23
			propeltidium, dorsolateral in the region of leg 1, posterior to first branch	23
			propeltidium, dorsolateral in the region of leg 1, posterior to second branch	23
E4	paired	anterodorsal at branch of endosternite in the region of leg 1, just posterior to E3	propeltidium, dorsolateral and posterior in the region of leg 2	23
E5	paired	anterodorsal at branch of endosternite in the region of leg 1, just posterior to E4	propeltidium, dorsolateral and anterior in the region of leg 2	23
E6	paired	anterodorsal at branch of endosternite in the region of leg 1, just posterior to E5	anterodorsal at pleural membrane, where chelicera articulates with prosoma	23
E7	paired	ventral at branch of endosternite in the region of leg 2	ventrolateral at pleural membrane between coxa of leg 1 and 2, ventral to P6	23
E8	unpaired	ventromedial at bridge of endosternite in the region of leg 2	posteroventral and medial on pharynx	23
E9	paired	ventromedial at bridge of endosternite in the region of leg 2, posterior to E8	ventrolateral at pleural membrane, just posterior where leg 1 articulates with prosoma	23
E10	paired	dorsolateral and in the center of the anterior-posterior axis on anterior bridge of endosternite in the region of leg 2	posterolateral at pleural membrane in the region of leg 2	23
E11	paired	dorsolateral and posterior on anterior bridge of endosternite in the region of leg 3	propeltidium, dorsolateral and posterior in the region of leg 3	23
E12	paired	dorsolateral and posterior on anterior bridge of endosternite in the region of leg 3, outside of E11	metapeltidium, dorsolateral in the region of leg 4, adjacent to E14 and E16	23
E13	paired	lateral at branch of endosternite in the region of leg 3, posterior to E12	ventral at tergite, at the border of segments 8 and 9, immediately anterior to origin of V	23

Tab. 5 continued

Muscle		Origin	Insertion	Fig.
E14	paired	dorsolateral and in the center of the anterior-posterior axis on posterior bridge of endosternite in the region of leg 3	propeltidium, dorsolateral and posterior in the region of leg 3, just anteromedial of E11	23
E15	paired	dorsolateral and posterior on posterior bridge of endosternite in the region of leg 3, posterior to E13	metapeltidium, dorsolateral, in the region of leg 4, adjacent to E12 and E16	23
E16	paired	posterolateral on upturned U section of endosternite in the region of leg 4	anterolateral at pleural membrane in the region of leg 4	23
E17	paired	dorsolateral at posterior section of endosternite in the region of leg 4, two branches merge just after origin	metapeltidium, dorsolateral, in the region of leg 4, adjacent to E12 and E14	23
E18	paired	lateral at posterior section of endosternite in the region of leg 4, ventral to E16	Lateral at pleural membrane, where leg 4 articulates with prosoma	23
E19	paired	ventrolateral and posterior at posterior section of endosternite in the region of leg 4	anterolateral at pleural membrane, where leg 4 articulates with prosoma, between E15 and E17	23
E20	paired	posterolateral at posterior section of endosternite in the region of leg 4, just posterior to E18	lateral at pleural membrane and in the center of the anterior-posterior axis in segment 8	23
Opisthosoma:				
D1	paired	metapeltidium, dorsolateral and anterior in the region of leg 4	dorsal at tergite of segment 9, just medial of D2	21C, 22B
D2	paired	dorsal at the anterior end of the tergite of segment 9	dorsal at tergite of segment 17, immediately posterior to the border of segments 16 and 17	21C, 22B
DV1	paired	FEMALE: anterodorsal at tergite of segment 9, lateral to D1	anteroventral at sternite of segment 9, just medial of V	21A, 22A
		MALE: anterodorsal at tergite of segment 9, outside of D1	anteroventral at sternite of segment 9, just medial of V	21B, 22B
		MALE: posterodorsal to the segmental overhang of segment 9		
DV2	paired	FEMALE: anterodorsal at tergite of segment 10, between D2 and JII1	anteroventral at sternite of segment 10, just posterior to genital lobe and medial of V	21A, 22A
		MALE: anterodorsal at tergite of segment 10, between D2 and JII1, splits in two branches ventral	dorsolateral at genital atrium	21B, 22B
			anteroventral at sternite of segment 10, just posterior to genital lobe 3 and medial of V	21B, 22B
DV3–4	paired	anterodorsal at tergite of segments 11 and 12, between D2 and JIII1 and JIV1, respectively	anteroventral at sternite of segments 11 and 12, just medial of V	21A, B, 22B
DV5	paired	anterodorsal at tergite of segment 13, between D2 and JV1, splits in two branches at half point	anteroventral at sternite of segment 13, just medial of V, thicker	21A, B, 22B
			ventral and in the center of the anterior-posterior axis at sternite of segment 13, just medial of V, thinner	21A, B, 22B
JI1–4	paired	anterior at tergite of segment 9, outside of D1, strands 1–4 evenly distributed from dorsal to ventrolateral	in the center of the anterior-posterior axis at tergite of segment 9, outside of D2, strands 1–4 evenly distributed from dorsal to ventrolateral	21C, 22A
JII1–6	paired	in the center of the anterior-posterior axis at tergite of segment 9, posterior to JI and outside of D2, strands 1–6 evenly distributed from dorsal to ventrolateral	anterior at tergite of segment 10, outside of D2, strands 1–6 evenly distributed from dorsal to ventrolateral	21C, 22A

Tab. 5 continued

Muscle		Origin	Insertion	Fig.
JIII1–6	paired	posterior at tergite of segment 10, posterior to JII and outside of D2, strands 1–6 evenly distributed from dorsal to ventrolateral	anterior at tergite of segment 11, outside of D2, strands 1–6 evenly distributed from dorsal to ventrolateral	21C, 22A
JIV1–6	paired	posterior at tergite of segment 11, posterior to JIII and outside of D2, strands 1–6 evenly distributed from dorsal to ventrolateral	anterior at tergite of segment 12, outside of D2, strands 1–6 evenly distributed from dorsal to ventrolateral	21C, 22A
JV1–6	paired	posterior at tergite of segment 12, posterior to JIV and outside of D2, strands 1–6 evenly distributed from dorsal to ventrolateral	anterior at tergite of segment 13, outside of D2, strands 1–6 evenly distributed from dorsal to ventrolateral	21C, 22B
JVI1–5	paired	posterior at tergite of segment 13, posterior to JV and outside of D2, strands 1–5 evenly distributed from dorsal to ventrolateral	anterior at tergite of segment 14, outside of D2, strands 1–5 evenly distributed from dorsal to ventrolateral	21C, 22A
JVII1–4	paired	posterior at tergite of segment 14, posterior to JVI and outside of D2, strands 1–4 evenly distributed from lateral to ventrolateral	in the center of the anterior-posterior axis at sclerite of segment 15, outside of D2, strands 1–4 evenly distributed from lateral to ventrolateral	21C, 22A
JVIII1–3	paired	posterior at sclerite of segment 15, posterior to JVII and outside of D2, strands 1–3 evenly distributed from lateral to ventrolateral	posterior at sclerite of segment 16, outside of D2, strands 1–3 evenly distributed from lateral to ventrolateral	21C, 22B
JIX1–2	paired	posterolateral at sclerite of segment 16, posterior to JVIII, strands 1–2 evenly distributed lateral	posterolateral at sclerite of segment 17, strands 1–2 evenly distributed lateral	21C, 22A
TI1	paired	FEMALE: ventrolateral and in the center of the anterior-posterior axis at pleural membrane of segment 9	ventrolateral and anterior at accessory gland posterior in segment 9	21A, 22A
TI2	paired	ventrolateral and in the center of the anterior-posterior axis at pleural membrane of segment 9, in females ventral to TI1	ventromedial and in the center of the anterior-posterior axis at sternite of segment 9	21A, B 22A, B
TII1	paired	ventrolateral and in the center of the anterior-posterior axis at pleural membrane of segment 10	ventromedial and in the center of the anterior-posterior axis at sternite of segment 10	21A, 22A, B
TII2	paired	ventrolateral and in the center of the anterior-posterior axis at pleural membrane of segment 10, ventral and inward of TII1	ventromedial and in the center of the anterior-posterior axis at sternite of segment 10, ventral to TIII1	21A, B 22A
TIII1–TV1	paired	ventrolateral at tergite of segments 11–13, TIII1 posterior, TIV1 in the center of the anterior-posterior axis, TV1 anterior in the respective segment	ventromedial at sternite of segments 11–13, TIII1 posterior, TIV1 in the center of the anterior-posterior axis, TV1 anterior in the respective segment	21A, 22A
TIII2–TV2	paired	FEMALE: ventrolateral at pleural membrane of segments 11–13, ventral to TIII1–TV1, TIII2 posterior, TIV2 in the center of the anterior-posterior axis, TV2 anterior in the respective segment	ventromedial at sternite of segments 11–13, ventral to TIII1–TV1, TIII2 posterior, TIV2 in the center of the anterior-posterior axis, TV2 anterior in the respective segment	21A, 22A
		MALE: ventrolateral at pleural membrane of segments 11–13, ventral and inward of TIII1–TV1, TIII2 posterior, TIV2 in the center of the anterior-posterior axis, TV2 anterior in the respective segment	ventromedial at sternite of segments 11–13, ventral and outward of TIII1–TV1, TIII2 posterior, TIV2 in the center of the anterior-posterior axis, TV2 anterior in the respective segment	21B, 22B
TVI	paired	ventrolateral, posterior and outward at tergite of segment 14	ventrolateral and posterior at pleural membrane of segment 14, outside of V	21A, 22B

Tab. 5 continued

Muscle		Origin	Insertion	Fig.
Gf	paired	dorsomedial in the genital operculum in segment 9, splits in two branches just after origin	anteroventral to its origin in the genital operculum in segment 9	21A, 22A
			posteroventral to its origin in the genital operculum in segment 9	21A, 22A
Gm1	paired	ventromedial at the genital atrium in segment 9	anteroventral and medial in genital lobe 1 in segment 9	21B, 22B
Gm2	paired	ventromedial at the genital atrium in segment 9, just posteromedial of Gm1	ventromedial in genital lobe 2, just outside of Gm1 in segment 9	21B, 22B
Gm3	paired	ventromedial at the genital atrium in segment 9, just posteromedial of Gm2	ventromedial in genital lobe 2, just posterior and outside of Gm2 in segment 9	21B, 22B
Gm4	paired	posteroventral and medial at genital atrium in segment 9	anteroventral at sternite of segment 10, just posterior to genital lobe 3 and medial of V	21B, 22B
V	paired	ventral at tergite, at the border of segments 8 and 9, immediately posterior to the insertion of E13, gives off two side strands anterior in segments 9 and 11	ventral at sclerite at the border of segments 17 and 18	21A, B 22A, B
			ventrolateral at pleural membrane posterior in segment 9	21A, B 22A, B
			ventrolateral at pleural membrane just anterior to the border of segments 9 and 10	21A, B 22A, B
F1–3	paired	lateral at sclerite at the anterior end of segment 18, strands 1–3 distributed from dorsal to ventrolateral	lateral at membranous fold and immediately distal to the joint connecting segment 18 and flagellar base, strands 1–3 distributed from dorsal to ventrolateral	21C, 22B

3.2.5.1   Musculature of the extremities

The musculature of the extremities, i.e. the chelicerae, the pedipalps and leg 1–4, is described for the right side. Thirteen muscles insert on the chelicera. Three extrinsic muscle strands (C1, C3, and C4, Tabs. 5, 8) originate dorsally from the prosoma. These might be involved in the up and down movement of the chelicera, where muscle C1 and C3 are possible antagonists to C4 (Figs. 21B, 22A). The basal article of the chelicera contains three strands of prominent intrinsic musculature (C5–7) and two minor intrinsic muscle strands (C2 and C8). Muscle C5 and C7 are possibly the antagonists to C6 (Figs. 21A, 22A). The movable digit of the chelicera as well as the tip of the fixed digit are free of musculature. The movable digit may be moved by the cheliceral muscles 9–13, which attach immediately proximal to the joint connecting the movable digit to the fixed digit via sinewy extensions. The antagonist to these muscles is probably hemolymph pressure because no musculature with antagonist topography was found (Figs. 21A, 22A).

The pedipalp has a total of five muscles (PP1–PP5) in its proximal articles as well as five tendons (PP6t–PP10t) in its distal articles (Figs. 21A, B, 22A, C; Tabs. 5, 10, 11). One extrinsic muscle (PP1) originates dorsal from the prosoma. Like the pedipalp, leg 1 has muscles (LI1–LI8) in the proximal articles and tendons (LI9t–LI14t) in the distal articles. In both extremities, the tendons are attached to the cuticle by pulleys in each article. The two extrinsic muscles of legs 1–3 (LI1, LI2, LII1, LII2, LIII1, and LIII2), originate dorsally from the prosoma and at the endosternite, respectively. In addition, legs 2 and 3 have seven (LII3–LII9) and eight (LIII3–LIII10) intrinsic muscles, respectively. Leg 4 has 14 muscles, of which 11 are intrinsic (LIV4–LIV14) and three are extrinsic (LIV1–LIV3). The extrinsic muscle strands all originate from the endosternite (Fig. 21; Tab. 5). The analysis of serial sections of pedipalps and legs suggests that some pairs of intrinsic muscles may act as mutual antagonists, while origin and insertion of other muscles suggests that hemolymph pressure might act as antagonist. In the pedipalp, articles 7–9 have no intrinsic antagonistic pair of muscles. The same is true for articles 6–11 of leg 1. The muscle and tendon of article 6 span the entire article. Articles 6 and 7 in legs 2 and 3, and articles 6–8 in leg 4 also have no possible intrinsic antagonistic pair of muscles (Figs. 21A, 22C). Here, the hemolymph possibly acts as antagonist.

3.2.5.2   Musculature of the body wall

A total of 13 muscles (P1–13) originate from the body wall but are not directly associated with the extremities or the endosternite. Prosomal muscles 1 and 2 are associated with the functional upper lip of the rostrosoma. Each of the paired P2 muscles are possibly antagonistic to each other to enable lateral movement of the functional upper lip. However, an antagonistic muscle for P1 was not recognized. Here, hemolymph is likely to provide the counter movement. The muscles associated with the pharynx (unpaired P3 and paired P4) are antagonistic to the circular muscle fibers of the pharynx (see 3.2.10.1).
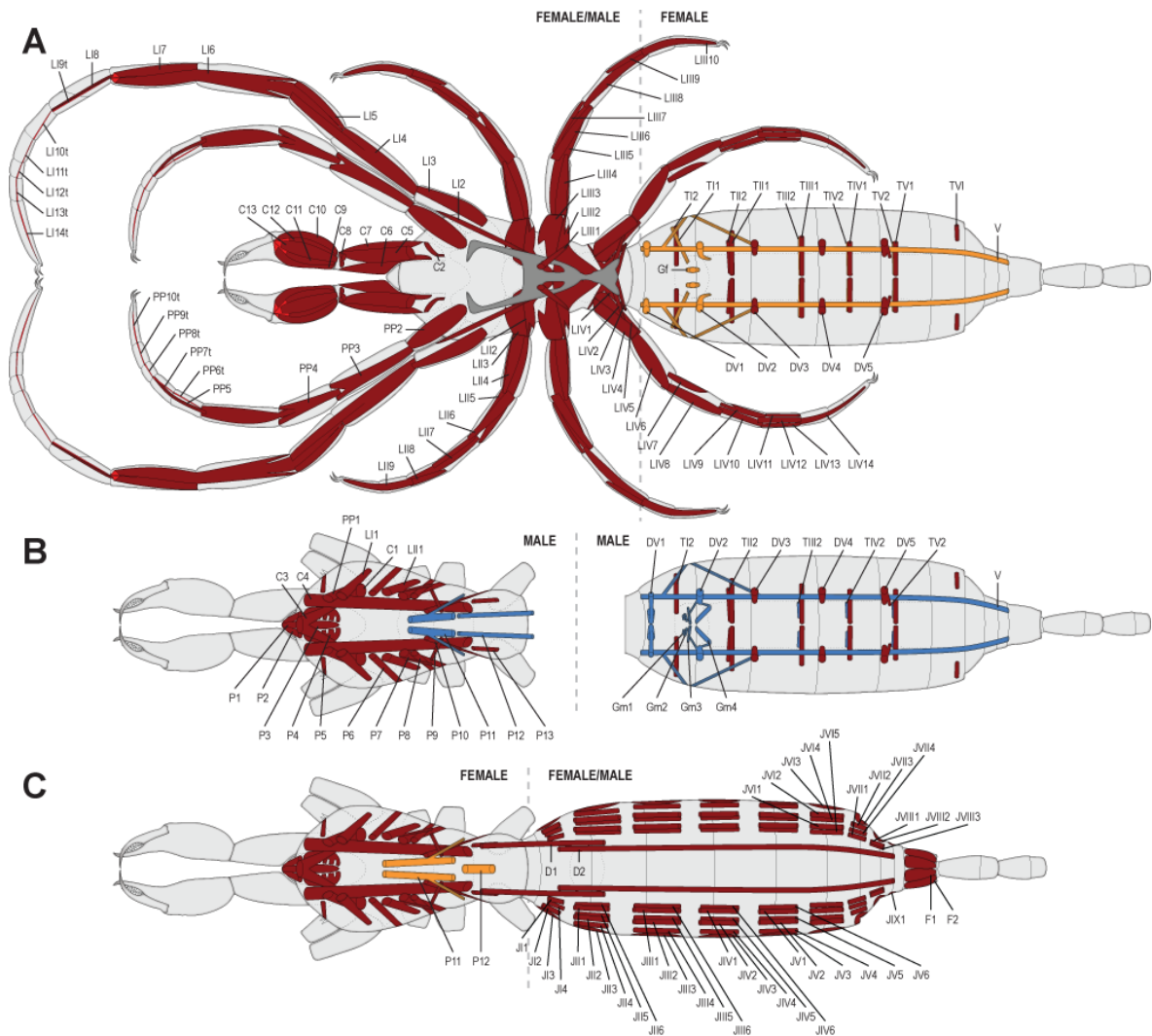
Fig. 21. *Eukoenenia spelaea*, dorsal schematic drawing of the musculature. Female/Male indicates that the musculature is identical in both sexes. Female or male indicates sex specificity of musculature. (**A**) Within the prosoma only endosternite musculature associated with the legs as well as cheliceral musculature are depicted. The remaining prosomal musculature is shown in B and C. Tendons in the chelicerae, pedipalps, and leg1 are marked bright red. Tendons are identified by a terminal 't' in their name. Within the opisthosoma, the dorsal, intersegmental and flagellar musculature was omitted for clarity. Sex-specific opisthosomal muscles for females are marked orange. (**B**) Male. Here, the remaining prosomal musculature not shown in A is depicted. Sex-specific prosomal and opisthosomal musculature is marked blue. (**C**) Here, the prosomal and opisthosomal musculature omitted from A is depicted. Sex-specific prosomal musculature is marked orange (female). Abbreviations: C1–13: cheliceral muscle; D1–2: dorsal muscle; DV1–5: dorsoventral muscle; F1–2: flagellar muscle; Gf: genital muscle female; Gm1–4: genital muscle male; JI1–4: intersegmental muscle 1; JII1–6: intersegmental muscle 2; JIII1–6: intersegmental muscle 3; JIV1–6: intersegmental muscle 4; JV1–6: intersegmental muscle 5; JVI1–5: intersegmental muscle 6; JVII1–4: intersegmental muscle 7; JVIII1–3: intersegmental muscle 8; JIX1: intersegmental muscle 9; LI1–14t: leg 1 muscle/tendon; LII1–9: leg 2 muscle; LIII1–10t: leg 3 muscle; LIV1–14: leg 4 muscle; P1–13: prosomal muscle; PP1–10t: pedipalps muscle/tendon; TI1–2: transversal muscle 1;TII1–2: transversal muscle 2; TIII1–2: transversal muscle 3; TIV1–2: transversal muscle 4; TV1–2: transversal muscle 5; TVI1: transversal muscle 6; V: ventral muscle.
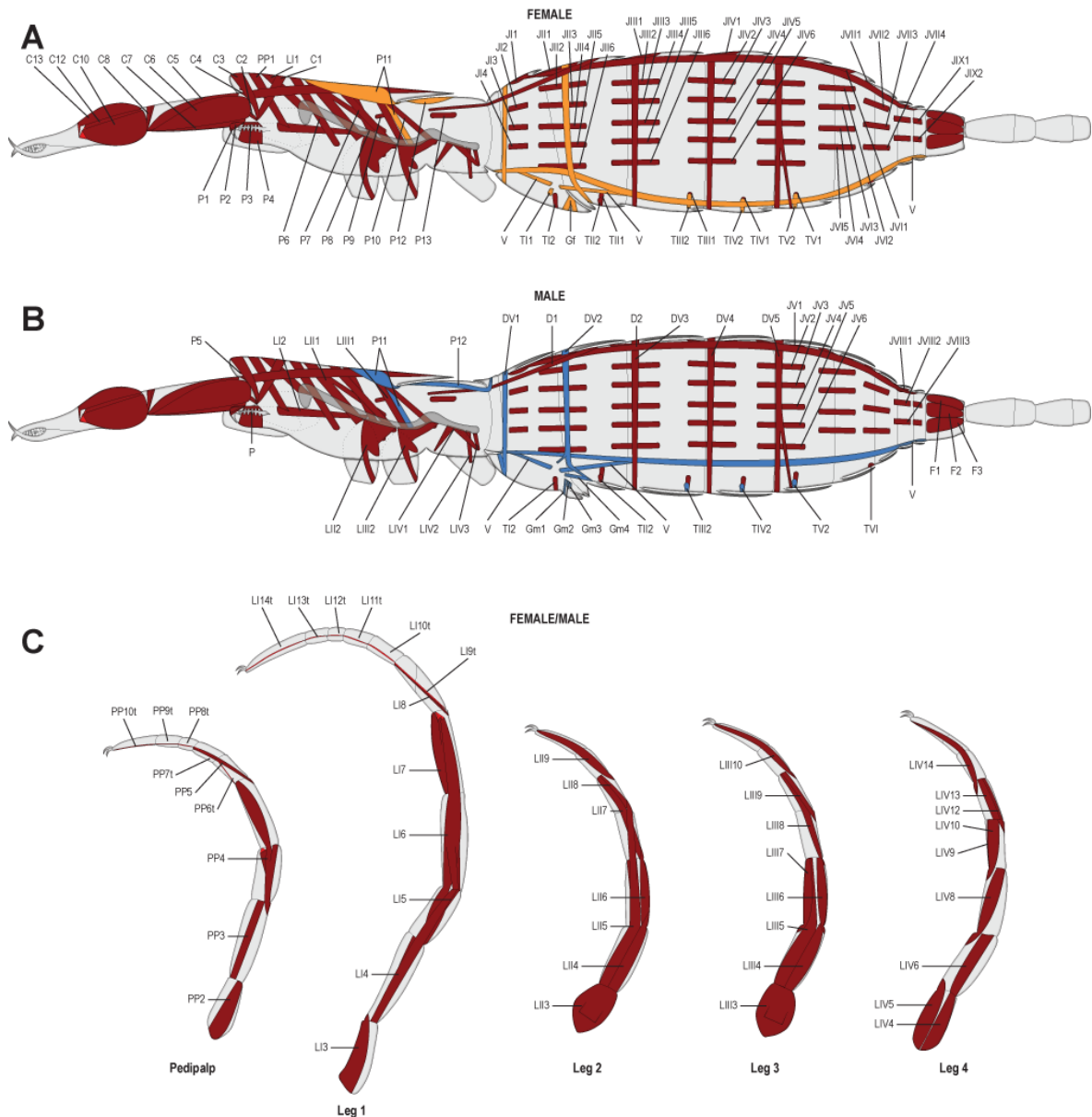
Fig. 22. *Eukoenenia spelaea*, schematic drawing of the musculature. (**A**) Lateral view of a female. The right body half is depicted. Endosternite musculature only associated with the legs are shown. Sinewy sections within the chelicerae are marked bright red. Sex-specific opisthosomal muscles for females are marked orange. (**B**) Lateral view of a male. Only the right body half is depicted. Sex-specific prosomal and opisthosomal musculature is marked blue. (**C**) Lateral view of the pedipalps and legs. Tendons are identified by a terminal 't' in their name. Abbreviations: C1–13: cheliceral muscle; D1–2: dorsal muscle; DV1–5: dorsoventral muscle; F1–3: flagellar muscle; Gf: genital muscle female; Gm1–4: genital muscle male; JI1–4: intersegmental muscle 1; JII1–6: intersegmental muscle 2; JIII1–6: intersegmental muscle 3; JIV1–6: intersegmental muscle 4; JV1–6: intersegmental muscle 5; JVI1–5: intersegmental muscle 6; JVII1–4: intersegmental muscle 7; JVIII1–3: intersegmental muscle 8; JIX1–2: intersegmental muscle 9; LI1–14t: leg 1 muscle/tendon; LII1–9: leg 2 muscle; LIII1–10t: leg 3 muscle; LIV1–14: leg 4 muscle; P: pharynx; P1–13: prosomal muscle; PP1–10t: pedipalps muscle/tendon; TI1–2: transversal muscle 1; TII1–2: transversal muscle 2; TIII1–2: transversal muscle 3;TIV1–2: transversal muscle 4; TV1–2: transversal muscle 5; TVI1: transversal muscle 6; V: ventral muscle.

The majority of the other prosomal muscles (P5–12) originates dorsally, and inserts posterolaterally on the body wall. Muscles are not confined to one segment but may cross segmental borders or even span several segments, e.g. muscles P6–10 span two segments and only P5 stays within a single segment (Figs. 21B, 22A; Tab. 5).

47

Sex-specific differences in the musculature of the body wall can be found in P11 and P12. Prosomal muscle 11 is almost twice as long in females as in males and extends anteriorly to the region of the 1st leg. In males, it extends anteriorly to the region of the 2nd leg. Thickness and branching of the muscle, however, show no differences between females and males (Figs. 21B, C, 22A, B).

3.2.5.3   Musculature of the endosternite

According to the box-truss axial muscle system (BTAMS) described by Shultz (2007*b*; Tab. 8) five segmental muscle groups are associated with the endosternite (E1–E20), i.e. dorsal suspensors, anterior oblique suspensor, posterior oblique suspensors, lateral suspensors, ventral suspensors. In addition, there are muscles extending to the anterior, or into the opisthosoma (Fig. 23; Tab. 5).

Five muscles can be described (E3, E5, E11, E14, E17) originating dorsal from the endosternite and inserting posterodorsal on the body wall (Fig. 23; Tabs. 5, 8). Those muscles are interpreted as the segmental dorsal suspensor muscles. Muscle E3 originates from the anterior end of the endosternite and extends straight dorsal where it inserts on the propeltidium. Muscle E5 originates posterior to E3 in the region of leg 1 and extends dorsal but with some posterior orientation; it also inserts on the propeltidium. Muscles E11 and E14 originate anterior and posterior from the region of leg 3, respectively. Both muscles insert in the same posterior position of

Fig. 23. *Eukoenenia spelaea*, schematic drawing of the endosternite musculature of female and male. No sex-specific differences were found. Only endosternite musculature not associated with the legs is depicted. Endosternite musculature is color coded as follows: orange = dorsal suspensors, purple = anterior and posterior oblique suspensors, dark red = lateral suspensors, blue = ventral suspensors, yellow = muscles extending anterior or into the opisthosoma. Endosternite musculature associated with the legs (LI2, LII2, LIV1–3) is only shown with its point of origin (yellow shaded). (**A**) Dorsal view. Mostly, the muscles do not extend perpendicular to the endosternite and in some cases muscles appear to span several segments. (**B**) Lateral view. Muscles mostly extend diagonally along the dorso-ventral axis. Abbreviations: E1–20: endosternite muscle; EaB: endosternite anterior bridge; EBr, endosternite branch; EcB: endosternite central bridge; EpB: endosternite posterior bridge; EpS: endosternite posterior section; EU: endosternite upturned U section; P: pharynx.

the propeltidium in the region of leg 3. Thus, the course of E11 is directed oblique towards posterior. Muscle E17 is associated with the region of leg 4 and extends straight dorsal to insert on the metapeltidium. E3 and E17 are the only dorsal suspensors, which insert dorsal to their origin.

Muscle E6 originates dorsal from the endosternite in the region of the most anterior dorsal suspensor and extends to the pleural membrane where the chelicera articulates with the prosoma. Based on the topography of its origin and insertion, it is the only anterior oblique suspensor muscle found in the prosoma (Fig. 23; Tabs. 5, 8).

The segmental posterior oblique suspensors originate dorsal from the endosternite and insert posterolaterally on the body wall. I described four segmental muscles (E4, E12, E15, E20) that can be assigned to this group (Fig. 23; Tabs. 5, 8). Muscle E4 is located in the region of leg 1 and inserts posterior in the region of leg 2. Muscles E12 and E15 anterior and posterior from the region of leg 3, respectively, but insert in the same region anterior in the region of leg 4 adjacent to dorsal suspensor E17. Muscle E20, which is possibly also part of the posterior oblique suspensors, originates at the terminal end of the endosternite, posterior to E17 and inserts laterally at the pleural membrane of segment 8 (Fig. 23; Tabs. 5, 8).

The lateral suspensors originate lateral from the endosternite and insert lateral at the pleural membrane. I recognized four muscles in two clusters (E10, E16, E18, E19) that can be considered to be the lateral suspensor muscles (Fig. 23; Tabs. 5, 8). Muscles E16, E18, and E19 are clustered and originate in the same region of leg 4. Muscle E10 is located in the region of leg 2.

The ventral suspensors (E1, E2, E7, E9) originate ventral from the endosternite and insert at the pleural membrane (Fig. 23; Tabs. 5, 8). Muscles E1 and E2 are grouped as they originate both at the anterior end of the endosternite. Muscle E1 has an anterior and a posterior branch and is the only muscle which inserts straight ventral. Its anterior branch inserts at the intersegmental membrane between ventral plate and prosternum; its posterior branch inserts at the prosternum (Fig. 23; Tabs. 5, 8). Muscles E7 and E9 are also clustered due to their origin in the region of leg 2 and the lateral suspensor muscle E10. Both ventral suspensor muscles insert anterolaterally on the pleural membrane.

Two muscles were observed that do not fit into the pattern of BTAMS. Muscle E8 originates medial from the anterior endosternal bridge and extends to the posteroventral end of the pharynx (Fig. 23; Tab. 5). Endosternal muscle 13 originates from the lateral branch of the endosternite and extends into the opisthosoma where it inserts at the border of segment 8 and 9 (Fig. 23). There is one insertion cluster dorsolateral on the metapeltidium, where three muscles, E12, E15, and E17, insert right next to each other. These appear to be the antagonists to LII2 and LIII2 which also originate from the endosternite (Fig. 23).

3.2.6   Musculature of the opisthosoma

In *Eukoenenia spelaea*, the opisthosomal musculature consists of the dorsal longitudinal, dorsoventral, intersegmental, transversal, genital, ventral longitudinal, and flagellar musculature. This pattern contains the BTAMS, i.e. the dorsal longitudinal, dorsoventral, and ventral longitudinal musculature are part of the BTAMS. Sex-specific differences can be found in the dorsoventral, posterior oblique, genital, and ventral longitudinal musculature. The following description is an account on the general topography of the musculature. Detailed descriptions with points of origin and insertion for each muscle are given in table 5. Possible antagonists are described according to the topography of their origin and insertion points.

The dorsal longitudinal musculature is divided into a paired anterior strand (D1) and a paired posterior strand (D2; Figs. 21C, 22B; Tab. 5). The anterior strand, D1, originates from the prosoma, dorsolateral from the metapeltidium in segment 7. From there, it passes into the opisthosoma and inserts dorsally on segment 10 lateral to the body median line. Muscle D2 originates dorsally from segment 9, medial of D1, and inserts on the anterior margin of segment 17. Consequently, both muscles, D1 and D2, overlap in segments 9 and 10 (Figs. 21C, 22B). The topography of these two muscles suggest that they enable the animals to bend their opisthosoma upward against the position of the prosoma in these segments.

The ventral longitudinal musculature consists of a paired strand (V) which extends from segment 8 to the border between segments 17 and 18. It branches twice, once in segment 9 and once in segment 11. However, both lateral branches insert posterolaterally on segment 9 (Figs. 21A, B, 22A, B; Tab. 5). The sex-specific

difference in the ventral muscle is the location relative to the ventral body wall. In females, the ventral longitudinal muscle has a more lateral position except in the genital region (Figs. 21A, 22A). In males, the muscle is more medial but more lateral in the metasoma, i.e. segments 15–18 (Figs. 21B, 22B).

Segmental dorsoventral musculature (DV1–DV5) is found in opisthosomal segments 9–13. These pairs of muscles span the opisthosoma from dorsal to ventral, anteriorly in each segment. Dorsally, the strands originate just lateral to the dorsal musculature. Ventrally, the strands terminate just medial of the ventral musculature. The first two strands, DV1 and DV2, are sexually dimorphic. In females, DV1 and DV2 are simple strands with no branching (Figs. 21A, 22A; Tab. 5). Muscle DV2, however, bends slightly toward posterior bevor inserting just posterior to the base of the genital lobes. In males, both muscles branch ventrally. The anterior branch of DV1 inserts on the dorsal side of the ventral overlap of segment 9. Muscle DV2 splits just dorsally of the genital atrium. Its anterior branch then inserts lateral on the center of the genital atrium's anterior-posterior axis (Figs. 21B, 22B; Tab. 5). The posterior branch inserts just posterior to the base of the third pair of genital lobes. In both sexes, DV5 branches, with the posterior branch inserting close to the transversal muscle TV (Figs. 21A, B, 22B).

The intersegmental musculature forms several parallel strands that span the pleural membranes in anterior-posterior direction (Figs. 21C, 22A, B; Tab. 5). These parallel muscle strands are evenly spaced from dorsal to ventrolateral along the body wall. There are a total of nine sets of intersegmental muscle strands (JI–JIX). Six strands on each side of the opisthosoma are present in segments 9/10–12/13 (JII1–6, JIII1-6, JIV1-6, and JV1–6). Set JVI consists of five strands, in the following sets the number of strands gets reduced by one per set. Segment 8 does not have any intrinsic musculature. Interestingly, I find four small muscle strands in the anterior half of segment 9, JI1–4, in a position similar to other intersegmental muscles, but not bridging over to segment 8. All other sets, JII–JVII, originate posterior from the preceding segment, span the segment border and insert on the following segment (Figs. 21C, 22A, B; Tab. 5). There is no intersegmental musculature spanning segments 17 and 18 (Figs. 21C, 22A, B).

The most distinct sexual difference of the opisthosomal musculature can be found in the genital musculature. Whereas females have only one paired genital muscle (Gf), males possess four pairs of genital muscles (Gm1–Gm4). In females, the genital muscle is located inside the genital operculum, lateral to the body median line. It inserts on the dorsal opercular wall, which is oriented toward the genital opening. Muscle Gf then splits into two branches and inserts anterior and posterior on the ventral opercular wall (Figs. 21A, 22A; Tab. 5). This pair of muscles might be associated with the widening of the genital opening.

The male genital musculature consists of four thin paired muscle strands which are associated with the genital lobes and the genital atrium. Muscles Gm1–Gm3 are grouped together and originate from the ventral wall of the atrium. The most anterior muscle strand (Gm1) extends ventrally and inserts on the anterior wall of the first genital lobe. It might be associated with the down movement of genital lobe 1. The muscle pairs Gm2 and Gm3 insert on the second pair of genital lobes and possibly move them up and medial. Muscle Gm4 originates from the lower third of the genital atrium. It inserts on the ventral body wall and might widen the genital atrium towards posterolateral (Figs. 21B, 22B).

The transversal musculature (TI–TVI) consists of paired strands of two parallel muscles in each segment. It is located ventrally below the nerve cord in segments 9–14, thus, it is not present in the metasoma. The transversal musculature spans the short pleural membrane and inserts on the sternite. There are paired transversal muscle strands per body half with the exception of TI in males and TVI in both females and males, which consist of only one strand per body half (Figs. 21A, B, 22A, B; Tab. 5). Muscle TI1 of females inserts ventrolaterally and is possibly involved in aiding the widening of the genital opening. The ventral strands TIII2, TIV2, and TV2 are longer in females than in males. Muscle TVI is located towards posterolateral in segment 14. It is as short as the ventral transversal muscle strands of the male, thus, shorter than the dorsal strands of both females and males (TIII1, TIV1, and TV1; Figs. 21A, B, 22A, B).

The last opisthosomal segment carries the flagellar musculature. It consists of three paired thick parallel muscle strands (F1–F3). The muscles are arranged parallel to the body axis and encircle almost the entire segment. The most ventral part of

segment 18 is free of musculature. Muscles F1–F3 insert anterior on the basal article of the flagellum. Muscle F1 might be associated with the up movement of the flagellum, F2 and F3 are possibly associated with down and lateral movement (Figs. 21A, 22B). The flagellum itself is free of musculature (see 3.2.13).

3.2.7 Nervous system

The nervous system of *Eukoenenia spelaea* consists of a prominent prosomal ganglial mass, the synganglion, which fills large parts of the prosoma and is the origin of the prosomal nerves as well as a pair of parallel opisthosomal nerve cords (Figs. 24, 25). The synganglion can be divided into the supraesophageal ganglion and subesophageal ganglion. The supraesophageal ganglion is located between the base of the chelicerae and the posterior end of the propeltidium (SupEG; Fig. 24). Using standard light microscopic histology, I could identify three major commissures: (1) the most anterior commissure is located dorsal to the esophagus in the median region of the pedipalpal coxae. It is possibly the protocerebral commissure (PCC; Figs. 26A, 27). (2) the most prominent commissure is located dorsal to the esophagus in the posterior region of the pedipalpal coxae and the median region of the coxae of leg 1. It is possibly the cheliceral commissure (ChC; Figs. 26B, 27). (3) The posterior commissure is located ventral to the esophagus between esophagus and endosternal muscle E8 in the posterior region of the coxae of leg 1. It is possibly the pedipalpal commissure, because nerve fibers from the commissure lead to the base of the pedipalpal coxae (PPC; Figs. 26C, 27).

The subesophageal ganglion is larger than the supraesophageal ganglion. It extends from the base of the pedipalps to the genital plate in the opisthosoma (SubEG; Fig. 24). The parts of the subesophageal ganglion relating to a specific prosomal segment are tightly merged, however, the ganglial lobes of the respective legs can be distinguished. Neuropil around the esophagus (circumesophageal commissure) connects the supra- and subesophageal ganglia (Fig. 39C). Just anterior to the anterior endosternal bridge, the supra- and subesophageal ganglia separate. The supraesophageal ganglion is never in contact with the endosternal bridge, as the midgut lies between these two structures (Fig. 19A). The subesophageal ganglion extends into the opisthosoma (Fig. 24). A hemolymph space surrounding the ganglia which is typical for euchelicerates, was not found
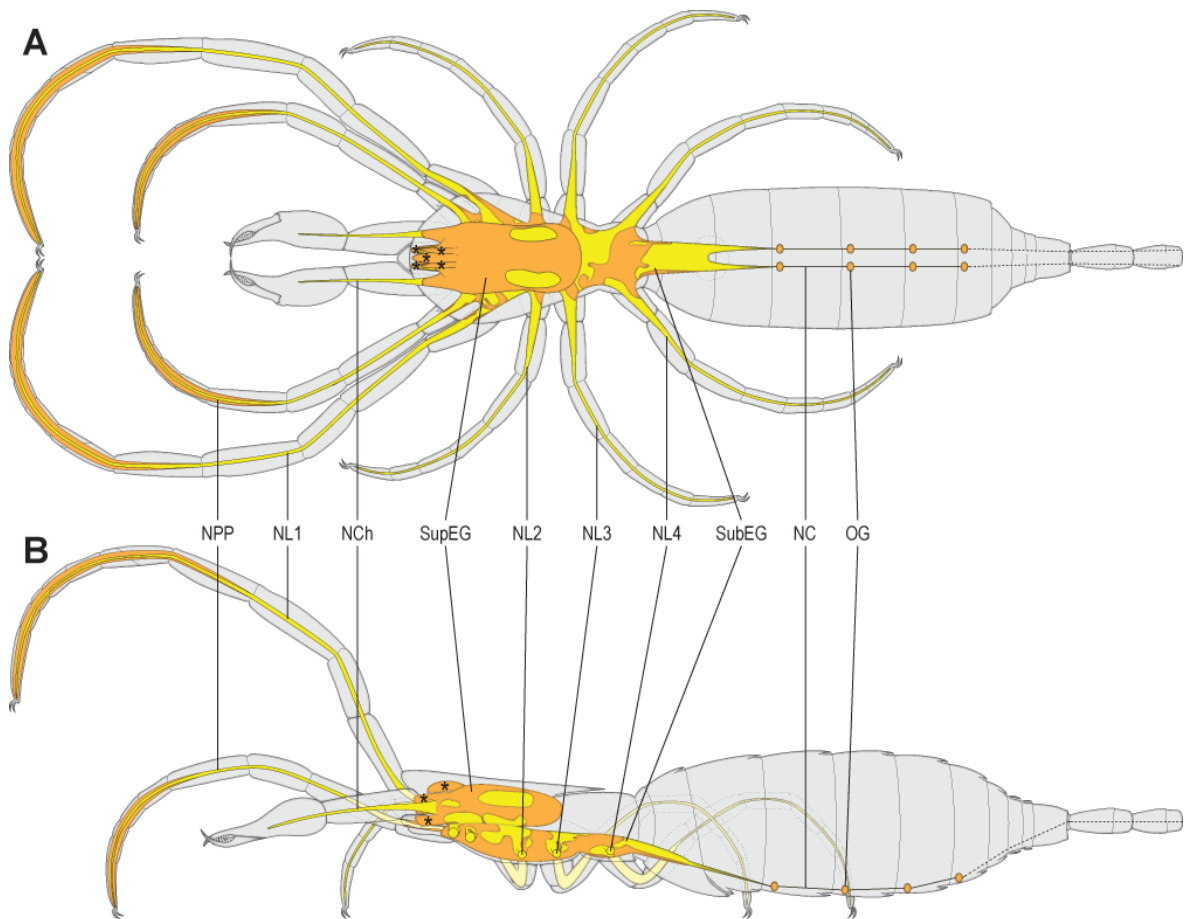
Fig. 24. *Eukoenenia spelaea*, schematic drawing of the nervous system. (**A**) Dorsal view. The supraesophageal ganglion is the prominent feature of the dorsal prosoma in the area of the propeltidium. It gives rise to the cheliceral nerves as well as several lobes (asterisk) into the anterior part of the propeltidium and into the rostrosoma. The subesophageal ganglion is larger than the supraesophageal ganglion and is the prominent feature of the ventral prosoma. It extends into the opisthosoma into segment 9. The pericarya layer (orange) is patchy all over the prosomal ganglial mass, leaving areas of neuropil (yellow) exposed. The distal articles of pedipalps and leg 1 are predominantly filled with sensory cells of the sensory setae and trichobothria (orange). Paired opisthosomal ganglia are found in segments 11–14. The nerve leaving the last opisthosomal ganglion are depicted with a dashed line because the actual topography is unclear. (**B**) Lateral view. The prosomal ganglia fill up most of the prosoma, especially in the area of the propeltidium. The thickness of the leg nerves decreases in the extremities from proximal to distal. Abbreviations: asterisk: ganglial lobes; NC: nerve cord; NCh: cheliceral nerve; NL1–4: leg nerve 1–4; NPP: pedipalpal nerve; OG: opisthosomal ganglion; SubEG: subesophageal ganglion; SupEG: supraesophageal ganglion.

(Fig. 25A, 28A, B). The ganglia are enveloped in a sheath-like structure, the neurilemma. The neurilemma is an extracellular matrix. It displays uniform thickness of approx. 50–100 nm around all structures adjacent to the ganglia, e.g. esophagus and muscles (Figs. 28A, B, 39C). A glial cell sheath, the perineurium that is typically found in arthropods is present (Figs. 28A, B).

The prosomal ganglia consist of neuropil surrounded by a patchy and incomplete cortex of the pericarya (Figs. 24, 25A). In the supraesophageal ganglion, the pericarya layer extends far anterior, sending out several lobes into the rostrosoma

(*; Fig. 24). Both ganglia are crossed by muscle strands which are dorsally, ventrally, and laterally attached to the body wall as well as the endosternite (see 3.2.5.3; Figs. 19A, 25B). In regions where the ganglial mass envelops musculature or the endosternite, no pericarya are present.

Following the neuron categorization by Babu (1985), two types of neurons can be recognized: (1) type B neurons. These neurons have a nucleus of approx. 1–2 µm in diameter. They can predominantly be found in the cortex of the posterior part of the subesophageal ganglion and the opisthosomal ganglia (Figs. 28C, D). In light microscopy, their nucleus stains darker and their cytoplasm lighter. The nucleus is the prominent structure of the neuron in transmission electron microscopy, the cytoplasm is largely reduced. (2) Type D neurons. These are larger neurons with a nucleus of approx. 3–4 µm in diameter (Figs. 17A, B, D, 28C). They can mainly be found in the cortex of the supraesophageal ganglion and the anterior part of the subesophageal ganglion. Their nucleus stains lighter in and the cytoplasm darker in light microscopy (Figs. 17B, 28C). Cell organelles, glycogen granules and free ribosomes are present in the cytoplasm of both types of neurons. Neurons of type A (typically associated with the mushroom bodies of the visual center) and type C (neurosecretory) could not be identified. The nucleus is large and surrounded by a small amount of cytoplasm in type B and type D neurons. The neuropil consists of axons and dendrites from the cortical neurons, and nerve fibers with microtubules, free ribosomes and glycogen granules (Fig. 28B).

Several nerves originate from the syncerebrum. Due to the fusion of the different ganglia, and the unclear differentiation into deuto-, and tritocerebrum, the description of the nerve origins will be attributed to the supra- and subesophageal ganglion based on the relative location of the nerve origins, only. The nerve supplying the chelicerae (NCh; Figs. 24, 27), originates laterally on each side of the supraesophageal ganglion just above the pharynx (Fig. 24B). The nerves of the pedipalps and legs 1–4 originate laterally from the subesophageal ganglion and decrease in diameter in article 2 (NL1–4, NPP, PrC-B, PrC-D; Figs. 24, 28C). In the pedipalp and leg 1, the number of type B and D neurons increases towards the more distal articles. Therefore, their distal articles are almost entirely filled with nerve cells. In contrast, legs 2–4 have only a few neurons distributed along the leg, with musculature instead of nerves being the prominent features within the leg (Fig. 24).
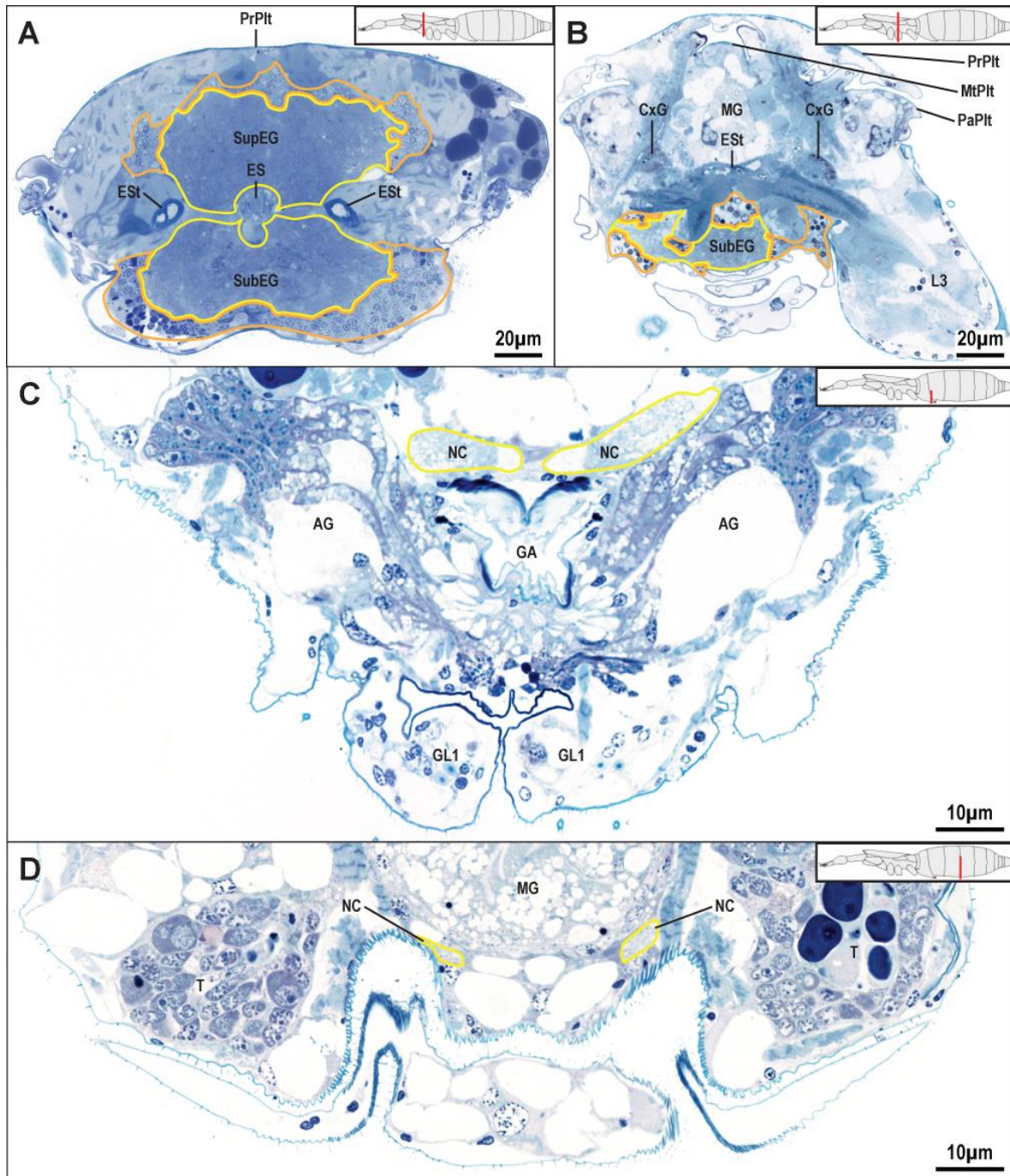
Fig. 25. *Eukoenenia spelaea,* light microscopic cross-sections of the nervous system. (**A**) Area of the border of segments 4 and 5. The prosomal ganglia fill a large portion of the prosoma. The pericarya layer (orange) forms an incomplete cortex to the more central neuropil (yellow). Mostly large type D pericarya are present. (**B**) Cross-section of the area of leg 3. The posterior section of the subesophageal ganglion displays a reduced central neuropil. The surrounding pericarya layer, consisting of mostly small type B neurons, is incomplete. In some areas, the neuropil is in direct contact with musculature and epidermis. (**C**) Light micrograph of a cross-section through segment 9 with the genital atrium. At their origin, the paired nerves supplying the posterior section of the body are enlarged. They are located dorsal to the genital atrium and accessory gland. (**D**) Area of the border of segments 11 and 12, just anterior to the opisthosomal ganglia of segment 12. The nerve cords of the rope ladder system of the opisthosomal nervous system are located ventral, and medial of the dorsoventral musculature. Abbreviations: AG: accessory gland; CxG: coxal gland glandular section; ES: esophagus; ESt: endosternite; GA: genital atrium; GL1: genital lobe 1; L3: leg 3; MG: midgut; MtPlt: metapeltidium; NC: nerve cord; PaPlt: parapeltidium; PrPlt: propeltidium; SubEG: subesophageal ganglion; SupEG: supraesophageal ganglion; T: testes.

56
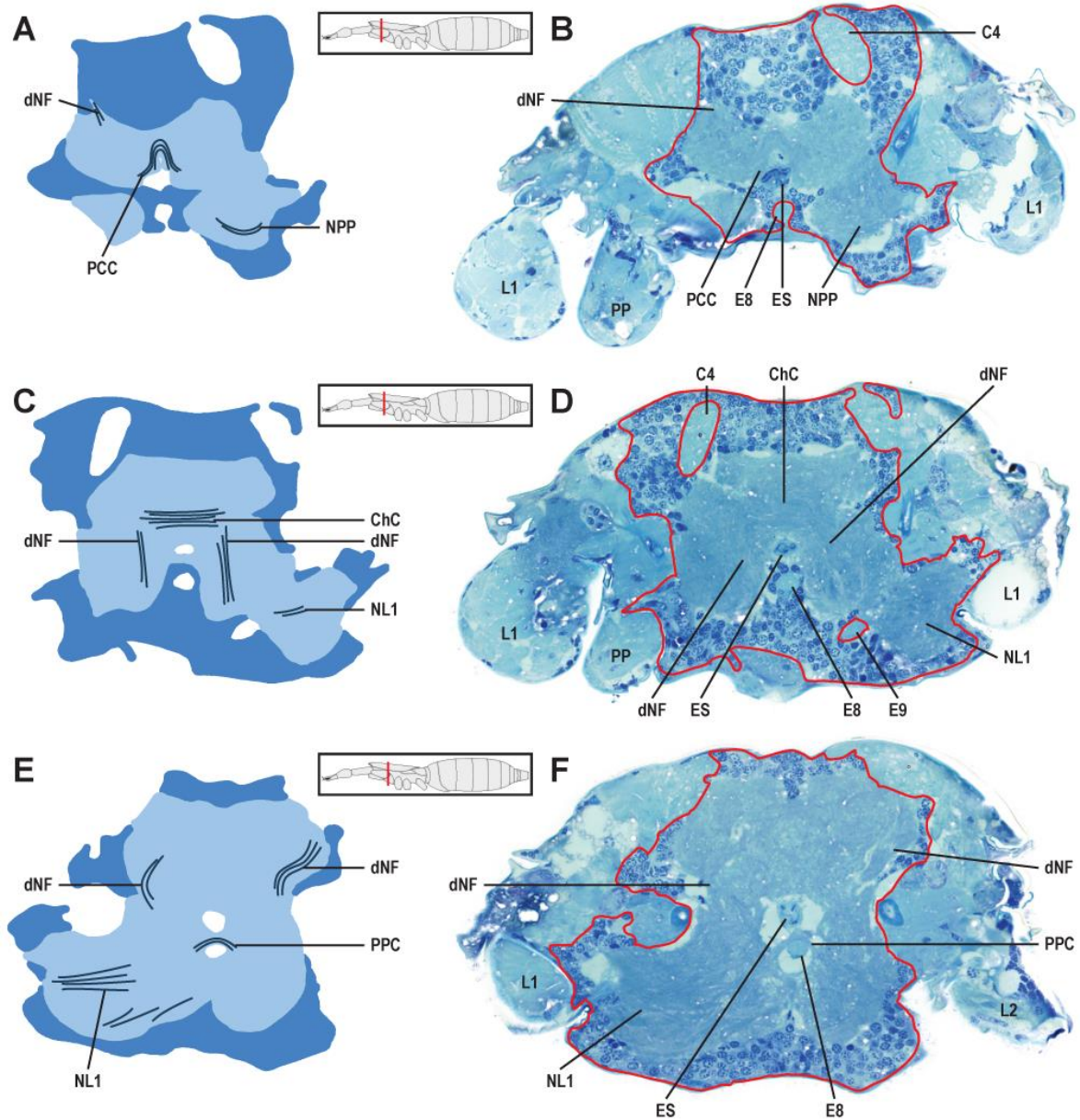
**Fig. 26**. *Eukoenenia spelaea*, locations of prominent commissures in the synganglion. (**A**) Schematic drawing of the pericarya layer (dark blue) and neuropil (light blue) in the region of the pedipalp and leg 1. The protocerebral commissure is located dorsal to the esophagus. (**B**) Light micrograph of a slightly oblique cross-section through the same region as in A. Dorsally, the pericarya partially envelop the cheliceral muscle C4. Ventrally, endosternal muscle E8 is also partially enveloped by pericarya. The pedipalpal nerve is broad at its base. (**C**) Schematic drawing of the pericarya layer and neuropil in the region between pedipalp and leg 1. The cheliceral commissure is more pronounced than all other commissures within the synganglion. The lateral nerve fibers are potentially part of the circumesophageal commissure. (**D**) Light micrograph of a slightly oblique cross-section through the same region as in C. The pericarya layer still envelops in part cheliceral muscle C4. Muscle E8 is now fully enveloped by pericarya. Similar to the pedipalpal nerve, the nerve of leg 1 is broad at its base. (**E**) Schematic drawing of the pericarya layer and neuropil in the region between leg 1 and 2. The delicate pedipalpal commissure is nestled between the esophagus and endosternal muscle E8. (**F**) Light micrograph of a slightly oblique cross-section through the same region as in E. The pedipalpal commissure fills the entire space between esophagus and muscle E8. Several descending fibers are located in the neuropil. The broad base of the nerve of leg 1 is clearly visible. Abbreviations: C4: cheliceral muscle; ChC: cheliceral commissure; dNF: descending fiber; E8–9: endosternal muscle; ES: esophagus; L1–2: leg 1–2; NL1: nerve of leg 1; NPP: nerve of pedipalp; PCC: protocerebral commissure; PP: pedipalp; PPC: pedipalpal commissure.
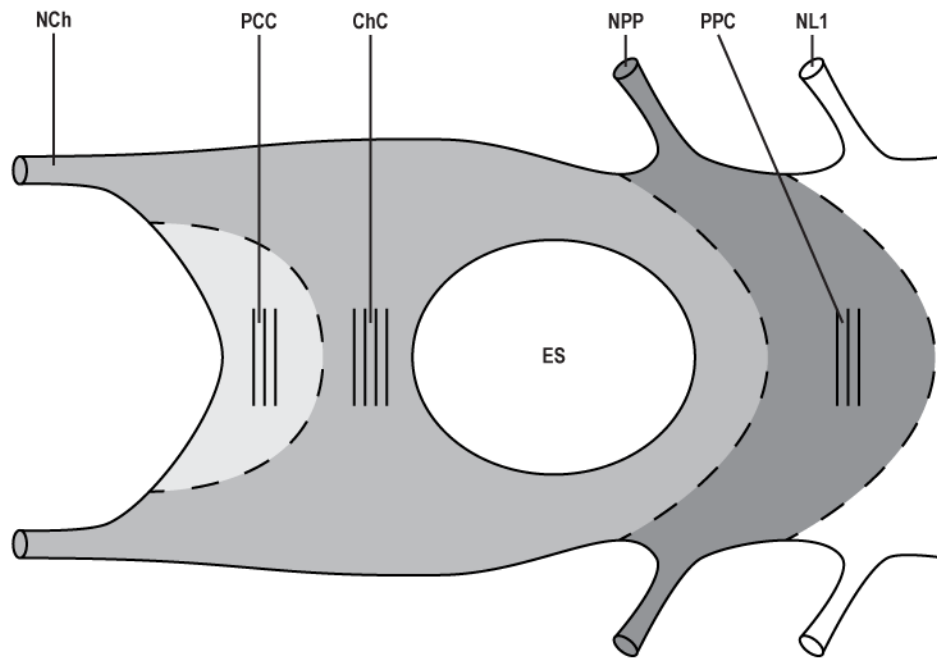
Fig. 27. *Eukoenenia spelaea*, schematic drawing of the anterior region of the synganglion. The protocerebrum with its commissure has shifted its location posterior between the anterior ends of the synganglion associated with the chelicerae. Thus, the cheliceral nerves originate from the most anterior part of the synganglion. The cheliceral commissure is located dorsally of the esophagus. The pedipalpal commissure, located ventrally of the esophagus, has shifted its location posterior between the bases of the nerves of leg 1. Abbreviations: ChC: cheliceral commissure; ES: esophagus; NL1: nerve of leg 1; NPP: nerve of pedipalp; PCC: protocerebral commissure; PPC: pedipalpal commissure.

Several pericarya lobes originating from the supraesophageal ganglion reaching anterior in the prosoma (*; Fig. 24). These lobes cannot be associated with prosomal structures like the frontal organ or lateral organs and appear to be pericarya displaced between the muscles of the prosoma due to limited space.

From the posterior end of the subesophageal ganglion in segment 9 two parallel nerve cords extend into the opisthosoma (Fig. 24). These nerve cords contain four pairs of opisthosomal ganglia in segments 11–14 and their respective connectives (OG; Fig. 24). At their origin, the nerve cords have a larger diameter than further distal (Figs. 25C, D). Each opisthosomal ganglion consists of approx. 25 type B neurons (Fig. 28D). The connectives are thicker in diameter than the ganglia and are connected to the ganglia dorsally (cNF; Fig. 28D). Additional nerve fibers are located mediolaterally of the connective (NF; Fig. 28D). One of these nerves is possibly a nerve connecting the left and right opisthosomal ganglia, a commissure. Distinct commissures, however, could not be identified in light microscopy. The origin of nerves supplying the sensory setae of segments 15–18 and the flagellum could also not be identified.
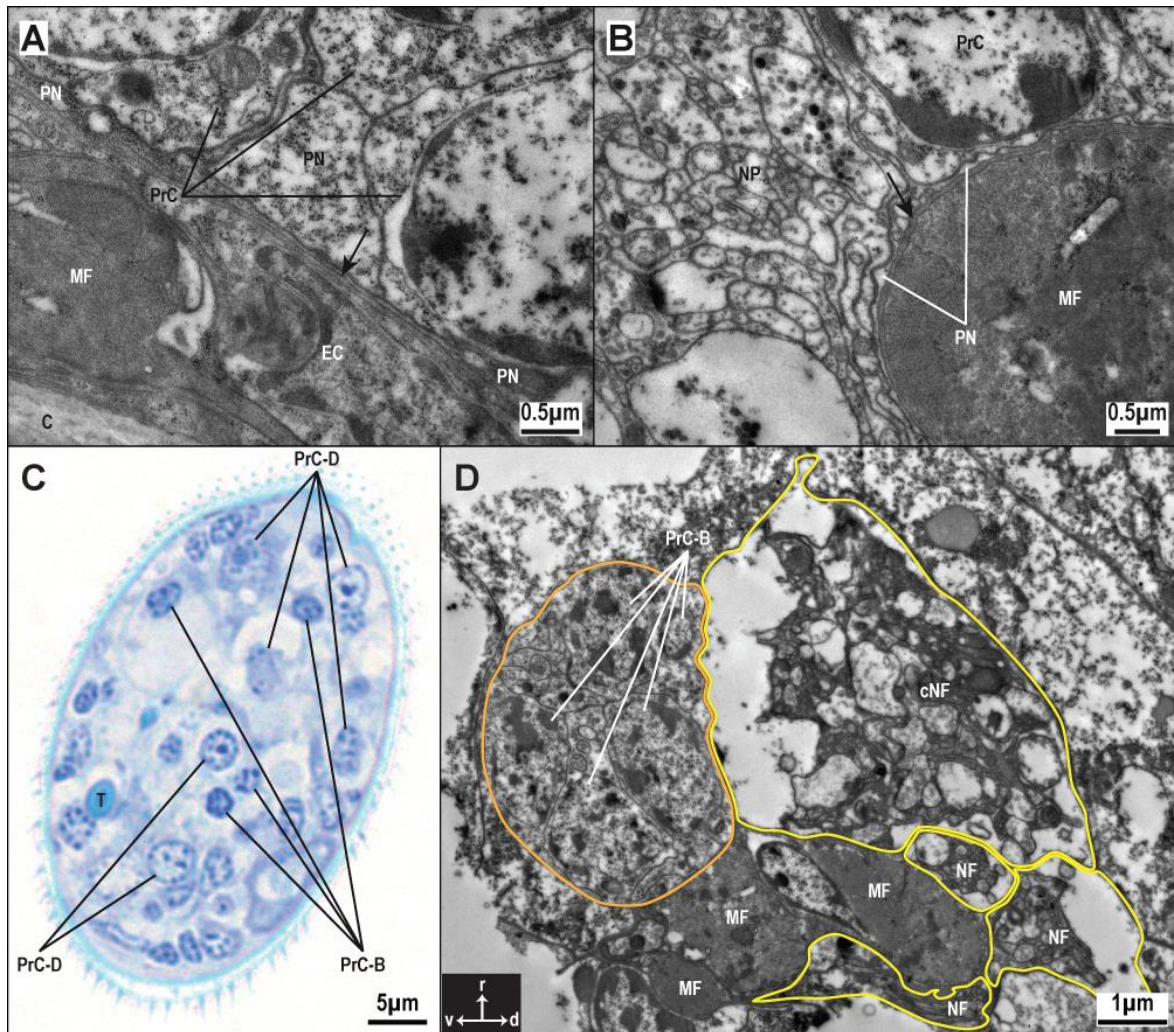
Fig. 28. *Eukoenenia spelaea*, nervous system. (**A**) Transmission electron micrograph of the supraesophageal ganglion just below the body wall. A thin neurilemma (arrow) separates the pericarya from the epidermis. (**B**) Transmission electron micrograph of the subesophageal ganglion in close association with a muscle. The neuropil is close to the muscle fiber. The thin neurilemma separates the muscle and the ganglion (arrow). (**C**) Light micrograph of a cross-section through a distal article of leg 1. Neurons are dispersed throughout the leg. The enlarged nuclei are surrounded by darker staining cytoplasm. (**D**) Transmission electron micrograph of an opisthosomal ganglion. The connective nerve lies (yellow) dorsal to the ganglion (orange) and is thicker in diameter than the ganglion itself. One of the adjacent nerve fibers is possibly the commissure. Abbreviations: C: cuticle; cNF: connective nerve fibers; d: dorsal; EC: epidermal cell; MF: muscle fiber; NF: nerve fiber; PN: perineurium; PrC-B: type B pericarya; PrC-D: type D pericarya; r: right; T: tendon; v: ventral.

3.2.8   Sensory organs

Sensory organs of *Eukoenenia spelaea* are the frontal organ, the lateral organs, the sensory setae, and the trichobothria. They all have the same basic structure: (1) outer cuticular structure, like a hair or modified hair, (2) a group of two or more sensory cells, and (3) several enveloping cells. The nervous elements are the same in all sensory organs: (1) the inner dendritic segment containing the mitochondria, (2) the ciliary segment with the typical 9 x 2 + 0 arrangement of microtubules, and

(3) the outer dendritic segment with more or less loosely arranged microtubules in varying numbers.

3.2.8.1 Frontal organ

The unpaired frontal organ is located medially at the most anterior part of the prosoma, just below the propeltidium and dorsal to the chelicerae (FO; Figs. 6A, B, 29A). It has a broad base with two finger-like modified setae extending anterodorsal (Figs. 9A, 29A). The setae are approx. 25 µm long and have a diameter of approx. 5–10 µm. Ridges and pits of the cuticle of the frontal organ form a honeycomb pattern. Transmission electron micrographs of these ridges show an electron-translucent base and an electron-denser tip (cR; Fig. 29B). The base of a ridge is anchored within the cuticle wall, the tip protrudes between the pits (cP; Figs. 29B, 30B). The cuticle of the pits is rich in cuticular grooves and covered with an electron-translucent epicuticle (cGr; Fig. 29B). The procuticle in this region has an electron-dense base and is less electron-dense in the pockets between the porous grooves (ProC; Fig. 29B). In the region of the ridges, the cuticle is approx. 0.35–0.5 µm thick, in the pits, it is only 0.2 µm thick. The cuticular grooves are approx. 0.1 µm deep. The diffusion distance through the cuticle is therefore
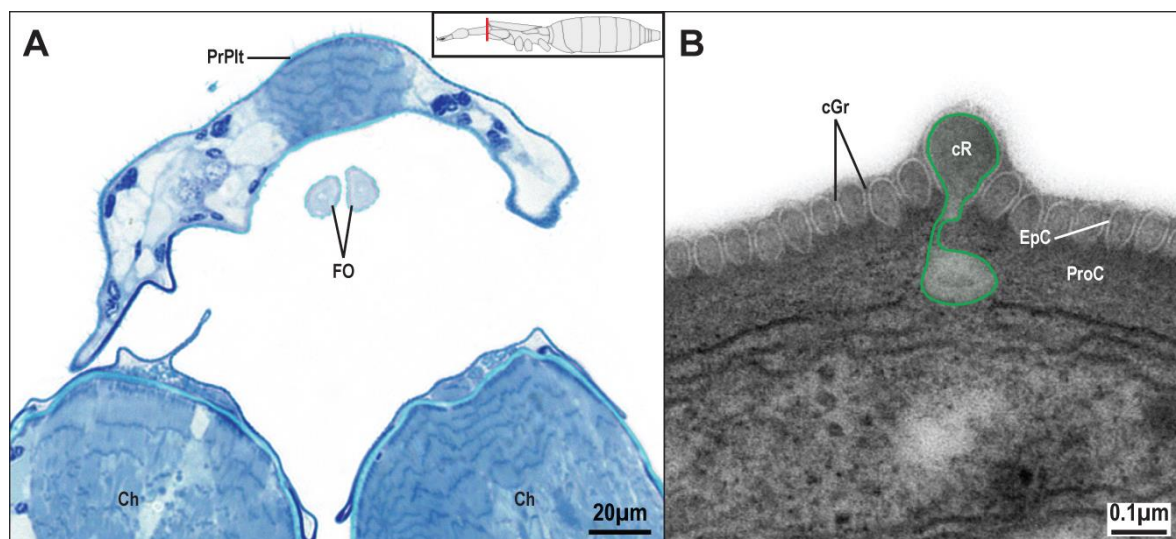
Fig. 29. *Eukoenenia spelaea*, frontal organ. (**A**) Light microscopic cross-section through the modified setae of the frontal organ. The frontal organ is located in a medial position at the anterior end of the prosoma, but partially covered by the propeltidium. (**B**) Transmission electron micrograph of a cross-section of the cuticular wall of a modified seta of the frontal organ. The procuticle is electron-translucent basally of the cuticular ridge (green). The cuticular ridge as well as the areas of the wall pores/grooves are built from less electron-dense procuticle and are covered by epicuticle. The epicuticle extends to the basal part of the wall pores/grooves. Abbreviations: cGr: cuticular groove; Ch: chelicera; cR: cuticular ridge; EpC: epicuticle; FO: frontal organ; PrPlt: propeltidium; ProC: procuticle.

approx. 0.1 µm. The base of the frontal organ (Fig. 30A) is filled with electron-dense material and displays fewer pores than the setae.

Within the base, the right seta has two mitochondria-rich (diameter 0.2 µm) dendrites which are enclosed by nine enveloping cells (IDS 1/2, EnvC; Figs. 30A, 31A). The electron density of the cytoplasm of both dendrites and the enveloping cells is equally high and similar to the electron density of the surrounding dense material. There are large vacuole-like spaces between the cells which could be part of the receptor lymph cavity. Distally, the dendrites branch cylindrically multiple times (dBr; Figs. 30B, 31B). The diameter of the branches varies between 0.1 and 2.5 µm. The dendritic branches show an irregular arrangement of microtubules and are enveloped in dense material (DM; Figs. 30B, 31B). In addition, some branches have small electron-dense regions, or so called droplets as well as deteriorated vacuoles and lamellar bodies (*; Fig. 30B). The dense material is mostly found just below the setal wall.

The left seta also has two mitochondria-rich dendrites; however, the mitochondria are larger than in the right seta (diameter 0.5 µm). In addition, the dendrites are surrounded by twelve enveloping cells (IDS 3/4, EnvC; Figs. 30A, 31A). Dendrites and enveloping cells have the same cytoplasm electron density. The vacuole-like spaces between the enveloping cells are larger than in the right receptor and could be part of the receptor lymph cavity. Further distal, one dendrite branches and folds, and displays an irregular arrangement of microtubule doublets (IDS 4, ODS, MT; Figs. 30C, F, 31C, F). Along the course of the seta, the intensity of branching, flattening and folding of this dendrite increases. Within the branches, the microtubuli doublets become single microtubuli and the arrangement becomes regular (Figs. 30D, G, 31D, G). Towards the distal end of the seta, the dendrite displays concentrically wrapped laminae. Within this lamellate section, microtubules are no longer recognizable (Figs. 30E, H, 31E, H). Many vacuoles in the center of the dendrite show deterioration and indicate incomplete fixation. The second dendrite branches cylindrically and is pushed towards the periphery of the seta by the first dendrite (Figs. 30C–E, 31C–E). The second dendrite is also dominated by numerous deteriorated vacuoles and lamellar bodies. However, there are more of these in the left seta than in the right seta (*; Figs. 30C–E). Regions where vacuoles
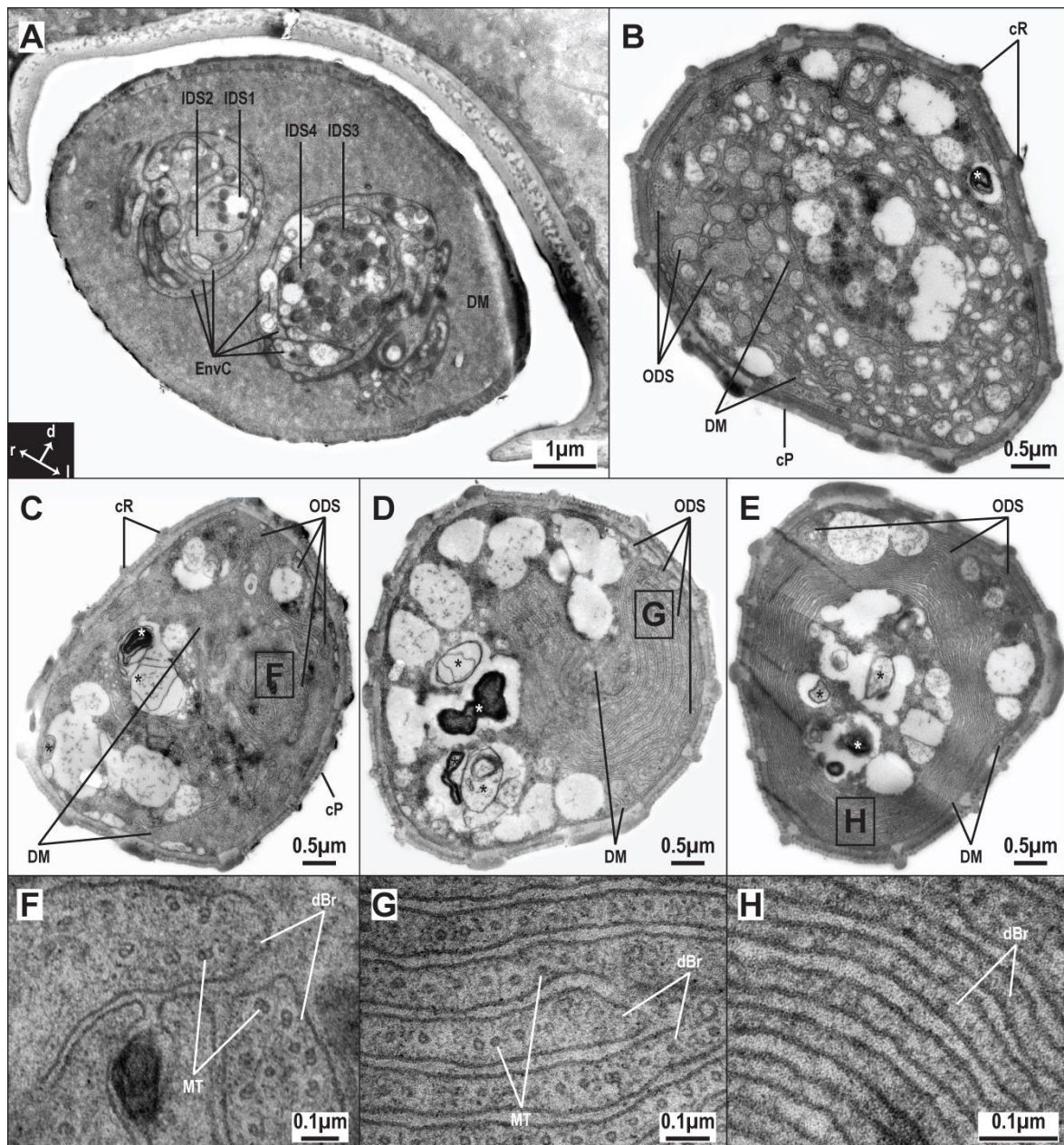
Fig. 30. *Eukoenenia spelaea*, transmission electron micrographs of cross-sections through the frontal organ. (**A**) Section through the unpaired basal part of the frontal organ. Two distinct units of two dendrites each surrounded by enveloping cells can be found. The dendritic units are surrounded by large amount of dense material. (**B**) Right seta. The dendrites have branched cylindrically. In cross-section, cuticular ridges and pits are easily distinguishable. A lamellar body is closely associated with a dendritic branch (asterisk) (**C**) Basal part of the left seta. In addition to the cylindrically branched dendrite, a dendrite with flattened branches is present. In the left seta, lamellar bodies are found in close association with dendrites as well (asterisk). (**D**) Medial part of the left seta. The dendritic branches have become more flattened. (**E**) Proximal part of the left seta. The flattened dendritic branches have become lamellate. (**F**) Close-up of the flattened dendritic branches in C. The microtubule doublets are clearly visible. (**G**) Close-up of the flattened dendritic branches in D. The microtubules are now all single. (**H**) Close-up of the flattened dendritic branches in E. No microtubules are present. Abbreviations: cP: cuticular pit, cR: cuticular ridge; dBr: dendritic branch; d: dorsal; DM: dense material; EnvC: enveloping cell; IDS1–4: inner dendritic segment 1–4; l: left; MT: microtubule; ODS: outer dendritic segment; r: right.
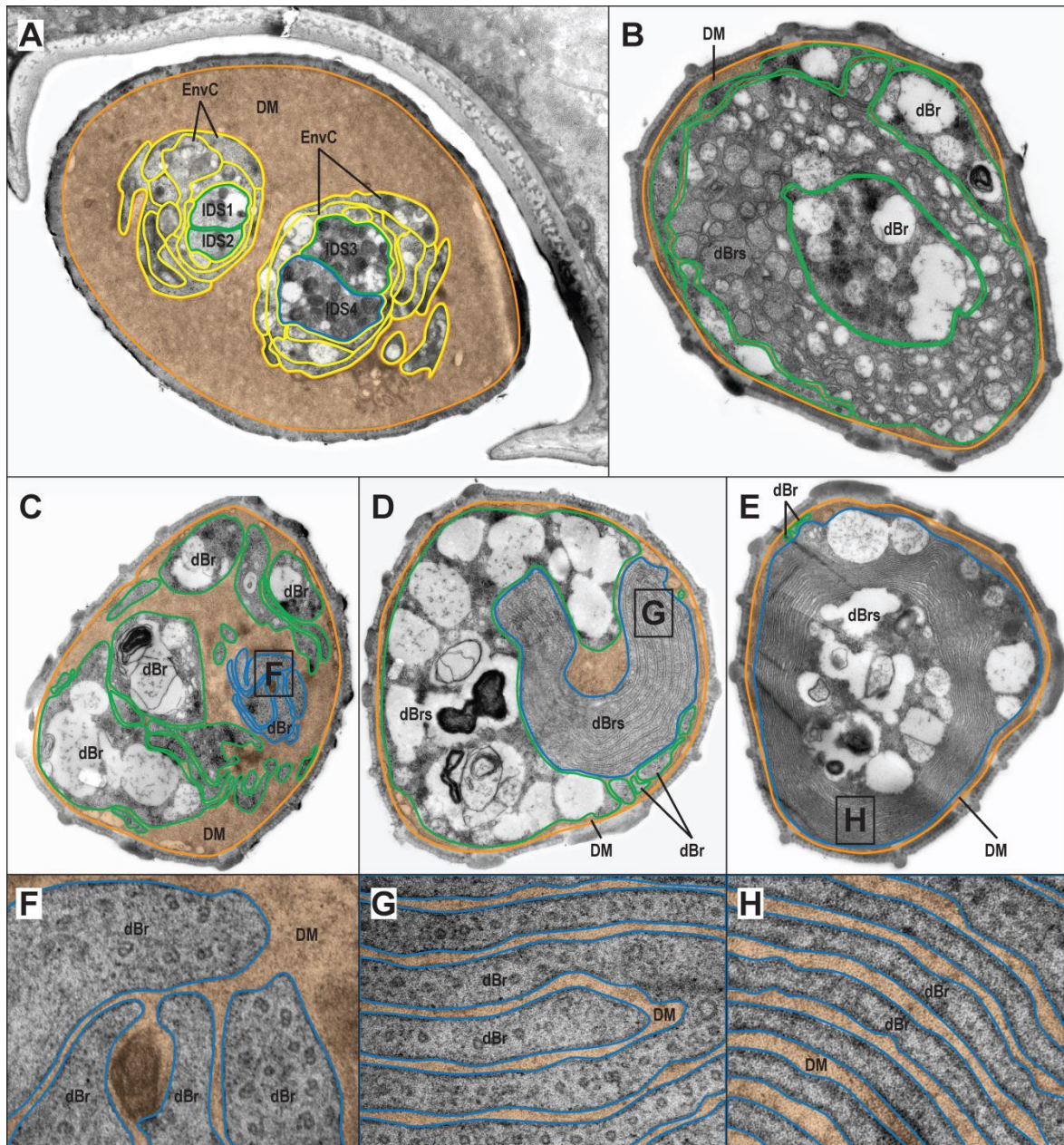
Fig. 31. *Eukoenenia spelaea*, transmission electron micrographs of the frontal organ from Fig. 30 with colored overlay. (**A**) Inner dendritic segments 1 and 2 (right seta, green) are enveloped in nine enveloping cells, whereas inner dendritic segments 3 and 4 (left seta, blue, green) have 12 enveloping cells. The inner dendritic segment is characterized by the presence of mitochondria. (**B**) The right seta is filled with a large number of dendritic branches (green). The dense material (orange) is largely reduced. (**C**) The cylindrically branched dendrite 3 (green) of the left seta displays irregularly sized branches. (**D**) As the dendrites increase their branching, the amount of dense material is reduced. (**E**) Distally, dendrite 3 is reduced to two small branches, whereas the lamellate branches of dendrite 4 (blue) take up most of the space within the seta. Dense material is reduce to a thin layer towards the setal wall. (**F**) The flattened dendritic branches of dendrite 4 at the basal part of the left seta are still similar in thickness to cylindrically branched dendrites. (**G**) The arrangement of the flattened branches of dendrite 4 becomes more regular, the branches themselves become more flattened. (**H**) Distally, the dendritic branches of dendrite 4 are now so flat, that they appear as lamella. Abbreviations: dBr: dendritic branch; dBrs: dendritic branches; DM: dense material; EnvC: enveloping cell; IDS1–4: inner dendritic segment 1–4.

also show small electron-dense droplets. Similar to the right seta, the dense material is mostly found just below the setal wall. However, in the left seta the amount of dense material decreases from proximal to distal (Figs. 30C–E, 31C–E).

3.2.8.2 Lateral organ

The lateral organ is a bilateral structure on the prosoma, just below the propeltidium and anterior to the base of the pedipalps (LO; Figs. 6A, C, 32A). It consists of four single, finger-like modified setae extending anteroventral (Figs. 11B, 32A). The setae are arranged slightly diagonally from anterior to posterior along the ventral side of the propeltidium. The size of the setae is similar to the setae of the frontal organ with an approximate length of 25 µm and an approximate thickness of 4.5 µm. Like in the frontal organ, the cuticle is rich in cuticular grooves and reinforced with honeycomb patterned cuticular ridges (cP, cR; Figs. 32C, D). The ultrastructure of the cuticle is the same as in the frontal organ.

The nerve supplying the lateral organ consists of eight dendritic units (IDS; Fig. 32B). This suggests that two dendrites extend into each seta. The enveloping cells could not be identified, because the transmission electron microscopic section of the nerve is too far proximal. The dendrites branch cylindrically within the setae (dBr; Figs. 32C, D). The branches display an uneven thickness which ranges between 0.1 and 4.2 µm and show only few microtubules. Like in the frontal organ, the dendritic branches have accumulations of dense material between them (DM; Figs. 32C, D). The dense material is largely located towards the inside of the setae. In contrast to the frontal organ, all dendritic branches of the lateral organ display many small electron-dense droplets as well as few electron-translucent droplets. Deteriorated vacuoles were not found.
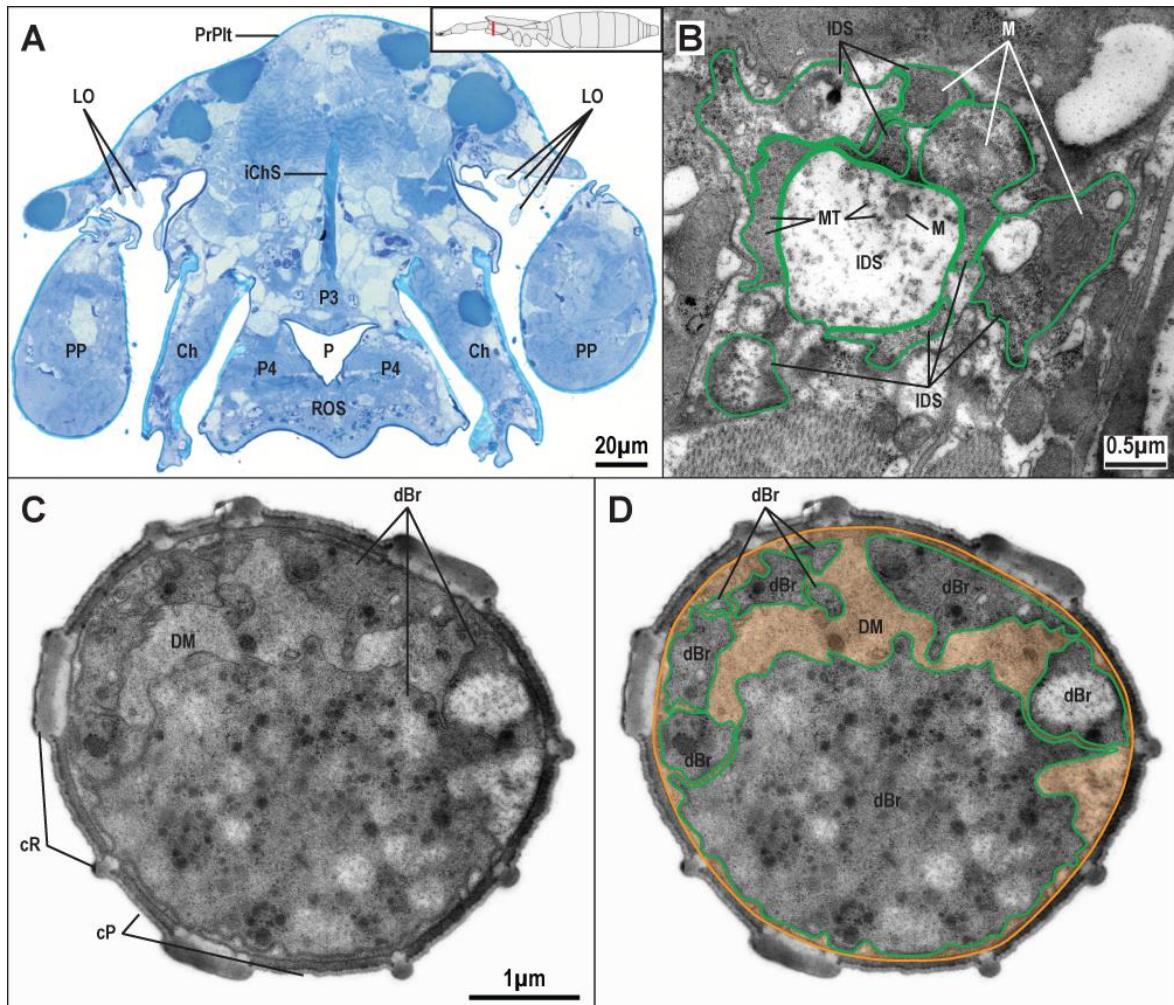
Fig. 32. *Eukoenenia spelaea*, lateral organ. (**A**) Light micrograph of a cross-section at the level of the chelicerae and pedipalps of a male. The lateral organs are located laterally beneath the propeltidium. Each modified seta is attached separately to the body. (**B**) Transmission electron micrograph of the eight inner dendritic segments (green) associated with the four lateral organs of one body half. The microtubules are arranged irregularly. (**C**) Transmission electron micrograph of a cross-section of a modified seta. The dendrites are branched cylindrically. Like in the frontal organ, the cuticular wall consists of cuticular ridges, which build the honeycomb pattern, and cuticular pits, which carry the wall pores. (**D**) Same as C with colored overlay. The dendritic branches vary in size. The dense material (orange) is largely located towards the inside, while the dendritic branches are oriented towards the setal wall. Abbreviations: Ch: chelicera; cP: cuticular pit; cR: cuticular ridge; dBr: dendritic branch; DM: dense material; iChS: intercheliceral septum; IDS: inner dendritic segment; LO: lateral organ; M: mitochondrion; MT: microtubule; P: pharynx; P3–4: prosomal muscle; PP: pedipalp: PrPlt: propeltidium; ROS: rostrosoma.

3.2.8.3   Sensory setae

Numerous sensory setae are found all over the body and flagellum (see 3.1). They are nested flexibly within the cuticle. At the region of insertion, the procuticle differentiates into an endocuticle and an electron-dense exocuticle (EnC, ExC, ProC; Figs. 33B, 34C). The epicuticle is electron-translucent. At the base of each of the seta I found seven sensory cells in a circular arrangement around a central enveloping cell. This enveloping cell has apical microvilli which extend into the inner
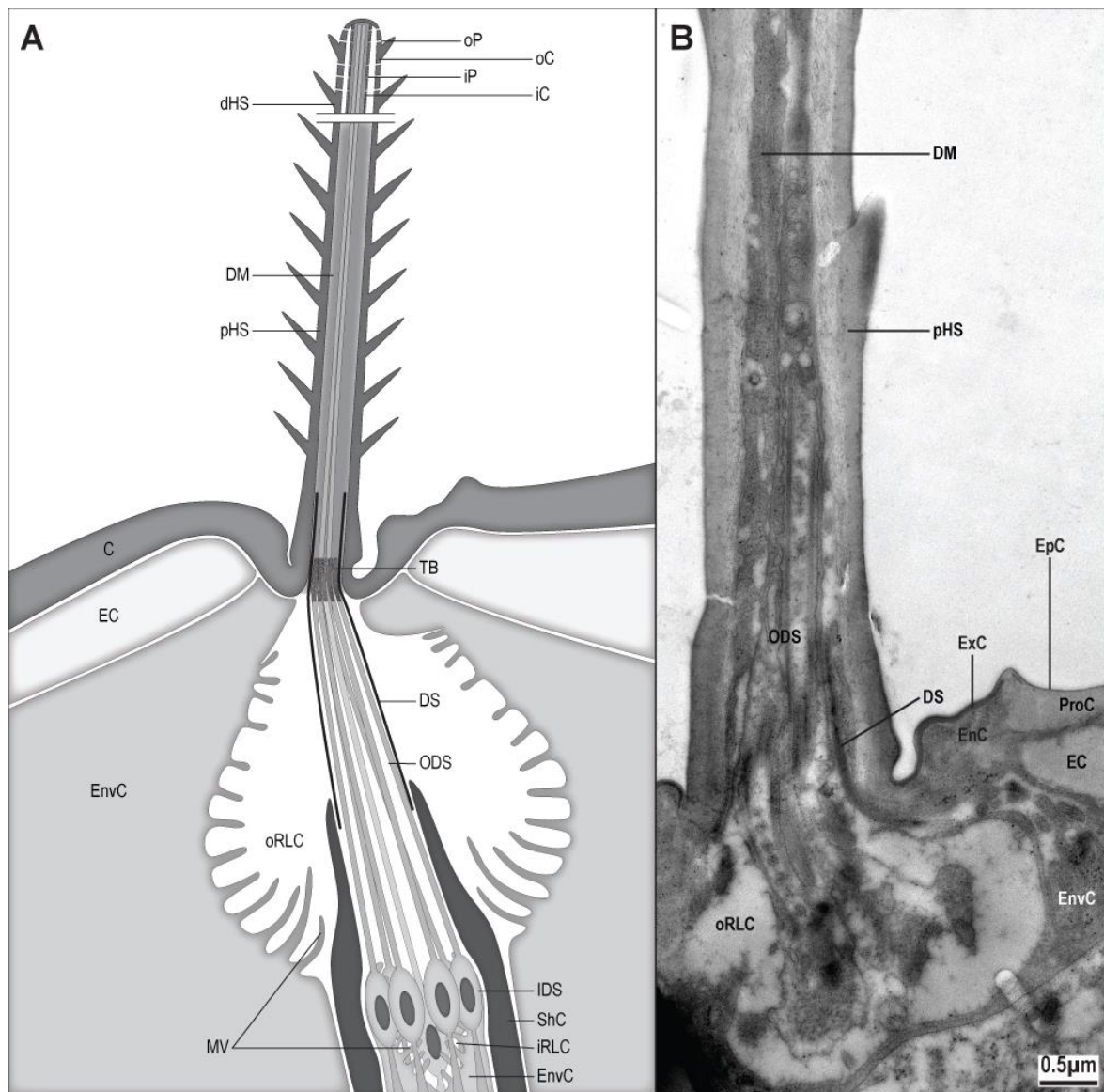
Fig. 33. *Eukoenenia spelaea*, sensory seta. (**A**) Schematic drawing of the microscopic anatomy of the sensory seta. Seven dendrites are associated with the seta, two of which extend into the hair shaft. The distal part of the hair shaft displays double walls and wall pores. (**B**) Transmission electron micrograph of a longitudinal section of the basal part of a sensory seta. The outer dendritic segments extend into the hair shaft. Abbreviations: C: cuticle; dHS: distal hair shaft; DM: dense material; DS: dendritic sheath; EC: epidermal cell; EnvC: enveloping cell; ExC: exocuticle; iC: inner cuticle; IDS: inner dendritic segment; iP: inner pore; iRLC: inner receptor lymph cavity; oC: outer cuticle; ODS: outer dendritic segment; oP: outer pore; oRLC: outer receptor lymph cavity; pHS: proximal hair shaft; ShC: sheath cell; TB: tubular body.

receptor lymph cavity (EnvC, IDS, MV; Figs. 33A, 34A). The inner dendritic segment of the sensory cells is characterized by the presence of mitochondria (IDS, M; Fig. 34A).

The outer dendritic segments of the sensory cells are characterized by a 9 x 2 + 0 arrangement of microtubules (ODS; Figs. 33A, 34B) and are arranged as a circle with one dendrite in the center. In contrast to the surrounding six dendrites, the

66
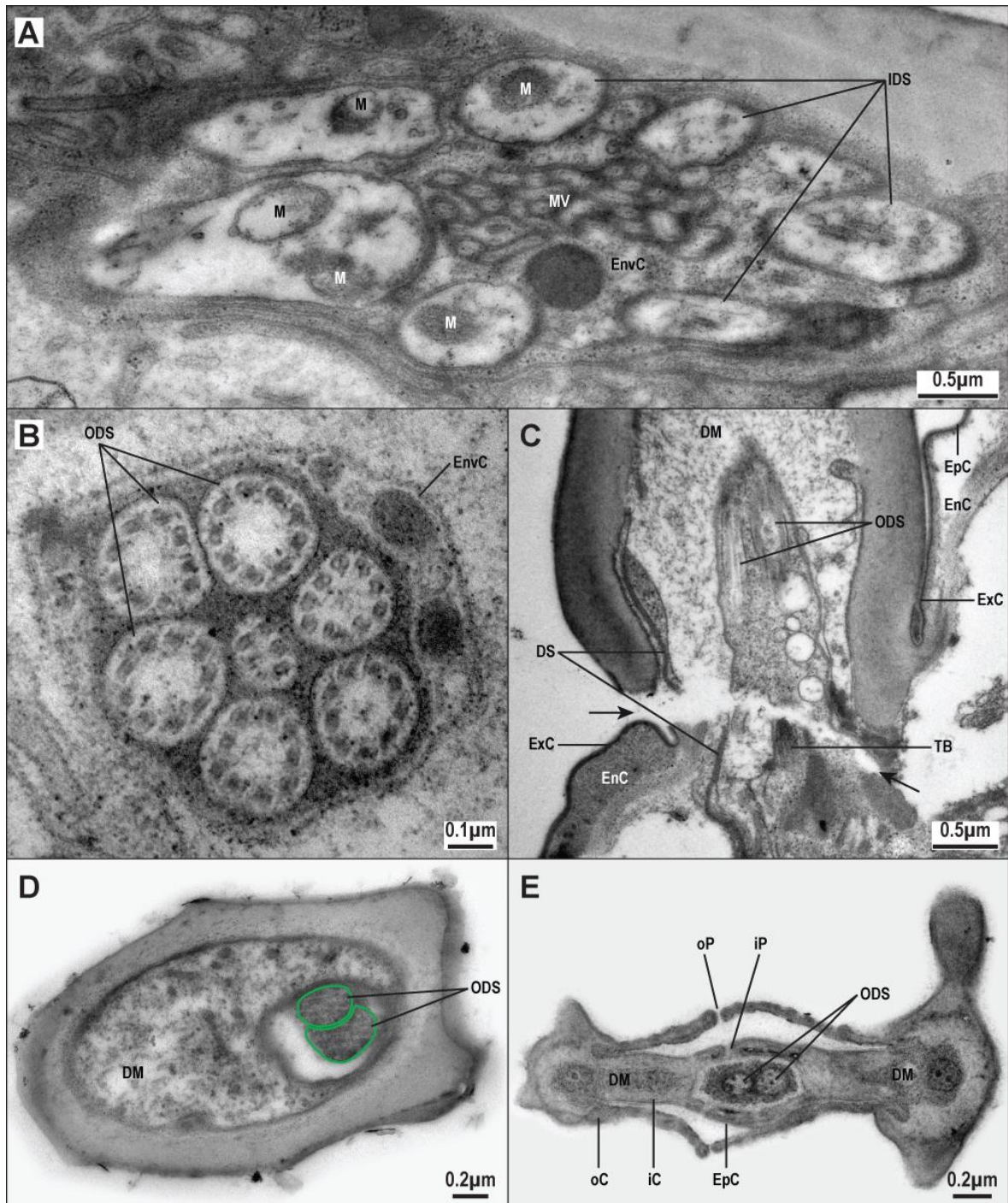
Fig. 34. *Eukoenenia spelaea*, transmission electron micrographs of sections through a sensory seta. (**A**) Cross-section of the area of the inner receptor lymph cavity. Seven dendrites are arranged in a circle around the microvilli of the central enveloping cell. (**B**) Cross-section of the area below the sensory seta. Six outer dendritic segments are arranged in a circle with the seventh dendrite located centrally. The central dendrite has a reduced number of microtubule doublets. (**C**) Longitudinal section of the basal part of the sensory seta. The dendritic sheath extends into the hair shaft. Two of the original seven dendrites continues into the hair. Arrows indicate an artefact. (**D**) Cross-section of the proximal hair shaft containing two closely neighboring dendrites (green). (**E**) Cross-section of the distal hair shaft. The two dendrites are located centrally within the hair. The hair itself has now an inner and outer cuticle with wall pores. The outer pore is open, the inner pore is clogged with electron-translucent material. The inner wall is covered with epicuticle. Abbreviations: DM: dense material; DS: dendritic sheath; EnC: endocuticle; EnvC: enveloping cell; EpC: epicuticle; ExC: exocuticle; iC: inner cuticle; IDS: inner dendritic segment; iP: inner pore; M: mitochondrion; MV: microvilli; oC: outer cuticle; ODS: outer dendritic segment; oP: outer pore; TB: tubular body.

central dendrite displays a 6 x 2 + 0 arrangement (Fig. 34B). The outer dendritic segments of the dendrites extend through the outer receptor lymph cavity and are embedded in an electron-dense dendritic sheath. This sheath is present only in the region of the cuticular socket and the proximal part of the seta (DS, oRLC; Figs. 33, 34C).

Two of the seven dendrites of a sensory seta extend to the tip of the seta, the other dendrites form a number of tubular bodies at the seta's point of insertion (TB; Figs. 33A, 34C). The two dendrites extending to the tip of the seta are unbranched and surrounded by dense material (Figs. 33, 34C–E). The number of microtubules found within the dendrites decreases towards the tip of the seta. At the distal part of the hair shaft, the cuticle wall is doubled and displays wall pores (iC, oC, iP, oP; Figs. 33A, 34E). The exact number of wall pores could not be established. The outer cuticular wall is approx. 0.05 µm thick, while the inner cuticular wall is only approx. 0.1 µm. The pores of the outer wall are completely open, whereas the pores of the inner wall are plugged and covered with epicuticle (Figs. 33A, 34E).

3.2.8.4 Trichobothria

Trichobothria are found on leg 1. The hair is nested in a cup-shaped socket which is divided into an inner and an outer compartment (cS; Figs. 35A, 36A, C). Both compartments have a cuticle intima. The outer compartment is open apically, the opening being surrounded by a ring of cuticular teeth (tBR; Figs. 35A, B, 36). The diameter of the outer segment is approx. 6.2 µm. It is surrounded by epidermal cells. The inner compartment of the socket is separated from the outer compartment by a thin cuticular membrane (cMB; Figs. 35A, B, 36). The diameter of the inner compartment of the socket is approx. 4.5 µm.

The receptor lymph cavity is separated into two parts, the inner and outer receptor lymph cavity (iRLC, oRLC; Figs. 36A, C). The inner receptor lymph cavity is located centrally between the inner dendritic segments. The outer receptor lymph cavity has a basal and an apical part. The basal part is located ventrolateral to the inner compartment of the socket (Figs. 36A, C). The apical part of the outer receptor lymph cavity forms the inside of the inner compartment. Enveloping cells with microvilli surround the entire outer receptor lymph cavity (EnvC; Figs. 36A, C). The
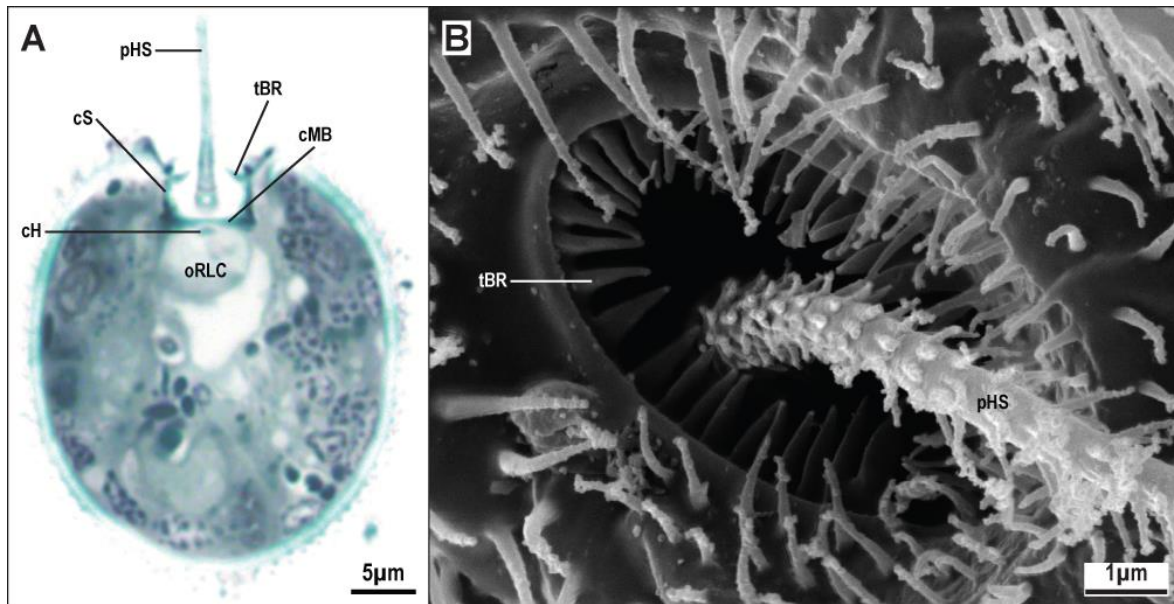
Fig. 35. *Eukoenenia spelaea*, trichobothrium. (**A**) Light micrograph of a cross-section through leg 1, with a longitudinal section of a trichobothrium. The hair shaft is located within a cuticular socket. The outer receptor lymph cavity is separated from the socket with a cuticular membrane. (**B**) Scanning electron micrograph of the basal part of the trichobothrium. The hair shaft is covered with small cuticular spikes which are arranged regularly along the shaft. A row of cuticular teeth is located along the rim of the socket. Abbreviations: cH: cuticular helmet; cMB: cuticular membrane; cS: cuticular socket; oRLC: outer receptor lymph cavity; pHS: proximal hair shaft; tBR: toothed bothrial rim.

cuticular wall of the socket only leaves a small opening for the enveloping cells to enter the inner compartment of the socket. This cuticular opening is also, where the dendrites enter the inner compartment.

Like in the outer receptor lymph cavity, the enveloping cells which form the inner receptor lymph cavity have apical microvilli (MV; Fig. 36C). A total of five dendrites is associated with a trichobothrium (IDS, ODS; Figs. 36A, C). The dendrites enter the outer receptor lymph cavity and are enveloped by a dendritic sheath which is built by sheath cells (DS, ShC; Figs. 36A, C). The dendrites connect to the helmet (cH). The helmet is a cuticular structure connected to the base of the hair shaft which is located centrally in the outer compartment of the socket (pHS; Figs. 36A, C). In contrast to described trichobothria of other arachnids, the helmet is open and ciliary sections of four dendrites continue through the opening into the proximal part of the shaft (Fig. 36). The arrangement of microtubules is the typical 9 x 2 + 0. Distally, only one outer dendritic segment is present inside the shaft. It is surrounded by dense material (DM; Fig. 36B). Cuticular pores could not be observed on the hair shaft.

69
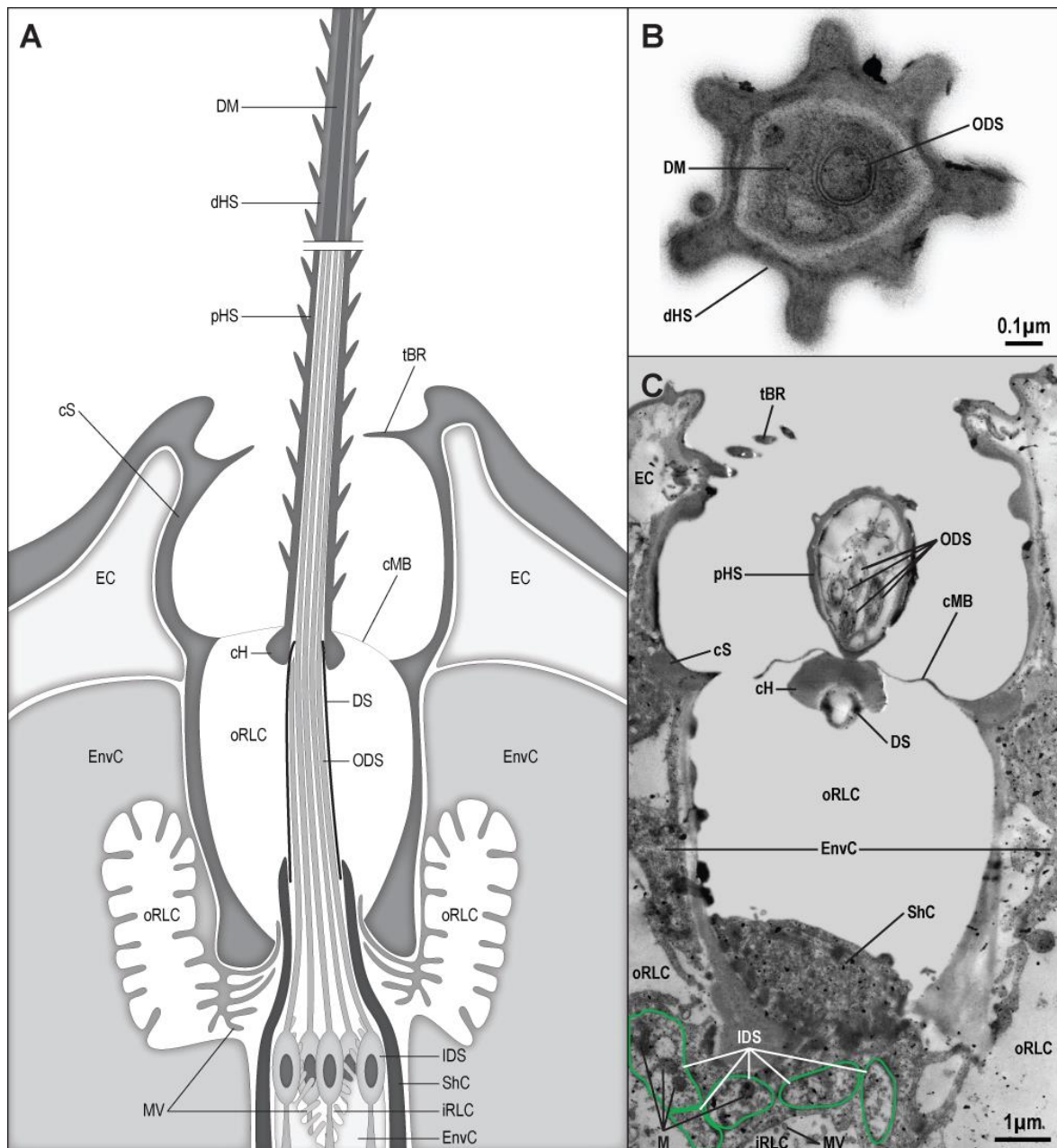
Fig. 36. *Eukoenenia spelaea*, trichobothrium. (**A**) Schematic drawing of the proposed microscopic anatomy of a trichobothrium, reconstructed based on several TEM sections. The cuticular socket of the bothrial wall extends basally to the sheath cells. The cuticular helmet is most likely apically open allowing the outer dendritic segments to pass into the hair shaft. (**B**) Transmission electron micrograph of a cross-section of the distal hair shaft. Of the four dendrites entering the hair shaft proximally, only one dendrite extends to the distal part of the hair. The outer dendritic segment is enveloped by dense material. (**C**) Transmission electron micrograph of a longitudinal section of the socket area. The sheath cells extend into the basal part of the cuticular socket. Four of the five inner dendritic segments (green) extend into the hair shaft. The dendritic sheath terminates at the cuticular helmet. Abbreviations: cH: cuticular helmet; cMB: cuticular membrane; cS: cuticular socket; dHS: distal hair shaft; DM: dense material; DS: dendritic sheath; EC: epidermal cell; EnvC: enveloping cell; IDS: inner dendritic segment; iRLC: inner receptor lymph cavity; ODS: outer dendritic segment; M: mitochondrion; MV: microvilli; oRLC: outer receptor lymph cavity; pHS: proximal hair shaft; ShC: sheath cell; tBR: toothed bothrial rim.

3.2.9 Heart

The heart is a muscular tube located in the dorsal midline of segments 7–14 (H; Fig. 37). The heart is flat in cross-section in the central region of segments but more roundish with a widened lumen in the transitional region between adjacent segments (Figs. 38A, B). Ostia, which are part of the ground pattern of the heart in arthropods, could not be found. Using transmission electron microscopy I did not detect any hemolymph cells in the heart lumen. The heart is surrounded by hemolymph and connective tissue. The heart tube consists of one thin layer of circular musculature. Over its entire length, the heart is built from approx. 80 cells (Fig. 38). Dilator musculature has not been identified. The heart tube is a delicate and small structure that is difficult to analyze in light microscopy. In transmission electron microscopic cross-sections, the heart tube appears as a syncytium with loosely scattered, irregular bundles of contractile filaments. A sarcoplasmic reticulum could not be clearly identified. The myofibrils seem to be interrupted and the filaments are
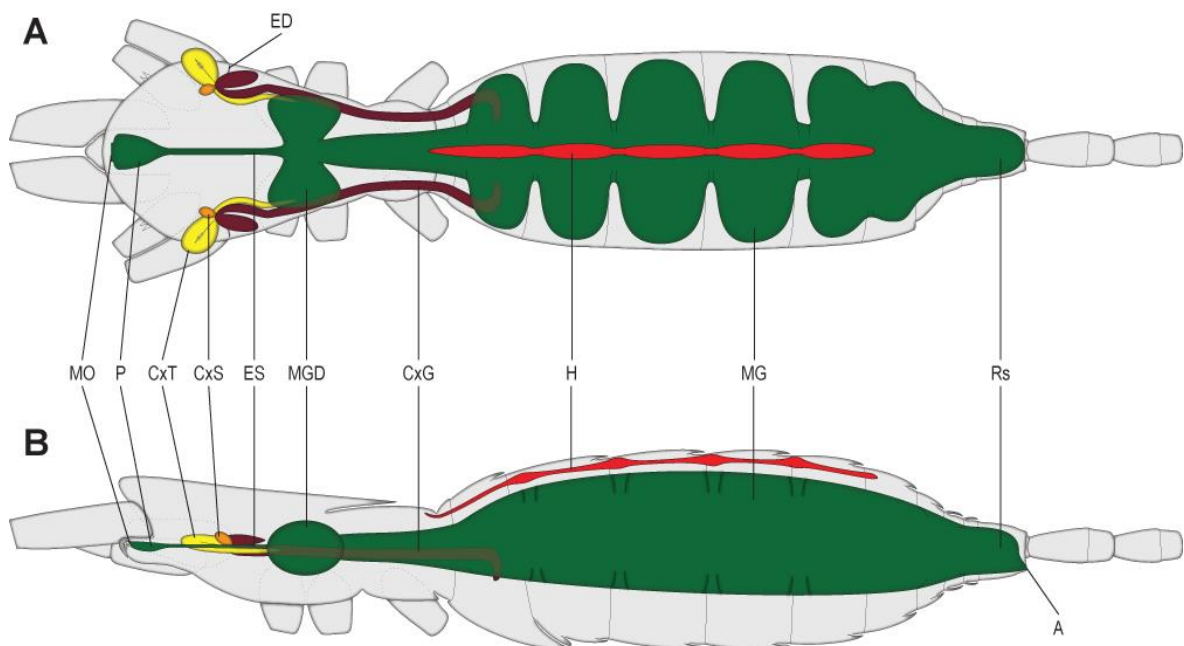
Fig. 37. *Eukoenenia spelaea*, schematic drawing of the heart, the alimentary system, and the coxal gland. (**A**) Dorsal view. In the prosoma, the midgut (red) has two lateral diverticula in the area of leg 2 and 3, just posterior to where the esophagus terminates. The opisthosomal midgut is a sac with indentations where the dorsoventral musculature is located. The saccule (orange) as well as the anterior structures of the tubule (yellow) and glandular section of the coxal gland (brown) are located in the area of leg 1. The tubule extends into the coxa of leg 1. The excretory duct opens to the outside just posterior to the coxa of leg 1. The coxal gland's glandular section extends into segment 9. The heart (purple) extends from the posterior end of the prosoma to segment 14. (**B**) Lateral view. The heart has a flattened appearance within a segment and has a roundish diameter at the junction of two segments. The anal opening lies in the membranous fold between segment 18 and the flagellum's basal article. Abbreviations: A: anus; CxG: coxal gland glandular section; CxS: coxal gland saccule; CxT: coxal gland tubule; ED: excretory duct; ES: esophagus; H: heart; MG: midgut; MGD: midgut diverticula; MO: mouth opening; P: pharynx; Rs: rectal sac.

irregularly scattered throughout the fibril (arrowheads; Figs. 38D, E). A sarcomere structure is barely recognizable, with the membrane of the muscle cells forming lateral infoldings wherever a Z-lines is located (arrows; Figs. 38D, E). These membrane infoldings might be considered representing elements equivalent to the T-tubular system. The muscle cell is enlarged in the region of the heterochromatin-rich oblong nucleus. Few mitochondria of various sizes are dispersed throughout the muscle cell. A nerve for stimulation of the heart muscle has also not been found.
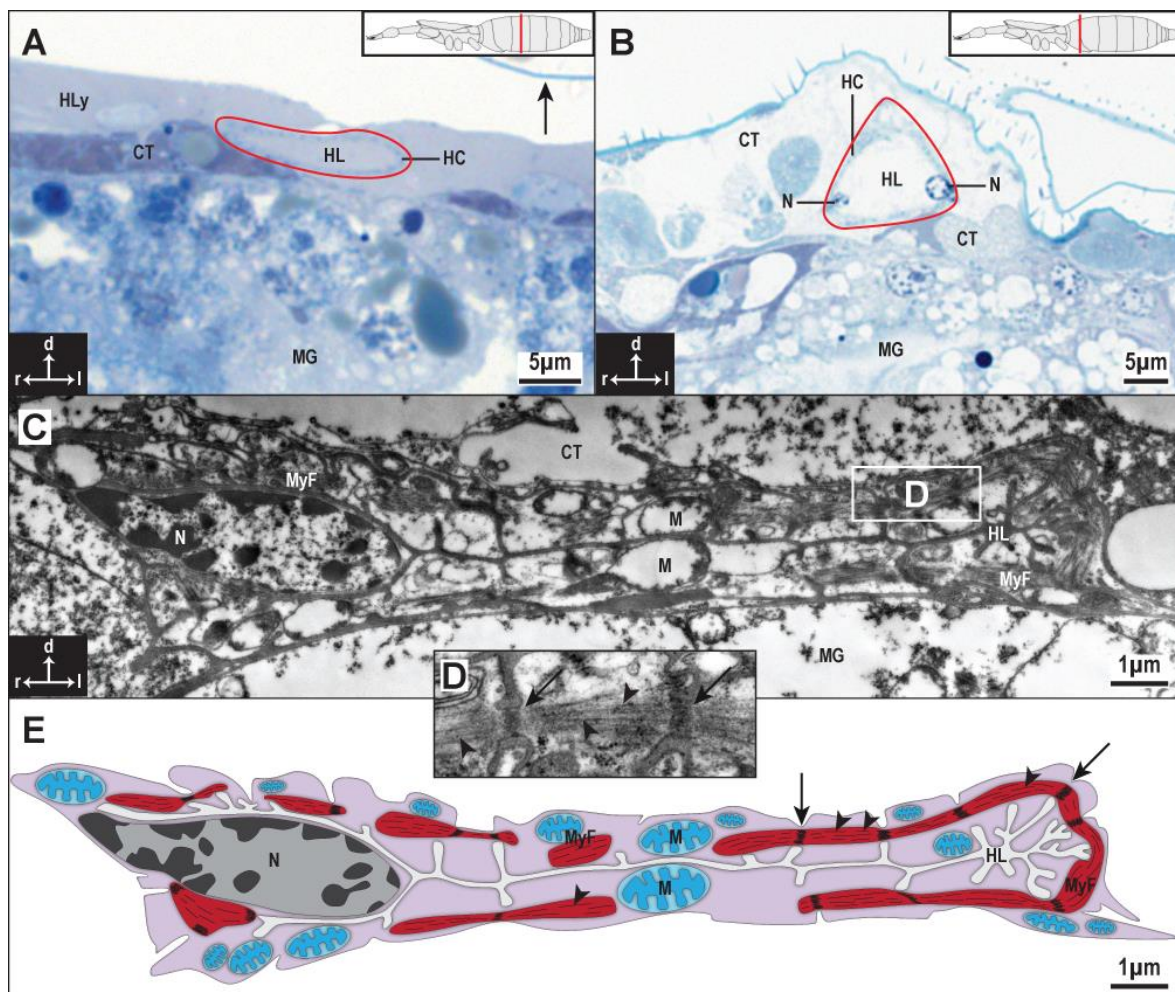
Fig. 38. *Eukoenenia spelaea*, cross-sections through the heart. (**A**) Light micrograph of the heart in segment 11 of the opisthosoma. The overall shape of the heart is flattened. The heart is surrounded by hemolymph and connective tissue. The arrow indicates an artificial separation of the cuticle from the body. (**B**) Light microscopic image of the heart in the area between segment 9 and 10. The lumen of the heart is open and extended as compared to the flattened appearance in a more middle position of a segment (see A). (**C**) Transmission electron micrograph of a cross section through the heart. The lumen is greatly reduced. No distinct pericardial wall was found. The heart is located adjacent to the midgut. (**D**) Transmission electron micrographic close-up of a myofibril. Dark areas similar to Z-lines (arrows) are associated with the infoldings of the cell membrane. Between these areas are muscle filaments visible (arrowheads). (**E**) Schematic drawing of C. The cell is enlarged in the area of the nucleus. The thick filaments (arrowheads) are distributed irregularly within the myofibril. Abbreviations: CT: connective tissue; d: dorsal; HC: heart cells; HL: heart lumen; HLy: hemolymph; l: left; M: mitochondrion; MG: midgut; MyF: myofibril; N: nucleus; r: right.

3.2.10 Digestive tract

The digestive tract consists of the foregut (mouth opening and pharynx within the rostrosoma, and esophagus), the midgut, prosomal midgut diverticula, and the rectal sac. A postcerebral stomach, as reported for other arachnid groups, is not present. The pharynx and esophagus are lined with a cuticle intima. The midgut, the prosomal midgut diverticula and the rectal sac have no cuticle lining. A cuticle-lined hindgut, typical for arthropods, is not present. The midgut was free of identifiable food particles. The anal opening is located in the membrane between segment 18 and the flagellar base ring (A; Fig. 37).

3.2.10.1 Pharynx

The pharynx begins at the mouth opening. The pharynx is X-shaped. The two arms of the upper part of the X are wide open, whereas the lower part of the X is narrow and there is no open lumen of the arms (P; Fig. 39A). Four strands of musculature attach to the pharynx forming the precerebral suction pump: two strands of lateral musculature (P4), one strand of dorsal musculature (P3), and one strand of endosternal musculature (E8; Fig. 23). One layer of circular musculature is located around the pharynx. The circular muscle fibers are located alternating between the muscle fibers of pharyngeal muscles P3 and P4 (Figs. 21B, 22A). The lumen of the pharynx is covered by a thick cuticle (EnC, EpC, ExC; Fig. 39B). The cuticle consists of an electron-translucent endocuticle which is covered by an electron-dense exocuticle. The exocuticle is approximately twice as thick as the endocuticle and shows regions of increased electron density (Fig. 39B). The epicuticle is a thin layer on top of the exocuticle and also appears to be electron-dense.

3.2.10.2 Esophagus

The esophagus extends from the posterior end of the pharynx to the region of the 2nd leg (Fig. 37). It is enveloped by the connectives between the supra- and subesophageal ganglia, and is separated from the neuropil by the neurilemma. The esophageal lumen has the shape of a stylized X and is thin. The esophagus is surrounded by a few irregularly placed thin fibers of longitudinal musculature followed by an outer ring of thin circular musculature (cMC, lMC; Fig. 39C). The circular musculature is a syncytium, which is indicated by the presence of two
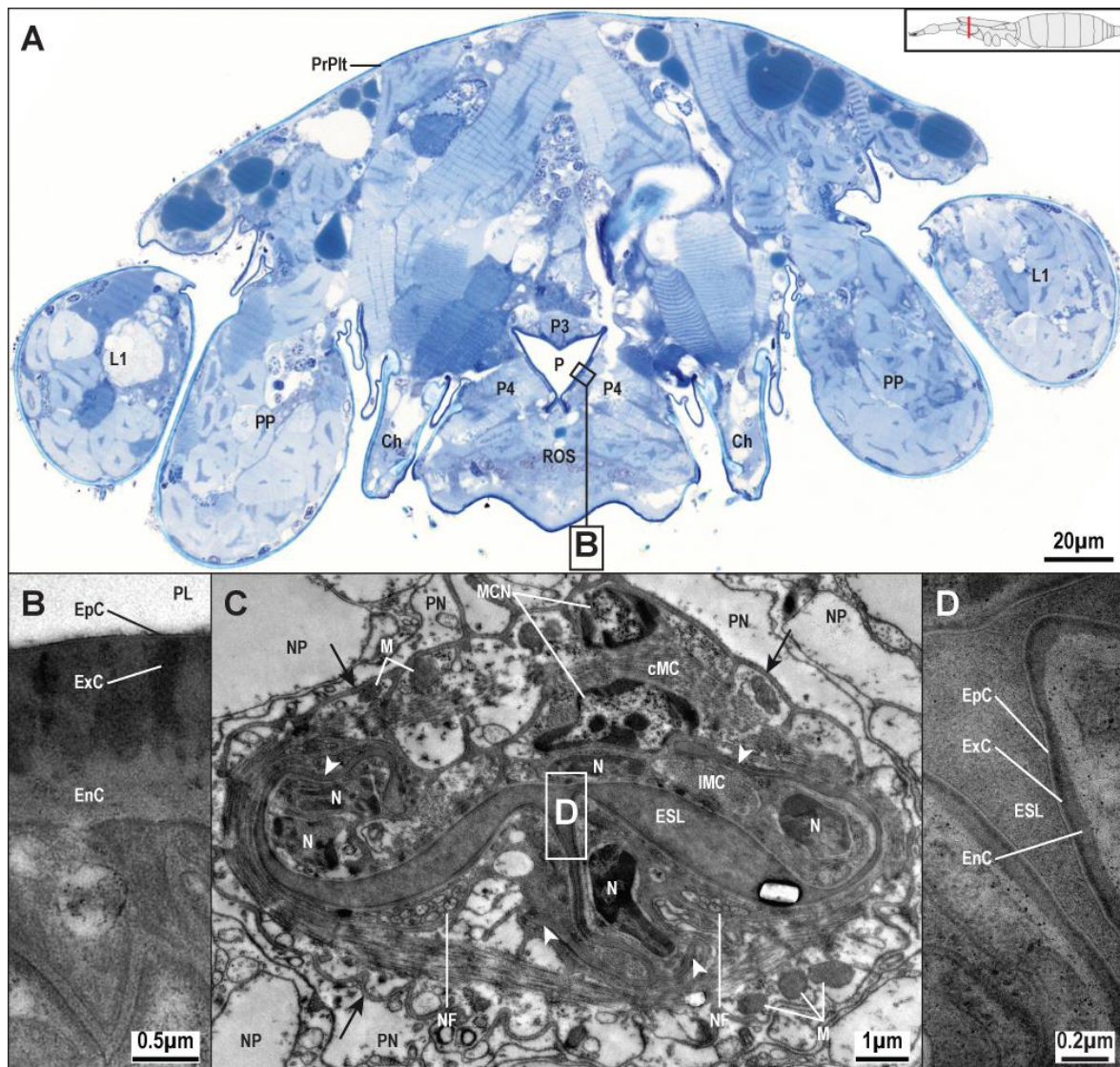
Fig. 39. *Eukoenenia spelaea*, pharynx and esophagus. (**A**) Light micrograph of a cross-section at the level of the pedipalps of a female. The pharynx is X-shaped; however, the lower shanks of the pharynx have no open lumen, thus, in cross-section, the actual open lumen of the pharynx resembles a "V". (**B**) Transmission electron micrograph of the cuticular intima of the pharynx. The exocuticle is heterogeneous electron-dense and thicker than the electron-translucent endocuticle. (**C**) Transmission electron micrograph of a cross-section through the esophagus. The lumen in the lateral branches of the esophagus is largely reduced/collapsed (white arrowheads). Two nuclei can be found in the circular muscle cell indicating its syncytial character. Two nerve fibers are located ventrolateral. The esophagus is surrounded by the neurilemma (black arrows), which is produced by the perineurium. (**D**) Close-up transmission electron micrograph of the cuticular intima of the esophagus in C. The endocuticle is the thickest of the three cuticle layers. The epicuticle is electron-translucent. Abbreviations: Ch: chelicera; cMC: circular muscle cell; EnC: endocuticle; EpC: epicuticle; ESL: esophagus lumen; ExC: exocuticle; L1: leg 1; lMC: longitudinal muscle cell; M: mitochondrion; MCN: muscle cell nucleus; N: nucleus; NF: nerve fiber; NP: neuropil; P: pharynx; P3/P4: prosomal muscle 3/4; PL: pharynx lumen; PN: perineurium; PP: pedipalp; PrPlt: propeltidium; ROS: rostrosoma.

neighboring nuclei. The cell membrane of the circular muscle cells is invaginated at the Z-lines, similar to the heart muscle. The paired nerve supplying the esophagus is located ventrolateral between the circular musculature and the epithelial cells (NF; Fig. 39C). Cross-sections show a minimum of five epithelial cells forming the esophagus (Fig. 39C). These cells have irregularly shaped nuclei, perinuclear

cytoplasm, and few mitochondria. The lumen of the esophagus is covered by cuticle with a thick electron-translucent layer of endocuticle, a thin electron-dense layer of exocuticle, and a thin electron-translucent layer of epicuticle (EnC, EpC, ExC; Fig. 39D).

3.2.10.3 Midgut

The prosomal midgut is tube-shaped and forms two lateral diverticula in the region of the 3rd leg (MGD; Fig. 37). The diverticula are simple evaginations of the midgut tube. The epithelium of the midgut and the diverticula have few strands of longitudinal and incomplete circular musculature which appear to consist of one myofibril per muscle cell (lMC, cMC; Fig. 40C). The lumen of the midgut and diverticula is narrow. The epithelium appears pseudo-stratified and is identical in the midgut tube and the diverticula. It consists of two distinct types of cells, digestive cells and secretory cells (DC, SC; Figs. 40A, B). Digestive cells are more numerous than secretory cells, high prismatic and have a basal nucleus. Numerous lipid vesicles can be seen in the lightly stained cytoplasm of the digestive cells (LV; Fig. 40B). Secretory cells are fewer in number and are easily recognized in LM due to the dark staining cytoplasm as well as the high number of intensively staining secretory vesicles (*, SC; Figs. 40A, B). As in the digestive cells, the nuclei are located at the base of the cells. Transmission electron micrographs show a microvilli border in both cell types. The microvilli are numerous and extend into the small midgut lumen (MV; Fig. 40B). Apical tubuli are more abundant in digestive cells than in secretory cells (AT; Fig. 40B).

The opisthosomal midgut (Fig. 40A) has the general shape of a sac with indentations caused by the dorsoventral musculature segmentally intersecting the midgut (Fig. 37A). The epithelium of the opisthosomal midgut is identical to that of the prosomal midgut. A distinction between midgut and midgut diverticula is not possible.
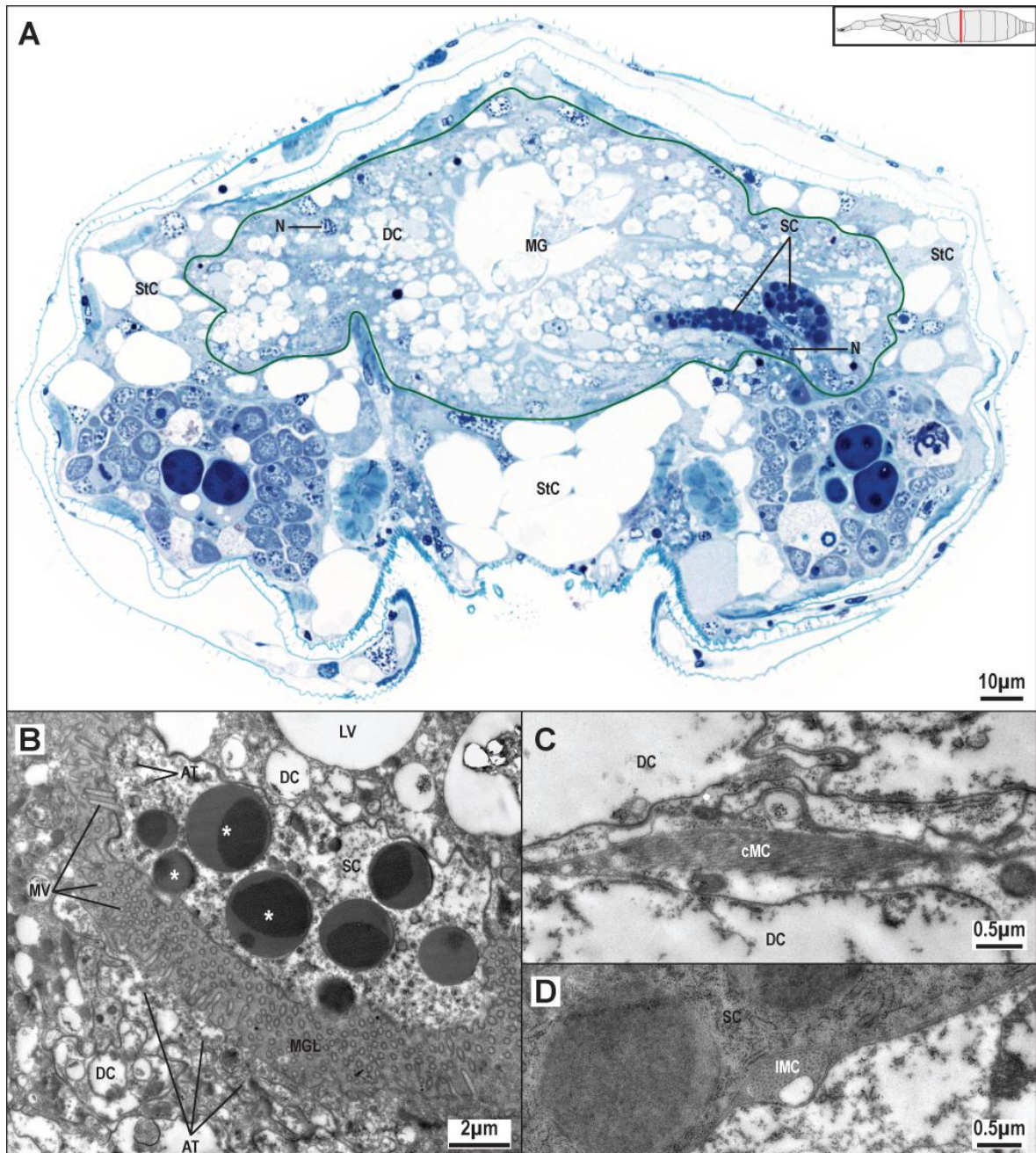
Fig. 40. *Eukoenenia spelaea*, midgut of the opisthosoma. (**A**) Light micrograph of a cross-section through segment 10 of a male. The midgut (red) is a simple sac with indentations caused by the dorsoventral opisthosoma musculature. Secretory cells can be easily distinguished from digestive cells. (**B**) Transmission electron micrograph of the midgut epithelium. Secretory cells are recognized by the electron-dense secretion granules (asterisk). The microvilli of the secretory and digestive cells extend into the midgut lumen. Apical microtubuli are more numerous in digestive cells than in secretory cells. The digestive cells have large electron-translucent excretory vesicles. (**C**) Transmission electron micrograph of the semicircular midgut musculature. The muscle cells are located within indentations between digestive cells. (**D**) Transmission electron micrograph of the longitudinal midgut musculature. The thin muscle cells can be found spread sparsely along the midgut. Abbreviations: AT: apical microtubule; cMC: circular muscle cell; DC: digestive cell; ExV: excretory vesicle; IMC: longitudinal muscle cell; MG: midgut; MGD: midgut diverticula; MV: microvilli; N: nucleus; SC: secretory cell; StC: storage cell.

76

3.2.10.4 Rectal sac

The rectal sac is located in the metasoma, segments 15–18 (Rs; Fig. 37). It is differentiated from the midgut by a single-layered epithelium consisting of large, high-prismatic cells (RsC; Figs. 41A, B) with more or less basal nuclei of the rectal
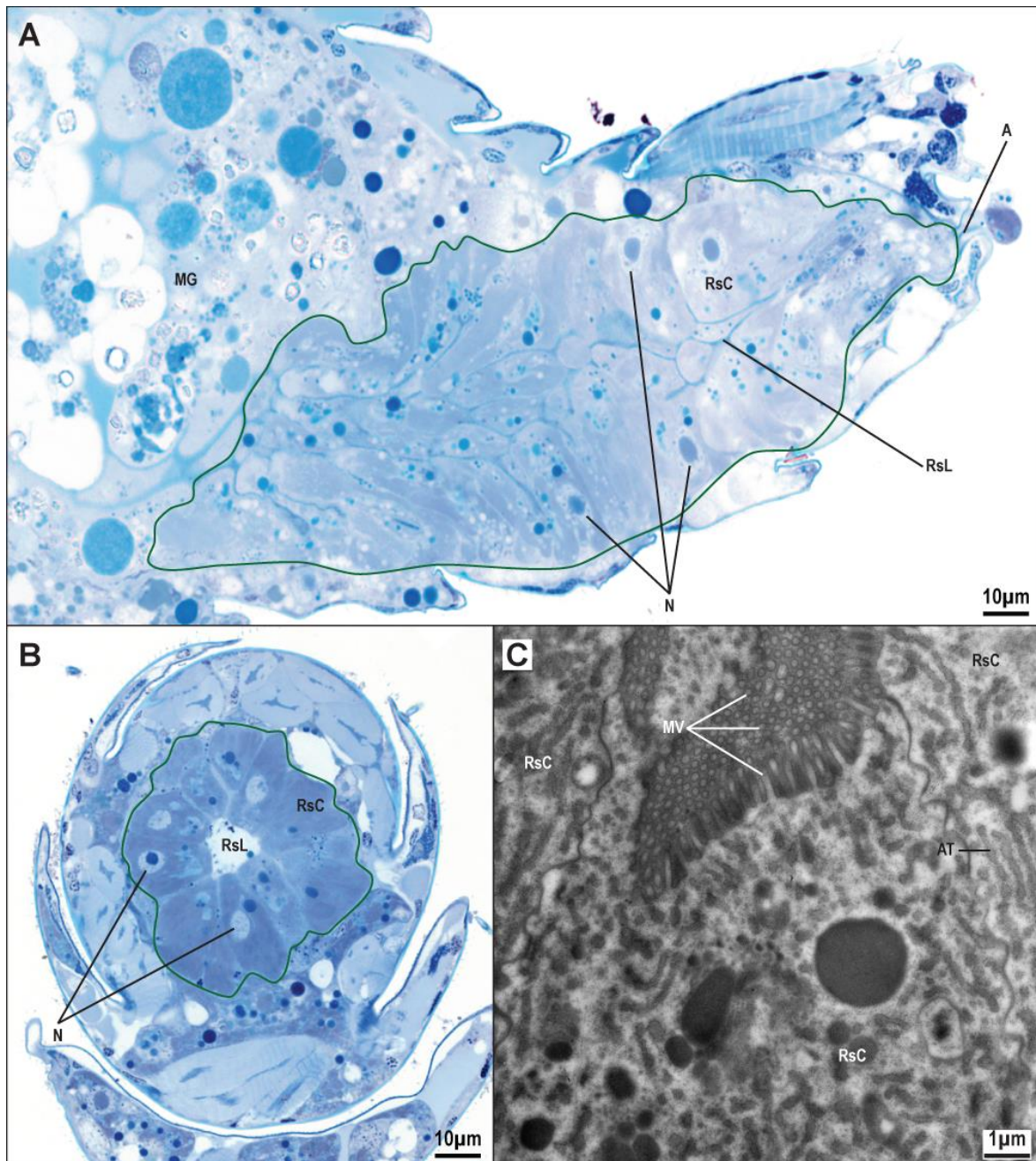
Fig. 41. *Eukoenenia spelaea*, rectal sac. (**A**) Light micrograph of a sagittal section of the metasoma of a female. The rectal sac (green outline) fills almost the entire metasoma. The nuclei of the high prismatic cells are located mostly basally. The lumen of the rectal sac is narrow. A distinct ectodermal (cuticula covered) hindgut is missing. (**B**) Light microscopic oblique cross-section of the rectal sac (red) of segments 16–18. Small droplets are located mostly apically in the cells of the rectal sac. (**C**) Transmission electron micrograph of the rectal sac epithelium. The dense microvilli of the rectal sac epithelial cells extend into the lumen. Abbreviations: A: anus; AT: apical tubule; MG: midgut; MV: microvilli; N: nucleus; RsC: rectal sac cells; RsL: rectal sac lumen.

sac cells. The cytoplasm stains intensively in light microscopy. Transmission electron micrographs show an apical microvilli border with a higher microvilli density than in the midgut epithelium. Small (secretory?) granules and larger lipid vesicles are located mostly apical (Figs. 41A, B). The epithelial cells of the rectal sac are rich in apical tubuli (AT; Fig. 41C). – It should be noted that no cuticle covered posterior segment of the gut was found and the rectal sac continues directly into the anus which is located ventral to the flagellum within the membrane of segment 18 (A; Figs. 37, 41A). The membrane surrounding the anal opening is arranged in folds (Fig. 16).

3.2.11 Excretory organ

Eukoenenia spelaea has a pair of coxal glands as the only excretory organs. The coxal gland consists of a saccule, a tubule, a glandular section, an excretory duct, and an excretory pore (CxG, CxS, CxT, ED, EP; Figs. 37, 42, 43).

The saccule is located in the region of the 1st leg, just posterior to the insertion of the coxa of the first leg on the prosoma. It consists of seven to eight podocytes (PC; Figs. 42B, D). The pedicels of the podocytes are oriented towards the surrounding hemolymph. The center of the saccule has a narrow lumen (CxSL; Fig. 42D). The nuclei of the podocytes are oblong and central in the cytoplasm. The cytoplasm is rich in rough endoplasmic reticulum, free ribosomes and glycogen granules, but has few electron-dense droplets. The saccule connects to the most anterior end of the glandular section (Fig. 42A). A distinct collecting tubule could not be identified.

The glandular section is a long, blind ending tube, extending straight along the lateral body wall into segment 9 (Fig. 37). Anteriorly, the glandular section makes a U-shaped bend, where it connects to the saccule and the tubule of the coxal gland (Fig. 42A). Posterior, it bends ventral and slightly towards the median line before ending. The glandular section of the coxal gland has a prismatic epithelium with an apical cytoplasmic part and a basal labyrinth (CxGA, CxGB, BL; Figs. 42C, E, F). Cross sections of the glandular section consists of three cells (Fig. 42F). The heterochromatin-rich nuclei are located in the cytoplasmic part of the cells. The cytoplasmic parts of the cells are connected by interdigitations and separated by a thin layer of extra cellular matrix (Fig. 42F). Secretion granules are also present.
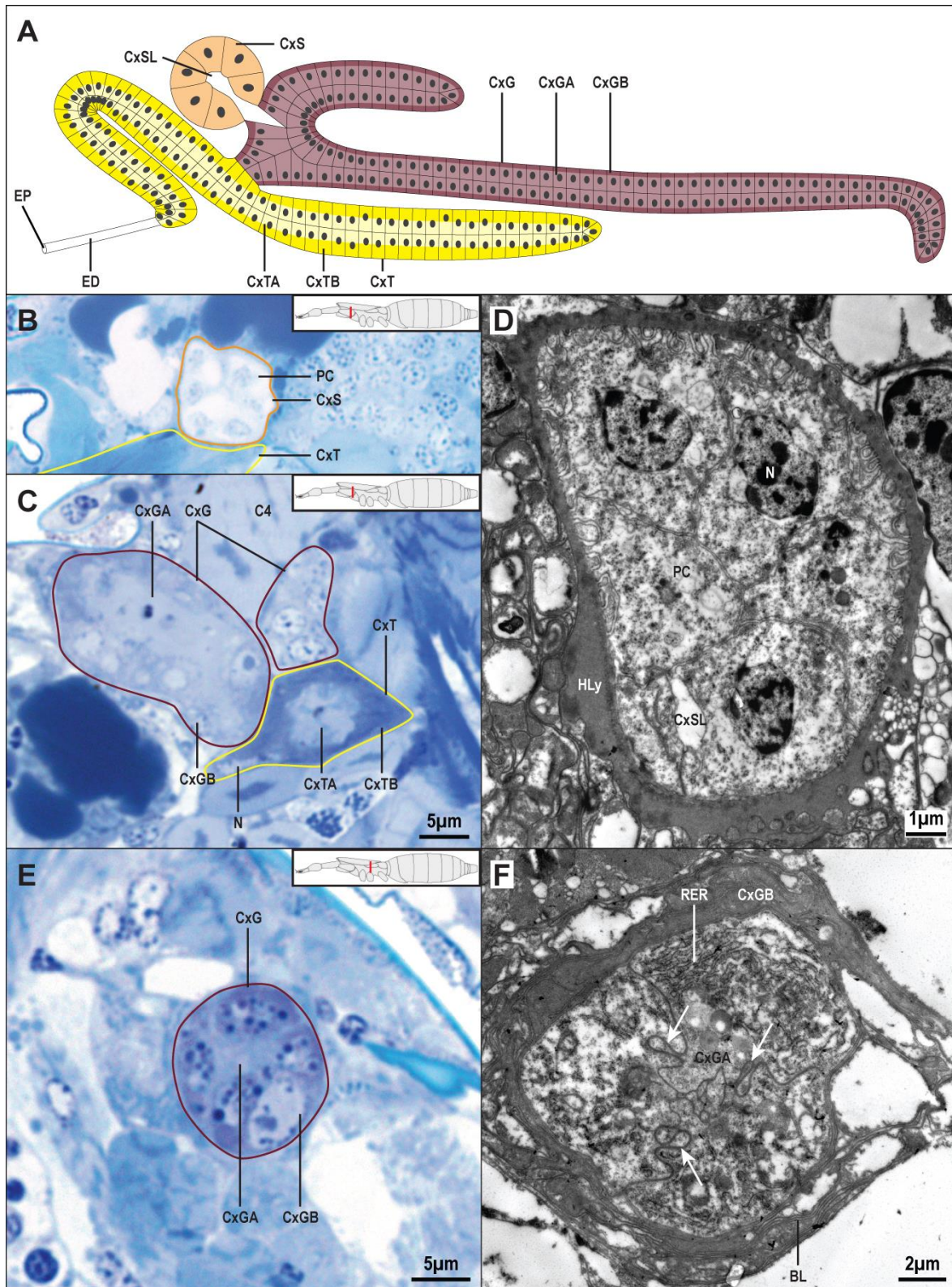
Fig. 42. *Eukoenenia spelaea*, coxal gland. (**A**) Schematic drawing of the coxal gland. It consists of the saccule (orange), tubule (yellow), and glandular section (brown). Tubule and glandular section both have a basal labyrinth (dark) and an apical cytoplasmic part (light). The excretory duct is connected with the cytoplasmic part of the tubule cells. (**B**) Light micrograph of a cross-section through the coxal gland region at the level of the 1st leg of a female. The saccule is not attached to musculature. The podocytes stain light and no lumen is present. (**C**) Light micrograph of a cross-section posterior to the saccule. The glandular section stains lighter than the tubule. Within the tubule, the nucleus is sometimes found in the basal region of the cells. (**D**) Transmission electron micrograph of the saccule. It is completely surrounded by hemolymph. The saccule has a small lumen.

The basal labyrinth displays few electron-dense as well as electron-translucent vesicles. The glandular section has no open lumen. This appearance is uniform from the transition zone between glandular section and saccule to the distal end.

The anterior part of the tubular part of the coxal gland is located within the coxa of leg 1 (Fig. 37). It originates from the glandular section in close neighborhood to the opening of the saccule into the glandular part. The anterior part of the tubule forms a hairpin turn before it connects to the excretory duct (Figs. 42A, 43C). The posterior part of the tubule extends parallel to the glandular section to the region of the 2nd leg. The epithelium of the tubule consists of prismatic cells with an extensive basal labyrinth (Fig. 43A). A minimum of three cells is found to build the tubule in cross-section (Fig. 43A). The nuclei are located mostly apically, however, they can also be found within the basal labyrinth (N; Fig. 43C). The cells of the basal labyrinth contain various electron-dense and electron-translucent vesicles. As in the glandular section, the apical cytoplasmic parts of the tubule cells are connected by interdigitations and septate junctions, and show no lumen (arrows; Fig. 43B). The tubule ends in the cuticle-lined excretory duct (ED; Fig. 43D). The excretory pore is covered by thick cuticle and is opens posteroventral to the coxa of leg 1, at the transition region between coxa and prosoma.

Caption **Fig. 42** continued

(**E**) Light micrograph of a cross-section of the coxal gland region at the level of the 3rd leg of a male. The basal part of the glandular cells contain dark staining secretion granules. (**F**) Transmission electron micrograph of the glandular section. The basal labyrinth is filled with electron-dense material. Interdigitations connect the apical parts of the glandular cells (arrows). Abbreviations: BL: basal labyrinth; C4: cheliceral muscle 4; CxG: coxal gland glandular section; CxGA: glandular cell apical region; CxGB: glandular cell basal region; CxS: coxal gland saccule; CxSL: coxal gland saccule lumen; CxT: coxal gland tubule; CxTA: tubular cell apical region; CxTB: tubular cell basal region; ED: excretory duct; EP: excretory pore; HLy: hemolymph; N: nucleus; PC: podocyte; RER: rough endoplasmic reticulum.
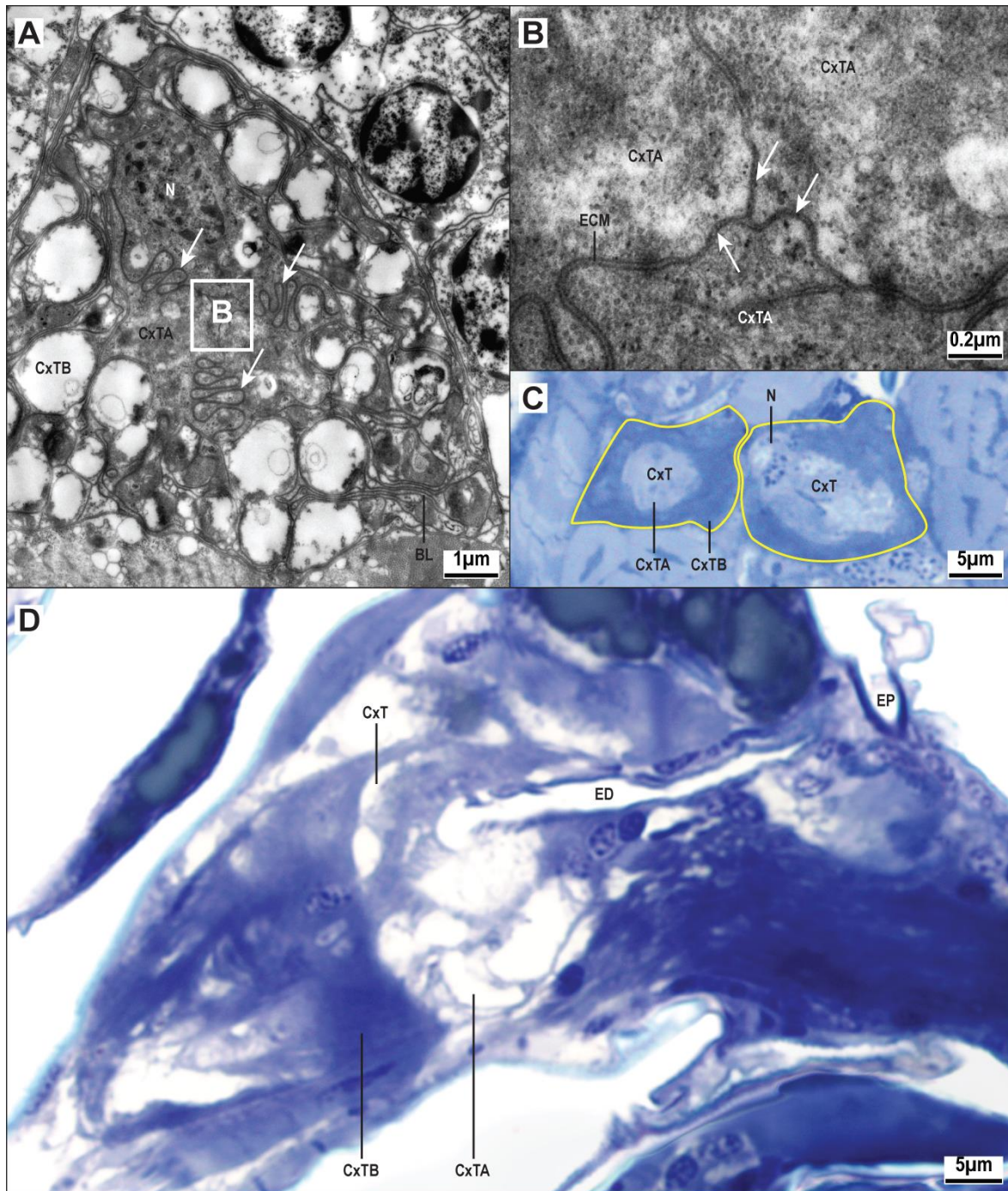
Fig. 43. *Eukoenenia spelaea*, coxal gland. (**A**) Transmission electron micrograph of the tubule of the coxal gland. A large number of electron-translucent [almost empty] vesicles occurs within the basal labyrinth. The cells are tightly connected via interdigitations (arrows). (**B**) Close-up transmission electron micrograph of the apical cell region in A, where septate junctions connect the cells apically (arrows). There is no lumen due to the tight connection of the cells, only a thin layer of extra-cellular matrix. (**C**) Light micrograph of a cross-section of the anterior loop of the tubule. Both arms of the tubule are closely neighboring each other. (**D**) Light micrograph of an oblique longitudinal section of the excretory duct. The duct originates between the apical parts of the tubule cells. It is lined with a thin cuticle intima. The excretory pore has a thicker cuticle. Abbreviations: BL: basal labyrinth; CxT: coxal gland tubule; CxTA: tubular cell apical region; CxTB: tubular cell basal region; ECM: extra-cellular matrix; ED: excretory duct; EP: excretory pore; N: nucleus.

3.2.12 Reproductive organs

Details on the reproductive organs of *Eukoenenia spelaea* are based on light microscopic (LM) observations and transmission electron microscopic (TEM) analysis of the female ovary and accessory gland. Due to material limitations, the TEM was not as exhaustive as intended. However, for *Prokoenenia wheeleri* males, a detailed description of sperm was given by Alberti (1979*a*). All other male structures were described using LM serial sections.

3.2.12.1 Female

The female reproductive organs consist of the ovary, the ovarian ducts, the uterus interna, the uterus externa, the accessory gland, and the receptaculum seminis. The genital opening is located between the posterior genital operculum on segment 9 and the anterior pair of genital lobes on segment 10.

The ovary is a median, sac-shaped, unpaired organ and located in segments 10–13 (OV; Fig. 44). It consists of somatic cells, eggs of different sizes, oocytes as well as a lipid-rich secretion in larger specimens (Figs. 14C, 45C). No musculature was found associated with the ovary wall. The somatic cells are flattened, irregularly shaped cells which attach directly to the ovarian wall (Figs. 45C, 46A). The nuclei are also irregularly shaped. The oocytes are nested between the somatic cells. They have a characteristic large, heterochromatin-poor nucleus (Fig. 46A). The oocytes are found at the apex of the ovary while developed eggs were found close to the opening to the oviduct. One of the studied females carried 6–12 eggs. In the largest specimen, the eggs were between 15 µm and 60 µm in diameter. The eggs were located anterior in the ovary while the posterior region of the ovary was filled with of lipid-rich secretions (Fig. 14C). In the smallest specimen, the eggs were between 15 µm and 25 µm diameter, probably representing an earlier developmental stage. In this specimen the eggs were located posteriorly within the ovary and no secretion was found in the lumen of the ovary.

One pair of ovarian ducts originate laterally from the ovary at the border of segments 11 and 12 (OVD; Fig. 44). The ducts extend anterior into segment 9, where they connect to the unpaired uterus interna. The lumen of the ovarian ducts is narrow (Fig. 45).
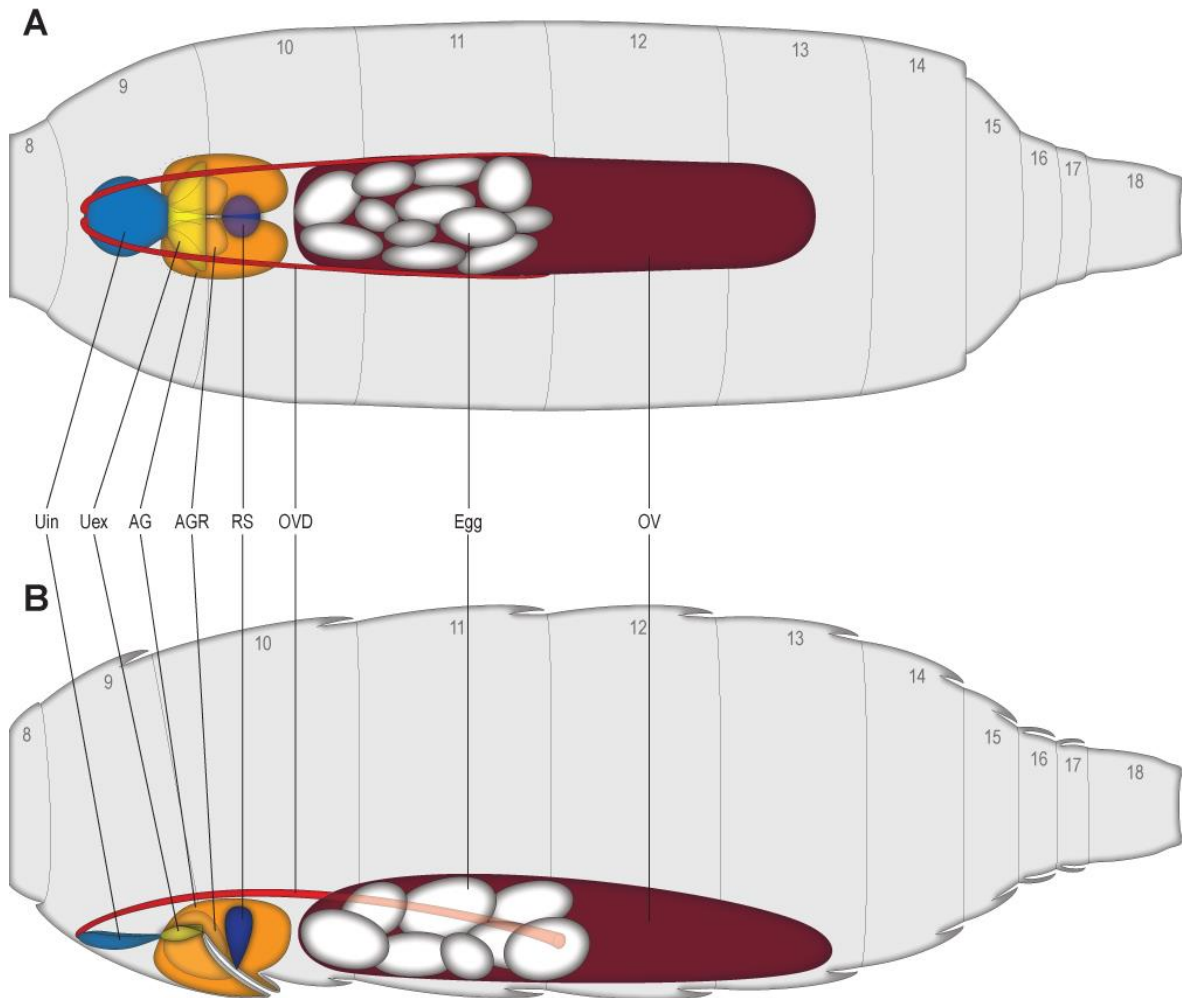
Fig. 44. *Eukoenenia spelaea*, schematic drawing of the female reproductive organs. (**A**) Dorsal view. The unpaired ovary (brown) extends from segment 10 to segment 13. The eggs are positioned in an anterior position within the ovary. The accessory gland (orange) is located anterior to the ovary. The reservoirs of the accessory gland are located anterior to the club-shaped receptaculum seminis. The accessory gland and the ovarian ducts (red) are the only paired internal structure of the female reproductive system. The ovarian ducts connect to the uterus interna (light blue) in segment 9. The uterus externa (dark blue) opens toward the outside. (**B**) Sagittal view. The ovarian duct originate from a middle position along the ovary in segment 12. The accessory gland is located within the genital operculum and the genital lobes. The receptaculum seminis opens halfway between genital opening and posterior end of the genital operculum. Arabic numbers indicate the segments. Abbreviations: AG: accessory gland; AGR: accessory gland reservoir; OV: ovary; OVD: ovarian duct; RS: receptaculum seminis; Uex: uterus externa; Uin: uterus interna.

The uterus interna is located in the anterior part of segment 9 (Uin; Fig. 44). It is flat, sac-shaped, and has a thin squamous epithelium. It continues into the uterus externa which is also located in segment 9 but posterior to the uterus interna (Uex; Fig. 44). Like the uterus interna, the uterus externa has a squamous epithelium, however, it displays many infoldings and it is lined with a thin cuticle intima (Fig. 45A). The nuclei are located basally (Fig. 45A).
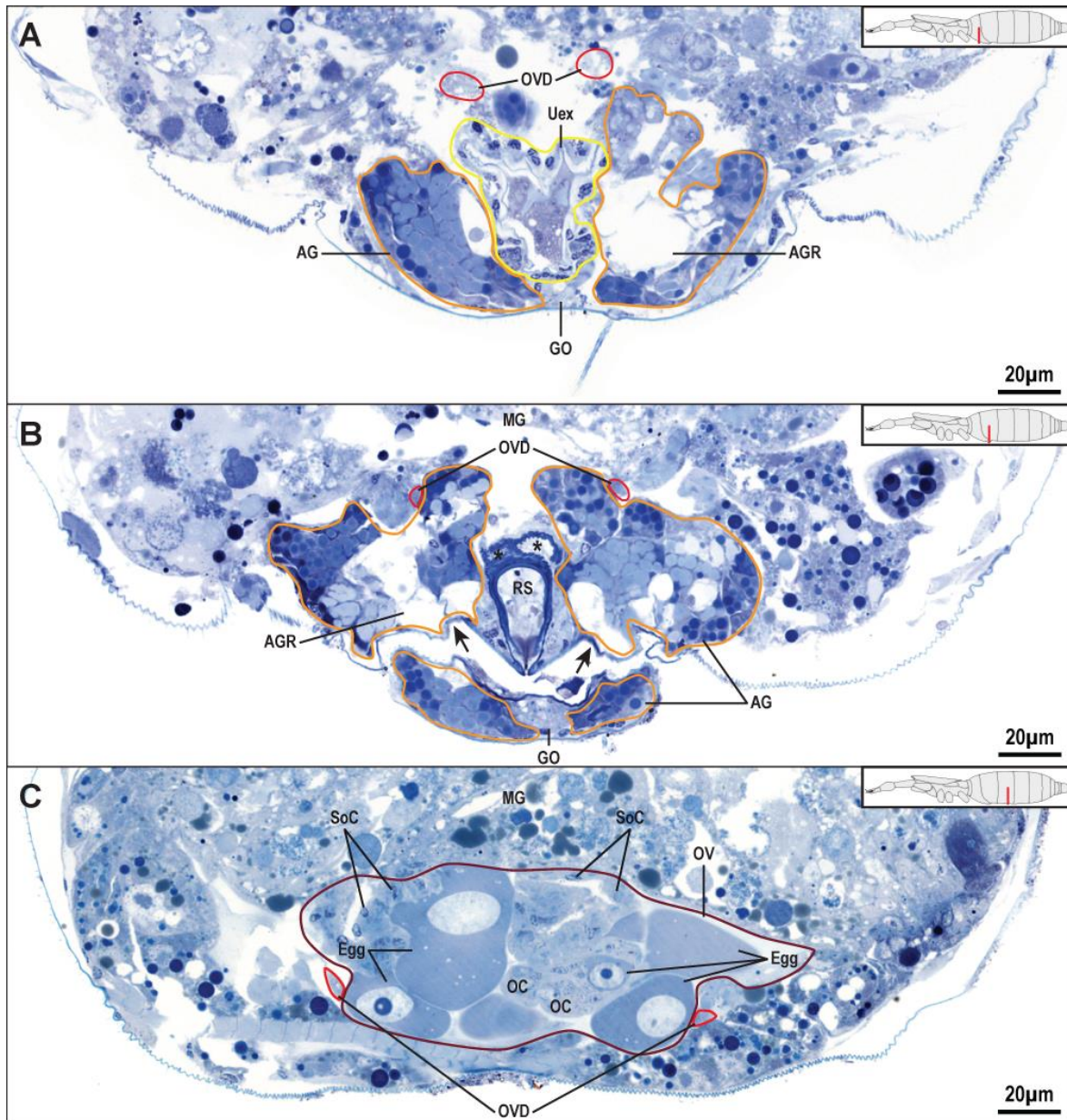
Fig. 45. *Eukoenenia spelaea*, light micrographs of cross-sections through the female reproductive organs. (**A**) Area of the genital operculum in segment 9. The cells of the paired accessory glands (orange) contain numerous secretion vesicles. The uterus externa (yellow) has numerous infoldings and a thin cuticle intima. (**B**) Area of the receptaculum seminis in segment 10. The accessory gland extends into the genital operculum. The cuticle next to the reservoirs (arrows) differs from the neighboring cuticle. The receptaculum seminis has a thick cuticle lining. (**C**) Area of the ovary (brown) in segment 11. The lumen of the ovarian duct (red) is narrow and barely visible. The eggs next to the oocytes vary in size. Abbreviations: AG: accessory gland; AGR: accessory gland reservoir; GO: genital operculum; MG: midgut; OC: oocyte; OV: ovary; OVD: ovarian duct; RS: receptaculum seminis; SoC: somatic cell; Uex: uterus externa.

The receptaculum seminis is an unpaired structure located in segment 10, medioposterior to the genital opening (RS; Fig. 44). The overall shape of the receptaculum is club-shaped in a dorsal-ventral axis, with the opening ventral in the gap between the genital operculum and the base of the genital lobes (Figs. 44B; 45B). The epithelium is flattened and barely distinguishable in light microscopy. The

84

lumen of the receptaculum is covered by a thick cuticle intima (Fig. 45B). Dorsal, the cuticle is arranged in two wrinkled lobes, originating medial and extending towards lateral (*; Fig. 45B). These lobes build a closed tube anterior, but are open posterior. In the studied individuals, I did not find spermatozoa in the receptaculum.

The paired accessory glands extend from the junction of uterus interna and uterus externa to just anterior to the ovary in segments 9 and 10 (AG; Fig. 44). The gland is lobed, and extends into the genital operculum as well as the genital lobes (Figs. 44B, 45B, 46B). The epithelium consists of high prismatic cells which are filled with numerous secretory vesicles (Fig. 45B). Two lateral reservoirs are located within the accessory glands. They extend anterior from the genital operculum to both sides of the receptaculum seminis posterior. Both reservoirs are oriented towards the uterus externa and genital opening (AGR; Figs. 44, 45B). A glandular opening could not be identified, however, in regions where the reservoir touches the body wall, i.e. just past the genital opening, the epidermis and the cuticle are thin (arrows; Fig. 45B).
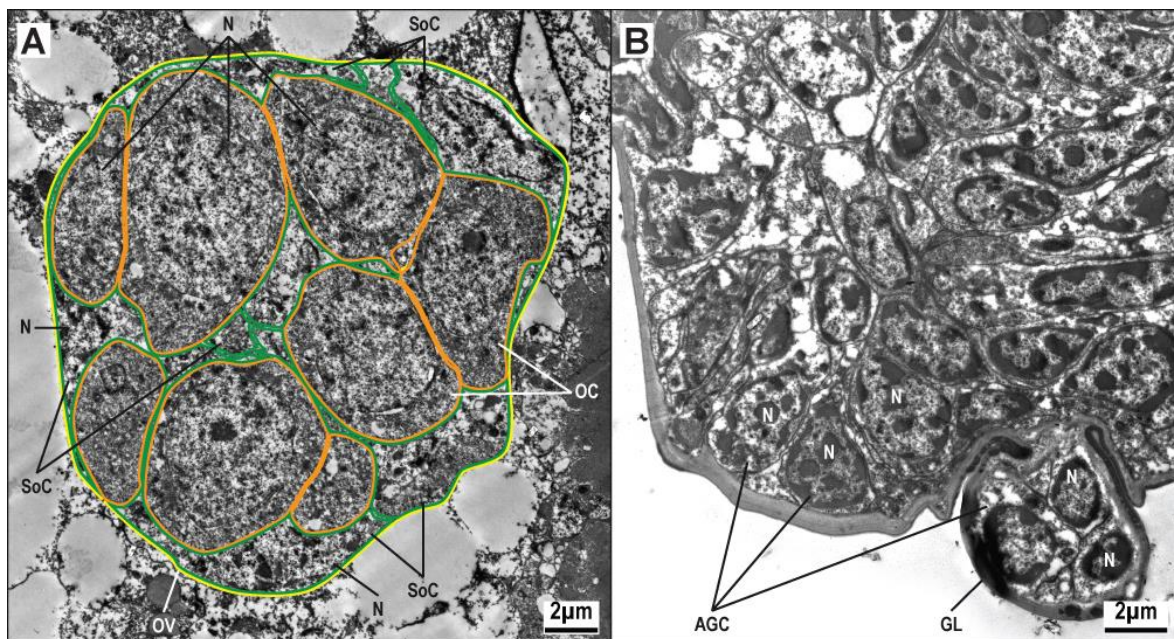
Fig. 46. *Eukoenenia spelaea*, transmission electron micrographs of female reproductive organs. (**A**) Cross-section through the ovary (yellow) in segment 11. The large roundish oocytes (orange) are nestled between the irregularly shaped somatic cells (green). The somatic cells are located towards the wall of the ovary. (**B**) Cross-section of the right genital lobe in segment 10. The epithelial cells of the accessory gland are high-prismatic with a basal nucleus. The gland extends into the genital lobe. Abbreviations: AGC: accessory gland cells; GL: genital lobe; N: nucleus; OC: oocyte; OV: ovary; SoC: somatic cell.

3.2.12.2 Male

The male reproductive organs consist of the testes, the vas deferens, a paired anterior accessory gland, an unpaired posterior accessory gland, and the genital atrium. The genital opening is located between the second and third pair of genital lobes at the border of segments 9 and 10.

The testes are paired and located lateroventrally in segments 10–13 (T; Fig. 47). They extend lateral and parallel to the ventral musculature. No musculature was found associated with the testes wall. The epithelium consists of squamous cells and is barely discernible in light microscopy (Fig. 49B). Two cell types are present, somatic cells and germ cells. The somatic cells are small, of equal shape and size, and the cytoplasm stains bluish (SoC; Fig. 49B). They are irregularly dispersed between the germ cells. Germ cells vary in size and the cytoplasm stains purple in light microscopy (GC; Fig. 49B). Spermatozoa of different developmental stages, i.e. spermatogonia, spermatocytes, and spermatids, are found throughout the entire length of the testes (SpC, SZ; Figs. 48, 49). The largest spermatozoa are 12–15 µm in diameter and have a large vacuole (diameter 10–14 µm) with five spherical enclosures (diameter 4.5–5 µm) each (* in inset; Figs. 47B, 48B). These enclosures contain several small droplets. The droplets in the periphery of an enclosure stain light in LM, the droplets in the center of the enclosure stain intensively (Figs. 47B, 48). The nucleus of the large spermatozoa is located basal and is difficult to diagnose in LM because it is comparatively small and oblong. Two small, dark staining, oblong structures are located at the apex of the spermatozoa (arrows, N; Figs. 47B, 48B). The nature of these structures is unclear. During development of the spermatozoa, the vacuole with the spherical enclosures increases in size, the nucleus changes shape from round to oblong, and the paired apical structure is still missing.

The vas deferens extends from the anterior end of the testes in segment 10 all the way into segment 8, where it merges into a short single tube before opening into the genital atrium in segment 9 (VD; Fig. 47). The course of the vas deferens is not straight but winding (Fig. 47). It is located laterally of the dorsoventral musculature of segments 9 and 10 (DV2, DV3; Fig. 21A). In segment 9, the vas deferens is oriented towards the median line, in segment 10, it is oriented towards the body wall.
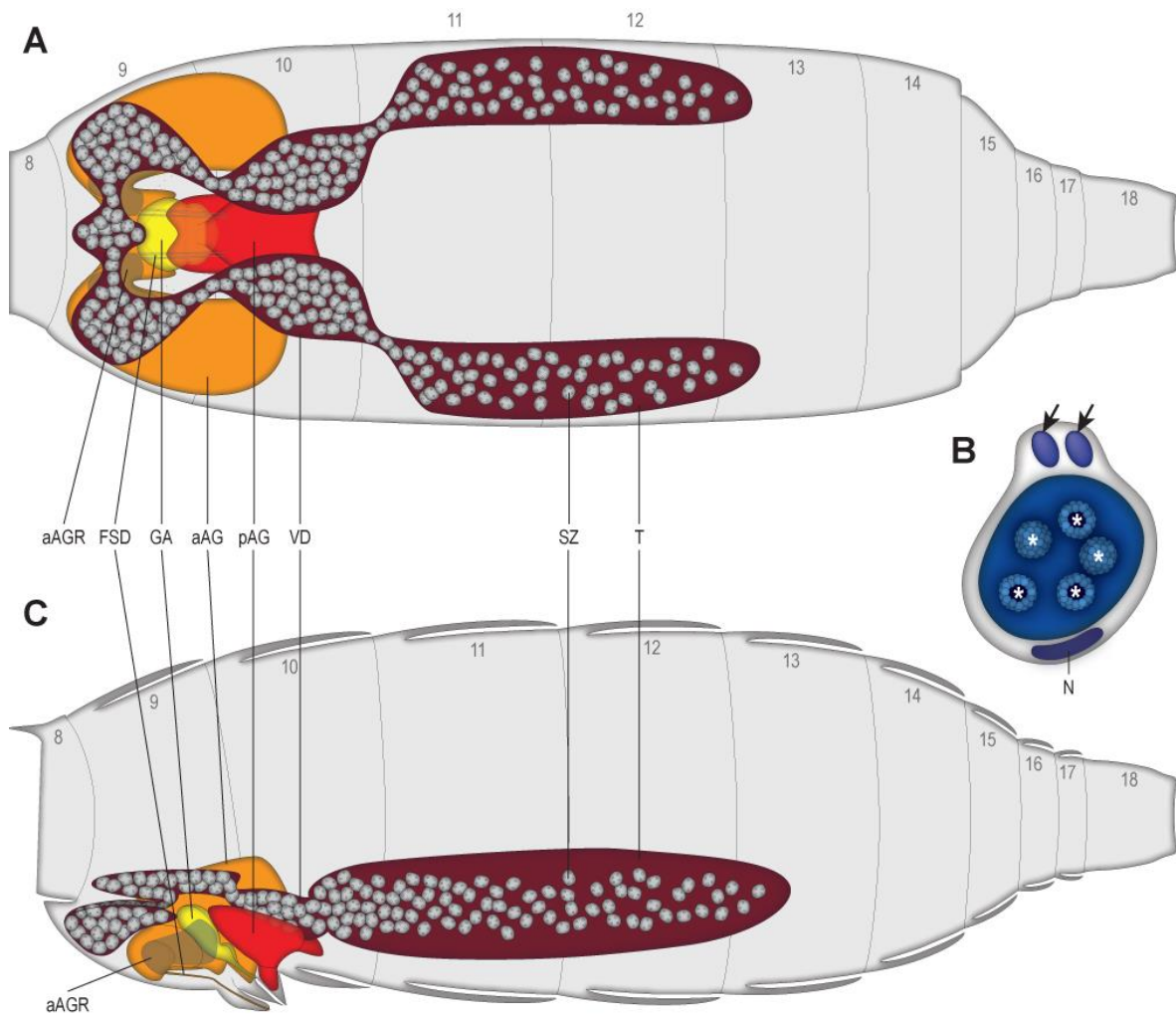
Fig. 47. *Eukoenenia spelaea*, schematic drawing of the male reproductive organs. (**A**) Dorsal view. The paired testes (brown) transition into the winding deferent ducts which fuse anteriorly before terminating at the genital atrium (yellow). The paired anterior accessory gland (orange) is located ventral and lateral to the genital atrium and deferent ducts. The unpaired posterior accessory gland (red) is dorsal to the genital atrium and extends far into segment 10. (**B**) Reconstruction of a large spermatozoon. The oblong nucleus is located basally. The large vacuole includes five dark staining spherical vesicles surrounded by several smaller light staining vesicles (asterisk). Two oblong structures are located at the apex of the spermatozoon (arrows). (**C**) Sagittal view. A large number of large spermatozoa within the vas deferens. Two fusule ducts originate from an anterior accessory gland reservoir and extend into genital lobe 1. The posterior accessory gland has extensions into genital lobe 3. Arabic numbers indicate the segments. Abbreviations: aAG: anterior accessory gland; aAGR: anterior accessory gland reservoir; pAG: posterior accessory gland; FSD: fusule duct; GA: genital atrium; N: nucleus; SZ: spermatozoon; T: testes; VD: vas deferens.

The tubes are filled with spermatozoa. The epithelium consists of flat squamous epithelial cells (Figs. 47, 49A).

The paired anterior accessory gland is located ventral to the vas deferens in segments 9 and 10 (aAG; Fig. 47). The two glandular sacs have anterior extensions which form an anterior loop. The extensions are oriented toward posterior, just anterior to the genital atrium. The sacs extend posterior and are located close to the

87
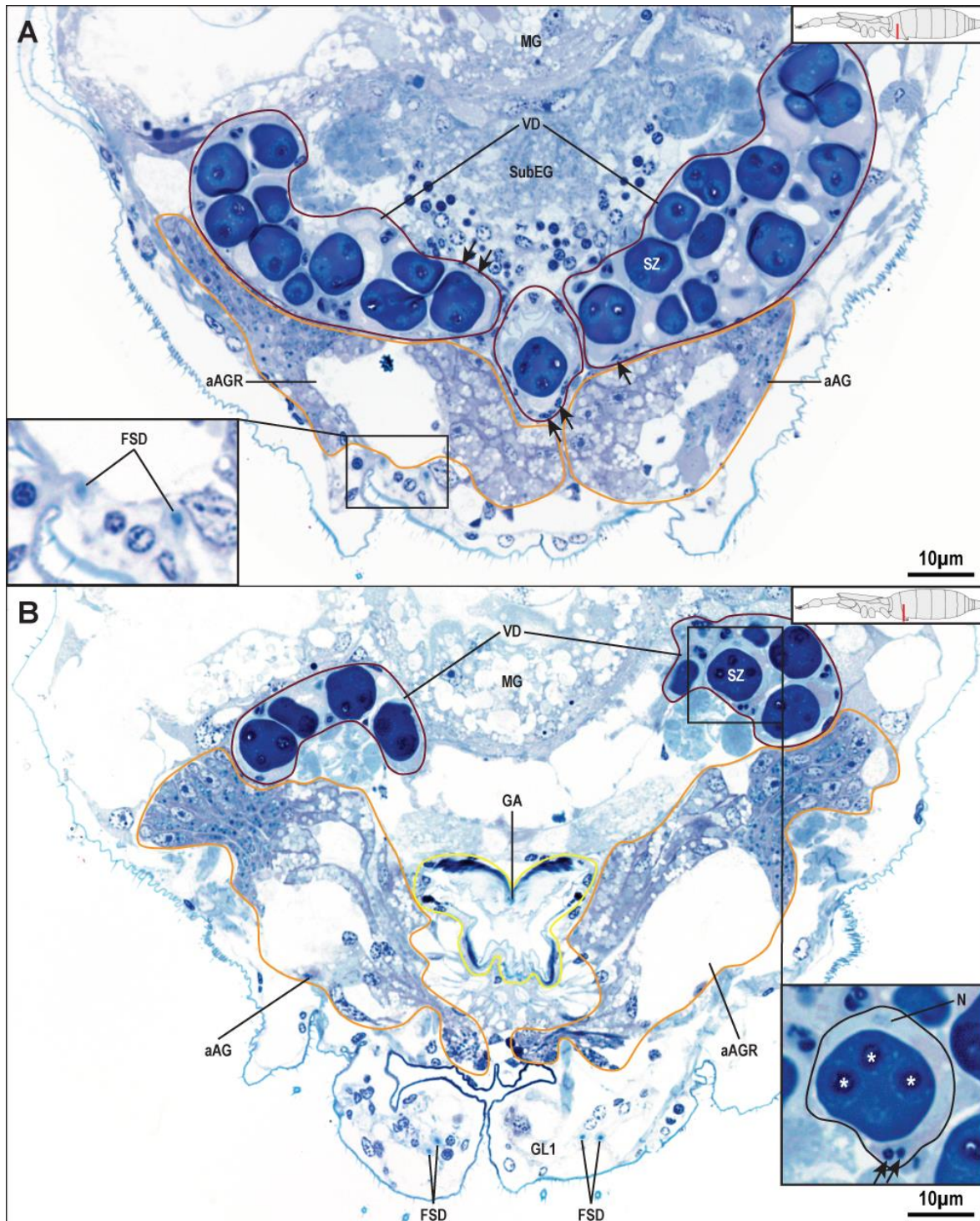
Fig. 48. *Eukoenenia spelaea*, light micrograph of a cross-sections of the male reproductive organs. (**A**) Area of the anterior section of vas deferens (brown) and anterior accessory gland (orange) in segment 9. The middle section is the fused part of the vas deferens. The vas deferens has a flat squamous epithelium (arrows) and is filled with fully developed spermatozoa. The posterior end of the subesophageal ganglion is located dorsal to the vas deferens. The secretory vesicles of the anterior accessory gland epithelial cells display different staining. The fusule ducts originate at the anterior accessory gland's reservoir (inset). (**B**) Area of the genital atrium (yellow) in segment 9. The spherical enclosures of the spermatozoan vacuole have lighter outer and darker inner vesicles (asterisk, inset). The spermatozoa have paired structures located in their apex (arrows, inset). Parts of the nucleus can be seen at the base of the spermatozoon. The genital atrium is lined with a thick layer of cuticle. The fusule ducts are located inside genital lobe 1. Abbreviations: aAG: anterior accessory gland; aAGR: anterior accessory gland reservoir; FSD: fusule duct; GA: genital atrium; GL1: genital lobe 1; MG: midgut; N: nucleus; SubEG: subesophageal ganglion; SZ: spermatozoon; VD: vas deferens.

88
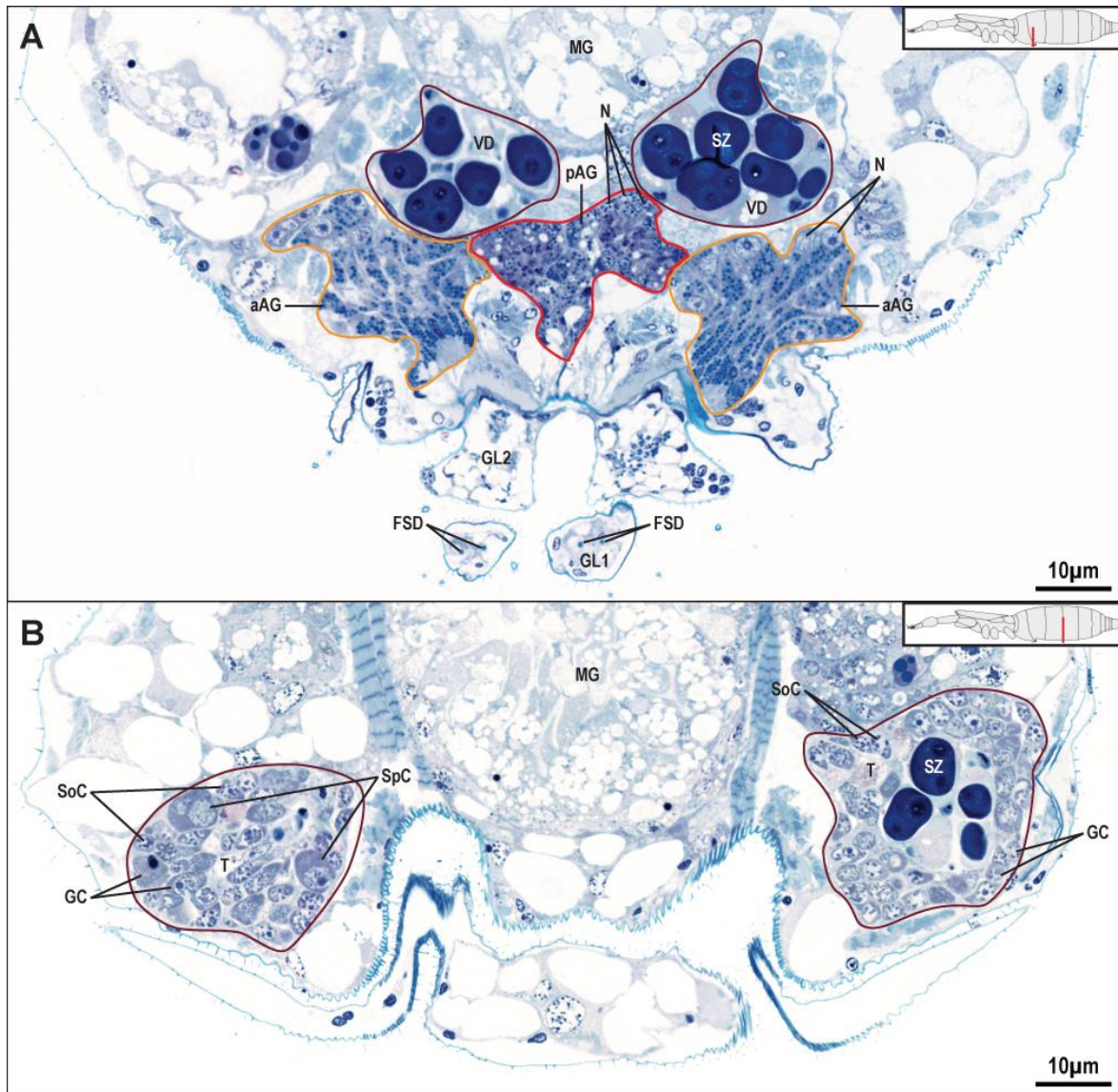
Fig. 49. *Eukoenenia spelaea*, light micrographs of cross-sections through the male reproductive organs. (**A**) Area of the anterior part of the second genital lobe in segment 9. The epithelial cells of the posterior section of the anterior accessory gland (orange) have only smaller and darker staining secretory vesicles. The unpaired posterior accessory gland (red) has prismatic cells with nuclei located basally. (**B**) Area of the testes (brown) at the border of segments 11 and 12. The number of fully developed spermatozoa is greatly reduced. The posterior section of the testes is filled with different developmental stages of spermatozoa. Abbreviations: aAG: anterior accessory gland; pAG: posterior accessory gland; FSD: fusule duct; GC: germ cell; GL1/2: genital lobe 1/2; MG: midgut; SoC: somatic cell; SpC: spermatocyte; SZ: spermatozoon; T: testes; VD: vas deferens.

body wall and lateral to the dorsoventral muscle DV2. The anterior accessory gland's epithelium consists of high prismatic cells with the nuclei located basally (Figs. 48, 49A). The cytoplasm is filled with secretory vesicles of different composition, large and lightly stained, and small and darker stained in light microscopy (LM). The larger vesicles are found within cells oriented toward the median line and closely associated with the reservoirs (Fig. 48). The smaller vesicles, however, are found in cells oriented toward the body wall and posteriorly

within the glandular sac (Figs. 48, 49A). Anteriorly within the loop, the anterior accessory gland has large reservoirs, which stain lightly in LM (aAGR; Figs. 47, 48). Connected to these reservoirs are the fusule ducts. There are two fusule ducts per gland. These cuticle lined tubules extend through the first genital lobes to the fusules, two per genital lobe (FSD, GL1; Figs. 15E, F, 47, 48A).

The posterior accessory gland is unpaired, sac-like in appearance, and is located in segments 9 and 10. It lies posteriorly to the genital atrium and has extensions into the third pair of genital lobes. Posteriorly it extends mid-section in segment 10 (SG; Fig. 47). The posterior accessory gland consists of prismatic cells filled with two types of secretory vesicles, one small type staining dark and one larger type staining light (Fig. 49A). The nuclei are located basally within the cells. No secretory duct was found, but a region with a thin epidermis and cuticle just posterior to the genital opening.

The genital atrium is located in the posterior half of segment 9 (GA; Fig. 47). It is a flattened sac which is oriented in an anterodorsal/posteroventral axis and terminates at the genital opening between genital lobes 2 and 3. In cross-section, the atrium's lumen displays a stylized W shape in the anterior region (Fig. 48B). Towards the genital opening, the lumen is flattened. The genital atrium has a squamous epithelium which secretes a thick layer of cuticle into the lumen. The cuticle is stained darker dorsally and ventrolaterally than the surrounding cuticle of the genital atrium (Fig. 48B). This might be an indication for varying chemical composition.

3.2.13   Flagellum

The terminal flagellum is a prominent feature of *Eukoenenia spelaea*. Its sclerotized basal ring connects to the last opisthosomal segment. The cuticle is thinner in the transitional zone between flagellar articles than in the articles themselves (arrowheads; Fig. 50A). The flagellum is free of musculature (Fig. 50). Just distal to a set of sensory setae, the cuticle has a groove, optically separating the proximal and distal part of the article. The distal part carries the cuticular spikes (Sp; Fig. 50A). Like in the rest of the body, the epidermis of the flagellum is a squamous epithelium with oblong nuclei. The epidermal cells contain light staining vesicles of different sizes (Fig. 50). A pair of nerves is located lateral and in the middle of the dorsoventral axis in the flagellum (Fig. 50C). The central lumen of the flagellum is
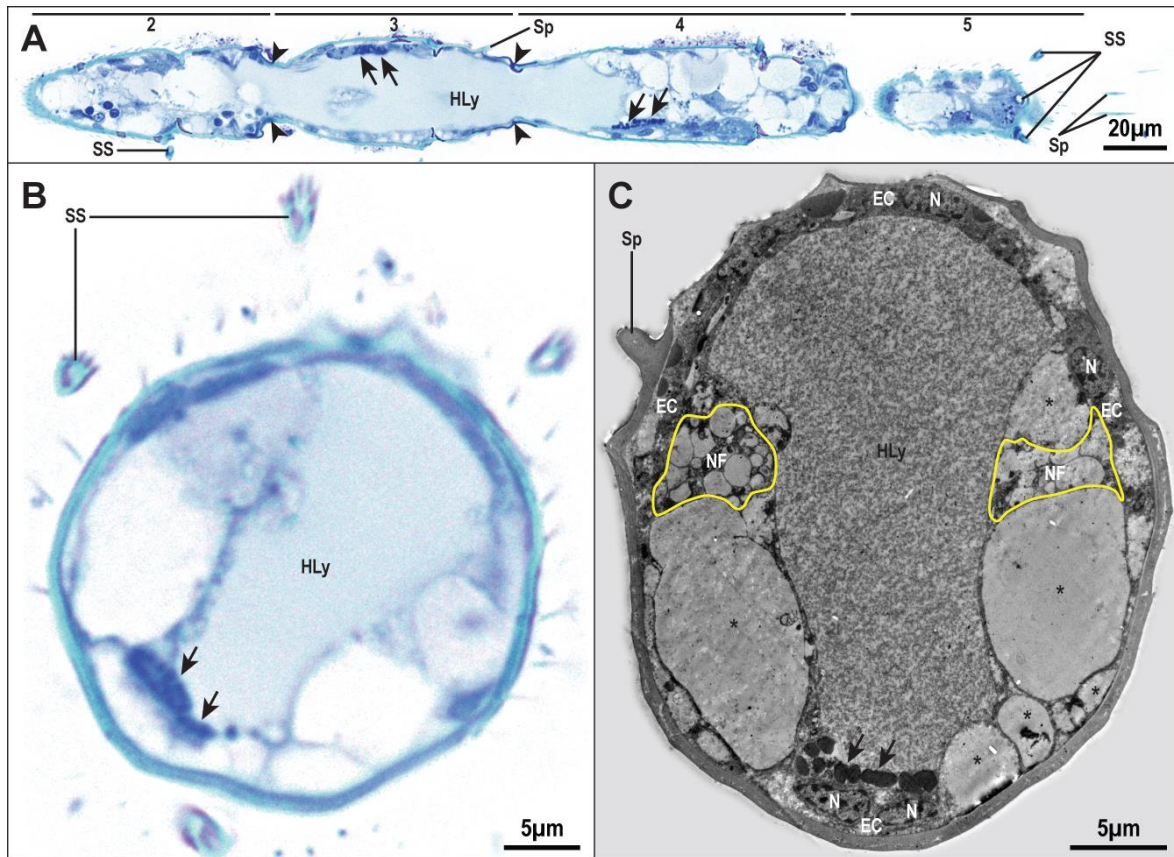
Fig. 50. *Eukoenenia spelaea*, flagellum. (**A**) Light micrograph of a longitudinal section of flagellar articles 2–5. The flagellum has no intrinsic musculature and mostly filled with hemolymph. The cuticle is thinner where the flagellar articles connect (arrowheads). Secrete vesicles are located lateral in the hemolymph space (arrows). Numbers indicate flagellar articles. (**B**) Light microscopic cross-section of a flagellar article. The hemolymph space is surrounded by large vesicles. Secrete vesicles are only found towards one side of the flagellar article (arrows). (**C**) Transmission electron micrographic cross-section of a flagellar article with a pair of lateral nerve fibers (yellow). Vesicles of varying sizes are found adjacent to the nerves. The secrete vesicles appear to be located within the hemolymph (arrows). Abbreviations: EC: epidermal cell; HLy: hemolymph; N: nucleus; NF: nerve fibers; SS: sensory seta; Sp: spike.

filled with hemolymph, which makes up approx. 50 % of the total flagellar volume. Within the hemolymph, small dark staining vesicles can be found. These vesicles are clustered and located adjacent to the epidermis. The nature of the vesicles is unclear.

3.3 Phylogenetic analysis

3.3.1 Phylogenetic position of *Eukoenenia spelaea* using Shultz's (2007*a*) original character matrix

When using Shultz's (2007*a*) original character matrices either for extant or for extant and fossil taxa, and simply adding *Eukoenenia spelaea* using his character coding (Tabs. A1, A2), the two unweighted analyses resulted in consensus trees

similar to Shultz's (2007*a*) original analysis before collapsing weakly supported branches (Figs. 51A, 52A). Differences between tree topographies were limited to relationships within the major groups.

Phylogeny based on extant taxa

For the phylogeny based exclusively on extant taxa, the analysis produced four minimal-length trees (length 415, consistency index 0.557; Fig. 51A). Four monophyletic groups with bootstrap percentage (BP) above 80 were recovered, i.e. Arachnida (BP 100), Uropygi (Schizomida + Thelyphonida, BP 99), Pedipalpi (Uropygi + Amblypygi, BP 99), and Tetrapulmonata (Pedipalpi + Araneae, BP 97). Anactinotrichida (Opilioacariformes + Parasitiformes) were reconstructed as sister group to Ricinulei. The placement of *Eukoenenia spelaea* with Palpigradi showed a nodal support of BP 85 (Fig. 51A). All other groups showed nodal support below BP 60.

The implied weights analyses (IWA) of extant taxa with $k = 1$ (1 tree, best score = 57.44048), $k = 2$ (2 trees, best score = 42.70714), $k = 3$ (1 tree, best score = 34.20952), $k = 4$ (1 tree, best score = 28.63651), $k = 5$ (1 tree, best score = 24.67045), and $k = 6$ (1 tree, best score = 21.69199) all resulted in the same major group topology (Fig. 51B). Palpigradi were recovered at the base of Arachnida as sister group to all other arachnids. Acari were recovered as monophyletic and as sister group to Ricinulei. Stomothecata (Opiliones + Scorpiones), Haplocnemata (Pseudoscorpiones + Solifugae), and Tetrapulmonata were recovered in all weighted analysis. Conflicts were limited to relationships within terminal taxa.

Phylogeny based on extant and fossil taxa

The unweighted analysis of extant and fossil taxa resulted in 32 minimal-length trees (length 463, consistency index 0.533; Fig. 52A). Two monophyletic groups with bootstrap percentage above 80 were recovered, i.e. Uropygi (Schizomida + Thelyphonida, BP 87), and Pedipalpi (Uropygi + Amblypygi, BP 91). Arachnida showed a nodal support of BP 74. Like in the analysis of extant taxa only, Acari were reconstructed as diphyletic with Anactinotrichida (Opilioacariformes + Parasitiformes) as sister group to Ricinulei. The placement of *Eukoenenia spelaea*

with Palpigradi showed a nodal support of BP 82. All other groups showed nodal support below BP 50 (Fig. 52A).

The IWA of extant and fossil taxa with k = 1 (3 trees, best score = 65.74762) resulted in the same topology as the IWA of extant taxa with the addition of Eurypterida s.lat. as the sister group to Arachnida as well as Trigonotarbida and Haptopoda within Pantetrapulmonata (Trigonotarbida + Araneae + Haptopoda + Pedipalpi; Fig. 52B). The fossil *Chimerarachne yingi* was recovered within Araneae. With k = 2 (3 trees, best score = 49.02857), k = 3 (3 trees, best score = 39.42976), k = 4 (5 trees, best score = 33.10952), and k = 5 (5 trees, best score = 28.59307), Palpigradi remained at the base of Arachnida, however, Haplocnemata were now recovered as the sister group to Acaromorpha and Pantetrapulmonata (Fig. 52C).
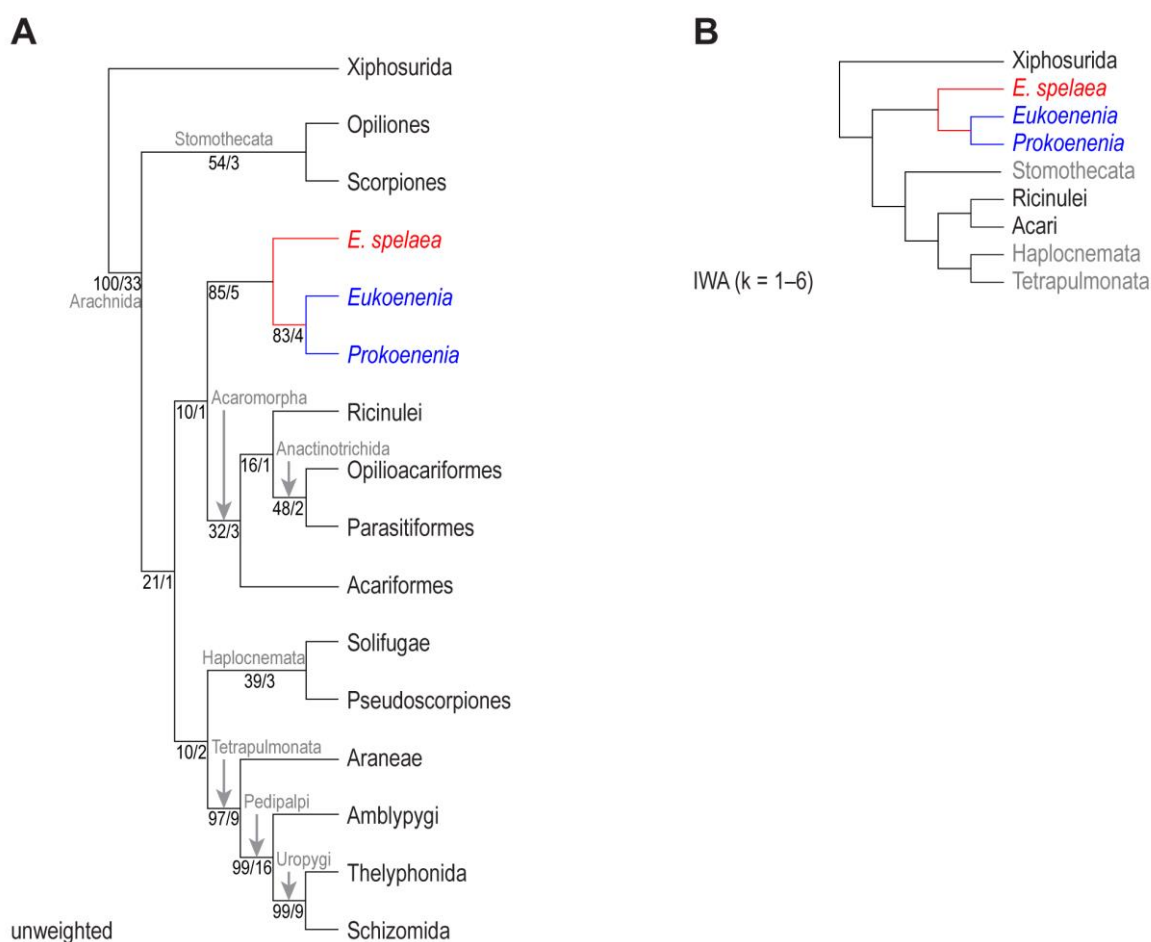
Fig. 51. Results of the analysis of extant taxa. (**A**) Minimal-length topology. Numbers below internodes indicate bootstrap percentages/Bremer support values. *Eukoenenia spelaea* as well as *Eukoenenia* and *Prokoenenia* are placed as sister group to Acaromorpha, however, nodal support is low. (**B**) Implied weights topology. All implied weights analyses resulted in the same major group topology. Conflicts were limited to relationships between terminal taxa of the groups listed in A. Palpigradi are placed at the base of Arachnida as sister group to all other arachnids.

The IWA with k = 6 (5 trees, best score = 25.17229) resulted in the same topology as the unweighted analysis (Fig. 52D). Conflicts were limited to relationships within terminal taxa.
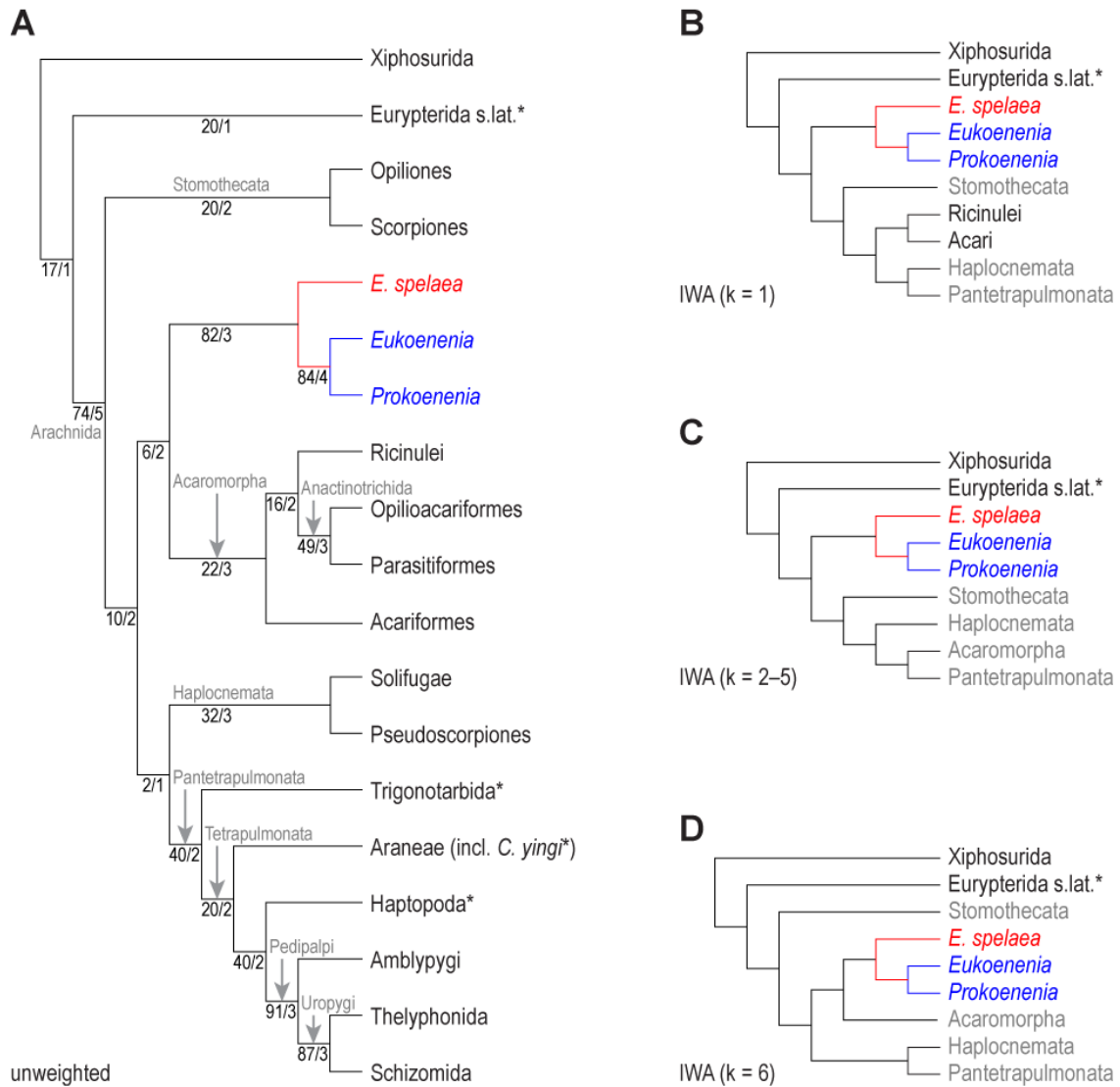
Fig. 52. Results of the analysis of extant and fossil taxa. (**A**) Minimal-length topology. Numbers below internodes indicate bootstrap percentages/Bremer support values. Like in the analysis of extant taxa only, *Eukoenenia spelaea* as well as *Eukoenenia* and *Prokoenenia* are placed as sister group to Acaromorpha. Nodal support for this relationship is low. (**B**) Implied weights topology with k = 1. Again, Palpigradi are placed at the base of Arachnida as sister group to all other arachnids. Ricinulei are placed as sister group to the monophyletic Acari. (**C**) Implied weights topology with k = 2–5. Palpigradi are placed at the base of Arachnida as sister group to the other interordinal groups. (**D**) Implied weights topology with k = 6. The topology is identical to the unweighted analysis. For all implied weights analyses, conflicts were limited to relationships between terminal taxa of the groups listed in A.

3.3.2 Changes in character states and new characters in the data matrix

Based on my morphological analysis of *Eukoenenia spelaea*, I have modified existing character states in the matrix as well as created new character codes to augment the data matrix of Shultz (2007*a*; Tabs. 6, 7).

The first modified character state (6) is the division of the carapace with distinct pro-, meso- or metapeltidial sclerites. In the original matrix, there was no association between the sclerites and prosomal segments. My analysis of the musculature of *Eukoenenia spelaea* (see 3.2.5.3) showed that the mesopeltidial sclerites are not associated with a segment, as previously assumed. In order to improve the analysis and separate groups with segment association of the mesopeltidia from groups without this specific morphology, the character state was changed to include association with segments. The coding was adjusted for *E. spelaea*, Palpigradi, Schizomida, and Solifugae (Tabs. 6, 7).

The character state involving the rostrosoma (32) took only structures into account that included the pedipalp coxae and anterior elements of the prosoma. However, the rostrosoma of *Eukoenenia spelaea* does not meet all of these criteria (see 3.1.4) and would, therefore, be coded as absent. To accommodate the presence of the palpigrade rostrosoma without pedipalpal involvement, the character state was rephrased in a more neutral way and the coding was adjusted for *E. spelaea* and Palpigradi (Tabs. 6, 7).

Character (61) coding for a trochanter-femur joint with dorsal hinge or pivot operated by flexor muscles only, was deleted. It was an assumed autapomorphy for Palpigradi, however, my analysis revealed that an antagonistic pair of muscles is present in legs 2 and 3 (see 3.2.5.1; Figs. 21A, 22C).

The number of metasomal sclerites (116) lacked an appropriate number for *Eukoenenia spelaea*. The original coding included only zero, two, three, five and nine sclerites. However, palpigrades have four metasomal sclerites (see 3.1.8). Thus, the character coding was adjusted to include four sclerites (Tabs. 6, 7).

My analysis of the box-truss axial muscle system (BTAMS) in the prosoma of *Eukoenenia spelaea* revealed the presence of anterior oblique muscles in this tagma (see 3.2.5.3). In the original data matrix of Shultz (2007*a*), such a character

95

was not available, because it was assumed that this type of musculature was reduced in all euchelicerates. To accommodate the presence of this muscle type in *E. spelaea*, I created the new character (128a) "anterior oblique muscles of BTAMS anterior to postoral somite VI (state 1 only in *E. spelaea*)" (Tabs. 6, 7). The character coding was adjusted for all taxa.

The suboral suspensor was originally included in the matrix (Shultz 2007*a*) with the character state "a tendon that arises from the BTAMS and inserts on the ventral surface of the oral cavity via muscle" (131). My morphological analysis of *Eukoenenia spelaea* showed that muscle E8 (Fig. 23; Tab 5) does not insert on the oral cavity but posteriorly on the pharynx (see 3.2.5.3). In order to include this result,

Tab. 6. Changes applied to the character states in the character matrix of Shultz's (2007a) phylogeny based on morphological characters. Character 61 was deleted, and characters 128a and 178a are introduced. Autapomorphic characters of *Eukoenenia spelaea* and Palpigradi are marked grey.

Character	Description by Shultz (2007a)	New description	(New) Coding
6	carapace with distinct pro-, meso- or metapeltidial sclerites	carapace with distinct pro-, meso- or metapeltidial sclerites associated with segments	0 = absent, 1 = two peltidia, 2 = three peltidia
32	rostrosoma: long, narrow, subcylindrical epistome projecting anteriorly with base fixed to dorsal surface of palpal coxae, bordered laterally by lobes projecting from palpal coxae; ventral wall of preoral chamber formed by anterior element of prosoma (sternapophysis)	rostrosoma: long, narrow, subcylindrical epistome projecting anteriorly, bordered laterally by lobes	0 = absent, 1 = fixed to pedipalpal coxae, 2 = no association with pedipalp
61		deleted, because it was a supposed autapomorphy	
116	number of metasomal somites: 0, zero; 1, two; 2, three; 3, five; 4, nine	number of metasomal somites	0 = zero, 1 = two, 2 = three, 3 = four, 4 = five, 5 = nine
128a	-	anterior oblique muscles of BTAMS anterior to postoral somite VI (state 1 only in *E. spelaea*)	0 = absent, 1 = present
131	suboral suspensor: a tendon that arises from the BTAMS and inserts on the ventral surface of the oral cavity via muscle	suboral suspensor: a tendon that arises from the BTAMS and inserts on the ventral surface of the foregut via muscle	0 = absent, 1 = ventral on oral cavity, 2 = ventral and posterior on pharynx
148	intercheliceral median organ	supracheliceral median organ	0 = absent, 1 = present
178a	-	coxal gland with additional glandular section	0 = absent, 1 = between saccule and tubule, 2 = between tubule and excretory pore
198	dilator muscle of precerebral pharynx and/or preoral cavity attaching to ventral surface of prosoma	dilator muscle of precerebral pharynx and/or preoral cavity attaching to prosoma or rostrosoma	0 = absent, 1 = ventral on prosoma, 2 = ventrolateral on rostrosoma

Tab. 7. Additional character coding changes applied to the original data matrix of Shultz (2007a).

Taxa	Character	Original coding	New coding
Acariformes	178a: coxal gland with additional glandular section	n/a	2 = between tubule and excretion porus
Eukoenenia *Prokoenenia* *E. spelaea*	3: Anterior end of dorsal prosoma with median marginal or submarginal pointed process	0 = absent	1 = present
	6: carapace with distinct pro-, meso- or meta-peltidial sclerites associated with segments	2 = three peltidia	1 = two peltidia
	32: rostrosoma: long, narrow, subcylindrical epistome projecting anteriorly, bordered laterally by lobes	0 = absent	2 = no association with pedipalp
	46: appendage III (= arachnid leg 1) extremely elongate, antenniform	? = unknown	1 = present
	116: number of metasomal somites	2 = three	3 = four
	128a: anterior oblique muscles of BTAMS anterior to postoral somite VI	n/a	1 = present
	178a: coxal gland with additional glandular section	n/a	1 = between saccule and tubule
	199: postcerebral pharynx (in *Prokoenenia*)	1 = present	0 = absent
E. spelaea only	68: patella of appendage of postoral somite III (= arachnid leg 1) proportionally much longer than those of more posterior appendages	0 = absent	? = unknown
	69: femur–patella joint	2 = hinge, one axis of movement, flexor muscles without muscular antagonists	0 = monocondylar, several axes of movement and multifunctional muscles
	72: patella–tibia joint	0 = monocondylar with or without CZY (73)	2 = hinge, one axis of movement, muscles without muscular antagonists
	73 and 74 (dependent on character 72)	0 = absent	- = inapplicable
	76: anterior femur–tibia or femoropatella–tibia (transpatellar) muscle	? = unknown	1 = present
	83: circumtarsal ring	0 = absent	? = unknown
	106: megoperculum	1 = present	0 = absent
	128: anterior oblique muscles of BTAMS posterior to postoral somite VI	? = unknown	0 = absent
	130: endosternite fenestrate	0 = absent	1 = present
	131: suboral suspensor: a tendon that arises from the BTAMS and inserts on the ventral surface of the foregut via muscle	1 = present (ventral on oral cavity)	2 = ventral and posterior on pharynx
	132: perineural vascular membrane in adult	1 = present	0 = absent
	162: nucleus with manchette of microtubules	0 = absent	? = unknown
	163: axoneme	0 = absent	? = unknown
	164: coiled axoneme	- = inapplicable	? = unknown
	165: microtubule arrangement in axoneme	- = inapplicable	? = unknown
	166: helical or corkscrew shaped nucleus	0 = absent	? = unknown
	167: vacuolated-type sperm	0 = absent	1 = present
	194: dorsal dilator muscle of precerebral pharynx attaching to dorsal surface of prosoma or intercheliceral sclerite	1 = present (dorsal on prosoma)	2 = dorsal on intercheliceral sclerite

Tab. 7 continued

Taxa	Character	Original coding	New coding
E. spelaea only	198: dilator muscle of precerebral pharynx and/or preoral cavity attaching to prosoma or rostrosoma	1 = present (ventral on prosoma)	2 = ventrolateral on rostrosoma
Schizomida	6: carapace with distinct pro-, meso- or meta-peltidial sclerites associated with segments	1 = present	2 = three peltidia
Solifugae	6: carapace with distinct pro-, meso- or meta-peltidial sclerites associated with segments	1 = present	2 = three peltidia
	178a: coxal gland with additional glandular section	n/a	1 = between saccule and tubule
Mastigoproctus	62: superior trochanter–femur muscle (or homologue) originating broadly in femur, inserting on distal margin of trochanter	0 = absent	1 = present
	69: femur–patella joint	2 = hinge, one axis of movement, flexor muscles without muscular antagonists	1 = bicondylar hinge, one axis of movement and antagonistic muscles
Palaeocharinus	44: apotele (claw), position	? = unknown	0 = terminal

the term "oral cavity" was replaced with "foregut" and the character coding was adjusted to include the options "ventral on oral cavity" and "ventral and posterior on pharynx" (Tabs. 6, 7).

The frontal organ of *Eukoenenia spelaea* is located dorsal to the chelicerae (see 3.2.8.1). Therefore, character (148) was rephrased from "intercheliceral" to "supracheliceral" to accommodate that fact (Tab. 6).

My analysis of the coxal gland in *Eukoenenia spelaea* showed, that it includes a prominent glandular section (see 3.2.11). A glandular section can also be found in other arachnids. To allow for a more complete phylogenetic analysis, I have added the character state "coxal gland with additional glandular section" (178a). To accommodate the differences between groups with a glandular section in the coxal gland, the coding includes the options "between saccule and tubule" and "between tubule and excretory pore" (Tabs. 6, 7). The coding was adjusted for Acariformes, *E. spelaea*, Palpigradi, and Solifugae.

The character state involving the dilator muscle of the precerebral pharynx and/or preoral cavity (194) was included in the original data matrix (Shultz 2007*a*) as "attaching to ventral surface of prosoma". However, in *Eukoenenia spelaea*, these dilator muscles attach ventrolateral on the rostrosoma (see 3.2.5.2). The character

state was expanded to "attaching to ventral surface of prosoma or rostrosoma" and the coding was adjusted accordingly for *E. spelaea* and Palpigradi (Tabs. 6, 7).

3.3.3 Results for updated character matrix including data for *Eukoenenia spelaea*

The unweighted analysis of the adjusted matrix (Tabs. 6, 7, A2) for the extant taxa produced 12 minimal-length trees (length 427, CI 0.531). Four monophyletic groups with bootstrap percentage above 80 were recovered, i.e. Arachnida (BP 99), Uropygi (Schizomida + Thelyphonida, BP 99), Pedipalpi (Uropygi + Amblypygi, BP 100), and Tetrapulmonata (Pedipalpi + Araneae, BP 91). Acaromorpha (Acariformes, Anactinotrichida, and Ricinulei) were reconstructed as unresolved. The deepest interordinal relationships within Arachnida are also unresolved (Fig. 53A). The placement of *Eukoenenia spelaea* with Palpigradi showed a nodal support of BP 98. All other groups showed nodal support below BP 60.

The implied weights analysis (IWA) of the adjusted matrix for extant taxa with k = 1 (1 tree, best score = 59.40714), k = 2 (1 tree, best score = 44.00714), k = 3 (1 tree, best score = 35.20952), k = 4 (1 tree, best score = 29.43651), k = 5 (1 tree, best score = 25.33712), and k = 6 (1 tree, best score = 22.26342) all resulted in the same major group topology (Fig. 53B). It is the same topology as the IWA of the original character matrix (Fig. 51B). Conflicts were limited to relationships within terminal taxa.

The unweighted analysis of the adjusted matrix of extant and fossil taxa resulted in 32 minimal-length trees (length 479, CI 0.522; Fig. 53C) which have the same consensus tree as my analysis using the original character coding. However, the bootstrap percentages and Bremer support values differ (Figs. 52A, 53C). Thus, only two monophyletic groups with bootstrap percentage above 80 were recovered, i.e. Uropygi (Schizomida + Thelyphonida, BP 87), and Pedipalpi (Uropygi + Amblypygi, BP 91). Arachnida showed a nodal support of BP 73. Like in the analysis of the original matrix, Acari were reconstructed as diphyletic with Anactinotrichida (Opilioacariformes + Parasitiformes) as sister group to Ricinulei. The placement of *Eukoenenia spelaea* with Palpigradi showed a nodal support of BP 92. All other groups showed nodal support below BP 50 (Fig. 53C).
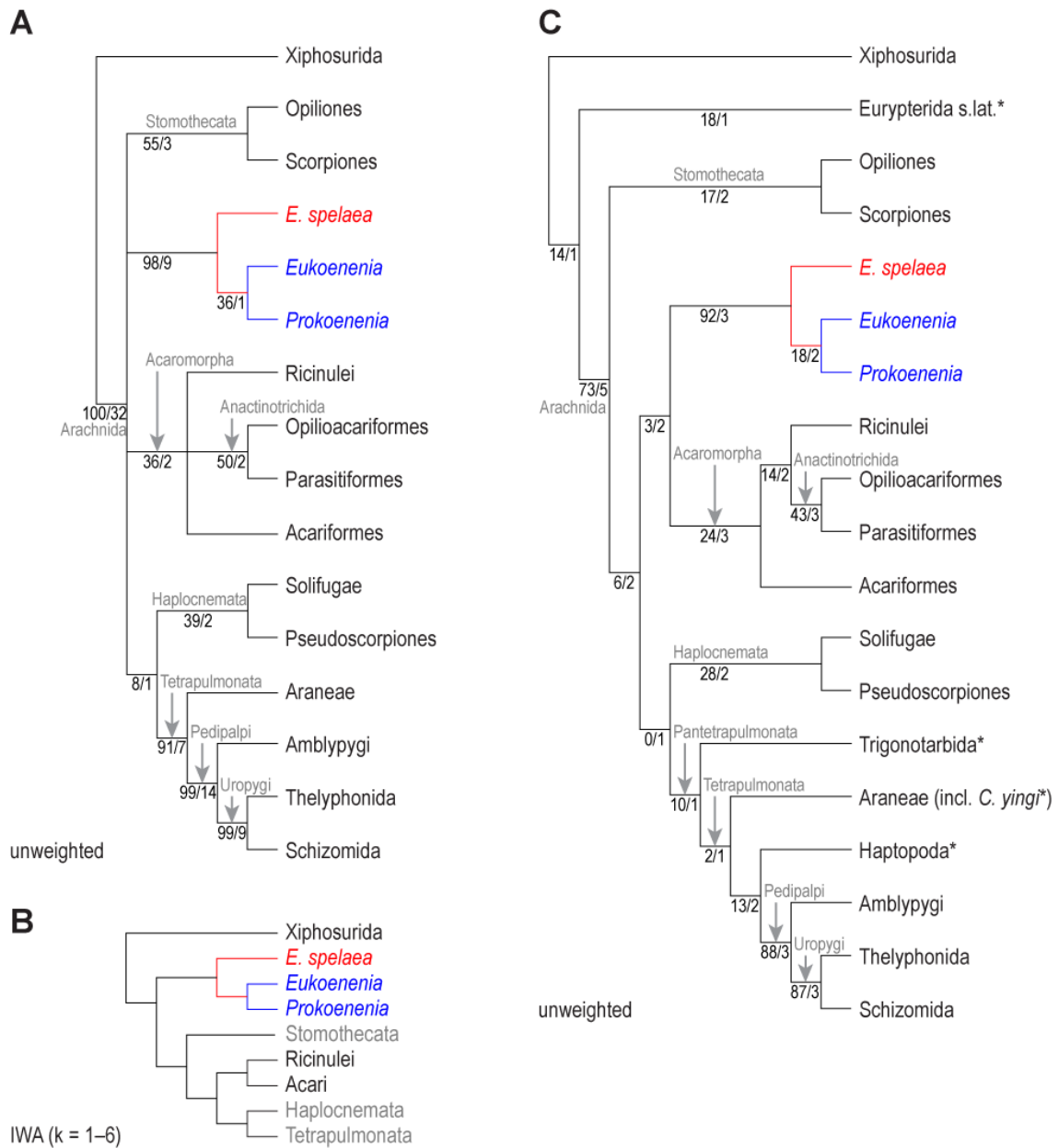
Fig. 53. Results of the analysis of the updated character matrix. (**A**) Minimal-length topology of the unweighted analysis of extant taxa. Numbers below internodes indicate bootstrap percentages/Bremer support values. Deepest relationships within Arachnida as well as Acaromorpha are unresolved. (**B**) Implied weights topology of extant taxa. The topology is identical to the implied weights analyses of the original character matrix (Fig. 51B). Palpigradi are placed at the base of Arachnida as sister group to all other arachnids. Ricinulei are placed as sister group to the monophyletic Acari. Conflicts were limited to relationships between terminal taxa of the groups listed in A. (**C**) Minimal-length topology of the unweighted analysis of extant and fossil taxa. Numbers below internodes indicate bootstrap percentages/Bremer support values. The topology is identical to the unweighted analysis of extant and fossil taxa of the original character matrix (Fig. 52A). Implied weights analysis resulted in topologies identical to the implied weights analysis with k = 2–5 of extant and fossil taxa of the original character matrix (Fig. 52C). Conflicts were limited to relationships between terminal taxa.

The IWA of the adjusted matrix for extant and fossil taxa with k = 1 (3 trees, best score = 65.97976), k = 2 (3 trees, best score = 50.72540), k = 3 (3 trees, best score = 40.77619), k = 4 (3 trees, best score = 34.23795), k = 5 (3 trees,

best score = 29.57305), and k = 6 (3 trees, best score = 26.06054) resulted in topologies identical to the IWA with k = 2–5 of extant and fossil taxa of the original character matrix (Fig. 52C). Conflicts were limited to relationships between terminal taxa.

3.3.4 Proposed apomorphic characters for Palpigradi and their sister group relationship

The morphological character analysis resulted in six autapomorphies for Palpigradi (Tabs. 6, A2). The autapomorphic characters are: (6) two peltidia associated with segments; (32) rostrosoma without pedipalpal association; (128a) anterior oblique muscle of BTAMS present in prosoma; (131) suboral suspensor arising from BTAMS attached to posterior end of pharynx (only confirmed for *Eukoenenia spelaea*); (148) the suprachceliceral median organ (frontal organ); and (198) lateral pharyngeal dilator muscle attaching to rostrosoma (only confirmed for *E. spelaea*).

In the unweighted analysis of extant data (original matrix) as well as extant with fossil data (original and updated matrix), Palpigradi was placed as sister group to Acaromorpha based on the four possible synapomorphies: (72) the patella–tibia joint of legs 1–4 has a hinge, one axis of movement, and muscles without muscular antagonists. (180) The adult coxal organ opening is located on or near the coxa of appendage III (= arachnid leg 1). (199) A lack of a postcerebral pharynx might be considered a synapomorphy for Palpigradi and Acaromorpha. Vacuolated-type sperm (167) would only be a synapomorphy for a Palpigradi-Anactinotrichida sister group relationship and not for Palpigradi and Acaromorpha.

The IWA of extant and fossil data (original and updated matrix), Palpigradi were recovered as basal arachnid group based on the six possible synapomorphies: (93) the inferior apotele muscle (= claw depressor) of legs 1–4 is attached at the tibia. (120) the respiratory medium is air for all recent arachnids. (127) Posterior oblique muscles of the BTAMS are present in postoral somites I–VI. (151) the gonads are located primarily in the opisthosoma in all recent Arachnida, and (154) there is only one gonopore. (184) Ingestion is primarily liquid food, with or without preoral digestion.

4. Discussion

4.1 Body tagmatisation

The arthropod body is organized as an array of segments. Blocks of segments may be integrated morphologically and/or functionally, forming tagmata. As recently reviewed by Fusco and Minelli (2013), the terms "segment" and "tagma" are descriptive, and the application of the terms is conceptually variable and differs between authors. Clearly, *[…] "their value as developmental units or units of evolutionary change should not be uncritically assumed" […]* (Fusco and Minelli 2013, p. 218). To circumvent this problem, some authors (e.g. Dunlop and Lamsdell 2017) differentiate between "somite" and "segment", with the "somite" representing the genetic/developmental blueprint and the "segment" being the externally expressed, morphologically recognizable expression of the "somite". Somites often match segments, but mismatches may occur when adjacent segments fuse. Fusion may affect the whole segment or only the dorsal or ventral part. Similarly, Lamsdell (2013) reviews concepts of "tagmosis", suggesting that true tagmata should be defined by functional differences related to appendages. While this approach includes a functional perspective, it remains fundamentally descriptive, because most frequently, function is deduced from morphological differentiation and almost always is an interpretation of morphology. – I follow Fusco and Minelli (2013) in their pragmatic approach, using "segment" and "tagma" as descriptive terms of modular organization of arthropods, and do not imply a priori homology when referring to segment numbers or tagmata. Because segment borders and tagmata can vary according to methods used, life stages, and phylogenetic relationship, they need to be determined explicitly for each taxon studied.

The body of euchelicerates is conventionally divided into prosoma and opisthosoma. In some taxa, the opisthosoma is further subdivided into meso- and metasoma (e.g. Amblypygi, Ricinulei, Schizomida, Scorpiones, and Thelyphonida). When various groups of euchelicerates are compared, the border between prosoma and opisthosoma varies along the longitudinal axis and may differ between the dorsal and the ventral side of the body (e.g. Ricinulei, Schizomida, Scorpiones, Thelyphonida, and Xiphosurida; Dunlop and Lamsdell 2017). Assigning clear and explicit segment numbers to the tagmata is difficult, at least by external examination.

It requires analyzing independent morphological landmarks like origin and insertion of the serial musculature to assign segment numbers to certain tagmata (van der Hammen 1986, Shultz 1993, 2007*b*).

4.1.1   Prosoma, dorsal aspect

In the (eu)chelicerate ground pattern, the prosoma consists of seven segments (Weygoldt and Paulus 1979*b*, Dunlop and Lamsdell 2017) that form a single dorsal shield and carry six appendages on the ventral side. Indeed, most euchelicerate groups, including fossil (e.g. Eurypterida) and basal extant groups (e.g. Xiphosurida) have a fused prosomal shield spanning the entire prosoma (Beier 1931, Gerhardt 1931, Gerhardt and Kästner 1931, Kästner 1931*b, c, d*, Vitzthum 1931, Dunlop and Lamsdell 2017). This morphology has been modified in several arachnid groups, e.g. in Palpigradi, Schizomida and Solifugae, in which the prosomal shield is dorsally divided into a pro-, meso-, and metapeltidium. The propeltidium is associated with the chelicerae, the pedipalps, and the first two pairs of walking legs. The meso- and the metapeltidium are associated with segments of walking leg 3 and 4, respectively (Kästner 1931*e*). The mesopeltidia of Schizomida are paired, dorsolateral sclerites. However, they are medially fused in Solifugae forming just one unpaired sclerite (Kästner 1931*e, f*). – The morphological reorganization of the prosoma, actually the entire body, is more substantial in Opiliones and Acari. However, because of their clearly derived, clade specific reorganization, the tagmatisation of these two clades is not discussed here.

At the first glimpse, the morphology of the prosoma of palpigrades appears similar to that of Schizomida and Solifugae, i.e. possessing pro-, meso- and metapeltidium. However, this study provides the opportunity to assign sclerites to segments by comparing muscle architecture with the cuticular sclerites. The (presumptive) ground pattern of musculature in the prosoma of euchelicerates recognizes serial/segmental dorsal and ventral suspensor muscles for each of the six post-ocular segments (Shultz 2007*b*). Based on this pattern, I would expect four dorsal suspensor muscles connecting the endosternite and the propeltidium (for the segments of the chelicerae, pedipalps, and the first two pairs of walking legs), and one pair for each, the mesopeltidium and the metapeltidium. However, the association of muscles in *Eukoenenia spelaea* differs from that expectation. Indeed,

I find four dorsal suspensor muscles associated with the propeltidium (E3, E5, E11, E14; Figs. 23, 54; Tabs. 5, 8), but, based on their origin and insertion they are assigned to prosomal segments 3–6 with the second prosomal segment missing a dorsal suspensor muscle. Therefore, I suggest that the propeltidium is the common dorsal shield (tergum) of segments 1 through 6. No musculature is associated with the mesopeltidium, but one dorsal suspensor muscle with the metapeltidium (E17; Figs. 23, 54; Tabs. 5, 8). Because the mesopeltidium has no muscle insertion I suggest it is not a segmental tergite. Instead it is considered a dorsolateral sclerotization of the pleural fold. Therefore, and to avoid confusion with a true tergite of the 6th prosomal segment as it occurs in Solifugae and Schizomida, I suggest to term this element "parapeltidium". The pattern of musculature and their insertions suggest a different and independent evolutionary origin of the morphological organization of the dorsal prosomal shields of palpigrades as compared to Schizomida and Solifugae. However, detailed information on the musculature of Schizomida and Solifugae is missing.
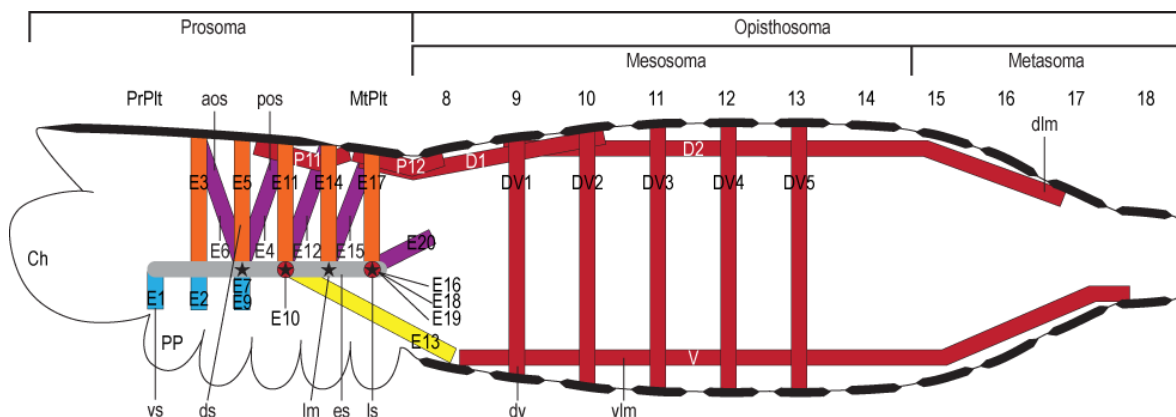
Fig. 54. *Eukoenenia spelaea*, musculature associated with the box-truss axial muscle system (BTAMS) based on Shultz (2007b). In the prosoma, dorsal suspensors are found in the region of the pedipalp, 1st, 2nd, 3rd, and 4th leg. Where dorsal suspensors are present, posterior oblique suspensors are present as well with the exception of the most anterior dorsal suspensor. From the second dorsal suspensor an anterior oblique suspensor arises. The posterior oblique suspensor at the posterior end of the endosternite inserts at the pleural membrane of segment 8. A ventral suspensor is present in the first three segments. A ventral muscle arising in the region of the 2nd leg terminates, where the ventral longitudinal muscle originates. There are two lateral suspensors in the prosoma in the region of E13 and the last dorsal suspensor. Two dorsal longitudinal muscles in the prosoma might be extensions of the dorsal longitudinal musculature of the opisthosoma. The first opisthosomal segment is free of dorsoventral and posterior oblique musculature. The following five opisthosomal segments follow the BTAMS but lack posterior oblique muscles. The last mesosomal segment lacks the dorsoventral musculature. Stars indicate the attachment sites of extrinsic leg musculature originating at the endosternite associated with legs 1–4. Abbreviations: aos: anterior oblique suspensor; Ch: chelicera; dlm: dorsal longitudinal muscle; ds: dorsal suspensor; dv: dorsoventral muscle; es: endosternite; ls: lateral suspensor; MtPlt: metapeltidium; PP: pedipalp; PrPlt: propeltidium; Po: posterior oblique muscle; pos: posterior oblique suspensor; vlm: ventral longitudinal muscle; vs: ventral suspensor.

This interpretation, of course, depends on the correct diagnosis of the dorsal suspensor muscles. However, this is straightforward because Palpigradi (like *Limulus polyphemus*) maintain the most complete set of dorsal suspensor muscles of the box-truss axial muscle system (BTAMS, see 4.4.1; Fig. 54; Tab. 8). Like in most other euchelicerates, the first dorsal suspensor muscle is reduced. The posterior oblique suspensor muscles and the ventral suspensor muscles would provide another independent system to determine segment regions. However, the posterior oblique suspensor muscles are reduced in the anterior segments. Ventral suspensor muscles are maintained in the anterior segments 2–4, but they are missing in the more posterior segments of the prosoma (Figs. 23, 54). Both suspensor types provide direct support for the propeltidium as the shield of segments 1–6. Additional, indirect support for the suggested interpretation of the mesopeltidium as a parapeltidium comes from the observation that no muscles at all insert on this sclerite (except P9 which is an intrinsic prosomal muscle). Comparisons with *Eukoenenia mirabilis* and *Prokoenenia wheeleri* reveal differences in the endosternal muscles associated with the peltidia. Millot (1943) reported four dorsal, five lateral, and six ventral suspensors in *E. mirabilis* (Tab. 8). The dorsal suspensor of segment 7 and parts of the dorsal suspensor of segment 5 (presumably dorsal oblique suspensors) attach to the posterior border of the propeltidium, where they insert in the same position. There is no mention of suspensor muscles associated with the meso- and metapeltidium. Thus, following the author's interpretation, the propeltidium of *E. mirabilis* spans segments 1–7. A similar endosternal suspensor muscle configuration was described by Firstman (1973) for *P. wheeleri*. However, the most posterior dorsal suspensor muscle was associated with segment 6 by the author, therefore, assigning the propeltidium to segments 1–6 (Tab. 8). An insertion of dorsal suspensor muscle to the meso- and metapeltidium were also not described.

While the published results for the three species of Palpigradi are different, they all converge in the observation that the mesopeltidium has no attachment of dorsal suspensor muscles. They also converge in the observation that the first prosomal segment has no suspensor axial muscles, and a variable morphology of dorsal and/or ventral suspensor muscles in the second prosomal segment. Thus, the

Tab. 8. Comparison of the endosternal musculature associated with the box-truss axial muscle system (BTAMS) by Shultz (2007a, 2001). The identification of the muscles of a specific suspensor and segment is based on origin and insertion points. Due to the unclear segment borders in the prosoma, assignment of suspensor muscles is additionally based on directionality of the muscles. The original terminology of the previous authors was used to aid recognition. Question marks indicate that the association with a segment is unclear. Color codes are as follows: orange = dorsal suspensors, purple = anterior and posterior oblique suspensors, red = lateral suspensors, blue = ventral suspensors. Abbreviations: aos: anterior oblique suspensor, ds: dorsal suspensor, ls: lateral suspensor, pos: posterior oblique suspensor, vs: ventral suspensor.

		Segment 1	Segment 2	Segment 3	Segment 4	Segment 5	Segment 6	Segment 7	References
Euarthropod BTAMS	ds		■	■	■	■	■	■	Firstman (1973), Shultz (2001, 2007*b*)
	vs		■	■	■	■	■	■	
	ls	■	■	■	■	■	■	■	
	aos		■	■	■	■	■	■	
	pos		■	■	■	■	■	■	
Eukoenenia spelaea	ds			E3	E5	E11	E14	E17	this study
	vs		E1	E2	E7/9				
	ls					E10		E16/18/19	
	aos				E6				
	pos				E4	E12	E15	E20	
Eukoenenia mirabilis	ds		d1	?	d3	d4		d5	Millot (1943)
	vs		v1	v2	v3	v4	v5	v6	
	ls			l	l	L	l	l	
	aos								
	pos				Sp			Sp	
Prokoenenia wheeleri	ds		ds		ds	Ds	ds		Firstman (1973)
	vs		vs	vs	vs	Vs	vs	vs	
	ls			ts	ts	Ts	ts	ts	
	aos								
	pos					■		■	
Limulus sp.	ds		13_I	13_{II}	13_{III}	13_{IV}	13_V	13_{VI}	Shultz (2001)
	vs		15		16_{III}?	16_{IV}	16_V	16_{VI}	
	ls								
	aos								
	pos							14	
Opiliones	ds				8			9	Shultz (2000)
	vs					12	12	12	
	ls								
	aos								
	pos								
Scorpiones	ds		EP1	EP3				ES4	Shultz (2007*b*)
	vs			EP6	$ES10_{III}$	$ES10_{IV}$	$ES10_V$		
	ls								
	aos								
	pos		EP2	EP4					
Amblypygi	ds				17_{III}	17_{IV}	17_V	17_{VI}	Shultz (1999)
	vs				19_{III}		19_V	19_{VI}	
	ls								
	aos								
	pos				18_{III}	18_{IV}	18_V		
Schizomida	ds			a? ds?	e1? ds?	c? ds?	d? ds?	1?	Börner (1904), Firstman (1973)
	vs			f? vs?	9? vs?				
	ls								
	aos								
	pos				e2?	h?	10?		
Thely-phonida	ds			13_{II}	13_{III}	13_{IV}	13_V	13_{VI}	Shultz (1993)
	vs			15_{II}	15_{III}	15_{IV}	15_V	15_{VI}	
	ls								
	aos								
	pos					14_{IV}	14_V	14_{VI}	
Pseudo-scorpiones	ds				?			?	Firstman (1973), Mehnert et al. (2018)
	vs							?	
	ls								
	aos								
	pos								
Ticks	ds			?	?			?	Firstman (1973)
	vs			?	?			?	
	ls							?	
	aos								
	pos								

assignment of suspensor muscles as presented here is in accordance and not in conflict with existing observations. The two other studies, even if they present slightly different observations, (indirectly) support my interpretation of the mesopeltidium being a sclerotization of the lateral pleural membrane rather than a tergite of the 6th segment. Without precise knowledge of the prosomal axial muscle system in Solifugae and Schizomida (the two other groups with split dorsal sclerites), but given the phylogenetic distance of Palpigradi and with the other taxa, I consider the dorsal division of the prosoma into a propeltidium and metapeltidium as evolved independently in Palpigradi.

4.1.2   Prosoma, ventral aspect

The ventral side of the prosoma of arachnids is morphologically variable. Distinct sclerites are present in many groups, but they may differ in their morphological origin (Moritz 1993, Shultz 1993, 1999). Thus, an a priori assignment of any ventromedial sclerite as a "sternite" is a terminological simplification that potentially creates confusion. As a "sternite" in a strict sense, I consider the ventral sclerotization of a segment, as compared to the dorsal "tergite" on the dorsal side. In the ancestral euchelicerate condition, the prosoma probably had no sternites, because the ventral food groove occupied the space between the legs. In scorpions, a single sternum is located between the coxae of legs 3 and 4, and possibly incorporates also parts of the sternite of the first opisthosomal segment (Farley 1999, 2005, Shultz 2007b). Schizomida and Thelyphonida have three sterna. The anterior sternum (traditionally tritotetrasternum) is the result of fusion of the sternites associated with legs 1 and 2. The posterior sternum (traditionally pentasternum) associated with leg 3 is small. The posterior sternum (traditionally metasternum) is prominent and occupies the region between the last pair of legs (Börner 1904, Millot 1949b, Moritz 1993). According to Shultz (1993) it represents the sternite of the first opisthosoma segment, thus, is morphologically derived from the opisthosoma.

Prosomal sternites may be fused forming one single sternum spanning the entire region between legs 1–4 as in Amblypygi (Millot 1949c, Shultz 1999) and Araneae (Millot 1949d). However, Shultz (1999) recognized the separate sternite located between the last pair of legs ("metasternum") in Amblypygi as the first opisthosomal sternite. Some species of Pseudoscorpiones have a rudimentary sclerotized

tubercle located between legs 3 and 4. This structure might be a residual sternite (Vachon 1949, Moritz 1993). Some species of Pseudoscorpiones (Weygoldt 1969), Ricinulei (Millot 1949*e*), and Solifugae (Millot and Vachon 1949*a*) lack any sternum sternite on the prosoma. Acari and Opiliones show a clear autapomorphic pattern of the ventral prosoma and are, thus, not further discussed.

In *Eukoenenia spelaea,* sclerites of the dorsal and the ventral side of the prosoma differ in number and segmental association. As documented above, the dorsal side consists of two dorsal shields, the ventral side displays four distinct sternites. The anterior sternum is conventionally considered representing the fused sternites of the 3rd (pedipalps) and 4th (leg 1) prosomal segment. The three posterior sterna correspond with segments 5–7 (legs 2–4, respectively). However, the anterior sternum is associated with the ventral suspensor muscles (E1, E2, E7/9), muscles that are assigned to segments 2–4 and, therefore, possibly represents the fused sternites of segments 2–4. With this interpretation I contrast the above mentioned conventional morphological interpretation as a deuto-tritosternum, and consider the anterior sternum a "prosternum" formed by the merged sternites of segments 2, 3, and 4. Prosomal segments 5, 6 and 7 do not have ventral suspensor muscles, however, a topographic association of these sterna with these three segments is straightforward because of their topographic association with the legs. There is no morphological evidence that would reject their interpretation as true sternites, i.e. segmental ventral sclerotizations of the body wall.

The prosternum and three free sternites in combination with the legs divide the ventral prosoma into clearly recognizable units. The formation of a prosternum supports the idea that the segments of the pedipalps and legs 1 together form a functional unit. It was reported that Palpigradi use the pedipalp as leg (hence the name; Kästner 1931*a*, Christian 2004). However, the internal structure of the pedipalp and leg 1 (see below) as well as the additional sensory hairs (trichobothria) and double number of sensory setae on the distal article compared with legs 2–4, suggest that the pedipalps and the first pair of walking legs are rather used for sensing than for walking. It might be possible that the pedipalps, equipped with contact chemoreceptors, are used to sense the chemical composition of the immediate way ahead, and that leg 1, equipped with trichobothria, is used to detect air movements. The interpretation of the first pair of legs as sensory appendages

rather than pedipalps, and the three following pairs of legs as walking legs is consistent with the sensory equipment of these animals, their ecology, and also with similar evolutionary transformations of the first pair of legs in other groups of arachnids (e.g. Amblypygi, Araneae).

4.1.3 Chelicerae

The plesiomorphic morphology of the chelicerae of euchelicerates is tripartite (Weygoldt and Paulus 1979*b*, Shultz 2007*a*), i.e. they consist of three articles, a basal article, a fixed digit, and a movable digit. Fixed digit and movable digit form the chela. This plesiomorphic morphology has been modified in various taxa of the euchelicerates by reducing the basal article, forming a subchela, and/or by adding combs, teeth or other cuticular structures to the surface of the chelicerae. The chelicerae of *Eukoenenia spelaea* consist of three articles. The basal article is as long as the chela. The fixed and movable digits display serrated cuticular teeth. Compared with the body size, the chelicerae of *E. spelaea* are large, as they have approximately the same length as the propeltidium. Large chelicerae and pincer-like structures are usually associated with raptorial function (Kaneko 1988, Moritz 1993). This would indicate, that *E. spelaea* hunts its prey. On one occasion, a palpigrade was observed presumably feeding on a collembolan using its chelicerae (Condé 1996). However, other observations as well as structures found in this study (see 4.2.2 and 4.11) indicate an alternative mode of feeding for *E. spelaea*.

4.1.4 Pedipalps and legs

Euchelicerate appendages have conventionally been described as consisting of seven articles: coxa (article 1), trochanter (article 2), femur (article 3), patella (article 4), tibia (article 5), basitarsus (article 6), and telotarsus (article 7; van der Hammen 1977, Shultz 1989). The terminology of these articles, however, is not entirely consistent between authors (Tab. 9), partly because the definition of what constitutes a specific leg article, e.g. joint articulation, muscle/tendon insertions, varies. The total number of leg articles can differ between legs. In the specialized antenniform legs of Amblypygi, the tibia can consist of up to 43 articles and the tarsus up to 105 (Weygoldt 1996). In Thelyphonida, leg 1 consists of 14 articles in total (Grams et al. 2018). A reduction to six articles can be observed in the pedipalps

Tab. 9. Comparison of leg article terminology of Palpigradi.

	Article 1	Article 2	Article 3	Article 4	Article 5	Article 6	Article 7–11
Shultz (1989)	Coxa	Trochanter	Femur	Patella	Tibia	Basitarsus	Telotarsus
van der Hammen (1982)	Trochanter	Femur 1	Femur 2	Genu	Tibia	Tarsus 1	Tarsus 2–7
Millot (1949*f*)	Coxa	Trochanter	Femur	Patella	Tibia	Basitarsus (1–4)	Tarsus (1–3)

of Amblypygi, Araneae (Moritz 1993), Opiliones (Pinto-da-Rocha et al. 2007), Pseudoscorpiones (Weygoldt 1969), Ricinulei (Millot 1949*e*), Schizomida (Moritz 1993), Scorpiones (Polis 1990), Solifugae (Punzo 2012), and Thelyphonida (Grams et al. 2018). As few as 2 pedipalpal articles can be found in Acari (Moritz 1993).

Eukoenenia spelaea shows a heterogeneous number of articles and variable topography of musculature within its extremities (see 4.4.6.2) and joint articulation could not clearly be established. Thus, labeling of articles according to traditional terminology of either author cannot be done correctly. Therefore, I decided to continue to use the neural term "article" throughout this study. *E. spelaea* displays a varying number of articles in pedipalps and legs. Pedipalp and leg 1 have a total of nine articles in the pedipalp and 11 articles in leg 1. Legs 2 and 3 follow the euchelicerate ground pattern of seven articles, however, leg 4 has one additional article. Although the number of articles of leg 1 is stated to be 11 in this study, article 6 of leg 1 in Palpigradi has been interpreted as two separate articles by previous authors (Kästner 1931*a*, Millot 1949*f*). However, this article in *E. spelaea* shows no cuticular joint structure. The present muscle (LI8) and tendon (LI9t; Figs. 21A, 22C) span the entire article and show no attachment points of muscles/tendons adjacent to the circular cuticular groove located medially on the article. Therefore, these structures also give no evidence to clarify, whether this article is the result of fusion of two separate articles or whether it is a single article.

4.1.5   Opisthosoma

The ground pattern of the opisthosoma of euchelicerates includes 12 segments with segmental musculature and ganglia (Fage 1949, Millot 1949*a*, Shultz 2001, 2007*b*). The heart and gonads occupy the anterior segments of the opisthosoma (Fage

1949, Millot 1949*a*, Alberti et al. 2007). In some groups, the opisthosoma is organized in two morphologically distinct regions, a meso- and a metasoma. Typically, in groups with a mesosoma and a metasoma (Scorpiones [Kästner 1931*b*, Polis 1990], Ricinulei [Millot 1949*e*], Schizomida, Thelyphonida [Kästner 1931*f*], and the extinct Araneae *Chimerarachne yingi* [Wang et al. 2018]), the mesosomal segments are divided into dorsal tergite and ventral sternite by lateral pleural folds, while the metasomal segments have sclerite rings without pleural folds. The number of mesosomal and metasomal segments differs among these groups (Tab. 10; Millot 1949*e*, Talarico et al. 2011, Fusco and Minelli 2013, Wang et al. 2018). It is apparent, that arachnid groups with a metasoma also have a terminal appendage, i.e. flagellum or sting (Fusco and Minelli 2013, Wang et al. 2018). Ricinulei are the only group that lacks such a terminal structure on the metasoma (Millot 1949*e*, Talarico et al. 2011).

The internal anatomy of meso- and metasoma also differs in various aspects (Tab. 10). In the mesosoma, Scorpiones have free ganglia (Millot and Vachon 1949*b*). In addition to the heart, dorsoventral and intersegmental (including dorsal and ventral) musculature and gonads are present in all mesosomal segments of scorpions (Millot and Vachon 1949*b*, Alberti et al. 2007, Shultz 2007*b*, Wirkner and Prendini 2007). In Ricinulei, dorsoventral musculature is present in all mesosomal segments similar to Scorpiones. The gonads are restricted to segments 8–13 (Millot 1949*e*, Talarico et al. 2008). The opisthosomal ganglion of Schizomida is located in the second opisthosomal segment. Like Scorpiones, Schizomida have the heart and gonads located in the entire mesosoma. The dorsoventral musculature, however, is missing in the last two mesosomal segments (Börner 1904, Millot 1949*b*). Thelyphonida have the last opisthosomal ganglion located in the second to last segment of the mesosoma. Their dorsoventral and intersegmental musculature as well as gonads also reach into this segment. The heart spans the entire mesosoma (Börner 1904, Millot 1949*b*, Shultz 1993). No information is available on internal structures of *Chimerarachne yingi*. In the metasoma of Scorpiones, free ganglia as well as serial intersegmental muscles are present (Millot and Vachon 1949*b*, Snodgrass 1965). Serial intersegmental muscles can also be found in Ricinulei (Talarico et al. 2011), Thelyphonida and Schizomida (Millot 1949*b*), however, no ganglia are present.

The opisthosoma of *Eukoenenia spelaea* is divided into a mesosoma (seven segments) and metasoma (four segments; Tab. 10). In the mesosoma of *E. spelaea* I find externally separate sclerites dorsal and ventral, which are connected by the pleural membrane. The metasoma is characterized by the presence of sclerite rings. Internally, the free opisthosomal ganglia, and the heart are restricted to the mesosomal segments 8–14 (mesosoma; Tab. 10). The segmental dorsoventral and transversal musculature, is located in segments 9–13, thus, lacks in the last mesosomal segment. The gonads are also restricted to segments 9–13. In the metasoma, serial intersegmental muscles are present.

There is variation in the external and internal morphology of the mesosoma and metasoma among the above mentioned arachnid groups. Assuming serial segmental anatomy for such organs as the gonads, nervous system, musculature,

Tab. 10. Morphological characters of the mesosoma (yellow) and metasoma (green) in arachnid groups with such a division of the opisthosoma. The presence of color equals the presence of the relevant structure in the respective segment. Where information on the character is missing, a lighter version of the respective color or question mark was used. Abbreviations: DV: dorsoventral muscle; I: intersegmental muscle including dorsal, ventral, transversal muscles.

Segment		8	9	10	11	12	13	14	15	16	17	18	19
Scorpiones	Muscles	DV/I	DV/I	DV/I	DV/I	DV/I	DV/I	DV/I	I	I	I	I	I
	Ganglia												
	Heart												
	Gonads												
C. yingi	Muscles												
	Ganglia												
	Heart												
	Gonads												
E. spelaea	Muscles	I	DV/I	DV/I	DV/I	DV/I	DV/I	I	I	I	I	I	
	Ganglia												
	Heart												
	Gonads												
Ricinulei	Muscles	DV/?	DV/?	DV/?	DV/?	DV/?	DV/?	DV/?	I	I	I		
	Ganglia												
	Heart												
	Gonads												
Schizomida	Muscles	DV/?	DV/?	DV/?	DV/?	DV/?	DV/?	DV/?					
	Ganglia												
	Heart												
	Gonads												
Thelyphonida	Muscles	DV/I	DV/I	DV/I	DV/I	DV/I	DV/I	DV/I	DV/I	I	I	I	I
	Ganglia												
	Heart												
	Gonads												

and the heart in the ground pattern of euchelicerates, topographic shifts and replacements are frequently observed. However, such variations are also evident in arachnid groups without an opisthosomal subdivision (André 1949, Berland 1949, Millot 1949*c, d*, Millot and Vachon 1949*a*, Alberti et al. 2007). This indicates, that fusion (ganglia), displacement (heart, gonads), and reduction (muscles) of morphological structures occurs independent of such a division. Intersegmental musculature for the movement of the metasoma is the single common character for all arachnid groups with meso- and metasoma. This suggests that a metasoma free of segmental organs, with the exception of intersegmental muscles and ganglia (Scorpiones only), is a reorganization of the posterior opisthosoma segments to facilitate the movement of the terminal appendage in these groups.

The relevant arachnid groups have developed different morphologies and functions for their metasoma and terminal appendage. Scorpiones have added a sting to their metasoma for overpowering prey and predators, but also use their metasoma for courtship (Stahnke 1966, Polis and Farley 1979, Polis 1990). The usage of the metasoma in Ricinulei is unclear and the terminal appendage is missing. Thelyphonida utilize their metasoma with attached flagellum as feeler and to deter predators (Moritz 1993, Alberti et al. 2007). Schizomida display a sex dimorphism of their flagellum, which indicates that movement of the flagellum and metasoma is relevant for courtship and mating (Hansen and Sørensen 1905, Moritz 1993, de Armas and Teruel 2002, Teruel and De Armas 2002, Pinto-da-Rocha et al. 2016).

Eukoenenia spelaea have also been observed raising their flagellum (and possibly metasoma) when irritated (Kováč et al. 2002). Involvement of the metasoma and flagellum in courtship and mating in *E. spelaea* is unknown. However, the presence of sensory setae along the flagellum suggests some type of sensory function.

A division of the opisthosoma into meso- and metasoma appears to be only apparent in groups which have a flagellum or sting and have to "wag their tail" for various reasons. This points to a purely functional division of the opisthosoma into mesosoma and metasoma in arachnid groups carrying a movable terminal flagellum or otherwise moving their posterior body region.

4.2 Cuticle

The cuticle of arthropods consist of a thick procuticle covered by a thin epicuticle. Depending on topographic and functional specializations, the procuticle can be differentiated into an inner endocuticle and an outer, sclerotized exocuticle (Hackman 1984, Neville 1984). Sclerotized cuticle can be either dark in color or colorless depending on its chemical composition and mode of sclerotization (Hackman 1984). The epicuticle is actually deposited on the cuticular surface through pore canals that penetrate the cuticle in large numbers. Soft cuticular membranes connect sclerotized regions (sclerites) allowing for movements and size changes, e.g. when feeding or during gestation.

The cuticle of *Eukoenenia spelaea* is mostly non-sclerotized, thus, lacks a clear differentiation into endo- and exocuticle. This might be due to their small body size. An absence of cuticle differentiation into exo- and endocuticle is also an indication of miniaturization (Polilov 2015*a*).

4.2.1 Cutaneous respiration

Arachnids typically breathe with book lungs and/or tracheae. Respiratory organs may be reduced with decreasing body size, and cutaneous respiration has been reported for numerous mites (Levi 1967). The theoretical size limit of the effective dimension an organism can obtain for cutaneous respiration depends on shape, oxygen partial pressure, diffusion distance, metabolic rate and a the diffusion constant for oxygen (and carbon dioxide, of course). A maximum diameter of 1 mm for a spherical animal was estimated (Graham 1988). *Eukoenenia spelaea* is well below the size limitation of diffusive respiration, given a maximum opisthosoma diameter of approx. 300 µm (left-right; 180 µm dorsoventral), and a prosoma diameter of approx. 280 µm (left-right; 150 µm dorsoventral). Also, the soft cuticle of *E. spelaea* is only 0.5 µm thick, and the underlying epidermis is single layered and flat so that the overall diffusion barrier through the integument below 1 µm. The hemolymph space is limited, thus, gas exchange may occur directly with /across the cells of the organs in close contact to each other and the body wall. For comparison, *Prokoenenia wheeleri* (Rucker 1901) which is larger (2–3 mm; Rucker 1903) than *E. spelaea*, has ventral lung sacks which are considered to function as respiratory organs.

4.2.2 Surface structures

Cuticular surface structures are common in arthropods representing a plethora of forms and functions (Gorb 2001*a*). For example, the hair density in spiders was associated with water repellence (Suter et al. 2004, Bush et al. 2007). *Eukoenenia spelaea* also displays an extensive pubescence on most parts of its body consisting of short cuticular protrusions (2–3 µm length). Given the morphological similarity of these structures, i.e. relative length and width as well as high hair density in two phylogenetically unrelated groups the interpretation of the pubescence as hydrophobic surface structure might be plausible. This in particular as even a drop of water represents a life threatening volume.

Grooming behavior has been discussed for spiders as well as several coleopterans in association with maintaining their hydrophobic character (Kovac and Maschwitz 2000, Suter et al. 2004). Such behavior has also been previously reported in palpigrades (Christian 2004). Different from spiders and coleopterans, palpigrades do not use their legs for grooming, but their chelicerae. Specialized cuticular structures can be found on the fixed and movable digits of the chelicerae. These display serrated cuticular teeth. The distance between the teeth is approx. 1–1.5 µm. Between the protrusions of the serration, the distance is approx. 0.05–0.1 µm. These structures match the thickness of the setae and trichobothria, the thickness of their spikes as well as the pubescence. Thus, the primary functions of the chelicerae might be removal of particles as well as maintaining water-repellence. I will discuss a potential additional function for feeding in section 4.11.

4.3 Ventral plate and underlying structure

A previously undocumented structure of *Eukoenenia spelaea* is the ventral plate with its modified epidermis and cuticular teeth. The cuticle of the ventral plate is similar to the common epidermal cuticle of *E. spelaea,* but it has enlarged pore canals. Microvilli from the underlying epidermal cells reach into these pore canals. Enlarged pore canals in which microvilli extend from epidermal cells, are consistent with cuticle found associated with a type 1 transport epithelium (Noirot and Quennedey 1974).

In *Eukoenenia spelaea*, the epidermis cells under the ventral plate show a specialized morphology also typical for type 1 transport epithelial cells with their large size, extensive apical microvilli brush border, and the glycogen granules. Conte (1984) called membrane amplification, as found in transport epithelia, a "hallmark of epithelial cells destined to transport electrolytes". A similar cellular morphology, i.e. polarization and extensive brush border, has been found in the ventral vesicles of collembolans, which is the main place for sodium uptake (Noble-Nesbitt 1963, Eisenbeis 1974). A similar morphology has been reported for the nuchal organ (neck organ, Hauptorgan, neck shield, cephalothoracic organ or salt organ) of Eucrustacea, which is involved in salt excretion (Conte 1984, Lowy and Conte 1985). In eucrustaceans, the epithelial cells also store glycogen granules, similar to my findings in *E. spelaea* (Hootman and Conte 1975, Lowy and Conte 1985). Thus, the ventral plate and associated transport epithelium in *E. spelaea* is likely involved in water uptake and/or osmoregulation.

4.4 Musculature

In the first part of this section, I compare and discuss the axial musculature of *Eukoenenia spelaea* in relation to the ancestral/plesiomorphic pattern of musculature anatomy as suggested by the euarthropod and euchelicerate box-truss axial muscle system (BTAMS), respectively. This will be followed by a comparative discussion of other muscle systems (e.g. pharyngeal musculature, appendages) in the second part of this section. This discussion is to some degree "opportunistic" because it depends on presence, availability, completeness, and quality of the published record.

4.4.1 Suspensor muscles originating from the prosomal endosternite

The BTAMS was suggested by Shultz (1993, 1999, 2001, 2007*b*) and derived from dissections of Xiphosurida, Scorpiones, Amblypygi, Thelyphonida, and extensive comparisons with other euarthropod taxa. The euarthropod box-truss axial muscle system assumes dorsal, ventral, and lateral (transverse connectors in terminology of Shultz [2007*b*]) suspensor muscles as well as anterior and posterior oblique muscles (Shultz 2007*b*). In the prosoma, all these muscles originate serially from the endosternite, i.e. each prosomal segment, except the first segment, carries a complete set of muscles. For BTAMS in arachnids, Shultz (2001, 2007*b*) proposed

that the anterior oblique suspensors were reduced. This was based on the assumption of serial muscle homology of the opisthosomal dorsoventral musculature with the dorsal and ventral suspensor muscles (but see below), and the observation that Xiphosurida have such anterior oblique muscles in the opisthosoma, while it is missing in all arachnids.

Table 8 gives an overview on the occurrence and published evidence of the prosomal axial musculature among Euchelicerates including *Eukoenenia spelaea*. The complete set of segmental, axial prosoma muscles occurring in the supposed euarthropod ground pattern is given in the top row and mirrored as the grid system underlying the empirically observed/described muscles in various groups of euchelicerates. I included the original muscle terminology in each cell of the table so that reference to the original literature is straightforward.

All described euchelicerates deviate from the supposedly ancestral euarthropod and even the euchelicerate BTAMS. However, on the basis of the available material, palpigrades show the most complete set of axial muscles (Tab. 8) including an anterior oblique suspensor muscle in segment 4 in *Eukoenenia spelaea* (Figs. 23, 54). Muscle E13 which is originating in segment 6 and inserting posteriorly in segment 8 might be interpreted as ventral suspensor that, untypically, spans several segments (but see discussion below). Lateral suspensors were described for segments 5 and 7. My description of five pairs of dorsal suspensor muscles (Figs. 23, 54) is in contrast to Börner (1904), Millot (1943, 1949*f*)), and Firstman (1973) who explicitly state that *Eukoenenia mirabilis* and *Prokoenenia wheeleri* have only four dorsal suspensor muscles, respectively. Given the fact that this study is the only study based on serial sections and a complete reconstruction of the ground pattern of the musculature, I respectfully consider the data presented here as more reliable.

Depending on the interpretation, I found three or four muscle pairs that could be assigned ventral suspensor muscles (Figs. 23, 54), while earlier descriptions of *Eukoenenia mirabilis* and *Prokoenenia wheeleri* reported the full set of six ventral suspensor muscles. Palpigrades with six ventral suspensor muscles would represent the plesiomorphic condition of the euarthropod BTAMS. *Eukoenenia spelaea* with only three ventral suspensor muscles appears rather

advanced, but, with three segmental ventral suspensor muscles, it is close to the euarthropod BTAMS. The lateral suspensor system shows a similar pattern, with the full set of segmental muscles in *E. mirabilis* and *P. wheeleri*, while *E. spelaea* has only two lateral suspensor muscles (Figs. 23, 54).

Interpretations of the axial muscle system in Palpigradi are straightforward. The prosomal axial muscle system resembles closely the plesiomorphic pattern as described in the euarthropod (!) BTAMS. Reference to the euarthropod BTAMS is necessary because of the occurrence of an anterior oblique muscle in segment 4.

4.4.2   Other prosomal muscles of the BTAMS

According to the euarthropod BTAMS (Shultz 2001), paired dorsal longitudinal musculature extends from the posterior prosoma segments (6 and 7) into the opisthosoma. These muscles have been documented for *Limulus polyphemus* (Shultz 2001), Amblypygi, Thelyphonida, and *Eukoenenia mirabilis* (Börner 1904). In the latter, these muscles also connect propeltidium and metapeltidium. This supports the hypothesis, that the metapeltidium is not a tergite, but a sclerotization of the pleural fold (see 4.1.1).

In *Eukoenenia spelaea*, two additional muscles might represent additional components of the dorsal longitudinal muscle system. These muscles are sexually dimorphic. In females, the longitudinal prosomal muscle P11 (Figs. 21C, 22A; Tab. 5) is paired and elongated, whereas P12 is unpaired, short, and does not extend into the following segment. In males, muscle P11 is paired but shorter as compared to females. Muscle P12 in males is paired (Figs. 21B, 22B; Tab. 5). These muscles have also been reported in *Eukoenenia mirabilis* by Börner (1904). However, Millot (1949*f*) who studied the same species did not document these muscles. Both muscles might be remnants from dorsal axial musculature, which extends into segments 7 and 6 of the prosoma and was retained in species with a partially segmented prosoma.

4.4.3   Muscles of the pharynx

In the arachnid ground pattern, two muscular pharyngeal pumps are present, a precerebral and a postcerebral pump (Snodgrass 1948). The presence of both muscular pumps varies among arachnids. The precerebral pharyngeal pump has

dorsal and lateral dilator muscles and circular constrictor musculature. The dorsal dilator is part of the epipharyngeal complex, which, again, consists of an anterior and a posterior component (Shultz 1993). Dorsal dilator muscles of the anterior complex span between the pharynx and the intercheliceral septum, the dorsal dilator muscles of the posterior component attach to the prosomal shield. Variation of the pharyngeal muscles occurs in all components of the pre- and postcerebral pump as well as the anterior and posterior components of the precerebral pump.

In Palpigradi, the postcerebral pharyngeal pump is missing (Millot 1942). As shown here for *Eukoenenia spelaea*, the precerebral pharyngeal pump is simplified, i.e. it consists only of the anterior component with a mediodorsal dilator muscle (P3) spanning between the pharynx and the intercheliceral septum/sclerite (iChS; Fig. 32, 39A). Additionally, *E. spelaea* has a muscle (E8) that originates from the anterior margin of the endosternite and inserts at the posterior end of the pharynx. The muscular topography of *E. spelaea* resembles that of *Eukoenenia mirabilis* (Millot 1942). However, Millot (1942, 1943) described two muscles attaching anterior to the pharynx (m2, m3) in a position where I find only muscle E8 attaching posterior. He also described an additional muscle (m4) spanning between the lower lip and the transition between mouth opening and pharynx. I could find no such muscle in *E. spelaea*.

Shultz (1993) stated that the epipharyngeal complex of *Eukoenenia mirabilis* consists of a smaller anterior and a larger posterior component. This statement was based on the studies by Roewer and Bronn (1934), and Millot (1942). My interpretation of these studies differs, however. The mediodorsal dilator of the pharynx in *E. mirabilis* (m1; Millot 1942) is the anterior component of the epipharyngeal complex, while the posterior component is missing. The small anterior muscle associated with the anterior end of the pharynx (L. sup.; Millot 1942) inserts in the upper lip and is, thus, not part of the epipharyngeal complex as defined by Shultz (1993).

4.4.4 Axial musculature of the opisthosoma

For the opisthosoma of euarthropods, Shultz (2001) proposed longitudinal dorsal and ventral muscles, segmental dorsoventral muscles, as well as anterior and posterior oblique muscles. The dorsal and ventral longitudinal muscles have a point

of attachment in each segment. The euchelicerate pattern deviates by the topographic arrangements of the anterior oblique muscles, i.e. converging at the border between pro- and opisthosoma (only *Limulus*). According to Shultz (2001), the anterior oblique muscles are reduced and the posterior oblique muscles insert on the lateral pleural membrane in all arachnids.

The dorsoventral musculature of the first opisthosomal segment requires special discussion. The morphology of the first opisthosomal segment is modified in many arachnid taxa, e.g. in Scorpiones (Shultz 2007*b*) it is integrated in the diaphragm, in Araneae (Gerhardt and Kästner 1931) it forms the pedicel, in Amblypygi, Schizomida, and Thelyphonida (Börner 1904, Kästner 1931*f*) the ventral parts of the first opisthosomal segment are transformed into the sternite of the prosoma. In other groups, the dorsoventral musculature is completely missing in the first opisthosomal segment, e.g. Pseudoscorpiones (Mehnert et al. 2018) and Solifugae (Kästner 1931*e*). In my documentation of the axial musculature of palpigrades, dorsoventral muscles are completely missing in the first opisthosomal segment. The described muscle E20 that originates from the posterior end of the endosternite is the posterior oblique muscle of the last prosomal segment because it inserts lateral on the pleural membrane of the first opisthosomal segment (as described in the BTAMS). This interpretation is in contrast to, but more parsimonious than that of Börner (1904) and Kästner (1931*a*) who suggested that the dorsoventral muscle of the 1st opisthosomal segment moved its insertion to the posterior end of the endosternite. However, if so, it must also have changed its origin from the dorsal sclerite of the first opisthosomal segment to the pleural membrane. Firstman (1973) reported about opisthosomal dorsoventral musculature, but does not provide necessary details about the segmental topography.

The dorsal and ventral longitudinal muscles of *Eukoenenia spelaea* have a single point of origin and insertion, respectively. Unusual are the two lateral branches of the ventral longitudinal muscles. Similarly noteworthy is the topography of dorsal muscle D1, which originates in the prosoma and inserts posterior to the origin of dorsal longitudinal muscle D2 in segment 10. This overlap of the dorsal longitudinal muscles is similar to the parallel muscle strands in Amblypygi, Thelyphonida, and Xiphosurida. However, the lack of segmental attachment of the longitudinal musculature, dorsal and ventral, appears to be unique for *E. spelaea*.

Börner (1904) and Kästner (1931*a*) suggested that muscle E13 is an anterior extension of the ventral longitudinal musculature inserting on the posterior region of the endosternite. Börner's (1904) and Kästner's (1931*a*) interpretation, assuming shift of the attachment from the ventral sclerite to the endosternite, is equally parsimonious to my interpretation, assuming shift of the insertion from the ventral sclerite of the last prosomal segment to the first opisthosomal segment.

The 2nd and 4th opisthosomal segment (segments 9 and 11) show two pairs of peculiar muscles that might be either interpreted as lateral branches of the ventral longitudinal muscle system, or as posterior and anterior oblique muscles of opisthosomal segments 2 and 4. Both situations would be unusual, because (1) the ventral longitudinal muscle system usually does not branch in arachnids, and (2) anterior and posterior oblique muscles are intersegmental, but the muscle of the 2nd opisthosomal segment is intrasegmental and the muscle of the 4th opisthosomal segment bridges two segments.

4.4.5   Other axial muscles (non-BTAMS)

Several additional muscles can be identified in the opisthosoma that do not fit the BTAMS. Intertergal and intersternal muscles, i.e. muscles connecting adjacent tergites and sternites, can be found in Amblypygi (Shultz 1999), Araneae (Whitehead and Rempel 1959), Scorpiones (Shultz 2007*b*), and Thelyphonida (Shultz 1993). An incomplete set of such muscles can be found in Opiliones (Shultz 2000). Börner's (1904) report of *Eukoenenia mirabilis* mentioned one pair of intersegmental muscles in each segment from segment 10–15. Additionally, muscles associated with the last opisthosomal segment and its appendage were reported in Thelyphonida (Shultz 1993) and Xiphosurida (Shultz 2001).

Eukoenenia spelaea has up to six pairs of intersegmental muscles in each segment 9–17. In the last opisthosomal segment, two paired and one unpaired strong longitudinal muscles attach to the basis of the flagellum. The large number of small intersegmental muscles is in contrast to earlier reports of *Eukoenenia mirabilis*.

4.4.6 Musculature of the appendages

4.4.6.1 Chelicerae

The musculature associated with the chelicerae varies within the euchelicerate groups. In groups with tripartite chelicerae, the movement of the basal article is facilitated by a differing number of extrinsic antagonistic muscles (Tab. 11). The chela is opened and closed by an antagonistic pair of muscles/tendons in both tripartite and bipartite chelicerae (Millot and Vachon 1949*a*, Steinbach 1952, Whitehead and Rempel 1959, van der Hammen 1966, 1967, Dubale and Vyas 1968, Vyas 1974, van der Hammen 1982, Shultz 1993, Alberti and Coons 1999, Shultz 1999, 2000, 2001, Meijden et al. 2012). The depressor/adductor of the movable digit is generally more prominent than the levator/abductor.

The tripartite chelicerae of *Eukoenenia spelaea* is moved by three extrinsic and ten intrinsic muscles, two muscles (C1, C3; Tab. 11) possibly facilitate the downward movement, a third muscle (C4; Tab. 11) possibly facilitates upward movement. The downward movement of the chela is possibly controlled by three intrinsic muscles (C5, C7, C8; Tab. 11), which share a common insertion point. Different from other euchelicerates, a muscular antagonist is missing, because muscle C6 is possibly used for rotation. Thus, the upward movement might be achieved through hemolymph pressure. Another unique character of *E. spelaea* is the lack of a muscular antagonist to the prominent closing musculature of the fixed digit (C9–13; Tab 11). It can be assumed that hemolymph is the antagonist here as well. To my knowledge, *E. spelaea* is the only euchelicerate which varies from the general ground plan of euchelicerate musculature.

Although a quick closing of the chela is possible, opening is likely regulated by hemolymph pressure, thus, potentially slower. This supports the hypothesis of grooming as primary function (see 4.2.2) of the chelicerae in *Eukoenenia spelaea* in addition to a possible involvement in feeding (see 4.11).

Tab. 11. Musculature of chelicerae of *Eukoenenia spelaea* in comparison with other euchelicerate groups (where data is available). The muscles are color coded according to their associated article (grey = basal article, orange = fixed digit, purple = movable digit).

	Depressor Adductor	Levator Abductor	Depressor Adductor Remotor	Levator Abductor Promotor	Depressor Adductor Remotor	Levator Abductor Promotor
Xiphosurida (Shultz 2001)	51	52	50	49	48	45-47
Scorpiones (Vyas 1974)	17	18	12, 13, 15	14, 16	1, 3, 4, 6, 8–10	2, 5, 7, 11
Opiliones (Shultz 2000)	38	39	35, 36	34, 37	27–29, 32, 33	30, 31
E. mirabilis (van der Hammen 1982)	t_s	t_i	tf_i	tf_s	ttr_i	ttr, ttr_s
E. spelaea	C9-13		C6	C5, C7, C8	C1, C3	C4
Solifugae (Millot and Vachon 1949*a*, Meijden et al. 2012)	depressor digiti mobilis	levator digiti mobilis	depressor	levator		
Araneae (Steinbach 1952, Whitehead and Rempel 1959)	70–72	69	Add, De, Re / 11c–15c	Abd, Le, Pro / 9c, 10c, 16c		
Amblypygi (Shultz 1999)	33	34	25-28	29-32		
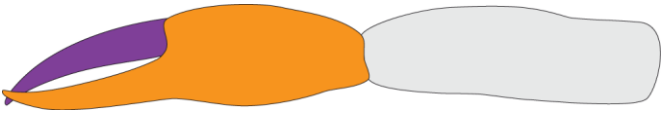
4.4.6.2   Pedipalps and legs

In euchelicerates, the pedipalp and legs are typically attached to the prosoma with a coxa. The coxa of the arachnid ancestor was probably moved by nine extrinsic muscles. Of these muscles, five originated on the dorsal shield and four originated from the endosternite (Shultz 1991). For the legs of *Eukoenenia mirabilis*, van der Hammen (1982) proposed that the first article is not a coxa, but a trochanter. The author based his interpretation on the muscle insertion and articulation found in the first leg article. According to his study, a pair of muscles/tendons insert laterodorsal and lateroventral, the articulation is located ventral. This view was rejected by Shultz (1989), who reasoned that the number of extrinsic muscles in *Eukoenenia* sp., three originating at the dorsal shield and two originating at the endosternite, is consistent with the muscle arrangement of the coxa in most euchelicerates.

Extrinsic musculature is found in all extremities of *Eukoenenia spelaea*. The number and origin of these muscles varies. Extrinsic musculature originating on the endosternite is present in legs 1–4, legs 1–3 have one endosternal muscle each and leg 4 has three endosternal muscles. One extrinsic muscle originating on the dorsal shield is present in the pedipalp, and legs 1–3. Leg 4 has no extrinsic musculature originating from the dorsal shield.

Whether the first article of the legs in *Eukoenenia spelaea* is a coxa or not, is not trivial, even with the criteria presented by van der Hammen (1982) and Shultz (1989). This is due to the fact that the number and origin/insertion points of the musculature varies between the extremities. The muscle/tendon configuration proposed by van der Hammen (1982) for the first article in *Eukoenenia mirabilis* was only found in part in leg 4 of *E. spelaea*. Muscle LIV4 fits the description, however, LIV5 does not. For the other leg joints, only few muscles matched the suggested configuration. This could be due to interspecific variation. It could also indicate, that the first article of *E. spelaea* is not a trochanter, as proposed by van der Hammen (1982). The muscle configuration reported by Shultz (1989) for the coxa in *Eukoenenia* sp. can be partially found in legs 2–4. As mentioned above, in *E. spelaea*, deviations from the proposed ground pattern are the reduced number of muscles originating from the dorsal shield and the endosternite. However, despite these variations, the presence of endosternal musculature inserting in the coxa supports the definition of the first article as coxa.

The intrinsic locomotor musculature of Euchelicerata was described by Shultz (1989, 2001). The proposed ground pattern for Arachnida consists of 13 muscles (Tab. 12). Extensors in articles 3–7 are present in Opiliones, Pseudoscorpiones, Scorpiones, Solifugae (Shultz 1989), and Xiphosurida (Shultz 1989, 2001). For *Eukoenenia mirabilis*, the analysis of leg 4 shows only muscles 1–3, 6–8, and 11 of the arachnid ground pattern and no extensors in articles 3–7 (Shultz 1989).

It is apparent, that the number of muscles as well as their overall origin and insertion varies between legs in *Eukoenenia spelaea* (Tabs. 5, 13). The terminal articles of pedipalp and leg 1 all have a single tendon each (PP6t–PP10t) attached to the joints with a pulley. This differs from the free tendon (1) in the ground pattern of

Tab. 12. Musculature of leg 4 of *Eukoenenia spelaea* in comparison with the proposed euchelicerate ground pattern and other euchelicerate groups for leg 4 (Shultz 1989). For better distinguishability of the separate muscles, the ground pattern was divided into two schematics. Muscle color codes in the table are identical to the schematic in the header. Light color code for *E. spelaea* indicates muscles which are not a good fit to the proposed ground pattern. Muscle 8 is coded as one muscle, but it is divided into several smaller muscles in most euchelicerate.
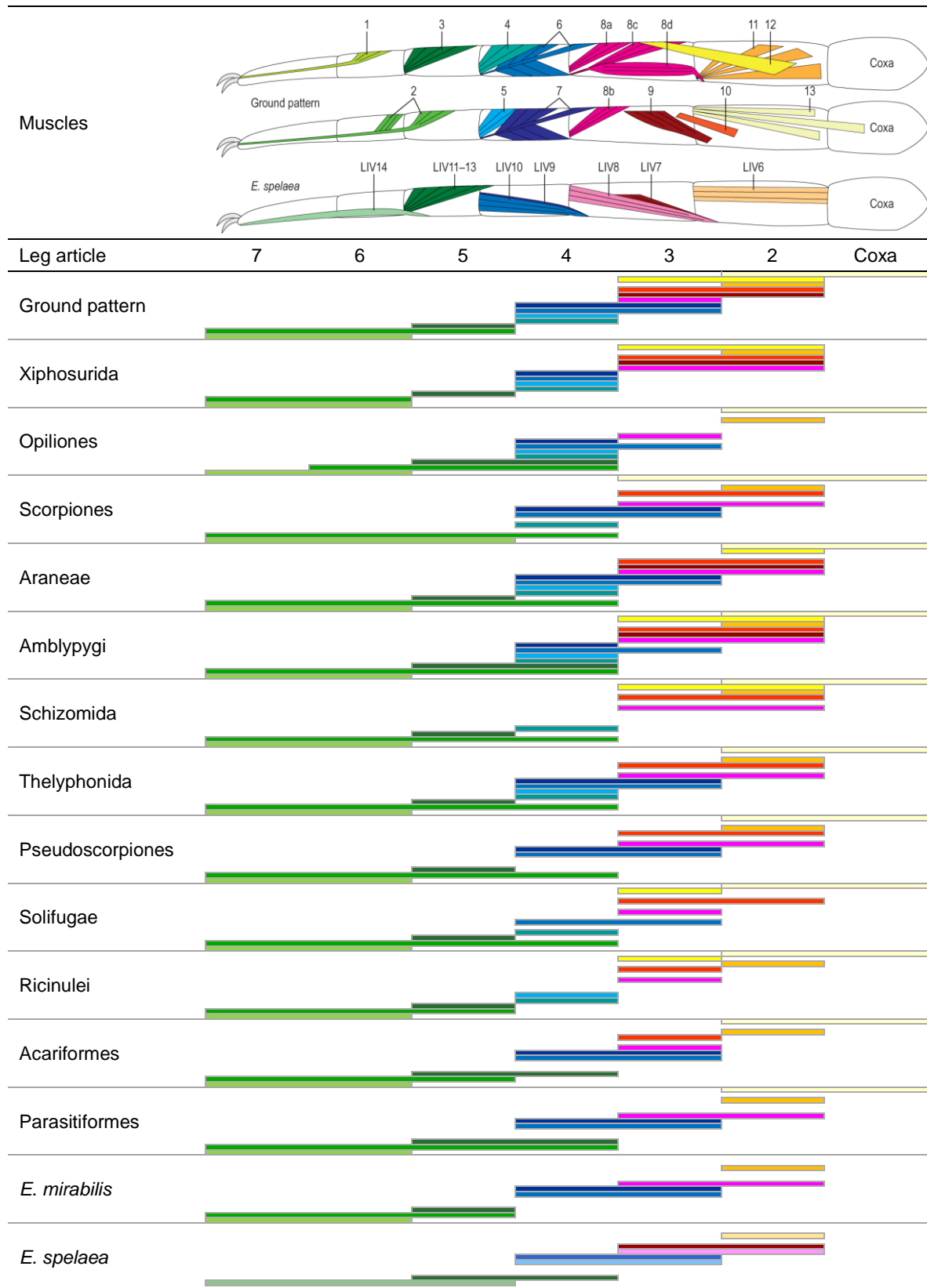
euchelicerates. Legs 2–4 do not have a muscle or tendon which can be considered homologous to muscle 1 of Shultz (1989).

Only muscle 2 of the proposed euchelicerate ground pattern can be matched with muscles in all the pedipalp and legs 1–4 (PP5, LI8, LII9, LIII10, LIV14; Tab. 13). In leg 4, however, the muscle (LIV14) originates ventral in article and does not insert at or near the tarsal claw. This is not fully in accordance with the proposed ground pattern, therefore, its origin and insertion point either moved considerably or this muscle cannot be matched with muscle 2 (Figs. 21A, 22C; Tab. 13).

Muscle 3 is missing in the pedipalp. In leg 1, muscle LI7 is not a clear match with muscle 3, its point of origin is lateral, not dorsal. Thus, it can only be considered a match with muscle 3, if the point of origin has shifted. Muscles LII8 (leg 2), LIII9 (leg 3), and LIV11–13 (leg 4) can be identified as muscle 3 of the ground pattern (Tab. 13). The slightly shifted points of origin and insertion in these muscles are possibly due to difficulty in properly orienting the legs.

Similar to *Eukoenenia mirabilis*, Acariformes, Parasitiformes and Pseudo-scorpiones, muscles 4 and 5 are missing in all pedipalp and legs in *E. spelaea* (Tab. 13).

Muscle 6 of the ground pattern is present in pedipalps and legs 1–4, however, in the pedipalp and leg 1, the muscle (PP4, LI6) is a side branch of a larger muscle. In legs 2 and 3, the muscle (LII7, LIII8) continues on into the following article, and in leg 4 (LIV10) the point of origin is ventral, not dorsal (Figs. 21A, 22C). Thus, a clear match to muscle 6 is not possible (Tab. 13).

A similar situation can be found with muscle LIV9 of leg 4. It too, has the point of origin shifted to ventral and is, thus, not a clear match with muscle 7 of the ground pattern (Figs. 21A, 22C; Tab. 13). Homologues of muscle 7 are missing in pedipalps and legs 1–3.

Poor matches for muscle 8 are present in legs 1–4 (LI5, LII6, LIII6/7, LIV8; Tab. 13). Discrepancies are present in the point of origin and insertion (Figs. 21A, 22C). The pedipalp lacks this muscle.

Tab. 13. *Eukoenenia spelaea*, comparison of musculature in pedipalps and legs. Color coding is identical to table 12. Light color code indicates muscles which are not a good fit to the proposed ground pattern. The muscles are coded according to their presence in one or more leg articles (the additional articles of pedipalp and leg 1 are assumed to follow article 7).

Muscle 9 of the ground pattern was only observed in leg 4 (LIV7). It is missing in the pedipalp and legs 1–3. This is similar to leg 4 in Amblypygi, Araneae, and Xiphosurida.

The lack of muscle 10 in pedipalp and all legs is similar to *E. mirabilis*, Parasitiformes, and Opiliones (Tab. 13).

Muscle 11 is only present in the pedipalp (PP3) and leg 4 (LIV6) in *E. spelaea*. However, there is a shift in point of origin and insertion which makes a match with the ground pattern difficult (Figs. 21A, 22C; Tab. 13).

A possible homologue of muscle 12 can be found in legs 1–3 (LI4, LII5, LIII5) but shifts in points of origin/insertion as well as muscle LII5 spanning three articles does not match the ground pattern (Figs. 21A, 22C; Tab. 13).

Additional possible matches are muscles LII4 and LIII4 of legs 2 and 3 with muscle 13, however, shifts in points of origin and insertion are apparent. Muscle 13 is missing in the pedipalp, leg 1, and leg 4 (Figs. 21A, 22C; Tab. 13).

It is evident, that the leg musculature of *Eukoenenia spelaea*, although variable between legs, shows most similarities to Acariformes and Parasitiformes (Tab. 12).

However, the presence of antagonistic muscle pairs, thus, extensors in articles 3–5 in *E. spelaea*, is similar to Opiliones, Pseudoscorpiones, Scorpiones, Solifugae, and Xiphosurida. Discrepancies between origin and insertion points of muscles described by Shultz (1989) for *Eukoenenia* sp. and in this study might be due to interspecific differences. Difficulty in orienting the legs properly might also lead to different interpretations of muscle attachment points.

4.5   Nervous system

4.5.1   Ground pattern

According to recent interpretations, the prosomal syncerebrum (supraesophageal ganglion) of arachnids is comprised of the proto- (ocular segment), deuto- (cheliceral segment), and tritocerebrum (pedipalpal segment; Damen et al. 1998, Telford and Thomas 1998, Mittmann and Scholtz 2003, Harzsch et al. 2005, Scholtz and Edgecombe 2006, Loesel et al. 2013, Wolf 2016). Developmental

studies of *Limulus polyphemus* suggested that the stomodaeum is enveloped by the deutocerebrum, not as previously suggested, the tritocerebrum, and that this is possibly a feature of the euarthropod ground pattern (Harzsch et al. 2005). However, the morphological evidences supporting this view are not unequivocally accepted, and there is still considerable discussion about the segmental nature of the syncerebrum (Babu 1965, Weygoldt 1985, Wegerhoff and Breidbach 1995, Bitsch and Bitsch 2007).

The subesophageal ganglion complex contains the pedal ganglia and a variable number of opisthosomal ganglia (Gottlieb 1926, Hanstrom 1928, Beier 1931, Kästner 1931*b, d, e*, Babu and Barth 1984, Wegerhoff and Breidbach 1995). The syncerebrum and the subesophageal ganglion are connected by a pair of circumesophageal connectives (Horn and Achaval 2002) and, together, form the synganglion. If a deutocerebrum is present, the circumesophageal connectives connect the supraesophageal with the subesophageal part of the deutocerebrum. If a deutocerebrum is not present, the circumesophageal connectives connect the respective parts of the tritocerebrum (Bitsch and Bitsch 2007).

Within the opisthosoma, the arthropod ground pattern shows a ladder nervous system with free ganglia (Handlirsch 1926). In most euchelicerate taxa, opisthosomal ganglia are reduced. However, in (juvenile) *Limulus* sp. the first opisthosomal ganglion is fused to the prosomal synganglion, but the following seven pairs of ganglia form a typical ladder nervous system. The opisthosomal ganglia are (later) medially fused (Tanaka et al. 2013, Battelle 2017). Scorpions have three pairs of ganglia in the mesosoma and four pairs in the metasoma. A small unpaired opisthosomal ganglion can be found in Thelyphonida and Solifugae, other arachnids lack opisthosomal ganglia (Millot 1949*a*, Babu 1985).

4.5.2   The brain of *Eukoenenia spelaea*

The brain of *Eukoenenia spelaea* is proportionally large and shows a high degree of fusion. My analysis revealed three commissures, two supraesophageal, i.e. the protocerebral and cheliceral commissure, and one subesophageal commissure associated with the pedipalps (Figs. 26, 27). I cannot definitively say that the portion of the supraesophageal ganglion associated with the chelicerae is the deutocerebrum, and the portion of the supraesophageal ganglion associated with

the pedipalps is the tritocerebrum. My analysis suggests, that the esophagus is enveloped by the portion of the supraesophageal ganglion associated with the chelicerae (Fig. 27).

A clear division of the synganglion of *Eukoenenia spelaea* into a supraesophageal proto- and deutocerebrum as well as a subesophageal tritocerebrum followed by the ganglia of the legs could not be established, it is, however, likely. This is further supported by morphological similarities with the larval synganglion of *Limulus polyphemus*, where the brain was described as tripartite (Mittmann and Scholtz 2003, Harzsch et al. 2005). The central portion of the protocerebrum in *L. polyphemus* is slightly bent. In *E. spelaea*, the protocerebrum is likely also bent to accommodate the nerve structures leading to the chelicerae in the anterior region of the supraesophageal ganglion. Similar to the larval synganglion of *L. polyphemus*, the cheliceral commissure of *E. spelaea* is located supra-esophageally and the pedipalpal commissure is subesophageal. In addition, the visual center, which is lacking in *E. spelaea* is only developed in postembryonic phase in *L. polyphemus*. This might also be an indication for paedomorphosis in *E. spelaea*.

The ganglia of the first three opisthosomal segments of *Eukoenenia spelaea* are probably fused to the subesophageal ganglion because it reaches into the second opisthosomal segment. The ganglia of the third opisthosomal segment were possibly displaced anteriorly due to this fusion. Such anterior displacement of opisthosomal ganglia and fusion to the subesophageal ganglion have been reported in other arachnids (Babu 1985). Opisthosomal segments 4 through 7 show individual small ganglia. This is consistent with the arthropod ground pattern. The number of neurons within the opisthosomal ganglia of *E. spelaea* is approx. 25, a number that is usually found in arthropod embryos (10–90 neurons per ganglion; Gerberding and Scholtz 2001, Harzsch 2003) and not in adults where neuron numbers vary between approx. 110 neurons in the fused opisthosomal ganglion of the mite *Ornithodoros parkeri* (Pound and Oliver JR 1982) to more than 4000 neurons per ganglion in *L. polyphemus* (Bursey 1973). Whereas the presence of free ganglia represents a plesiomorphic condition, the small number of neurons suggests a paedomorphic morphology of the opisthosomal ganglia in *E. spelaea*.

The ground pattern of euchelicerates has a perineural vascular sheath, that surrounds the synganglion and (probably) supplies it with oxygen and nutrients (Firstman 1973, Alberti and Coons 1999, Coons and Alberti 1999, Klußmann-Fricke et al. 2012, Wirkner and Huckstorf 2013, Göpel and Wirkner 2015, Klußmann-Fricke and Wirkner 2016). In many euchelicerates, the perineural vascular sheath has been modified into a network of arteries and capillaries. In other groups, tracheate arachnids, it has been reduced (solifuges [Klann 2009] and mites [Alberti and Coons 1999]).

Firstman (1973) documented a perineural vascular sheath in *Prokoenenia wheeleri*, however, I found no evidence for such structure or any residue of it. In *Eukoenenia spelaea*, the synganglion is surrounded by a thin and probably incomplete perineurium (glia cells surrounding the pericarya layer). The perineurium produces a thin extracellular matrix that might be considered a neural lamella. – I would like to reiterate that the cuticle of the prosoma is thin and all observed dimensions of the prosoma of *E. spelaea* suggest that diffusion is sufficient to ensure continuous oxygen supply of the prosomal ganglia.

4.6   Frontal Organ

The frontal organ of *Eukoenenia spelaea* consists of two modified setae that share a common base, thus, forming a sensory unit. Each seta of the frontal organ has its own set of enveloping cells. The setae's surface is covered with a multitude of cuticular grooves. The topographic position of the frontal organ and its construction from two setae on a common basis makes it a unique structure among arthropods.

While the topographic anatomy is unique, its ultrastructure characterizes it as a sensory unit and allows to recognize features typical for sense modalities in terrestrial arthropods, i.e. hygroreception, thermoreception and chemoreception. Different sense modalities may be combined in sensory units of terrestrial arthropods, i.e. hygro- and thermoreceptors, or chemo-/thermo-/hygroreceptors. All sensory cells are embedded in dense material/receptor lymph. A hygroreceptive unit usually consists of two cells, a moist cell and a dry cell, however, single cell hygroreceptors have been reported as well (Anton and Tichy 1994, Tichy and Loftus 1996, Barth 2002, Gainett et al. 2017*a*). Ultrastructurally they are characterized by branched dendrites. Thermoreceptors contain lamellate dendrites (Davis and

Sokolove 1975, Altner et al. 1978, Yokohari 1999). Chemoreceptors contain branched dendrites (Steinbrecht 1969, Altner and Prillinger 1980, Foelix 1985, Tichy and Barth 1992, Tichy and Loftus 1996) in combination with one pore at the tip of the hair for contact chemoreception, or numerous pores evenly distributed along the hair shaft for non-contact chemoreception (Altner and Prillinger 1980, Foelix and Hebets 2001, Barth 2002).

Thus, ultrastructural analysis can, to some degree, provide evidence of the receptive modalities of sensory hairs, i.e. (two) branching dendrites in combination with a smooth cuticle surface usually are associated with hygroreception, branched dendrites in combination of cuticle pores are associated with chemoreception (contact/non-contact), and lamellate dendrites are associated with thermoreception. This ultrastructural distinction describes a general pattern, however, some arachnids have thermo- and/or hygroreceptors in combination with pored sensory setae (Foelix and Axtell 1972, Foelix and Chu-Wang 1973, Foelix 1985, Anton and Tichy 1994, Tichy and Loftus 1996), thus, morphological evidence must be considered carefully as suggestive of sense modalities but requires additional experimental testing.

Among terrestrial arthropods combined thermo- and hygroreceptors are common (Waldow 1970, Altner et al. 1973, Loftus 1976, Altner 1977, Altner et al. 1978, 1983). Thermo-/hygroreceptors or combination chemo-/thermo-/hygroreceptors were described in Acari (Foelix and Axtell 1972, Hess and Loftus 1984), Araneae (Foelix and Chu-Wang 1973, Ehn and Tichy 1994) and Opiliones (Gainett et al. 2017*a*). They were specifically found on legs of arachnids (Anton and Tichy 1994, Gainett et al. 2017*a*). The tarsal organ in some arachnid groups (Foelix and Chu-Wang 1973, Foelix and Schabronath 1983, Talarico et al. 2005) and Haller's organ in Parasitiformes (Acari; Alberti and Coons 1999, Foelix and Axtell 1972) act as sensory unit consisting of several closely neighboring sensory structures, thus, possibly improving sensory resolution (Anton and Tichy 1994).

The frontal organ of *Eukoenenia spelaea* is unusual for terrestrial arthropods because of its asymmetrical organization, i.e. left and right setae contain dendrites with obviously different sense modalities. The base of the frontal organ contains two pairs of sensory cells that reach into the left and right seta. The left seta receives

two cylindrically branching dendrites. In combination with a smooth surface this would be indicative of hygroreception, in combination with pore(s) it would suggest (non-)contact chemoreception. Obviously it is not that easy in palpigrades: as described above, the surface of the seta has cuticular grooves, but they are shallow and do not penetrate the entire procuticle. Thus, the dendritic branches cannot get in direct contact with the substances outside. The cuticular honeycomb patterns in combination with an extremely thin cuticle (< 0.2 µm) could be interpreted as a lightweight construction as found in, e.g. beetle forewings (Chen et al. 2012). This might further suggest that the seta is more similar to a smooth seta. However, on the basis of my ultrastructural analysis, it is impossible to ultimately decide, if the two branching dendrites in the left seta in combination with the cuticular grooves stand for chemo- or hygroreception. The right seta of the frontal organ contains one cylindrically branched dendrite and a lamellate dendrite. Like on the left seta, the cuticular grooves on the surface of the right seta do not penetrate the procuticle. Therefore, the branching dendrite could be either non-contact chemoreceptor or hygroreceptor, while the lamellate dendrite is possibly a thermoreceptor.

Lamellate receptors also indicate a correlation between the extent of lamellation and the range of the operating temperature. A lower range of the operating temperature seems to be correlated with an increase in the number of dendritic lamellae (Loftus and Corbière-Tichané 1981, Corbière-Tichané and Loftus 1983, Altner and Loftus 1985). Such receptors are often found in small arachnids such as Opiliones, for which temperature and humidity are an integral part of their lives (Todd 1949, Wiens and Donoghue 2004, Curtis and Machado 2007). The lamellation within the proposed thermoreceptive dendrite in *Eukoenenia spelaea* is extensive. The environment in which these animals live is cool and moist. The temperature within the cave is stable between +7.9 and +10.7 °C, and the humidity is always around 97 % (Kováč et al. 2002, 2014). This provides indirect support for the idea that the right seta is a thermoreceptor.

4.7 Lateral organ

The lateral organs of *Eukoenenia spelaea* are also a unique sensory organ of palpigrades. Each consists of four modified sensory hairs. However, these sensory hairs have no common base like in the frontal organ. The ultrastructure of all setae

is identical and resembles very much the ultrastructure described for the left seta of the frontal organ. Thus, based on the ultrastructural results the interpretation is the same, i.e. branching dendrites in combination with the numerous cuticular grooves suggests that the lateral organs function as non-contact chemoreceptors or hygroreceptors.

4.8   Sensory setae

The combination of chemo- and mechanoreceptive sensory cells in setae is common in arthropods (Chu-Wang and Axtell 1973, Foelix and Chu-Wang 1973, Harris and Mill 1973, Ozaki and Tominaga 1999). Especially eyeless soil arthropods possess such combined sensory organs (Eisenbeis and Wichard 1987).

In contrast to the modified setae of the frontal and the lateral organ, the dendrites are unbranched in chemoreceptive sensory setae of arthropods. Few pores on the tip of the seta are usually interpreted as contact chemoreception while many pores along a large portion of the shaft of the seta are interpreted as non-contact chemoreception. Also, the cuticular wall of the seta can be single or double with two or three canals. The dendrites are located in the inner canal whereas the outer canal(s) is either filled with dense material/receptor lymph or it is empty. The outer canal is typically crescent-shaped in cross-section (Foelix and Chu-Wang 1973, Foelix et al. 1975). Mechanoreceptive cells typically end in a tubular body at a cuticular socket at the basis of the hair (Foelix et al. 1975, Gaffal et al. 1975, McIver 1975, Keil 1997, Barth et al. 2004, Dechant et al. 2006). Thus, ultrastructural features of combined chemo-mechanoreceptors are distinct, i.e. pored surface in combination with one or few unbranched dendrites, and a cuticular socket with a tubular body at the base of the sense hair.

Numerous examples of combined chemo-mechanoreceptors representing this ultrastructural organization, together with the taxon specific variations, have been published (Scorpiones: 4 dendrites; Tab. 14 [Foelix and Schabronath 1983, Cushing et al. 2014], and Solifugae: 4–7 dendrites [Haupt, 1982]). In Acari (Foelix and Chu-Wang 1972, Chu-Wang and Axtell 1973, Hess and Vlimant 1982), Amblypygi (Foelix et al. 1975, Foelix and Hebets 2001), and Araneae (Foelix and Chu-Wang 1973, Harris and Mill 1973), the number is reduced to two mechanoreceptive dendrites per seta (Tab. 14).

Tab. 14. Number of chemo- and mechanoreceptive dendrites within sensory setae in Arachnida.

	Chemoreceptive dendrites	Mechanoreceptive dendrites	References
Acari	3–8	2	Foelix and Chu-Wang (1972), Chu-Wang and Axtell (1973), Hess and Vlimant (1982)
Amblypygi	9–12	2	Foelix et al. (1975), Foelix and Hebets (2001)
Araneae	~20	2	Foelix and Chu-Wang (1973), Harris and Mill (1973)
Opiliones	~16	unknown	Foelix (1976), Gainett et al. (2017*b*)
Pseudoscorpiones	3–5	unknown	Foelix (1985)
Scorpiones	~20	4	Foelix and Schabronath (1983), Cushing et al. (2014)
Solifugae	12	4–7	Haupt (1982)
E. spelaea	2	5?	this study

In *Eukoenenia spelaea*, the sensory setae of the body and the flagellum have few cuticular pores at their tip and the seta is double walled with an empty outer canal. At least two dendrites reach to the tip of the hair shaft. All sensory setae have a cuticular socket with tubular bodies at which five dendrites terminate. These ultrastructural features clearly suggest that these hairs function as (contact)chemo-mechanoreceptors. – Among euchelicerates, there seems to be a correlation between the number of chemoreceptive dendrites and body size (Tab. 14). While most larger-bodied groups have 10–20 dendrites, taxa with small body size like Acari or Pseudoscorpiones have only 3–8 or 3–5 dendrites, respectively. *E. spelaea* is among the smallest euchelicerates and has only two chemoreceptive dendrites.

Typically, double-walled contact-chemoreceptors of arthropods have plugged pores in the outer wall; also the outer canal is filled with dense material/receptor lymph (Foelix and Chu-Wang 1973). Again, *Eukoenenia spelaea* is special, because the outer pore on each side of the seta is open and the outer canal is empty, but the inner pore plugged. Such a configuration might be associated with receptor specificity, as chemicals pass differently through dense material/receptor lymph and cuticular plugs (Altner et al. 1977).

4.9 Trichobothria

Trichobothria are common and characteristic mechanoreceptive sensory organs of terrestrial arthropods. The typical structure of an arachnid trichobothrium includes a thin hair which is directly or indirectly connected to sensory cells in a cuticular socket. This socket has either bilateral symmetry as in spiders (Görner 1965, Harris and Mill 1977) or it is circular like in scorpions (Hoffmann 1967, Messlinger 1987). The socket has either smooth ridges (Scorpiones [Messlinger 1987, Farley 1999], and Araneae [Barth 2014]) or is ridged and teethed (orbatid mites [Alberti et al. 1994]). The socked consists of an outer and inner cavity that are separated by a thin cuticular membrane. The inner cavity is an extension of the outer receptor lymph cavity and filled with receptor lymph. Dendrites are surrounded by the dendritic sheath and terminate in a tubular body at the base of the hair. Bending of the hair may cause displacement of the cuticular helmet at the basis of the hair resulting in deformation of the tubular body and ultimately in the creation of an action potential in the sensory cell. The seta itself is either massive with only a short lumen at its proximal end (Alberti et al. 1995) or hollow (Reißland and Görner 1985), but it does not contain dendrites. This overall fine structure of a trichobothrium is specific and widely found among arachnids.

The trichobothria of *Eukoenenia spelaea* follow this general arachnid pattern. They have a circular socket with cuticular teeth. However, they differ in one important detail, i.e. of the five dendrites associated with the trichobothrium, four continue on into the hair shaft, with one extending into the distal section of the hair. In the base of the hair, the dendrites retain their 9 x 2 + 0 microtubule configuration. I found a cuticular thickening at the base of the hair which I interpret as the residue of a cuticular helmet. A true helmet-like structure was not developed because of the dendrites reaching into the hair. I did not find tubular bodies. However, my material was limited and the presence of tubular bodies cannot be entirely ruled out. Dendrites inside the hair shaft are unusual and might indicate a second sense modality in addition to mechanoreception.

I could not identify pores along the hair shaft but my material was limited. A general similarity to a chemoreceptor is evident. Similar unusual trichobothria were described for the millipede *Polyxenus*. In this species, three unbranched dendrites

enter the hair and retain their 9 x 2 + 0 microtubule configuration in the outer dendritic segments. A cuticular helmet structure as well as tubular bodies were not found (Tichy 1975). In addition, the trichobothrium of *Polyxenus* has several plugged pores along its shaft and, thus, its function was proposed to be chemoreceptive (Tichy 1975).

In *Eukoenenia spelaea*, the cuticular teeth of the socket might serve three functions: (1) the teeth might prevent sediment particles from entering the socket and, thus, obstructing the movement of the hair. The sediment reported in the Ardovská Cave consists of particles smaller than 2 µm among others (Kučera 1964, Guggenheim and Martin 1995, ISO 2017). Such small particles could be held back by the cuticular teeth, which are spaced at approx. 10 nm. Similar retention structures are known from mites (Alberti et al. 1994, Gorb 2001*b*) where they may also hinder microorganisms from entering the socket (Alberti et al. 1994). (2) The teeth might prevent breakage of the hair due to overextension while moving through sediment. The thin cuticle teeth might bend more easily when the hair shaft gets pressed against them, thus, be more flexible than a solid ridge. (3) The cuticular teeth might prevent the seta from adhering to the side of the socket, thus, impairing its flexibility.

4.10 Heart

In the ground pattern of arthropods, the heart is a dorsal muscular tube surrounded by a pericardium and suspended by musculo-elastic ligaments which act as antagonist to the circular muscles of the heart tube (Shear 1999). Hemolymph enters the heart through paired segmental ostia. The heart of arachnids is typically supplied with a nerve to regulate the contraction of the cardiac muscle (Zwicky and Hodgson 1965, Sherman et al. 1969, Bursey and Sherman 1970, Obenchain and Oliver, Jr 1975, Alberti and Seeman 2004). Pure myogenic hearts can be found in some ticks (Schriefer et al. 1987, Coons and Alberti 1999). The muscle cells of the heart tube are typical striated muscles, with clearly defined sarcomeres. The Z-line, A- and I-band, T-tubular system as well as the sarcoplasmic reticulum (SR) are well developed (Tjønneland et al. 1987). The heart pumps the hemolymph through the body. The hemolymph-vascular system of euchelicerates can be morphologically complex in pulmonate euchelicerates (Wirkner et al. 2013), but tends to be simplified

in tracheate arachnids (Crome 1953, Levi 1967), or reduced in some miniaturized mites (Crome 1953, Levi 1967, Wirkner et al. 2013).

During embryogenesis, the heart develops from paired lateral coelomic cavities that merge in the dorsal midline of the embryonic body. From this, it differentiates into an originally closed tube (Strubell 1892, Kästner 1931*f*, Scholl 1977, Rugendorff et al. 1994). Ostia and dilatator muscles develop during later development stages, as has been shown for *Limulus* (Scholl 1977) and *Drosophila* (Rugendorff et al. 1994, Bodmer 1995, Molina and Cripps 2001). Thus, a simple tube without ostia represents an early stage in arthropod heart development. The heart tube of *Eukoenenia spelaea* is such a muscular tube, without ostia and without a pericard and thus, appears to be arrested on an early developmental stage, i.e. might be paedomorphic.

The paedomorphic morphology of the adult heart is corroborated on the ultrastructural level. The number of mitochondria is low, the sarcoplasmic reticulum is poorly developed, myofilaments are irregularly placed throughout the myofibril, and the Z-lines are not clearly differentiated. Such poorly developed cytological appearance of myocardial cells has also been described from the heart of juvenile ticks (Coons and Alberti 1999, p. 360; Fig. 67) and the heart of larval *Drosophila* (Lehmacher et al. 2012). The microscopic anatomy and the ultrastructure of the heart of adult *Eukoenenia spelaea* resembles that of juvenile or larval stages of other arthropods. Together they support the view that the heart of *E. spelaea* is paedomorphic.

The vestigial/rudimentary/paedomorphic morphology of the heart suggests a low degree of functionality and consequently that it is not involved in circulation of the hemolymph through the body. This is not surprising because the overall hemolymph space is extremely small or missing. Movement of the residual hemolymph can probably be driven by muscle contraction of the body musculature in prosoma and opisthosoma. Reduction of the heart goes also along with the lack of respiratory organs and dependence on cuticular gas exchange (Rucker 1901, Kästner 1931*a*). As discussed in 4.2.1, the small size of the animal and the thin cuticle place *Eukoenenia spelaea* well below the upper size limit for diffusive respiratory gas exchange. With these features respiratory gases can be exchanged directly

between cells of the body and the environment, and a heart for circulating the hemolymph is not necessary for convective gas transport.

4.11 Rostrosoma

All arachnids have a preoral cavity that is formed by various morphological contributions from the labrum, the chelicerae, the pedipalps, or sternal elements (Kästner 1931*g*, Collatz 1987, Moritz 1993, Farley 2001). These elements can be combined to form a more or less complex rostrosoma that may surround the preoral cavity, the mouth and parts of the pharynx. Preoral cavity and mouth may be equipped with cuticular teeth, ridges or other filtering structures that prevent larger particles from entering the pharynx. In some taxa, external cuticular surface structures on the lower lip might be involved in guiding secretions from salivary glands that open ventral on the body to the mouth. Obviously, the rostrosoma, preoral cavity and the various associated structures evolved independently and parallel in many groups of arachnids (Snodgrass 1948, Dunlop 2000).

The rostrosoma of *Eukoenenia spelaea* is comparatively simple as it consists of a cuticular tube that carries the functional upper lip and lower lip at its anterior part. The rostrosoma surrounds the preoral cavity, the mouth and the anterior part of the pharynx. The rostrosoma is a distinct morphological structure that does not involve parts from chelicerae, pedipalps or any other appendage. This appears to be a derived state for arachnids, as other arachnid groups (Kästner 1931*g*, Collatz 1987, Moritz 1993, Farley 2001) as well as their sister group Xiphosurida (Gerhardt 1931) have structures of the extremities involved in the formation of the rostrosoma. Adult morphology does not provide evidence of its morphological origin. However, comparative developmental evidence suggests that structures surrounding the mouth opening develop from the Anlagen of the labrum, the epistome or the epistomo-labral plate, i.e. derivatives of the pre-cheliceral segment (Araneae [Mittmann and Wolff 2012], Scorpiones [Farley 2001], and *Limulus polyphemus* [Haug and Rötzer 2018]). In case of *E. spelaea*, I can pretty safely exclude that other structures contribute to the formation of the rostrosoma, because I showed on the basis of the muscle morphology that the ventral sclerite of the cheliceral element is part of the prosternum (in my terminology) that also contains the deuto-, and tritosternum.

Historically, the functional lower lip has been derived from a protosternite (Börner 1902*a*, 1903). However, such structure has never been confirmed in either adult or developmental stages of euchelicerates. Also, my observation shows that segmental musculature of the cheliceral segment attaches to the prosternum. Snodgrass' (1948, p. 21) conclusion *"[…] If, therefore, the mouth of the palpigrades lies between the labrum and the sternum of the first postoral somite, we see here an embryonic condition retained in no other modern adult arthropod […]"* appears to be of merely historical interest.

Millot (1942) reported glandular structures in the lower lip of *Eukoenenia mirabilis* and postulated the secretion of saliva. However, I could not detect cells with an unequivocal secretory character. Some cells with large nuclei in the lower lip might correspond to what Millot (1943) described as glandular cells, but I did not see vesicles or structures that would indicate secretory activity.

Food uptake has never been reported for palpigrades. Like in all other arachnids, the cuticular ridges on the inside of the upper and lower lip are most likely used as filter mechanism to prevent large particles from entering the alimentary system. Wheeler (1900) and Rucker (1901) suggested that palpigrades feed on arthropod eggs. This idea was rejected by Millot (1942), who found that the reported vitellin vesicles were in fact not inside the midgut, but in the surrounding storage tissue. Smrž et al. (2013, 2015) suggested that *Eukoenenia spelaea* feeds on heterotrophic cyanobacteria which, indeed, have been identified in the gut of *E. spelaea*. The serrated cuticular teeth of the chelicerae might be used as a comb to graze cyanobacteria off the surrounding soil. The spacing of the teeth (1–1.5 µm) is considerably smaller than the diameter of most cyanobacteria found within the gut (6–8 µm; Smrž et al. 2013, 2015).

4.12   Digestive tract

The digestive tract of euchelicerates can be divided in an ectodermal foregut, comprising pharynx and esophagus, a mesodermal midgut, and an ectodermal hindgut (Millot 1949*a*, Alberti and Coons 1999, Coons and Alberti 1999, Farley 1999, Talarico et al. 2011). Along the foregut, dilator muscles attach to the precerebral and postcerebral pharynx forming suction pumps. Pre- and postcerebral suction pumps can be found in Amblypygi (Kästner 1931*f*), Araneae (Felgenhauer 1999), Ricinulei

(Ludwig et al. 1994, Talarico et al. 2011), Scorpiones (Farley 1999), and Thelyphonida (Kästner 1931*f*). The posterior suction pump is missing in Acari (Alberti and Coons 1999, Coons and Alberti 1999), Opiliones (Pinto-da-Rocha et al. 2007), Pseudoscorpiones (Weygoldt 1969), and Solifugae (Klann and Alberti 2010).

Eukoenenia spelaea also lacks a postcerebral suction pump. Rucker's (1901) and Börner's (1904) description of a postcerebral suction pump in *Prokoenenia wheeleri* is clearly a misinterpretation of the prosomal midgut (Millot 1942, Weygoldt and Paulus 1979*b*, Shultz 2007*a*, this study). The ectodermal esophagus of *E. spelaea* directly merges into the midgut tube and shows no sign of additional musculature. The midgut is a straight tube in the prosoma where it forms two diverticula. In the opisthosoma, the midgut is rather sac-like with indentations caused by the dorsoventral musculature; distinct midgut diverticula are missing in the opisthosoma. A similar sac-like midgut has been reported from instars of Araneae (Gerhardt and Kästner 1931), Pseudoscorpiones (Weygoldt 1969), Thelyphonida (Kästner 1931*f*), and Xiphosurida (Kimble et al. 2002). The morphological simplicity of the midgut in *E. spelaea,* and its overall similarity with that of developmental stages of other euchelicerate taxa is suggestive of a paedomorphic morphology.

The epithelium of the midgut and prosomal midgut diverticula in *Eukoenenia spelaea* are identical and contain secretory and digestive cells which are characterized by the numerous apical microvilli. It is a dimorphic epithelium like in most arachnids (Polis 1990, Ludwig et al. 1994, Farley 1999, Klann and Alberti 2010, Talarico et al. 2011) except Acari (Alberti and Coons 1999, Coons and Alberti 1999), Araneae (Felgenhauer 1999), and Opiliones (Becker and Peters 1985) where additional cell types like ferment cells, replacement cells, or excretion cells are present. Previous authors reported different structures and cell inclusions within the midgut epithelium of palpigrades. Wheeler (1900) and Rucker (1901) reported "yolk-bodies" within the midgut of *Eukoenenia mirabilis* and *Prokoenenia wheeleri*, which were later determined to be vitellin vesicles within the storage tissue surrounding the midgut in *E. mirabilis* (Millot 1942). Smrž et al. (2013, 2015) reported spherical inclusions in the midgut of *E. spelaea* which they identified as cyanobacteria (*Chroococcidiopsis*). My material shows lipid-rich vesicles within the storage cells, however, the midgut content could not be clearly identified.

A cuticle-lined hindgut is missing in *Eukoenenia spelaea*. Traditionally, the rectal sac has been interpreted as part of the hindgut (Kästner 1931*a*). However, it has no cuticular lining and its epithelium consists of high prismatic cells with long microvilli, thus, clearly relates to the mesodermal midgut and absorptive function. The rectal sac opens in the cuticle-lined anal opening. The ectodermal hindgut appears to be reduced to a short section, the anus.

4.13 Excretory organ

The coxal glands of arachnids typically consists of a saccule, tubule (labyrinth), bladder (vesicle), an excretory duct, and an excretory pore (Buxton 1913, 1917, Millot 1949*a*, Moritz 1993). The saccule may be connected to muscle fibers, e.g. in Acari (Alberti and Coons 1999) and Solifugae (Buxton 1913, Alberti 1979*b*, Klann 2009), supposedly allowing for extension of the saccule for creation of a pressure gradient. Among arachnid taxa the tubule varies in shape and morphological complexity (Buxton 1913, 1917, Alberti and Coons 1999). In Solifugae (Buxton 1913, 1917, Alberti 1979*b*, Klann 2009) and some ticks (Coons and Alberti 1999), an additional glandular section is associated with the coxal gland. The glandular section occurs in different topographic position in solifuges, where it is inserted between saccule and tubule, and in ticks where it forms the distal part of the tubule. Thus, the topographic morphology suggests an independent evolutionary origin of these glandular elements of the coxal gland in Solifugae and ticks.

The location of the excretory pore varies among Arachnida with little phylogenetic information. In Solifugae the pore is located in close proximity to the pedipalp (Buxton 1913, Alberti 1979*b*), in Acari on or adjacent to leg 1, in Amblypygi, Araneae (Buxton 1913, 1917), Opiliones (Pinto-da-Rocha et al. 2007), and Thelyphonida (Buxton 1913, 1917) next to leg 2, in Pseudoscorpiones (Weygoldt 1969) and Xiphosurida (Shultz 1990) close to leg 3, and in Scorpiones (Farley 1999) between leg 3 and 4. Some species of Amblypygi and Araneae have two excretory pores, one close to leg 2 and one close to leg 4 (Buxton 1913, 1917).

My description of the coxal gland of *Eukoenenia spelaea* is strikingly similar to that of Solifugae (Buxton 1913, 1917, Klann 2009). However, in Solifugae the glandular section is comparatively short and the tubule is long, while in *E. spelaea* the

glandular section extends far posterior into the opisthosoma and the tubule is short. The excretory pore is located posteriorly to leg 1.

In *Eukoenenia spelaea*, the saccule is a simple, small pouch with an epithelial wall of podocytes and a narrow lumen. No muscles were found associated with the saccule. In contrast to my description, Millot (1942) reported a muscle strand inserting on the saccule in *Eukoenenia mirabilis*. The organization of the saccule in *E. spelaea* equals the general basic organization of the epithelium of the saccule of euchelicerates. Of course, there is considerable variation in the size of the lumen of the saccule, e.g. in some species of Acari (Alberti and Coons 1999, Coons and Alberti 1999) and Thelyphonida (Buxton 1917) the lumen is only a small cavity while in other Acari (Alberti and Coons 1999, Coons and Alberti 1999), Amblypygi (Buxton 1913, 1917), Araneae (Buxton 1913, 1917, Lopez 1983), Scorpiones (Buxton 1913, 1917), Solifugae (Buxton 1913, 1917, Alberti 1979*b*, Klann 2009), and Xiphosurida (Fahrenbach 1999) the lumen can be extensive.

In *Eukoenenia spelaea*, a glandular section is intercalated between saccule and tubule. The glandular section has a short anterior section and a long posterior section that terminates in the opisthosoma. Millot (1942) described a secretion-filled lumen of the glandular section. Indeed transmission electron microscopy (TEM) shows that the apical part of the glandular cells are filled with vesicles, but TEM-images of *E. spelaea* do not show any tubular lumen, instead I described tight apical connections between the cells. Description on a lumen by Millot (1942) might be based on the lower resolution of light microscopy resulting in the apical parts of the tubule cells appearing like a lumen. In addition, the glandular cells display a basal labyrinth which is less intensively developed than in the tubule cells.

This is similar to what has been reported in Solifugae. Within the cells of their glandular section, secrete granules are present (Alberti 1979*b*). Because the excretory pore of Solifugae opens close to the pedipalp coxae, Alberti (1979) speculated about their function as salivary glands. This was supported by the presence of a fold in the cuticle, along which the secretion supposedly flow to the mouth (Buxton 1913). Indeed, Acari, Amblypygi, Araneae, Ricinulei, Schizomida, and Thelyphonida have similar ducts associated with a salivary gland (van der Hammen 1989). However, I could not identify such a duct in *Eukoenenia spelaea*.

The lack of a duct as well as the location of the excretory pore posterior to leg 1 do not suggest a function of the glandular section as salivary gland.

The tubule of *Eukoenenia spelaea* is a simple, bent tube with an additional posterior branch emerging from a position where the glandular section fuses with the tubule. It has not yet been reported for other palpigrades. The bend may be interpreted as a simplified labyrinth with no lumen. Whether a lumen opens in the transitory region to the excretory duct could not be determined. However, I found a tight connection between the apical poles of the tubule cells even in these distal parts of the tubule. A bladder is missing in *E. spelaea*. My findings are in slight contrast to description of *Eukoenenia mirabilis* by (Millot 1942) who described a bladder-like collecting vesicle instead of a bent tubule.

The cells of the tubule in arachnids typically display some form of microvilli, sometimes varying in number and length along the course of the tubule (Alberti 1979*b*, Coons and Alberti 1999, Fahrenbach 1999, Filimonova 2004, 2016, 2017). Increased basal cell infoldings are also known for tubule cells of Solifugae (Alberti 1979*b*) and the distal part of the tubule in mites (Alberti and Coons 1999). In the latter, the tubule cells which are typically three in cross-section are closely attached to each other, completely reducing the lumen of the tubule (Alberti and Coons 1999).

In *Eukoenenia spelaea*, the cellular structure of the tubule differs from the cell structure seen in other arachnids. Due to the lack of a lumen of the tubule, no microvilli are present. However, the increased basal cell infoldings as well as the close attachment of three cells in cross-section are similar to those described for Solifugae and mites.

4.14 Reproductive organs

4.14.1 Female reproductive organs

The female reproductive organs of arachnids consist of the ovaries, oviducts, seminal receptacle, and genital chamber. The detailed morphology of these structures varies considerably between groups and with the exception of ladder-like gonad morphology found in Schizomida, Scorpiones, and Thelyphonida (Shultz 2007*a*), contains little phylogenetic information. The ovaries can be paired or display various degrees of fusion (Kästner 1931*f*, Polis et al. 1990, Moritz 1993, Michalik et

al. 2005, Klann 2009, Foelix 2010). The oviducts are typically paired, originate anteriorly at the ovary, and vary in thickness (Moritz 1993, Alberti and Michalik 2004). A seminal receptacle may be found in groups with sperm transfer with gonopods or a penis (Alberti and Michalik 2004) but it is lacking in Amblypygi (Börner 1902*b*) and Solifugae (Millot and Vachon 1949*a*, Klann 2009), also groups with morphological structures for sperm transfer. A receptaculum seminis was described for *Prokoenenia wheeleri* by Rucker (1901), but was later disputed by Börner (1902). The genital chamber is generally lined with cuticle (Börner 1902*b*, Kästner 1931*d*, Millot and Vachon 1949*b*, Weygoldt 1969, Alberti and Coons 1999, Coons and Alberti 1999, Felgenhauer 1999, Klann 2009). In Acari (Alberti and Coons 1999, Coons and Alberti 1999), Amblypygi (Börner 1902*b*, Kästner 1931*f*), Pseudoscorpiones (Weygoldt 1969), Schizomida, and Thelyphonida (Börner 1902*b*, Kästner 1931*f*), an accessory gland is associated with the reproductive organs.

The unusual, slightly posterior origin of the paired ovarian ducts from the unpaired ovary of *Eukoenenia spelaea* appears to be unique among arachnids. The diameter of the ducts is small compared to the diameter of an egg. Although no transmission electron microscopic images of the ovarian ducts are available, it can be assumed that the epithelium is high prismatic and expandable to accommodate the eggs prior to laying. The seminal receptacle of *E. spelaea* is similar to that described by Rucker (1901) for *Prokoenenia wheeleri*. The paired accessory gland has no opening which indicates that the secretion collected in the reservoir is secreted through pores in the thin layer of cuticle in the region lateral to the genital opening. It is unclear, however, what type of secretion is produced in this gland. A low number of eggs within the ovary suggests that only few eggs are laid at a time.

4.14.2 Male reproductive organs

The male reproductive organs of arachnids typically consist of the paired testes, vas deferens, and genital atrium (Alberti et al. 2007). Like the female ovary, the morphology of the testes varies between groups and contains little phylogenetic information. Unpaired testes as well as testes in different stages of fusion are present (Weygoldt 1969, Polis 1990, Moritz 1993, Alberti and Coons 1999, Coons and Alberti 1999, Pinto-da-Rocha et al. 2007, Talarico et al. 2008, Klann 2009, Michalik 2009). The transfer of sperm can be coupled with the production of a

spermatophore. These sperm packages can display a species-specific morphology (e.g. Amblypygi [Weygoldt et al. 2010], Pseudoscorpiones [Weygoldt 1969], and Scorpiones [Polis 1990]. Spermatophores are built in Acari (Alberti and Coons 1999, Coons and Alberti 1999), Pseudoscorpiones (Weygoldt 1969), Scorpiones (Polis 1990), Solifugae (Klann 2009), Amblypygi, Schizomida, and Thelyphonida (Moritz 1993). A spermatophore transfer can be coupled with a transfer behavior or it can be simply left on the ground for the female to find (Shear 1999, Alberti and Michalik 2004).

The male reproductive system of *Eukoenenia spelaea* consists of paired testes, vas deferens, a genital atrium, and two accessory glands. The unpaired posterior gland has no secretory duct, but, similar to the accessory gland in females, possibly secretes through pores in the cuticle (Bereiter-Hahn et al. 1984). This gland corresponds to the paired accessory gland described for *Prokoenenia wheeleri* (Rucker 1901). The paired anterior accessory gland is larger than the posterior accessory gland and is associated with the glandular fusules of the first genital lobes. The general morphology of *E. spelaea's* male reproductive organs is similar to Amblypygi, Araneae, Ricinulei, Schizomida, and Thelyphonida. However, the morphology of the accessory glands differs greatly from these groups. The posterior accessory gland has no clear opening into the genital atrium. A unique character of *E. spelaea* appears to be the secretion ducts of the anterior accessory gland. The function of both accessory glands is unknown.

4.14.3 Sperm morphology

In contrast to the morphology of the testes and accessory glands, sperm morphology can be used in phylogenetic analyses of euchelicerates/arachnids (Alberti 1995). The sperm of euchelicerates shows a variety of shapes and complexity (Alberti 1995, Alberti and Michalik 2004, Pitnick et al. 2009). Xiphosurida have the most ancestral sperm, while most arachnids have more complex flagellate sperm. Aflagellate sperm have been reported from Acari, Opiliones, Solifugae (Alberti and Michalik 2004), and *Prokoenenia wheeleri* (Alberti 1979). The aflagellate sperm of *P. wheeleri* has an acrosomal complex that lacks the acrosomal filament, like in a few opilionid and acarine taxa (Alberti 1995). Despite the wide variability in shape the nucleus of the sperm may take in arachnids, the sperm

nucleus of *P. wheeleri* is unique because it is wound several times around the spermatozoon (Alberti 1979*a*, Alberti and Michalik 2004). Ticks as well as some anactinotrichid mites have vacuolated sperm. In this type of sperm, the large central vacuole develops through fusion of multiple peripheral vacuoles and the fully developed sperm itself is later turned inside out (Alberti and Michalik 2004). The spermatozoa of *P. wheeleri* also possess a large vacuole that gradually increases in size during differentiation.

The spermatozoa of *Eukoenenia spelaea* are similar to the spermatozoa of *Prokoenenia wheeleri*. They contain a large vacuole, with a constant number of spherical vesicles. The development of the vacuole appears to be identical to that in *P. wheeleri*. The nucleus of *E. spelaea* is oblong and located basally in the spermatozoon. It shows no evidence of winding like in *P. wheeleri*. However, it is unclear, whether the spermatozoa found in *E. spelaea* are matured or not and whether the nucleus develops into the unique spiral shape when the spermatozoon is matured. Unfortunately no transmission electron microscopic images could be obtained from spermatozoa in *E. spelaea*. Therefore, the nature of the two oblong structures located at the apex of the spermatozoon remains unclear.

4.15   Phylogenetic analysis

4.15.1 Autapomorphies of *Eukoenenia spelaea* and Palpigradi

To aid in the phylogenetic analysis, my morphological analysis of *Eukoenenia spelaea* provided several autapomorphic characters which separate *E. spelaea*/Palpigradi from other arachnid groups. Incidentally, all proposed autapomorphic characters are located in the prosoma. One of these autapomorphic characters is the dorsal division of the prosoma in two dorsal sclerites that are associated with segments (character 6; Tabs. 6, A2), i.e. are attachment sites for segmental suspensor muscles (see 4.1.1). This differs from Schizomida and Solifugae, which both appear to have three dorsal sclerites with segment association. Until now, the division of the prosoma into three sclerites could be interpreted as a parallel development in Palpigradi, Schizomida, and Solifugae. However, my analysis clearly showed that it is a unique character for *E. spelaea*, and possibly Palpigradi.

The frontal organ (suprecheliceral organ; character 148; Tabs. 6, A2) can only be found in Palpigradi. The location medial on the prosoma suggests that the left and right setae are associated with the left and right body half, respectively. Because Palpigradi are bilaterally symmetric, one would expect the same morphology/ultrastructure in both setae. However, the setae of the frontal organ in *Eukoenenia spelaea* display a varying ultrastructure of the dendrites indicating different sense modalities. To my knowledge, such a morphology is unique among Euchelicerata.

My analysis of *Eukoenenia spelaea* showed that the preoral cavity, mouth, and pharynx are nestled inside a cone-shaped rostrosoma (character 32; Tabs. 6, A2). A similar structure is present in Pseudoscorpiones and Solifugae (Shultz 2007*a*). Palpigradi, however, are the only arachnid groups without any involvement of pedipalp or leg structures in the formation of the rostrosoma. Thus, the palpigrade rostrosoma is an autapomorphic character with no common features with the rostrosoma of Pseudoscorpiones and Solifugae.

Within the rostrosoma, dilator muscles are attached to the pharynx (character 198; Tabs. 6, A2) which extend the pharynx in a ventral/ventrolateral direction in Palpigradi (Millot 1942), Araneae (Whitehead and Rempel 1959), Solifugae (Roewer 1934), und Xiphosurida (Shultz 2001). In Araneae, Solifugae, and Xiphosurida, the point of attachment for these dilator muscles is ventral on the prosoma. The situation for Palpigradi is unclear, because Millot (1942) who studied *Eukoenenia mirabilis*, did not clarify the attachment points of the pharynx dilators, however, Shultz (2007*b*) coded this character identical to Araneae, Solifugae, and Xiphosurida. In *Eukoenenia spelaea*, the lateral dilator muscles of the pharynx attach to the rostrosoma. This suggests that this muscle topology is unique in *E. spelaea*, thus, it is an autapomorphic character.

In addition to the above mentioned characters, several morphological features have no yet been reported in any euchelicerate except in this study for *Eukoenenia spelaea*. (1) The ventral plate has a unique morphology (i.e. cuticular teeth, specialized epidermal cells), however, its function is unclear. Whether this structure was overlooked in other palpigrades is not known. Thus, it cannot be said for certain, whether it is an autapomorphy for *E. spelaea* or all Palpigradi. (2) The prosternum,

i.e. the fused sternites of segments 2–4, has only been reported in this study. However, due to incomplete data on other species of Palpigradi it is not clear, whether it is an autapomorphic character for *E. spelaea* or for Palpigradi. (3) The ultrastructure of the trichobothria, with dendrites reaching into the hair shaft, is unique among euchelicerates. Further studies on other palpigrade species are necessary to determine autapomorphy in *E. spelaea* or Palpigradi. (4) *E. spelaea* lack a hindgut. Previous studies of palpigrades interpreted the rectal sac as rectum/hindgut (Kästner 1931*a*). To determine whether this interpretation is correct for other Palpigradi or whether a lack of a cuticular hindgut is an autapomorphy for all species, a detailed analysis of the rectal sac in all palpigrade taxa is needed.

4.15.2 Synapomorphies with Acaromorpha and other arachnid groups

Palpigradi were repeatedly placed as sister group to Acaromorpha (Figs. 51A, 52A, D, 53C). This was based on four possible synapomorphies that were recovered from the character set provided by Shultz (2007*a*) as well as the characters newly added to the character set. The first character, which unites Palpigradi and Acaromorpha is the patella-tibia joint of legs 1–4. It has a hinge, one axis of movement, and muscles that lack a muscular antagonist (72; Tabs. A1, A2; Shultz 1989). However, this character would have to have evolved in parallel in Solifugae (Shultz 1989) and Trigonotarbida (Selden et al. 1991) as this character state is the same in these groups. Given that this morphological character is possibly tied to a specific function of movement, a parallel development is not unlikely.

Another character associated with the legs is the opening of the coxal organ in adults (180; Tabs. A1, A2). In Palpigradi (Millot 1942) and Acaromorpha (Legg 1976, Alberti and Coons 1999) it is located on or near the coxa of appendage III (= leg 1). However, this character possibly evolved in parallel in (Pan)Tetrapulmonata. It might also be a synapomorphy of the sister group to Stomothecata and then was reduced in Haplocnemata (Buxton 1913, 1917). Both scenarios are equally parsimonious.

Palpigradi and Acaromorpha both lack a postcerebral pharynx (199; Tabs. A1, A2; Shultz 2007*a*). Thus, this character might be considered a synapomorphy for these two groups. However, a loss of the postcerebral pharynx must have occurred then in parallel in Opiliones and Pseudoscorpiones.

A possible synapomorphy for a Palpigradi-Anactinotrichida sister group relationship is vacuolated-type sperm (167, Tabs. A1, A2; Alberti 1979*a*, 1995, Alberti and Michalik 2004). This would only be a synapomorphy for these two groups and not for Palpigradi and Acaromorpha. However, it is unlikely, that it is present in the basal group Palpigradi and the derived Anactinotrichida but has retained its plesiomorphic arachnid-type, i.e. unvacuolated, morphology in the basal acaromorph groups Acariformes and Ricinulei.

In addition to the synapomorphic characters from the character set, several morphological features show similarity between *Eukoenenia spelaea*/Palpigradi and Acaromorpha. The leg musculature is such a feature. The comparison of the musculature of leg 4 especially between Acariformes, Parasitiformes, and Palpigradi reveals similarities in terms of deviation from the euchelicerate ground pattern and loss of specific muscles (see 4.4.6.2; Tab. 12; Shultz 1989).

Within the coxal gland tubule, the cell arrangement is also very similar between mites and *E. spelaea*. A tubule lumen is missing in both groups and there are always three cells present in cross-section (see 4.13; Alberti and Coons 1999). However, the general morphology of the coxal gland in *E. spelaea* shows more similarity to Solifugae (Buxton 1913, 1917, Alberti 1979*b*, Klann 2009).

The presence of a myogenic heart in some ticks (Schriefer et al. 1987, Coons and Alberti 1999) is also very similar to the proposed myogenic heart of *Eukoenenia spelaea*, thus, it is a character which these groups have in common.

Several characters were found which support a Palpigradi/Acaromorpha sister group relationship, however, the phylogenetic analysis with TNT resulted in low bootstrap percentage and Bremer support values, and the unweighted analysis of the updated character matrix of extant taxa left the deep arachnid relationships unresolved (Figs. 51–53). In general, bootstrap percentages and Bremer support values were lower in my analyses than in the most recent phylogenetic analysis based on morphological characters of extant and fossil taxa with a special focus on extant taxa by Shultz (2007*a*). Although I used the author's data matrix as basis for positioning *Eukoenenia spelaea* within the Arachnida, the variation in support values might be due to differences in program version as well as the fact that my entire analysis was conducted in TNT. The phylogenetic relationships between

major euchelicerate groups remain largely unresolved considering the weak support of the nodes (Figs. 51–53). However, my morphological analysis of *E. spelaea* indicates that there are morphological characters which support a sister group relationship between Palpigradi and Acaromorpha.

4.16 Miniaturization

Miniaturization is evolution toward small adult body size, thus, evolving from a larger ancestor. Such phylogenetic size decrease leads most commonly to structural simplification and reduction, but also to morphological novelty as well as an increase in variability in few cases (Hanken and Wake 1993, Polilov 2016). Several morphological features have been reported in miniaturized arthropods (Polilov 2008, Quesada et al. 2011, Polilov 2015*a*, *b*, 2016, Polilov and Shmakov 2016). There is a reduction or lack of structures like the heart, neurilemma, or respiratory organs. The brain is proportionally increased in relation to the body size. The mostly undifferentiated gut lacks musculature. Gonads are unpaired in some miniaturized arthropods and there is a reduced number of large eggs. High levels of fusion within the brain have been reported for ticks (Ioffe 1963, Wegerhoff and Breidbach 1995), a potentially miniaturized group with reduced body size.

Studies on miniaturized insects revealed additional morphological features associated with miniaturization. A lack of differentiation of the cuticle into exo- and endocuticle is such a feature. Reduction of muscles in some regions of the body was also reported. In miniaturized insects, the brain also displays a high level of fusion and the number of sensory organs is reduced. A reduction in the number of Malpighian tubules is also a characteristic feature of miniaturization (Polilov 2015*a*, *b*, Polilov and Shmakov 2016).

Developmental processes like progenesis (i.e. early maturation) or retention of larval structures in adults (neoteny; Gould 1977) may result in paedomorphotic features of the adult. Only progenesis, will also result in smaller body size. Thus, if one finds features of developmental stages in miniaturized adults, one may conclude that they reached small body size by progenesis.

Several morphological features found in *Eukoenenia spelaea* indicate miniaturization: (1) there is a lack of a distinct differentiation into endo- and

exocuticle over large regions of the body. (2) *Eukoenenia spelaea* has no respiratory organs but utilizes cutaneous respiration. (3) Several muscles, e.g. dorsoventral muscles in the posterior opisthosoma and posterior oblique muscles in all of the opisthosoma, are reduced. (4) The prosomal ganglia are proportionally large and display a high level of fusion. (5) *E. spelaea* has only 14 trichobothria in total. (6) The simplified structure of the coxal gland, i.e. the reduced number of cells and a simple tube instead of a complex labyrinth, could be an indication for miniaturization. However, some mites, despite their small body size, have complex labyrinths (Filimonova 2016), while some Solifugae have a simplified labyrinth (Alberti 1979*b*). Thus, the complexity of the coxal gland's tubule is a weak indicator at best. (7) In contrast to most arachnids, *E. spelaea* lacks Malpighian tubules. (8) The female gonads are an unpaired structure. (9) Within the ovary, the number of eggs is low and only few eggs appear to be fully developed.

In addition, *Eukoenenia spelaea* displays several characters which are indicative of paedomorphotic processes: (1) the portion of the supraesophageal ganglion associated with the chelicerae envelops the esophagus which is similar to the situation in larval *Limulus polyphemus*. (2) A reduced number of neurons within the opisthosomal ganglia can be found in *E. spelaea* as well as arthropod embryos. (3) Like the hearts of early developmental stage of arthropods, the heart of *E. spelaea* lacks ostia and the musculature (sarcomere structure) is weakly developed. (4) The midgut is a simple sac with no epithelial differentiation between the different regions. The musculature associated with the midgut is poorly developed. A similar morphology is found in juveniles of several arachnid groups.

In addition to morphological indicators of miniaturization, the last common ancestor had to have been large to confirm that a group is miniaturized. Within euchelicerates one can observe groups with a tendency to have larger body sizes (e.g. Eurypterida: up to 1.8 m body length, Alberti et al. 2007; Scorpiones: up to 210 mm body length, Polis et al. 1990; Solifugae: 10–70 mm body length, Punzo 2012; Xiphosurida: up to 850 mm body length, Alberti et al. 2007) and groups with a tendency to have smaller body sizes (e.g. Acari: up to 14 mm body length, Dunlop 2018; Opiliones: up to 22 mm body length, Pinto-da-Rocha et al. 2007; Pseudoscorpiones: 1–7 mm body length, Weygoldt 1969; Ricinulei: up to 10 mm body length, Alberti et al. 2007; Schizomida: approx. 5 mm body length, Harvey 2003).

The analysis of size relation between groups strongly depends on the phylogeny that is being used. According to the phylogenetic analysis presented above, Palpigradi are hypothesized as sister group to Acaromorpha (Figs. 51–53). Within this group are only species with a tendency toward small body size. This might indicate, that the ancestor was small as well. Based on my analysis, this last common ancestor of Palpigradi and Acaromorpha was sister to the last common ancestor of Haplocnemata + (Pan)Tetrapulmonata (Fig. 53C). Within this grouping are mainly groups whose taxa display larger body sizes. In addition, the sister group to Haplocnemata + Tetrapulmonata and Palpigradi + Acaromorpha are the Stomothecata (Fig. 53C), also a group with a large sized representative (Scorpiones). At the base of the phylogeny presented here are two groups with a tendency toward large body size, the extinct Eurypterida and the recent Xiphosurida. This could indicate that the common ancestor for both groups, Haplocnemata + Tetrapulmonata and Palpigradi + Acaromorpha, was large and that a miniaturization event might have taken place in the last common ancestor of Palpigradi + Acaromorpha.

My morphological analysis showed, that *Eukoenenia spelaea* displays numerous morphological characters which are indicative of miniaturization, i.e. paedomorphic features as well as reduced and simplified structures. Based on my phylogenetic analysis it is also likely, that the common ancestor of Haplocnemata + Tetrapulmonata and Palpigradi + Acaromorpha was large. These findings support the hypothesis that *E. spelaea* is likely miniaturized.

5. References

Alberch, P. 1980. Ontogenesis and morphological diversification. *American Zoologist* 20: 653–667.

Alberti, G. 1979a. Zur Feinstruktur der Spermien und Spermiocytogenese von *Prokoenenia wheeleri* (Rucker, 1901)(Palpigradi, Arachnida). *Zoomorphologie* 94: 111–120.

Alberti, G. 1979b. Licht- und elektronenmikroskopische Untersuchungen an Coxaldrüsen von Walzenspinnen (Arachnida: Solifugae). *Zoologischer Anzeiger* 203: 48–64.

Alberti, G. 1995. Comparative spermatology of Chelicerata: review and perspective. *Advances in spermatozoal Phylogeny and Taxonomy. Mémoires du Muséum National d'Histoire Naturelle* 166: 203–230.

Alberti, G.; Coons, B. 1999. Acari: Mites. In: Harrison, F.W.; Foelix, R.F. (Eds.), *Microscopic Anatomy of Invertebrates*, Vol. 8C, Wiley-Liss, New York, p.515–1265.

Alberti, G.; Seeman, O. 2004. Ultrastructural observations on Holothyrida (Acari: Anactinotrichida). *Phytophaga* XIV: 103–111.

Alberti, G.; Michalik, P. 2004. Feinstrukturelle Aspekte der Fortpflanzungssysteme von Spinnentieren (Arachnida). In: Biologiezentrum des Oberösterreichischen Landesmuseums (Ed.), *Diversität und Biologie von Webspinnen, Skorpionen und anderen Spinnentieren*, Neue Serie 14, Denisia 12, p.1–62.

Alberti, G.; Moreno, A.I.; Kratzmann, M. 1994. The fine structure of trichobothria in moss mites with special emphasis on *Acrogalumna longipluma* (Berlese, 1904)(Oribatida, Acari, Arachnida). *Acta Zoologica* 75: 57–74.

Alberti, G.; Moreno, A.I.; Kratzmann, M. 1995. Fine structure of trichobothria in moss mites (Oribatida). In: Kropczyńska, D.; Boczek, J.; Tomczyk, A. (Eds.), *The Acari: Physiological and Ecological Aspects of Acari-Host Relationships*, Vol. 2, Dabor, Warsaw, p.23–30.

Alberti, G.; Thaler, K.; Weygoldt, P. 2007. Chelicerata. In: Westheide, W.; Rieger, R. (Eds.), *Spezielle Zoologie. Teil 1: Einzeller und Wirbellose Tiere*, 2nd ed. Spektrum Akademischer Verlag, München, p.479–532.

Altner, H. 1977. Insect sensillum specificity and structure: an approach to a new typology. *Olfaction and Taste* 6: 295–303.

Altner, H.; Prillinger, L. 1980. Ultrastructure of invertebrate chemo-, thermo-, and hygroreceptors and its functional significance. *International Review of Cytology* 67: 69–139.

Altner, H.; Loftus, R. 1985. Ultrastructure and function of insect thermo-and hygroreceptors. *Annual Review of Entomology* 30: 273–295.

Altner, H.; Sass, H.; Altner, I. 1977. Relationship between structure and function of antennal chemo-, hygro-, and thermoreceptive sensilla in *Periplaneta americana*. *Cell and Tissue Research* 176: 389–405.

Altner, H.; Tichy, H.; Altner, I. 1978. Lamellated outer dendritic segments of a sensory cell within a poreless thermo-and hygroreceptive sensillum of the insect *Carausius morosus*. *Cell and Tissue Research* 191: 287–304.

Altner, H.; Ernst, K.D.; Kolnberger, I.; Loftus, R. 1973. Feinstruktur und adäquater Reiz bei Insektensensillen mit Wandporen. *Verhandlungen der Deutschen Zoologischen Gesellschaft* 66: 48–53.

Altner, H.; Schaller-Selzer, L.; Stetter, H.; Wohlrab, I. 1983. Poreless sensilla with inflexible sockets. *Cell and Tissue Research* 234: 279–307.

André, M. 1949. Ordre des Acariens. In: Grassé, P.-P. (Ed.), *Traité de Zoologie*, Vol. 6, Masson et Cie., Paris, p.794–892.

Anton, S.; Tichy, H. 1994. Hygro-and thermoreceptors in tip-pore sensilla of the tarsal organ of the spider *Cupiennius salei*: innervation and central projection. *Cell and Tissue Research* 278: 399–407.

de Armas, L.F.; Teruel, R. 2002. Un género nuevo de Hubbardiidae (Arachnida: Schizomida) de las Antilles Mayores. *Revista Ibérica de Aracnología* 6: 45–52.

Atyeo, W.T.; Kethley, J.B.; Perez, T.M. 1984. Paedomorphosis in *Metacheyletia* (Acari: Cheyletidae), with the description of a new species. *Journal of Medical Entomology* 21: 125–132.

Babu, K.S. 1965. Anatomy of the central nervous system of arachnids. *Zoologische Jahrbücher. Abteilung für Anatomie und Ontogenie der Tiere* 82: 1–154.

Babu, K.S. 1985. Patterns of arrangement and connectivity in the central nervous system of arachnids. In: Barth, F.G. (Ed.), *Neurobiology of Arachnids*, Springer, p.3–19.

Babu, K.S.; Barth, F.G. 1984. Neuroanatomy of the central nervous system of the wandering spider, *Cupiennius salei* (Arachnida, Araneida). *Zoomorphology* 104: 344–359.

Barranco, P.; Mayoral, J.G. 2007. A new species of *Eukoenenia* (Palpigradi, Eukoeneniidae) from Morocco. *Journal of Arachnology* 35: 318–324.

Barranco, P.; Mayoral, J.G. 2014. New palpigrades (Arachnida, Eukoeneniidae) from the Iberian Peninsula. *Zootaxa* 3826: 544–562.

Barth, F.G. 2002. *A spider's world: senses and behavior*. Springer Verlag, Berlin Heidelberg, 393p.

Barth, F.G. 2014. The slightest whiff of air: airflow sensing in arthropods. In: *Flow Sensing in Air and Water*, Springer, p.169–196.

Barth, F.G.; Németh, S.S.; Friedrich, O.C. 2004. Arthropod touch reception: structure and mechanics of the basal part of a spider tactile hair. *Journal of Comparative Physiology A* 190: 523–530.

Battelle, B.-A. 2017. Opsins and their expression patterns in the xiphosuran *Limulus polyphemus*. *The Biological Bulletin* 233: 3–20.

Becker, A.; Peters, W. 1985. Fine structure of the midgut gland of *Phalangium opilio* (Chelicerata, Phalangida). *Zoomorphology* 105: 317–325.

Beier, M. 1931. Ordnung Pseusoscorpionidae (Afterscorpione). In: Krumbach, T. (Ed.), *Handbook of Zoology Online*, Vol. 2, De Gruyter, Berlin Boston, p.118–192.

Bereiter-Hahn, J.; Matoltsy, A.G.; Richards, K.S. 1984. *Biology of the Integument. 1 Invertebrates*. In: Bereiter-Hahn, J.; Matoltsy, A.G.; Richards, K.S. (Eds.) Springer Verlag, Berlin Heidelberg, 841p.

Berland, L. 1949. Ordre des Opilions. In: Grassé, P.-P. (Ed.), *Traité de Zoologie*, Vol. 6, Masson et Cie., Paris, p.761–793.

Bitsch, J.; Bitsch, C. 2007. The segmental organization of the head region in Chelicerata: a critical review of recent studies and hypotheses. *Acta Zoologica* 88: 317–335.

Bodmer, R. 1995. Heart development in *Drosophila* and its relationship to vertebrates. *Trends in Cardiovascular Medicine* 5: 21–28.

Börner, C. 1902a. Arachnologische Studien. II. und III. *Zoologischer Anzeiger* 25: 433–466.

Börner, C. 1902b. Arachnologische Studien. IV. Die Genitalorgane der Pedipalpen. *Zoologischer Anzeiger* 26: 81–92.

Börner, C. 1903. Arachnologische Studien. V. Die Mundbildung bei den Milben. *Zoologischer Anzeiger* 26: 99–109.

Börner, C. 1904. Beiträge zur Morphologie der Arthropoden: I. Ein Beitrag zur Kenntnis der Pedipalpen. *Zoologica* 16: 1–174.

Bremer, K. 1994. Branch support and tree stability. *Cladistics* 10: 295–304.

Bursey, C.R. 1973. Microanatomy of the ventral cord ganglia of the horseshoe crab, *Limulus polyphemus* (L.). *Zeitschrift für Zellforschung und Mikroskopische Anatomie* 137: 313–329.

Bursey, C.R.; Sherman, R.G. 1970. Spider cardiac physiology, I. Structure and function of the cardiac ganglion. *Comparative and General Pharmacology* 1: 160–170.

Bush, J.W.M.; Hu, D.L.; Prakash, M. 2007. The Integument of water-walking arthropods: form and function. In: Casas, J.; Simpson, S.J. (Eds.), *Advances in Insect Physiology*, Vol. 34, Elsevier, p.117–192.

Buxton, B.H. 1913. Coxal glands of the arachnids. In: Spengel, J.W. (Ed.), *Zoologische Jahrbücher*, Supplement 14. Gustav Fischer Verlag, Jena, p.230–454.

Buxton, B.H. 1917. Notes on the anatomy of arachnids. *Journal of Morphology* 29: 1–31.

Chen, J.; Xie, J.; Zhu, H.; Guan, S.; Wu, G.; Noori, M.N.; et al. 2012. Integrated honeycomb structure of a beetle forewing and its imitation. *Materials Science and Engineering: C* 32: 613–618.

Christian, E. 2004. Palpigraden (Tasterläufer)–Spinnentiere in einer Welt ohne Licht. In: Biologiezentrum des Oberösterreichischen Landesmuseums (Ed.), *Diversität und Biologie von Webspinnen, Skorpionen und anderen Spinnentieren*, Neue Serie 14, Denisia 12. p.473–483.

Christian, E.; Isaia, M.; Paschetta, M.; Bruckner, A. 2014. Differentiation among cave populations of the *Eukoenenia spelaea* species-complex (Arachnida: Palpigradi) in the southwestern Alps. *Zootaxa* 3794: 052–086.

Chu-Wang, I.-W.; Axtell, R.C. 1973. Comparative fine structure of the claw sensilla of a soft tick, *Argas (Persicargas) arboreus* Kaiser, Hoogstraal, and Kohls,

and a hard tick, *Amblyomma americanum* (L.). *The Journal of Parasitology* 59: 545–555.

Collatz, K.-G. 1987. Structure and function of the digestive tract. In: Nentwig, W. (Ed.), *Ecophysiology of Spiders*, Springer Verlag, Berlin Heidelberg, p.229–238.

Condé, B. 1996. Les Palpigrades, 1885–1995: acquisitions et lacunes. *Proceedings of the XIIIth Congress of Arachnology : Geneva, 3-8 September 1995* 1: 87–106.

Conte, F.P. 1984. Structure and function of the crustacean larval salt gland. *International Review of Cytology* 91: 45–106.

Coons, L.B.; Alberti, G. 1999. Acari: Ticks. In: Harrison, F.W.; Foelix, R.F. (Eds.), *Microscopic Anatomy of Invertebrates*, Vol. 8B, Wiley-Liss, New York, p.267–514.

Corbière-Tichané, G.; Loftus, R. 1983. Antennal thermal receptors of the cave beetle, *Speophyes lucidulus* Delar. *Journal of Comparative Physiology A* 153: 343–351.

Crome, W. 1953. Die Respirations-und Circulationsorgane der *Argyroneta aquatica* Cl. (Araneae). *Wissenschaftliche Zeitschrift Humboldt-Universität Berlin* 2: 53–83.

Curtis, D.J.; Machado, G. 2007. Ecology. In: Pinto-da-Rocha, R.; Machado, G.; Giribet, G. (Eds.), *Harvestmen: The Biology of Opiliones*, Harvard University Press, p.280–308.

Cushing, P.E.; Casto, P.; Knowlton, E.D.; Royer, S.; Laudier, D.; Gaffin, D.D.; et al. 2014. Comparative morphology and functional significance of setae called papillae on the pedipalps of male camel spiders (Arachnida: Solifugae). *Annals of the Entomological Society of America* 107: 510–520.

Damen, W.G.; Hausdorf, M.; Seyfarth, E.-A.; Tautz, D. 1998. A conserved mode of head segmentation in arthropods revealed by the expression pattern of Hox genes in a spider. *Proceedings of the National Academy of Sciences* 95: 10665–10670.

Davis, E.E.; Sokolove, P.G. 1975. Temperature responses of antennal receptors of the mosquito, *Aedes aegypti*. *Journal of Comparative Physiology* 96: 223–236.

Dechant, H.-E.; Hößl, B.; Rammerstorfer, F.G.; Barth, F.G. 2006. Arthropod mechanoreceptive hairs: modeling the directionality of the joint. *Journal of Comparative Physiology A* 192: 1271–1278.

Dubale, M.S.; Vyas, A.B. 1968. The structure of the chela of *Heterometrus* sp. and its mode of operation. *Bulletin of the Southern California Academy of Sciences* 67: 240–244.

Dunlop, J.A. 2000. The epistomo-labral plate and lateral lips in solifuges, pseudoscorpions and mites. *Ekologia (Bratislava)* 19: 67–78.

Dunlop, J.A. 2018 (in press). Miniaturisation in Chelicerata. *Arthropod Structure & Development*.

Dunlop, J.A.; Lamsdell, J.C. 2017. Segmentation and tagmosis in Chelicerata. *Arthropod Structure & Development* 46: 395–418.

Dunlop, J.A.; Kamenz, C.; Talarico, G. 2009. A fossil trigonotarbid arachnid with a ricinuleid-like pedipalpal claw. *Zoomorphology* 128: 305.

Dybas, H.S. 1966. Evidence for parthenogenesis in the featherwing beetles: with a taxonomic review of a new genus and eight new species (Coleoptera: Ptiliidae). *Fieldiana Zoology* 51: 11–52.

Ehn, R.; Tichy, H. 1994. Hygro-and thermoreceptive tarsal organ in the spider *Cupiennius salei*. *Journal of Comparative Physiology A* 174: 345–350.

Eisenbeis, G. 1974. Licht-und elektronenmikroskopische Untersuchungen zur Ultrastruktur des Transportepithels am Ventraltubus arthropleoner Collembolen (Insecta). *Cytobiologie* 9: 180–202.

Eisenbeis, G.; Wichard, W. 1987. *Atlas on the biology of soil arthropods*. Springer Science & Business Media, Berlin Heidelberg, 436p.

Fage, L. 1949. Classe des Mérostomacés. In: Grassé, P.-P. (Ed.), *Traité de Zoologie*, Vol. 6, Masson et Cie., Paris, p.219–262.

Fahrenbach, W.H. 1999. Merostomata. In: Harrison, F.W.; Foelix, R.F. (Eds.), *Microscopic Anatomy of Invertebrates*, Vol. 8A, Wiley-Liss, New York, p.21–115.

Farley, R.D. 1999. Scorpiones. In: Harrison, F.W.; Foelix, R.F. (Eds.), *Microscopic Anatomy of Invertebrates*, Vol. 8A, Wiley-Liss, New York, p.117–222.

Farley, R.D. 2001. Development of segments and appendages in embryos of the desert scorpion *Paruroctonus mesaensis* (Scorpiones: Vaejovidae). *Journal of Morphology* 250: 70–88.

Farley, R.D. 2005. Developmental changes in the embryo, pronymph, and first molt of the scorpion *Centruroides vittatus* (Scorpiones: Buthidae). *Journal of Morphology* 265: 1–27.

Felgenhauer, B.E. 1999. Araneae. In: Harrison, F.W.; Foelix, R.F. (Eds.), *Microscopic Anatomy of Invertebrates*, Vol. 8A, Wiley-Liss, New York, p.223–266.

Felsenstein, J. 1985. Confidence limits on phylogenies: an approach using the bootstrap. *Evolution* 39: 783–791.

Filimonova, S.A. 2004. The fine structure of the coxal glands in *Myobia murismusculi* (Schrank)(Acari: Myobiidae). *Arthropod Structure & Development* 33: 149–160.

Filimonova, S.A. 2016. Morpho-functional variety of the coxal glands in cheyletoid mites (Prostigmata). I. Syringophilidae. *Arthropod Structure & Development* 45: 356–367.

Filimonova, S.A. 2017. Morpho-functional variety of the coxal glands in cheyletoid mites (Prostigmata). II. Cheyletidae. *Arthropod Structure & Development* 46: 777–787.

Firstman, B. 1973. The relationship of the chelicerate arterial system to the evolution of the endosternite. *Journal of Arachnology* 1: 1–54.

Foelix, R. 2010. *Biology of spiders*. 3rd ed. Oxford University Press, New York, 419p.

Foelix, R.; Hebets, E. 2001. Sensory biology of whip spiders (Arachnida, Amblypygi). *Eileen Hebets Publications* 32.

Foelix, R.F. 1976. Rezeptoren und periphere synaptische Verschaltungen bei verschiedenen Arachnida. *Entomologica Germanica* 3: 83–87.

Foelix, R.F. 1985. Mechano- and chemoreceptice sensilla. In: Barth, F.G. (Ed.), *Neurobiology of Arachnids*, Springer Verlag, Berlin Heidelberg, p.118–137.

Foelix, R.F.; Axtell, R.C. 1972. Ultrastructure of Haller's organ in the tick *Amblyomma americanum* (L.). *Cell and Tissue Research* 124: 275–292.

Foelix, R.F.; Chu-Wang, I.-W. 1972. Fine structural analysis of palpal receptors in the tick *Amblyomma americanum* (L.). *Zeitschrift für Zellforschung und Mikroskopische Anatomie* 129: 548–560.

Foelix, R.F.; Chu-Wang, I.-W. 1973. The morphology of spider sensilla II. Chemoreceptors. *Tissue and Cell* 5: 461–478.

Foelix, R.F.; Schabronath, J. 1983. The fine structure of scorpion sensory organs. I. Tarsal sensilla. *Bulletin of the British Arachnological Society* 6: 53–67.

Foelix, R.F.; Chu-Wang, I.-W.; Beck, L. 1975. Fine structure of tarsal sensory organs in the whip spider *Admetus pumilio* (Amblypygi, Arachnida). *Tissue and Cell* 7: 331–346.

Fusco, G.; Minelli, A. 2013. Arthropod segmentation and tagmosis. In: Minelli, A.; Boxshall, G.; Fusco, G. (Eds.), *Arthropod Biology and Evolution: Molecules, Development, Morphology*, Springer Verlag, Berlin Heidelberg, p.197–223.

Gaffal, K.P.; Tichy, H.; Theiß, J.; Seelinger, G. 1975. Structural polarities in mechanosensitive sensilla and their influence on stimulus transmission (Arthropoda). *Zoomorphology* 82: 79–103.

Gainett, G.; Michalik, P.; Müller, C.H.; Giribet, G.; Talarico, G.; Willemart, R.H. 2017a. Putative thermo-/hygroreceptive tarsal sensilla on the sensory legs of an armored harvestman (Arachnida, Opiliones). *Zoologischer Anzeiger* 270: 81–97.

Gainett, G.; Michalik, P.; Müller, C.H.; Giribet, G.; Talarico, G.; Willemart, R.H. 2017b. Ultrastructure of chemoreceptive tarsal sensilla in an armored harvestman and evidence of olfaction across Laniatores (Arachnida, Opiliones). *Arthropod Structure & Development* 46: 178–195.

Garwood, R.J.; Dunlop, J. 2014. Three-dimensional reconstruction and the phylogeny of extinct chelicerate orders. *PeerJ* 2: e641.

Gerberding, M.; Scholtz, G. 2001. Neurons and glia in the midline of the higher crustacean *Orchestia cavimana* are generated via an invariant cell lineage that comprises a median neuroblast and glial progenitors. *Developmental Biology* 235: 397–409.

Gerhardt, U. 1931. Ordnung Xiphosura/Poecilopoda (Schwertschwänze). In: Krumbach, T. (Ed.), *Handbook of Zoology Online*, Vol. 1, De Gruyter, Berlin Boston, p.47–96.

Gerhardt, U.; Kästner, A. 1931. Ordnung Araneae (Echte Spinnen oder Webspinnen). In: Krumbach, T. (Ed.), *Handbook of Zoology Online*, Vol. 2, De Gruyter, Berlin Boston, p.394–656.

Giribet, G.; Edgecombe, G.D.; Wheeler, W.C.; Babbitt, C. 2002. Phylogeny and systematic position of opiliones: A combined analysis of chelicerate relationships using morphological and molecular data. *Cladistics* 18: 5–70.

Giribet, G.; McIntyre, E.; Christian, E.; Espinasa, L.; Ferreira, R.L.; Francke, Ó.F.; et al. 2014. The first phylogenetic analysis of Palpigradi (Arachnida) – the most enigmatic arthropod order. *Invertebrate Systematics* 28: 350–360.

Goloboff, P.A. 1993. Estimating character weights during tree search. *Cladistics* 9: 83–91.

Goloboff, P.A.; Catalano, S.A. 2016. TNT version 1.5, including a full implementation of phylogenetic morphometrics. *Cladistics* 32: 221–238.

Goloboff, P.A.; Farris, J.S.; Nixon, K.C. 2008. TNT, a free program for phylogenetic analysis. *Cladistics* 24: 774–786.

Göpel, T.; Wirkner, C.S. 2015. An "ancient" complexity? Evolutionary morphology of the circulatory system in Xiphosura. *Zoology* 118: 221–238.

Gorb, S. 2001a. Principles of cuticular attachment in Arthropoda. In: *Attachment Devices of Insect Cuticle*, Kluwer Academic Publishers, Dordrecht, p.37–76.

Gorb, S. 2001b. Cuticular protuberances of insects. In: *Attachment Devices of Insect Cuticle*, Kluwer Academic Publishers, Dordrecht, p.21–36.

Görner, P. 1965. A proposed transducing mechanism for a multiply-innervated mechanoreceptor (trichobothrium) in spiders. *Cold Spring Harbor Symposia on Quantitative Biology* 30: 69–73.

Gottlieb, K. 1926. Über das Gehirn des Skorpions. *Zeitschrift für Wissenschaftliche Zoologie* 127: 195–243.

Gould, S.J. 1977. Heterochrony and the parallel of ontogeny and phylogeny. In: *Ontogeny and Phylogeny*, Belknap Press of Harvard University Press, Cambridge, p.209–266.

Graham, J.B. 1988. Ecological and evolutionary aspects of integumentary respiration: body size, diffusion, and the Invertebrata. *American Zoologist* 28: 1031–1045.

Grams, M.; Wirkner, C.S.; Runge, J. 2018. Serial and special: comparison of podomeres and muscles in tactile vs walking legs of whip scorpions (Arachnida, Uropygi). *Zoologischer Anzeiger* 273: 75–101.

Guggenheim, S.; Martin, R.T. 1995. Definition of clay and clay mineral: joint report of the AIPEA nomenclature and CMS nomenclature committees. *Clays and Clay Minerals* 43: 255–256.

Hackman, R.H. 1984. VIII Arthropoda - Cuticle: Biochemistry. In: Bereiter-Hahn, J.; Matoltsy, A.G.; Richards, K.S. (Eds.), *Biology of the Integument. 1 Invertebrates*, Springer Verlag, Berlin Heidelberg, p.583–610.

van der Hammen, L. 1966. Studies on Opilioacarida (Arachnida) I. Description of *Opilioacarus texanus* (Chamberlin & Mulaik) and revised classification of the genera. *Zoologische Verhandelingen* 86: 1–80.

van der Hammen, L. 1967. The gnathosoma of *Hermannia convexa* (C. L. Koch)(Acarida: Oribatina): and comparative remarks on its morphology in other mites. *Zoologische Verhandelingen* 94: 3–45.

van der Hammen, L. 1977. A new classification of Chelicerata. *Zoologische Mededelingen* 51: 307–319.

van der Hammen, L. 1982. Comparative studies in Chelicerata II. Epimerata (Palpigradi and Actinotrichida). *Zoologische Verhandelingen* 196: 3–70.

van der Hammen, L. 1986. Comparative studies in Chelicerata IV. Apatellata, Arachnida, Scorpionida, Xiphosura. *Zoologische Verhandelingen* 226: 4–52.

van der Hammen, L. 1989. *An introduction to comparative arachnology*. SPB Academic Publishing, The Hague, 567p.

Handlirsch, A. 1926. Arthropoda: Allgemeine Einleitung in die Naturgeschichte der Gliederfüsser. In: Krumbach, T. (Ed.), *Handbook of Zoology Online*, De Gruyter, Berlin Boston, p.211–276.

Hanken, J.; Wake, D.B. 1993. Miniaturization of body size: organismal consequences and evolutionary significance. *Annual Review of Ecology and Systematics* 24: 501–519.

Hansen, H.J. 1901. On six species of *Koenenia*, with remarks on the order Palpigradi. *Entomologisk Tidskrift*: 193–240.

Hansen, H.J.; Sørensen, W. 1897. The order Palpigradi Thorell (*Koenenia mirabilis* Grassi) and its relationships to other Arachnida. *Entomologisk Tidskrift*: 223–240.

Hansen, H.J.; Sørensen, W.E. 1905. The Tartarides: a tribe of the order Pedipalpi. *Arkiv för Zoologi* 2: 1–85.

Hanstrom, B. 1928. *Vergleichende Anatomie des Nervensystems der wirbellosen Tiere*. Springer Verlag, Berlin Heidelberg, 628p.

Harris, D.J.; Mill, P.J. 1973. The ultrastructure of chemoreceptor sensilla in *Ciniflo* (Araneida, Arachnida). *Tissue and Cell* 5: 679–689.

Harris, D.J.; Mill, P.J. 1977. Observations on the leg receptors of *Ciniflo* (Araneida: Dictynidae). *Journal of Comparative Physiology* 119: 37–54.

Hartmann, G. 1973. Zum gegenwärtigen Stand der Erforschung der Ostracoden interstitieller Systeme. *Annales de Spéléologie* 28: 417–426.

Harvey, M.S. 2002. The neglected cousins: what do we know about the smaller arachnid orders? *Journal of Arachnology* 30: 357–372.

Harvey, M.S. 2003. *Catalogue of the smaller arachnid orders of the world: Amblypygi, Uropygi, Schizomida, Palpigradi, Ricinulei and Solifugae*. CSIRO Publishing, Clayton South, 385p.

Harzsch, S. 2003. Ontogeny of the ventral nerve cord in malacostracan crustaceans: a common plan for neuronal development in Crustacea, Hexapoda and other Arthropoda? *Arthropod Structure & Development* 32: 17–37.

Harzsch, S.; Wildt, M.; Battelle, B.; Waloszek, D. 2005. Immunohistochemical localization of neurotransmitters in the nervous system of larval *Limulus polyphemus* (Chelicerata, Xiphosura): evidence for a conserved protocerebral architecture in Euarthropoda. *Arthropod Structure & Development* 34: 327–342.

Haug, C.; Rötzer, M.A. 2018. The ontogeny of *Limulus polyphemus* (Xiphosura s. str., Euchelicerata) revised: looking "under the skin." *Development Genes and Evolution* 228: 49–61.

Haupt, J. 1982. Hair regeneration in a solfugid chemotactile sensillum during moulting (Arachnida: Solifugae). *Wilhelm Roux's Archives of Developmental Biology* 191: 137–142.

Hess, E.; Vlimant, M. 1982. The tarsal sensory system of *Amblyomma variegatum* Fabricius (Ixodidae, Metastriata). I. Wall pore and terminal pore sensilla. *Revue Suisse de Zoologie* 89: 713–729.

Hess, E.; Loftus, R. 1984. Warm and cold receptors of two sensilla on the foreleg tarsi of the tropical bont tick *Amblyomma variegatum*. *Journal of Comparative Physiology A* 155: 187–195.

Hoffmann, C. 1967. Bau und Funktion der Trichobothrien von *Euscorpius carpathicus* L. *Zeitschrift für vergleichende Physiologie* 54: 290–352.

Hootman, S.R.; Conte, F.P. 1975. Functional morphology of the neck organ in *Artemia salina* nauplii. *Journal of Morphology* 145: 371–385.

Horn, A.C.M.; Achaval, M. 2002. The gross anatomy of the nervous system of *Bothriurus bonariensis* (L. C. Koch, 1842)(Scorpiones, Bothriuridae). *Brazilian Journal of Biology* 62: 253–262.

Ioffe, I.D. 1963. Structure of the brain of *Dermacentor pictus* Herm. (Chelicerata, Acarina). *Zoologicheskii Zhurnal* 42: 1472–1484.

ISO, E. 2017. 14688-1:2017: Geotechnical investigation and testing – Identification and classification of soil – Part 1: Identification and description. *International Organization for Standardization, Geneva*.

Kaneko, N. 1988. Feeding habits and cheliceral size of oribatid mites in cool temperate forest soils in Japan. *Revue d'Écologie et de Biologie du Sol* 25: 353–363.

Kästner, A. 1931a. Ordnung Palpigradi Thorell. In: Krumbach, T. (Ed.), *Handbook of Zoology Online*, Vol. 2, De Gruyter, Berlin Boston, p.77–98.

Kästner, A. 1931b. Ordnung Scorpiones (Schwertschwänze). In: Krumbach, T. (Ed.), *Handbook of Zoology Online*, Vol. 1, De Gruyter, Berlin Boston, p.117–240.

Kästner, A. 1931c. Ordnung Ricinulei. In: Krumbach, T. (Ed.), *Handbook of Zoology Online*, Vol. 2, De Gruyter, Berlin Boston, p.99–116.

Kästner, A. 1931d. Ordnung Opiliones Sundevall (Weberknechte). In: Krumbach, T. (Ed.), *Handbook of Zoology Online*, Vol. 2, De Gruyter, Berlin Boston, p.300–393.

Kästner, A. 1931e. Ordnung Solifugae (Walzenspinnen). In: Krumbach, T. (Ed.), *Handbook of Zoology Online*, Vol. 2, De Gruyter, Berlin Boston, p.193–299.

Kästner, A. 1931f. Ordnung Pedipalpi Latreille (Geißel-Scorpione). In: Krumbach, T. (Ed.), *Handbook of Zoology Online*, Vol. 2, De Gruyter, Berlin Boston, p.1–76.

Kästner, A. 1931g. Die Hüfte und ihre Umformung zu Mundwerkzeugen bei den Arachniden. *Zeitschrift für Morphologie und Ökologie der Tiere* 22: 721–758.

Keil, T.A. 1997. Functional morphology of insect mechanoreceptors. *Microscopy Research and Technique* 39: 506–531.

Kimble, M.; Coursey, Y.; Ahmad, N.; Hinsch, G.W. 2002. Behavior of the yolk nuclei during embryogenesis, and development of the midgut diverticulum in the horseshoe crab *Limulus polyphemus*. *Invertebrate Biology* 121: 365–377.

Klann, A.E. 2009. *Histology and ultrastructure of solifuges.* Ernst-Moritz-Arndt-Universität, Greifswald.

Klann, A.E.; Alberti, G. 2010. Histological and ultrastructural characterization of the alimentary system of solifuges (Arachnida, Solifugae). *Journal of Morphology* 271: 225–243.

Klußmann-Fricke, B.-J.; Wirkner, C.S. 2016. Comparative morphology of the hemolymph vascular system in Uropygi and Amblypygi (Arachnida): complex correspondences support Arachnopulmonata. *Journal of Morphology* 277: 1084–1103.

Klußmann-Fricke, B.-J.; Prendini, L.; Wirkner, C.S. 2012. Evolutionary morphology of the hemolymph vascular system in scorpions: a character analysis. *Arthropod Structure & Development* 41: 545–560.

Kovac, D.; Maschwitz, U. 2000. Protection of hydrofuge respiratory structures against detrimental microbiotic growth by terrestrial grooming in water beetles (Coleoptera: Hydropbilidae, Hydraeoidae, Dryopidae, Ebnidae, Curculiooidae). *Entomologia Generalis*: 277–292.

Kováč, Ľ.; Mock, A.; Ľuptácik, P.; Palacios-Vargas, J.G. 2002. Distribution of *Eukoenenia spelaea* (Peyerimhoff, 1902)(Arachnida, Palpigradida) in the Western Carpathians with remarks on its biology and behaviour. In: Tajovskỳ, K.; Balík, V.; Pižl, V. (Eds.), *Studies on Soil Fauna in Central Europe*, České Budějovice: Institute of Soil Biology AS CR, p.93–99.

Kováč, Ľ.; Elhottová, D.; Mock, A.; Nováková, A.; Krištůfek, V.; Chroňáková, A.; et al. 2014. *The cave biota of Slovakia.* State Nature Conservancy of the Slovak Republic, Slovak Caves Administration, Liptovský Mikuláš, 1–192p.

Kučera, B. 1964. Krasová morfologie a vỳvoj Ardovské jeskyně v Jihoslovenském krasu. *Československỳ kras, NČSAV Praha* 16: 41–56.

Lamsdell, J.C. 2013. Revised systematics of Palaeozoic 'horseshoe crabs' and the myth of monophyletic Xiphosura: re-evaluating the monophyly of Xiphosura. *Zoological Journal of the Linnean Society* 167: 1–27.

Landman, N.H.; Dommergues, J.L.; Marchand, D. 1991. The complex nature of progenetic species – examples from Mesozoic ammonites. *Lethaia* 24: 409–421.

Legg, G. 1976. The external morphology of a new species of ricinuleid (Arachnida) from Sierra Leone. *Zoological Journal of the Linnean Society* 59: 1–58.

Lehmacher, C.; Abeln, B.; Paululat, A. 2012. The ultrastructure of *Drosophila* heart cells. *Arthropod Structure & Development* 41: 459–474.

Levi, H.W. 1967. Adapations of respiratory systems of spiders. *Evolution* 21: 571–583.

Loesel, R.; Wolf, H.; Kenning, M.; Harzsch, S.; Sombke, A. 2013. Architectural principles and evolution of the arthropod central nervous system. In: Minelli, A.; Boxshall, G.; Fusco, G. (Eds.), *Arthropod Biology and Evolution: Molecules, Development, Morphology*, Springer Verlag, Berlin Heidelberg, p.300–342.

Loftus, R. 1976. Temperature-dependent dry receptor on antenna of *Periplaneta*. Tonic response. *Journal of Comparative Physiology* 111: 153–170.

Loftus, R.; Corbière-Tichané, G. 1981. Antennal warm and cold receptors of the cave beetle, *Speophyes lucidulus* Delar, in sensilla with a lamellated dendrite. *Journal of Comparative Physiology A* 143: 443–452.

Lopez, A. 1983. Coxal glands of the genus *Metepeira* (Araneae, Araneidae). *The Journal of Arachnology* 11: 97–99.

Lowy, R.J.; Conte, F.P. 1985. Morphology of isolated crustacean larval salt glands. *American Journal of Physiology-Regulatory, Integrative and Comparative Physiology* 248: R709–R716.

Ludwig, M.; Alberti, G. 1992. Fine structure of the midgut of *Prokoenenia wheeleri* (Arachnida: Palpigradi). *Zoologische Beiträge* 34: 127–134.

Ludwig, M.; Palacios-Vargas, J.G.; Albertif, G. 1994. Cellular details of the midgut of *Cryptocellus boneti* (Arachnida: Ricinulei). *Journal of Morphology* 220: 263–270.

McIver, S.B. 1975. Structure of cuticular mechanoreceptors of arthropods. *Annual Review of Entomology* 20: 381–397.

McNamara, K.J. 1986. A guide to the nomenclature of heterochrony. *Journal of Paleontology*: 4–13.

McNamara, K.J. 1988. The abundance of heterochrony in the fossil record. In: Mckinney, M. (Ed.), *Heterochrony in Evolution*, Springer Verlag, Berlin Heidelberg, p.287–325.

Mehnert, L.; Dietze, Y.; Hörnig, M.K.; Starck, J.M. 2018. Body tagmatization in pseudoscorpions. *Zoologischer Anzeiger* 273: 152–163.

Meijden, A. van der; Langer, F.; Boistel, R.; Vagovic, P.; Heethoff, M. 2012. Functional morphology and bite performance of raptorial chelicerae of camel spiders (Solifugae). *The Journal of Experimental Biology* 215: 3411–3418.

Messlinger, K. 1987. Fine structure of scorpion trichobothria (Arachnida, Scorpiones). *Zoomorphology* 107: 49–57.

Michalik, P. 2009. The male genital system of spiders (Arachnida, Araneae) with notes on the fine structure of seminal secretions. *Contributions to Natural History* 12: 959–972.

Michalik, P.; Reiher, W.; Tintelnot-Suhm, M.; Coyle, F.A.; Alberti, G. 2005. Female genital system of the folding-trapdoor spider *Antrodiaetus unicolor* (Hentz, 1842) (Antrodiaetidae, Araneae): ultrastructural study of form and function with notes on reproductive biology of spiders. *Journal of Morphology* 263: 284–309.

Millot, J. 1942. Sur l'anatomie et l'histophysiologie de *Koenenia mirabilis* Grassi (Arachnida, Palpigradi). *Revue Francais d'Entomologie Paris* 9: 33–51.

Millot, J. 1943. Notes complémentaires sur l'anatomie, l'histologie et la répartition géographique en France de *Koenenia mirabilis* Grassi (Arachnida Palpigradi). *Revue Francais d'Entomologie Paris* 9: 127–135.

Millot, J. 1949a. Classe des Arachnides. In: Grassé, P.-P. (Ed.), *Traité de Zoologie*, Vol. 6, Masson et Cie., Paris, p.263–385.

Millot, J. 1949b. Ordre des Uropyges. In: Grassé, P.-P. (Ed.), *Traité de Zoologie*, Vol. 6, Masson et Cie., Paris, p.533–562.

Millot, J. 1949c. Ordre des Amblypyges. In: Grassé, P.-P. (Ed.), *Traité de Zoologie*, Vol. 6, Masson et Cie., Paris, p.563–588.

Millot, J. 1949d. Ordre des Aranéides. In: Grassé, P.-P. (Ed.), *Traité de Zoologie*, Vol. 6, Masson et Cie., Paris, p.589–743.

Millot, J. 1949e. Ordre des Ricinuléides. In: Grassé, P.-P. (Ed.), *Traité de Zoologie*, Vol. 6, Masson et Cie., Paris, p.744–760.

Millot, J. 1949f. Ordre des Palpigrades. In: Grassé, P.-P. (Ed.), *Traité de Zoologie*, Vol. 6, Masson et Cie., Paris, p.520–532.

Millot, J.; Vachon, M. 1949a. Ordre des Solifuges. In: Grassé, P.-P. (Ed.), *Traité de Zoologie*, Vol. 6, Masson et Cie., Paris, p.482–519.

Millot, J.; Vachon, M. 1949b. Ordre des Scorpions. In: Grassé, P.-P. (Ed.), *Traité de Zoologie*, Vol. 6, Masson et Cie., Paris, p.386–436.

Mittmann, B.; Scholtz, G. 2003. Development of the nervous system in the" head" of *Limulus polyphemus* (Chelicerata: Xiphosura): morphological evidence for a correspondence between the segments of the chelicerae and of the (first) antennae of Mandibulata. *Development Genes and Evolution* 213: 9–17.

Mittmann, B.; Wolff, C. 2012. Embryonic development and staging of the cobweb spider *Parasteatoda tepidariorum* C. L. Koch, 1841 (syn.: *Achaearanea tepidariorum*; Araneomorphae; Theridiidae). *Development Genes and Evolution* 222: 189–216.

Molina, M.R.; Cripps, R.M. 2001. Ostia, the inflow tracts of the *Drosophila* heart, develop from a genetically distinct subset of cardial cells. *Mechanisms of Development* 109: 51–59.

Moritz, M. 1993. 1. Unterstamm Arachnata. In: Gruner, H.-E. (Ed.), *Lehrbuch Der Speziellen Zoologie. Band I: Wirbellose Tiere. 4. Teil: Arthropoda (Ohne Insecta)*, 4th ed. Gustav Fischer Verlag, Jena, p.64–447.

Neville, A.C. 1984. Cuticle: organization. In: Bereiter-Hahn, J.; Matoltsy, A.G.; Richards, K.S. (Eds.), *Biology of the Integument*, Springer Verlag, Berlin Heidelberg, p.611–625.

Noble-Nesbitt, J. 1963. Transpiration in *Podura aquatica* L. (Collembola, Isotomidae) and the wetting properties of its cuticle. *Journal of Experimental Biology* 40: 681–700.

Noirot, C.; Quennedey, A. 1974. Fine structure of insect epidermal glands. *Annual Review of Entomology* 19: 61–80.

Obenchain, F.D.; Oliver, Jr, J.H. 1975. The heart and arterial circulatory system of ticks (Acari: Ixodoidea). *Journal of Arachnology*: 57–74.

Ozaki, M.; Tominaga, Y. 1999. Contact chemoreceptors. In: Eguchi, E.; Tominaga, Y. (Eds.), *Atlas of Arthropod Sensory Receptors*, Springer, Tokyo, p.143–154.

Payne, C.M.; Allen, J.A. 1991. The morphology of deep-sea Thyasiridae (Mollusca: Bivalvia) from the Atlantic Ocean. *Philosophical Transactions of the Royal Society B: Biological Sciences* 334: 481–562.

Pinto-da-Rocha, R.; Machado, G.; Giribet, G. 2007. *Harvestmen. The Biology of Opiliones.* Harvard University Press, Cambridge London, 597p.

Pinto-da-Rocha, R.; Andrade, R.; Moreno-González, J.A. 2016. Two new cave-dwelling genera of short-tailed whip-scorpions from Brazil (Arachnida: Schizomida: Hubbardiidae). *Zoologia (Curitiba)* 33.

Pitnick, S.; Hosken, D.J.; Birkhead, T.R. 2009. Sperm morphological diversity. In: *Sperm Biology – An Evolutionary Perspective*, Elsevier, Oxford, p.69–149.

Platnick, N.I.; Forster, R.R. 1982. On the Micromygalinae, a new subfamily of mygalomorph spiders (Araneae, Microstigmatidae). *American Museum Novitates* 2734: 1–13.

Polilov, A.A. 2008. Anatomy of the smallest Coleoptera, featherwing beetles of the tribe Nanosellini (Coleoptera, Ptiliidae), and limits of insect miniaturization. *Entomological Review* 88: 26–33.

Polilov, A.A. 2015a. Consequences of miniaturization in insect morphology. *Moscow University Biological Sciences Bulletin* 70: 136–142.

Polilov, A.A. 2015b. Small is beautiful: features of the smallest insects and limits to miniaturization. *Annual Review of Entomology* 60: 103–121.

Polilov, A.A. 2016. *At the size limit – Effects of miniaturization in insects*. Springer International Publishing Switzerland, Cham, 325p.

Polilov, A.A.; Shmakov, A.S. 2016. The anatomy of the thrips *Heliothrips haemorrhoidalis* (Thysanoptera, Thripidae) and its specific features caused by miniaturization. *Arthropod Structure & Development* 45: 496–507.

Polis, G.A. 1990. *The biology of scorpions*. Stanford University Press, Stanford, 587p.

Polis, G.A.; Farley, R.D. 1979. Behavior and ecology of mating in the cannibalistic scorpion, *Paruroctonus mesaensis* Stahnke (Scorpionida: Vaejovidae). *Journal of Arachnology*: 33–46.

Pound, J.M.; Oliver JR, J.H. 1982. Syneganglial and neurosecretory morphology of female *Ornithodoros parkeri* (Cooley)(Acari: Argasidae). *Journal of Morphology* 173: 159–177.

Punzo, F. 2012. *The Biology of Camel-Spiders: Arachnida, Solifugae*. Springer Science & Business Media, 301p.

Quesada, R.; Triana, E.; Vargas, G.; Douglass, J.K.; Seid, M.A.; Niven, J.E.; et al. 2011. The allometry of CNS size and consequences of miniaturization in orb-weaving and cleptoparasitic spiders. *Arthropod Structure & Development* 40: 521–529.

Regier, J.C.; Shultz, J.W.; Zwick, A.; Hussey, A.; Ball, B.; Wetzer, R.; et al. 2010. Arthropod relationships revealed by phylogenomic analysis of nuclear protein-coding sequences. *Nature* 463: 1079–1083.

Reißland, A.; Görner, P. 1985. Trichobothria. In: Barth, F.G. (Ed.), *Neurobiology of Arachnids*, Springer Verlag, Berlin Heidelberg, p.138–161.

Reynolds, E.S. 1963. The use of lead citrate at high pH as an electron-opaque stain in electron microscopy. *The Journal of Cell Biology* 17: 208–212.

Roewer, C.F. 1934. 4. Buch: Solifugae, Palpigradi. In: Bronn, H.G. (Ed.), *Dr. H.G. Bronns Klassen und Ordnungen des Tierreichs*, Vol. 5, Akademische Verlagsgesellschaft, Leipzig, p.1–723.

Rucker, A. 1901. The Texan *Koenenia*. *The American Naturalist* 35: 615–630.

Rucker, A. 1903. A new *Koenenia* from Texas. *Quarterly Journal of Microscopical Science*: 215–231.

Rüdeberg, C. 1967. A rapid method for staining thin sections of vestopal W-embedded tissue for light microscopy. *Experientia* 23: 792–792.

Rugendorff, A.; Younossi-Hartenstein, A.; Hartenstein, V. 1994. Embryonic origin and differentiation of the *Drosophila* heart. *Wilhelm Roux's Archives of Developmental Biology* 203: 266–280.

Scholl, G. 1977. Beiträge zur Embryonalentwicklung von *Limulus polyphemus* L. (Chelicerata, Xiphosura). *Zoomorphologie* 86: 99–154.

Scholtz, G.; Edgecombe, G.D. 2006. The evolution of arthropod heads: reconciling morphological, developmental and palaeontological evidence. *Development Genes and Evolution* 216: 395–415.

Schriefer, M.E.; Beveridge, M.; Sonenshine, D.E.; Homsher, P.J.; Carson, K.A.; Weidman, C.S. 1987. Evidence of ecdysteroid production by tick (Acari: Ixodidae) fat-body tissues in vitro. *Journal of Medical Entomology* 24: 295–302.

Selden, P.A.; Shear, W.A.; Bonamo, P.M. 1991. A spider and other arachnids from the Devonian of New York, and reinterpretations of Devonian Araneae. *Palaeontology* 34: 241–281.

Shear, W.A. 1999. Introduction to Arthropoda and Cheliceriformes. In: Harrison, F.W.; Foelix, R.F. (Eds.), *Microscopic Anatomy of Invertebrates*, Vol. 8A, Wiley-Liss, New York, p.1–19.

Sherman, R.G.; Bursey, C.R.; Fourtner, C.R.; Pax, R.A. 1969. Cardiac ganglia in spiders (Arachnida: Araneae). *Experientia* 25: 438–439.

Shultz, J.W. 1989. Morphology of locomotor appendages in Arachnida: evolutionary trends and phylogenetic implications. *Zoological Journal of the Linnean Society* 97: 1–55.

Shultz, J.W. 1990. Evolutionary morphology and phylogeny of Arachnida. *Cladistics* 6: 1–38.

Shultz, J.W. 1991. Evolution of locomotion in Arachnida: the hydraulic pressure pump of the giant whipscorpion, *Mastigoproctus giganteus* (Uropygi). *Journal of Morphology* 210: 13–31.

Shultz, J.W. 1993. Muscular anatomy of the giant whipscorpion *Mastigoproctus giganteus* (Lucas)(Arachnida: Uropygi) and its evolutionary significance. *Zoological Journal of the Linnean Society* 108: 335–365.

Shultz, J.W. 1999. Muscular anatomy of a whipspider, *Phrynus longipes* (Pocock)(Arachnida: Amblypygi), and its evolutionary significance. *Zoological Journal of the Linnean Society* 126: 81–116.

Shultz, J.W. 2000. Skeletomuscular anatomy of the harvestman *Leiobunum aldrichi* (Weed, 1893)(Arachnida: Opiliones: Palpatores) and its evolutionary significance. *Zoological Journal of the Linnean Society* 128: 401–438.

Shultz, J.W. 2001. Gross muscular anatomy of *Limulus polyphemus* (Xiphosura, Chelicerata) and its bearing on evolution in the Arachnida. *Journal of Arachnology* 29: 283–303.

Shultz, J.W. 2007a. A phylogenetic analysis of the arachnid orders based on morphological characters. *Zoological Journal of the Linnean Society* 150: 221–265. By permission of the Linnean Society.

Shultz, J.W. 2007b. Morphology of the prosomal endoskeleton of Scorpiones (Arachnida) and a new hypothesis for the evolution of cuticular cephalic endoskeletons in arthropods. *Arthropod Structure & Development* 36: 77–102.

Smrž, J.; Kováč, Ľ.; Mikeš, J.; Lukešová, A. 2013. Microwhip scorpions (Palpigradi) feed on heterotrophic cyanobacteria in Slovak caves – a curiosity among Arachnida. *PLOS ONE* 8: e75989.

Smrž, J.; Kováč, Ľ.; Mikeš, J.; Šustr, V.; Lukešová, A.; Tajovsky, K.; et al. 2015. Food sources of selected terrestrial cave arthropods. *Subterranean Biology* 16: 37.

Snodgrass, R.E. 1948. The feeding organs of Arachnida, including mites and ticks. *Smithsonian Miscellaneous Collections* 110: 1–93.

Snodgrass, R.E. 1965. *A Textbook of Arthropod Anatomy*. Reprint ed. Hafner Publishing/Cornell University, 392p.

Stahnke, H.L. 1966. Some aspects of scorpion behavior. *Bulletin of the Southern California Academy of Sciences* 65: 65–80.

Steinbach, G. 1952. Vergleichende Untersuchungen zur Chelicerenmuskulatur einiger Araneen. *Wissenschaftliche Zeitschrift der Humboldt-Universität zu Berlin* 2.

Steinbrecht, R.A. 1969. Comparative morphology of olfactory receptors. In: Pfaffmann, C. (Ed.), *Olfaction and Taste*, Vol. 3, Rockefeller University Press, New York, p.3–21.

Strubell, A. 1892. Zur Entwicklungsgeschichte der Pedipalpen. *Zoologischer Anzeiger* 15: 87–93.

Suter, R.B.; Stratton, G.E.; Miller, P.R. 2004. Taxonomic variation among spiders in the ability to repel water: surface adhesion and hair density. *Journal of Arachnology* 32: 11–21.

Talarico, G.; Hernandez, L.G.; Michalik, P. 2008. The male genital system of the New World Ricinulei (Arachnida): ultrastructure of spermatozoa and spermiogenesis with special emphasis on its phylogenetic implications. *Arthropod Structure & Development* 37: 396–409.

Talarico, G.; Lipke, E.; Alberti, G. 2011. Gross morphology, histology, and ultrastructure of the alimentary system of Ricinulei (Arachnida) with emphasis on functional and phylogenetic implications. *Journal of Morphology* 272: 89–117.

Talarico, G.; Palacios-Vargas, J.G.; Silva, M.F.; Alberti, G. 2005. First ultrastructural observations on the tarsal pore organ of *Pseudocellus pearsei* and *P. boneti* (Arachnida, Ricinulei). *Journal of Arachnology* 33: 604–612.

Tanaka, G.; Hou, X.; Ma, X.; Edgecombe, G.D.; Strausfeld, N.J. 2013. Chelicerate neural ground pattern in a Cambrian great appendage arthropod. *Nature* 502: 364.

Telford, M.J.; Thomas, R.H. 1998. Expression of homeobox genes shows chelicerate arthropods retain their deutocerebral segment. *Proceedings of the National Academy of Sciences* 95: 10671–10675.

Teruel, R.; De Armas, L.F. 2002. Un género nuevo de Hubbardiidae (Arachnida: Schizomida) del occidente de Cuba. *Revista Ibérica de Aracnología* 6: 91–94.

Tichy, H. 1975. Unusual fine structure of sensory hair triad of the millipede, *Polyxenus*. *Cell and Tissue Research* 156: 229–238.

Tichy, H.; Barth, F.G. 1992. Fine structure of olfactory sensilla in myriapods and arachnids. *Microscopy Research and Technique* 22: 372–391.

Tichy, H.; Loftus, R. 1996. Hygroreceptors in insects and a spider: humidity transduction models. *Naturwissenschaften* 83: 255–263.

Tjønneland, A.; Økland, S.; Nylund, A. 1987. Evolutionary aspects of the arthropod heart. *Zoologica Scripta* 16: 167–175.

Todd, V. 1949. The habits and ecology of the British harvestmen (Arachnida, Opiliones), with special reference to those of the Oxford district. *The Journal of Animal Ecology*: 209–229.

Vachon, M. 1949. Ordre des Pseudoscorpions. In: Grassé, P.-P. (Ed.), *Traité de Zoologie*, Vol. 6, Masson et Cie., Paris, p.437–481.

Vitzthum, H. 1931. Ordnung Acari (Milben). In: Krumbach, T. (Ed.), *Handbook of Zoology Online*, Vol. 3, De Gruyter, Berlin Boston, p.1–160.

Vyas, A.B. 1974. The cheliceral muscles of the scorpion *Heterometrus fulvipes*. *Bulletin of the Southern California Academy of Sciences* 73: 9–14.

Waldow, U. 1970. Elektrophysiologische Untersuchungen an Feuchte-, Trocken- und Kälterezeptoren auf der Antenne der Wanderheuschrecke *Locusta*. *Journal of Comparative Physiology A* 69: 249–283.

Wang, B.; Dunlop, J.A.; Selden, P.A.; Garwood, R.J.; Shear, W.A.; Müller, P.; et al. 2018. Cretaceous arachnid *Chimerarachne yingi* gen. et sp. nov. illuminates spider origins. *Nature Ecology & Evolution* 2: 614–622.

Wegerhoff, R.; Breidbach, O. 1995. Comparative aspects of the chelicerate nervous systems. In: *The Nervous Systems of Invertebrates: An Evolutionary and Comparative Approach*, Springer, p.159–179.

Weygoldt, P. 1969. *The Biology of Pseudoscorpions*. Harvard University Press, Cambridge, 145p.

Weygoldt, P. 1985. Ontogeny of the arachnid central nervous system. In: Barth, F.G. (Ed.), *Neurobiology of Arachnids*, Springer Verlag, Berlin Heidelberg, p.20–37.

Weygoldt, P. 1996. Evolutionary morphology of whip spiders: towards a phylogenetic system (Chelicerata: Arachnida: Amblypygi). *Journal of Zoological Systematics and Evolutionary Research* 34: 185–202.

Weygoldt, P.; Paulus, H.F. 1979a. Untersuchungen zur Morphologie, Taxonomie und Phylogenie der Chelicerata II. Cladogramme und die Entfaltung der Chelicerata. *Journal of Zoological Systematics and Evolutionary Research* 17: 177–200.

Weygoldt, P.; Paulus, H.F. 1979b. Untersuchungen zur Morphologie, Taxonomie und Phylogenie der Chelicerata I. Morphologische Untersuchungen. *Journal of Zoological Systematics and Evolutionary Research* 17: 85–116.

Weygoldt, P.; Rahmadi, C.; Huber, S. 2010. Notes on the reproductive biology of *Phrynus exsul* Harvey, 2002 (Arachnida: Amblypygi: Phrynidae). *Zoologischer Anzeiger* 249: 113–119.

Wheeler, W.M. 1900. A singular arachnid *Koenenia mirabilis* (Grassi) occurring in Texas. *The American Naturalist* 34: 837–850.

Whitehead, W.F.; Rempel, J.G. 1959. A study of the musculature of the black widow spider, *Latrodectus mactans* (Fabr.). *Canadian Journal of Zoology* 37: 831–870.

Wiens, J.J.; Donoghue, M.J. 2004. Historical biogeography, ecology and species richness. *Trends in Ecology & Evolution* 19: 639–644.

Williams, D.S.; McIntyre, P. 1980. The principal eyes of a jumping spider have a telephoto component. *Nature* 288: 578.

Wirkner, C.S.; Prendini, L. 2007. Comparative morphology of the hemolymph vascular system in scorpions – A survey using corrosion casting, MicroCT, and 3D-reconstruction. *Journal of Morphology* 268: 401–413.

Wirkner, C.S.; Huckstorf, K. 2013. The circulatory system of spiders. In: *Spider Ecophysiology*, Springer, p.15–27.

Wirkner, C.S.; Tögel, M.; Pass, G. 2013. The arthropod circulatory system. In: Minelli, A.; Boxshall, G.; Fusco, G. (Eds.), *Arthropod Biology and Evolution: Molecules, Development, Morphology*, Springer Verlag, Berlin Heidelberg, p.343–391.

Wolf, H. 2016. Scorpiones. In: Schmidt-Rhaesa, A.; Harzsch, S.; Purschke, G. (Eds.), *Structure and Evolution of Invertebrate Nervous Systems*, Oxford University Press, Oxford, p.443–452.

Yokohari, F. 1999. Hygro- and Thermoreceptors. In: Eguchi, E.; Tominaga, Y. (Eds.), *Atlas of Arthropod Sensory Receptors*, Springer, Tokyo, p.191–210.

Zwicky, K.T.; Hodgson, S.M. 1965. Occurrence of myogenic hearts in arthropods. *Nature* 207: 778.

6.   Acknowledgements

I thank my family and friends, especially Gülperi Stenhouse, Dominic Anders, Sabrina and Katrin Lehmeier, Stefanie Geiger, and many more incredible people for their invaluable friendship, laughter, and unfaltering support.

To my wonderful wife Julia Guess: thank you my love for being who you are. Without your never-ending love and support, your patience and motivation, I would have never had the courage and endurance to finish this project. I love you more than I could ever put into words.

7. Appendix

7.1 Additional tables

Tab. A1. Original character list of Shultz (2007*a*). "A phylogenetic analysis of the arachnid orders based on morphological characters". Zoological Journal of the Linnean Society 150: 245–265. By permission of the Linnean Society.

Character	Character description	Character coding
1	dorsal sclerite formed by fusion of the prosomal carapace, the dorsal portion of the first opisthosomal somite and the dorsomedial (axial) portion of the second opisthosomal somite	0, absent; 1, present
2	single dorsal sclerite covering entire dorsal surface of body, no lines indicating original segmentation	0, absent; 1, present
3	anterior end of dorsal prosoma with median marginal or submarginal pointed process	0, absent; 1, present
4	ophthalmic ridges: pair of longitudinal crests intersecting or passing near the region of the lateral eyes or comparable region where lateral eyes are absent	0, absent; 1, present
5	carapace with demarcations (e.g. grooves, sclerites, phragmata) between pro-, meso- or metapeltidia	0, absent; 1, present
6	carapace with distinct pro-, meso- or metapeltidial sclerites	0, absent; 1, present; -, inapplicable due to absence of pro-, meso- or metapeltidial demarcations
7	sejugal furrow: circumferential zone of body flexibility that passes between the coxae of legs 2 and 3	0, absent; 1, present
8	prosomal ozopores	0, absent; 1, present
9	carapacal pleural doublure	0, absent; 1, present
10	cardiac lobe: a longitudinal axial elevation of the carapace	0, absent; 1, present
11	moveable cucullus	0, absent; 1, present
12	medial intercoxal 'sternal' region	0, all pedal coxae separated medially; 1, anterior pedal coxae abutting medially, posterior coxae separated; 2, anterior pedal coxae separated medially, posterior coxae abutting; 3, all pedal coxae abutting medially; 4, epimera: coxae undifferentiated medially from ventral body wall
13	postoral sternapophysis (= tritosternum, labium): a cuticular evagination of the ventral body wall posteriorly adjacent to the palpal coxae forming the posterior border of the preoral chamber in some taxa or displaced posteriorly by fusion of the palpal coxae in others	0, absent; 1, present
14	channels on the body surface linking openings of coxal organs to preoral chamber	0, absent; 1, present
15	podocephalic canal: cuticular channel and/or duct draining multiple glands and opening near mouthparts	0, absent; 1, present; -, inapplicable due to absence of channel
16	heavily sclerotized suboral sclerite serving, in part, as basal pivot point for coxae of appendages of postoral somites II–IV (= arachnid palp and legs 1 and 2)	0, absent; 1, present
17	genal angles	0, rounded; 1, pointed
18	cheliceral segmentation	0, three articles; 1, two articles

Character	Character description	Character coding
19	terminal cheliceral joint	0, laterally placed bicondylar hinge; 1, dorsally placed bicondylar hinge; 2, ventrally placed bicondylar hinge
20	chelicera articulating with carapace at anterolateral pivot	0, absent; 1, present
21	chelicera pivoting on dorsal protuberance of epistome	0, absent; 1, present
22	extrinsic cheliceral muscle arising on carapace and inserting on dorsal margin of nonbasal cheliceral article	0, absent; 1, present
23	extrinsic cheliceral muscle arising on carapace and inserting on ventral margin of nonbasal cheliceral article	0, absent; 1, present
24	extrinsic cheliceral muscles attaching to epistome	0, absent; 1, present
25	lateral tergocheliceral muscle with three heads	0, absent; 1, present; -, coded only for extant tetrapulmonates and the palpigrade *Eukoenenia*, homology is unclear in other taxa
26	cheliceral silk glands	0, absent; 1, present
27	cheliceral venom glands	0, absent; 1, present
28	cheliceral serrula interior and exterior	0, absent; 1, present
29	cheliceral 'flagellum' in male	0, absent; 1, present
30	palpal coxae fused ventromedially and forming posterior wall of preoral chamber	0, absent; 1, present
31	gnathosoma	0, absent; 1, present; -, inapplicable, palpal coxae not fused (30)
32	rostrosoma: long, narrow, subcylindrical epistome projecting anteriorly with base fixed to dorsal surface of palpal coxae, bordered laterally by lobes projecting from palpal coxae; ventral wall of preoral chamber formed by anterior element of prosoma (sternapophysis)	0, absent; 1, present
33	rutella/corniculi: hypertrophied setae modified as mouthparts located on the anterior processes of the palpal coxae	0, absent; 1, present
34	terminal segments specially modified in adult male as a clasper used to engage the female	0, absent; 1, present
35	robust, raptorial	0, absent; 1, present
36	orientation of robust, raptorial appendage	0, operating in subtransverse plane; 1, operating in subvertical plane; -, inapplicable, coded only for Pedipalpi
37	extrinsic muscle attaching to epistome	0, absent; 1, present
38	muscle originating and inserting within coxa	0, absent; 1, present
39	tarsus and/or tibia with venom glands	0, absent; 1, present
40	tarsal grooming organ	0, absent; 1, present
41	scorpionoid chela: a large, well-developed chela formed by tibia (manus + fixed finger) and tarsus (moveable finger)	0, absent; 1, present
42	modified in male as copulatory organ	0, absent; 1, present

Character	Character description	Character coding
43	apotele	0, apparently absent, not differentiated externally from penultimate article; 1, present
44	apotele (claw), position	0, terminal; 1, subterminal; -, inapplicable, coded only for taxa with a distinct apotele (43)
45	terminal adhesive organ	0, absent; 1, present; -, inapplicable, due to lack of an apotele (43)
46	appendage III (= arachnid leg 1) extremely elongate, antenniform	0, absent; 1, present
47	appendage V (= arachnid leg 3) of male specialized for sperm transfer	0, absent; 1, present
48	appendages V and VI (= arachnid legs 3 and 4) with femur shorter than patella and with principal site of flexion/extension at patella-tibia joint ('apatellate' condition sensu Van der Hammen, 1989)	0, absent; 1, present
49	appendage VI (= arachnid leg 4) with terminus modified as flattened blade	0, absent; 1, present
50	appendage III (= arachnid leg 1) with coxapophysis forming floor or wall of preoral chamber	0, absent; 1, present
51	appendage IV (= arachnid leg 2) with coxapophysis	0, absent; 1, present
52	at least one pair of coxal gnathobases on appendages III-VI (= arachnid legs 1–4)	0, absent; 1, present
53	coxae of appendages III–V (= arachnid legs 1–3) with jointed, moveable endites	0, absent; 1, present
54	intracoxal muscle: a muscle arising on anterior wall of coxa and inserting on posterior wall	0, absent; 1, present
55	coxae of appendages II–VI (= arachnid palp and legs) with dorsal articulation with carapace	0, absent; 1, present
56	flabellum (exite) on coxa of appendage VI (= arachnid leg 4)	0, absent; 1, present
57	insertion process of anteromedial tergocoxal muscle	0, weakly developed; 1, well to extremely well developed
58	musculi laterales: enlarged lateral tergocoxal muscle with attachment shifted from coxa to adjacent pleural membrane	0, absent; 1, present
59	coxa–trochanter joint with complex posterior articulation composed of two articulating sclerites	0, absent; 1, present
60	depressor muscle (or homologue) of trochanter-femur joint	0, absent; 1, present
61	trochanter–femur joint with dorsal hinge or pivot operated by flexor muscles only	0, absent; 1, present
62	superior trochanter–femur muscle (or homologue) originating broadly in femur, inserting on distal margin of trochanter	0, absent; 1, present
63	basifemur–telofemur joint of appendages III and IV (= arachnid legs 1 and 2) in adult	0, absent; 1, present
64	basifemur–telofemur joint of appendage V (= arachnid leg 3) in adult	0, absent; 1, present
65	basifemur–telofemur joint of appendage VI (= arachnid leg 4) in adult	0, absent; 1, present
66	cuticular differentiation of basifemur-telofemur joint absent, but muscles present	0, absent; 1, present; -, inapplicable due to presence of joint
67	circumfemoral ring	0, absent; 1, present
68	patella of appendage of postoral somite III (= arachnid leg 1) proportionally much longer than those of more posterior appendages	0, absent; 1, present

Character	Character description	Character coding
69	femur–patella joint	0, monocondylar, several axes of movement and multifunctional muscles; 1, bicondylar hinge, one axis of movement and antagonistic muscles; 2, hinge, one axis of movement, flexor muscles without muscular antagonists
70	patellar plagula	0, absent or with simple median attachment; 1, symmetrical, Y-shaped with long proximal stem; 2, symmetrical, U-shaped (= arcuate sclerite); 3, asymmetrical, attaching to patella only at anterior margin
71	tibiae divided by one or more joints	0, absent; 1, present
72	patella–tibia joint	0, monocondylar with or without CZY (73); 1, bicondylar hinge, one axis of movement, antagonistic muscles; 2, hinge, one axis of movement, muscles without muscular antagonists
73	patella–tibia joint with posterior compression zone ('CZY')	0, absent; 1, present; -, inapplicable due to absence of monocondylar articulation
74	patella–tibia joint of appendages III–VI (= arachnid legs 1–4) with deep-set monocondylar pivot bordered by a pair of tibial processes to which extensor muscles attach	0, absent; 1, present; -, inapplicable due to absence of monocondylar joint (72)
75	patella–tibia joint largely immobile, specialized for autotomy	0, absent; 1, present
76	anterior femur–tibia or femoropatella–tibia (transpatellar) muscle	0, absent; 1, present
77	proximal attachment of posterior femur–tibia or femoropatellar–tibia (transpatellar) muscle	0, muscle absent; 1, dorsoposterior surface of femur and/or posterior surface of patella; 2, distal process of femur, muscle acting as extensor of femur-patella joint
78	distal attachment of posterior femur–tibia (transpatellar) muscle	0, posterior; 1, dorsal, acting as extensor of patella–tibia joint; -, inapplicable due to absence of muscle (77)
79	anterior patella–tibia muscle	0, absent; 1, present
80	posterior patella–tibia muscle	0, absent; 1, present
81	patella–tibia joint spanned by elastic ('springlike') sclerite	0, absent; 1, present
82	tarsus divided into proximal basitarsus (= metatarsus) and distal telotarsus (= distitarsus or 'tarsus')	0, absent; 1, present
83	circumtarsal ring	0, absent; 1, present

Character	Character description	Character coding
84	telotarsus in adult with two or more tarsomeres	0, absent; 1, present; -, inapplicable due to absence of telotarsus (82)
85	three telotarsomeres on appendages of postoral somites IV-VI (= arachnid legs 2–4)	0, absent; 1, present; -, inapplicable due to absence of telotarsus (82) or absence of telotarsomeres (84)
86	tibia–tarsus joint spanned by well-developed elastic ('springlike') sclerite	0, absent; 1, present
87	appendage of postoral somite VI (= arachnid leg 4) with ring of large, basally articulated spatulate processes at tibia-tarsus joint	0, absent; 1, present
88	appendages postoral somites III–V (= arachnid legs 1–3) with tibiotarsus (tibia and tarsus not differentiated)	0, absent; 1, present
89	ambulacrum: peduncle-like extension of the tarsus with internal condylophores and terminating distally with apotele (e.g. claws) and/or pulvillus	0, absent; 1, present
90	apotele of appendage III (= arachnid leg 1)	0, absent or not apparent; 1, present
91	appendages of postoral somites III–VI (= arachnid legs) chelate with chela formed from tibiotarsus and apotele or tarsus and apotele	0, absent; 1, present
92	apotele with eversible or padlike empodium (= pulvillus) in adult	0, absent, although empodial claw may be present; 1, present
93	inferior apotele muscle (= claw depressor) with tibial attachment	0, absent; 1, present
94	inferior apotele muscle (= claw depressor) with patellar attachment	0, absent; 1, present
95	number of opisthosomal somites in adult	0, five; 1, eight; 2, nine; 3, 10, 4, 11; 5, 12; 6, 13
96	prosoma-opisthosoma coupling mechanism	0, absent; 1, present
97	pedicel	0, absent; 1, aranean type; 2, ricinuleid type
98	opisthosoma with three- segmented 'buckler'	0, absent; 1, present
99	thoracetron: consolidation of tergites of postgenital somites	0, absent; 1, present; -, inapplicable, coded only for Xiphosura
100	fusion of tergites of postoral somites VIII and IX (= opisthosomal somites 2 and 3) only	0, absent; 1, present
101	three diplotergites	0, absent; 1, present
102	paired opisthosomal defensive glands opening via ducts on either side of the anus	0, absent; 1, present
103	muscular diaphragm separating prosomal and opisthosomal compartments, formed by dorsoventral muscles of postoral somites VI–VIII and extrinsic muscles of leg 4	0, absent; 1, present
104	opisthosomal appendicular chondrites	0, absent; 1, present
105	paired appendages on ventral surface of postoral somite VII (= opisthosomal somite 1) in adult	0, absent; 1, present
106	megoperculum	0, absent; 1, present
107	postgenital operculum or 'sternite'	0, sclerotized; 1, not sclerotized; -, inapplicable, coded only for Pantetrapulmonata
108	genital opening of female guarded by four plates (one pregenital, one postgenital, two laterogenitals); genital opening of male guarded by two plates	0, absent; 1, present

Character	Character description	Character coding
109	anterior margin of genital opening in male with glands secreting via fusules	0, absent; 1, present
110	paired valve-like plates apparently formed from components of three somites covering triradiate genital opening	0, absent; 1, present
111	eversible 'appendages' on the ventral surface of postgenital somites	0, absent; 1, present
112	opisthosomal silk glands and spinnerets derived from appendages on postoral somites X and XI (= opisthosomal somites 4 and 5)	0, absent; 1, present
113	opisthsosomal spinnerets, location	0, near middle of opisthosoma; 1, near posterior end of opisthsosoma; -, inapplicable, coded only for Araneae
114	anterior medial 'spinnerets'	0, absent; 1, present; -, inapplicable, coded only for Araneae
115	opisthosomal tergites divided longitudinally into one median and two lateral plates	0, absent; 1, present
116	number of metasomal somites	0, zero; 1, two; 2, three; 3, five; 4, nine
117	postanal structure (telson)	0, absent or not obviously developed; 1, present
118	postanal structure, shape	0, caudal spine; 1, aculeus; 2, flagellum; 3, anal operculum; -, inapplicable due to absence of postanal structure (117)
119	specialized postanal flagellum in male (see 157–159)	0, absent; 1, present; -, inapplicable, coded only for taxa with postanal flagellum (118)
120	respiratory medium	0, water; 1, air
121	respiratory lamellae on opisthosomal somite 2 (= genital somite, postoral somite VIII)	0, absent; 1, present
122	respiratory lamellae on opisthosomal somite 3 (= postoral somite IX)	0, absent; 1, present
123	respiratory lamellae on opisthosomal somites 4–6 (= postoral somites X–XII)	0, absent; 1, present
124	respiratory lamellae on opisthosomal somite 7 (= postoral somite XIII)	0, absent; 1, present
125	kiemenplatten	0, absent; 1, present
126	tracheal system	0, absent; 1, paired ventral stigmata on postoral somite VIII (= opisthosomal somite 2); 2, paired ventral stigmata on postoral somites IX and X; 3, one pair of stigmata opening near legs 3 or 4; 4, paired stigmata associated with chelicerae; 5, four pairs of stigmata on dorsal surface of opisthosoma; -, inapplicable, aquatic (120)

Character	Character description	Character coding
127	posterior oblique muscles of BTAMS of postoral somites I–VI	0, absent; 1, present in one or more somites
128	anterior oblique muscles of BTAMS posterior to postoral somite VI	0, absent; 1, present
129	ventral attachments of posterior oblique muscles of opisthosomal btams located in prosoma	0, absent; 1, present
130	endosternite fenestrate	0, absent; 1, present
131	suboral suspensor: a tendon that arises from the btams and inserts on the ventral surface of the oral cavity via muscle	0, absent; 1, present
132	perineural vascular membrane in adult	0, absent; 1, present
133	ventral endosternal suspensor attaching on coxa of anteriorly adjacent somite	0, absent; 1, present
134	posteriormost postoral somite with a pair of dorsoventral muscles	0, VI; 1, VII; 2, VIII; 3, XII; 4, XIII; 5, XIV; 6, XV; 7, XVI
135	segmental ganglia	0, consolidated in prosoma; 1, one or more present in opisthosoma
136	dorsal median eyes	0, absent; 1, present
137	retinula cells of dorsal median eyes	0, organized into closed rhabdoms; 1, organized into network of rhabdomeres; 2, disorganized; -, inapplicable due to absence of median eyes (136)
138	ventral median eyes	0, absent; 1, present
139	lateral eyes	0, absent; 1, present
140	arrangement and number of lateral eyes	0, compound, many; 1, five or more pairs (includes microlenses); 2, three primary pairs (excludes microlenses); 3, two pairs; 4, one pair; -, inapplicable due to absence of lateral eyes (139)
141	lateral eyes with closed rhabdoms	0, absent; 1, present; -, inapplicable due to absence of lateral eyes (139)
142	slit sensilla	0, absent; 1, present
143	trichobothria	0, absent; 1, present
144	tibial trichobothria with 2-1-1-1 pattern on appendages III–VI (= arachnid legs 1–4)	0, absent; 1, present; -, inapplicable due to absence of trichobothria (143)
145	paired trichobothria on dorsal surface of prosoma	0, absent; 1, present; -, inapplicable due to absence of trichobothria (143)
146	malleoli	0, absent; 1, present
147	pectines	0, absent; 1, present

Character	Character description	Character coding
148	intercheliceral median organ	0, absent; 1, present
149	tarsal organ on appendage of postoral somite III (= arachnid leg 1) (= Haller's organ): sensilla contained within a cuticular depression on the superior surface of the tarsus of appendage III (= arachnid leg 1)	0, absent; 1, present
150	tarsal organ on appendage of postoral somite IV (= arachnid leg 2)	0, absent; 1, present
151	gonads	0, primarily prosomal; 1, primarily opisthosomal
152	ladder-like opisthosomal gonads/accessory glands (see 153)	0, absent; 1, present
153	male gonads in two distinct parts, one producing sperm and another (tubular gland) producing a holocrine secretion similar to degenerate sperm	0, absent; 1, present
154	number of gonopores	0, two; 1, one
155	genital opening (gonopore or gonostome) appearing to open in prosomal region (between leg coxae or anterior to posterior carapacal margin)	0, absent; 1, present
156	ovipositor	0, absent; 1, present
157	stalked spermatophore attached to substratum	0, absent; 1, present
158	male turns posterior end toward female during mating behaviour	0, absent; 1, present
159	female grasps male opisthosoma during mating behaviour	0, absent; 1, present
160	penis	0, absent; 1, present
161	median organ	0, absent; 1, present
162	nucleus with manchette of microtubules	0, absent; 1, present
163	axoneme	0, absent; 1, present
164	coiled axoneme	0, absent; 1, present; -, inapplicable due to absence of axoneme (163)
165	microtubule arrangement in axoneme	0, 9 + 0; 1, 9 + 1; 2, 9 + 2; 3, 9 + 3; -, inapplicable due to absence of axoneme (163)
166	helical or corkscrew shaped nucleus	0, absent; 1, present
167	vacuolated-type sperm	0, absent; 1, present
168	sperm aggregates	0, absent; 1, present
169	yolk in early embryo	0, concentrated (centrolecithal or telolecithal); 1, evenly distributed (isolecithal)
170	embryonic nutrition other than yolk	0, absent; 1, present
171	embryological growth zone	0, initiating segment addition within prosoma; 1, initiating segment addition posterior to prosoma
172	eggs/embryos maintained in external, attached brood sac secreted by genital glands	0, absent; 1, present

Character	Character description	Character coding
173	embryonic and early postembryonic 'lateral' or Claparède organs associated with coxa of postoral somite IV (= arachnid leg 2)	0, absent; 1, present
174	embryonic lateral organ associated with carapace	0, absent; 1, present
175	live birth	0, absent; 1, present
176	hexapodal larva and 1–3 nymphal stages	0, absent; 1, present
177	hexapodal prelarva	0, absent; 1, present
178	malpighian tubules	0, absent; 1, present
179	dorsomedian excretory organ	0, absent; 1, present
180	adult coxal organ opening on or near coxa of appendage III (= arachnid leg 1)	0, absent; 1, present
181	adult coxal organ opening on or near coxa of appendage V (= arachnid leg 3)	0, absent; 1, present
182	adult coxal organ opening on coxa of appendage II (= arachnid palp)	0, absent; 1, present
183	genital papillae	0, absent; 1, present; -, inapplicable, coded only for those taxa with eversible 'appendages' (111)
184	ingestion	0, solid food; 1, primarily liquid food, with or without preoral digestion
185	mouth	0, directed posteroventrally; 1, directed anteroventrally
186	oral cavity dilated by muscles arising from coxae and constricted by large circular sphincter	0, absent; 1, present
187	palate plate	0, absent; 1, present
188	lateral walls of epistome broadly fused to medial walls of palpal coxae, opposite sides connected by well-developed transverse epistomal muscle	0, absent; 1, present
189	epistome with a pair of lateral arms that projects posteriorly into the prosoma on either side of the pharynx	0, absent; 1, present
190	epistome with four pairs of suspensor muscles attaching to the carapace	0, absent; 1, present
191	intercheliceral epipharyngeal sclerite	0, absent; 1, present
192	epipharyngeal sclerite large, projecting posteriorly	0, absent; 1, present; -, inapplicable due to absence of sclerite (191)
193	dorsal dilator muscle of precerebral pharynx attaching to intercheliceral septum or associated epipharyngeal sclerite (191)	0, absent; 1, present
194	dorsal dilator muscle of precerebral pharynx attaching to dorsal surface of prosoma	0, absent; 1, present
195	lateral dilator muscle of precerebral pharynx attaching to endosternite	0, absent; 1, present
196	lateral dilator muscle of precerebral pharynx attaching to lateral surface of epistomal processes	0, absent; 1, present
197	lateral dilator muscle of precerebral pharynx attaching to medial process of coxa of appendage II (= arachnid palp)	0, absent; 1, present
198	dilator muscle of precerebral pharynx and/or preoral cavity attaching to ventral surface of prosoma	0, absent; 1, present
199	postcerebral pharynx	0, absent; 1, present

Character	Character description	Character coding
200	dilator muscle of postcerebral pharynx attaching to endosternite	0, absent; 1, present; -, inapplicable due to absence of postcerebral pharynx (199)
201	dilator muscle of postcerebral pharynx attaching to dorsal surface of prosoma	0, absent; 1, present; -, inapplicable due to absence of postcerebral pharynx (199)
202	crop and gizzard	0, absent; 1, present; -, inapplicable due to absence of postcerebral pharynx (199)

Tab. A2. Original character matrix of (Shultz 2007*a*). "A phylogenetic analysis of the arachnid orders based on morphological characters". Zoological Journal of the Linnean Society 150: 223–227. By permission of the Linnean Society. Updated character codes are marked blue, added character codes are marked red, the deleted character 61 is displayed with grey background.

Taxon	Character coding			
Allothrombium	0000???000 000--00000 000--00011 000004??0?? 000--00000 --	0001100?20 000?000001 0010?000-0 ????00-013 ?0100110211	0?0?-00001 00111-0020 000000-001 0110100000 0011100000	10000-0?00 02--011011 10--000--1 1001001000 0-0000000-
Alycus	00000?1000 000--00000 000--00011 000000??0?? 0???????0? --	0001100?20 000?000001 00101000-0 ????00-013 ????011?2?1	0?00-00001 00001?0020 000000-001 ?110100000 0010100000	10100-0?00 02--0??011 10--000--1 1?0100???? 0-0????00-
Archegozetes	00001?1000 000--00000 000--00011 000000??0?? 000--00000 -0	0401100?20 000?000001 0010?000-0 ????00-00- 00100110201	0?00-00001 0000000020 000000-001 -110100000 0010100000	10100-0?00 02--011011 10--000--1 1001011000 0-0000000-
Microcaeculus	0000??0000 000--00000 000--00011 000004??0?? 0?0--00?00 --	0001100?20 000?000001 0010?000-0 ????012013 ?0100?20211	0?0?-00001 00111-0020 000000-001 0110100000 001?100000	10000-0?00 02--011011 10--000--1 1001001??0 0-0000000-
Palaeacarus	00001?1000 000--00000 000--00011 000000??0?? 0?0--?0?0? --	0401100?20 000?000001 0010?000-0 ????01?0?? ?0100110201	0?00-00001 00111-0020 000000-001 ?110100000 0010100000	10100-0?00 02--011011 10--000--1 1?01011000 0-0??0000-
Aphonopelma	00000-0000 0110000000 0100-00001 11000010000 0111310000 10	0011000110 0000000110 00115010-0 0003111012 1000000101	0000001000 0000010022 0000011010 0110000011 1001101000	-0000-0000 0010011011 1110000--1 1001000000 1011100111
Hypochilus	00000-0000 0110000000 0100-00001 11000010000 0111310000 10	0011000110 0000000110 00115010-0 0003011012 1000000101	0000001000 0000010022 0000011010 0110000011 ?001101000	-0000-0000 0010011011 1110000--1 1001000000 1110100111
Liphistius	00000-0000 0110000000 0100-00001 11000010000 0111310000 10	0011000110 0000000110 00115010-0 0003011012 1000000101	0000001000 0000010022 0000010010 0110000011 1001101000	-0000-0000 0010011011 1101000--1 1001000000 1110100111
Charinus	00100-0000 0010010000 0101100000 11000010000 0111310000 10	0011000110 000?001011 01105000-0 1015010012 1110000101	0000100000 0000010023 0000010000 011000??? 1001100000	-000100?01 1000101011 10--020--1 1011001100 1110001011
Phrynus	00100-0000 0000-10000 0101100000 11000010000 0111310000 10	0011000110 0001001011 00105000-0 1015010012 1110000101	0000100000 0000010023 0000010000 011000??? 00-1100000	-000100101 1000101011 00--020--1 1011001100 1110001011
*Chasmataspis**	00000-0?11 ?????????? ????????0? ??00?-??0?? ?????????? ??	0??????1??? ?1???????? 1???6?01-0 ?????1??1? ??????????	????-????? ????????? 0?????-??? ?????0???? ??????????	?????-???? ?????????? ??-?1410-0 ????0????? ??????????
*Diploaspis**	000?0-0?1? ????????1? ??????0001 ??00?-??0?? ?????????? ??	0??????1??? ?????????? 0???6?01-0 ?????1??1? ??????????	????-????? ????????? 0?????-??? ?????????? ??????????	?????-???? ?????????? ??-?0410-0 ????0????? ??????????

Taxon	Character coding			
Octoberaspis*	0 0 ? 1 0 – 0 ? 1 ? ? ? ? ? ? ? ? ? 1 ? ? ? ? ? ? ? 0 ? 0 ? ? ? 0 0 ? – ? ? 0 ? ? 1 ? ? ? ? ? ? ? ? ? ?	0 ? ? ? ? ? 1 ? ? ? ? ? ? ? ? ? ? ? ? ? ? ? ? 6 ? 0 1 – 0 ? ? ? ? ? 1 ? ? 1 ? ? ? ? ? ? ? ? ? ?	? ? ? ? – ? ? ? ? ? ? ? ? ? ? ? ? ? ? ? 0 ? ? ? ? ? – ?	? ? ? ? ? – ? ? ? ? ? ? ? ? ? ? ? ? ? ? ? ? – ? 0 4 1 0 – 0 ? ? ? ? 0 ? ? ? ? ? ? ? ? ? ? ? ? ? ? ?
Baltoeurypterus*	0 0 0 0 0 – 0 ? 1 1 0 0 1 0 0 0 0 0 1 0 ? 1 0 0 – 0 0 0 0 1 ? ? ? 0 1 – ? ? 0 ? ? 1 ? ? ? ? ? ? ? ? ? ?	0 0 0 ? ? 0 0 0 0 0 0 1 1 ? 0 0 0 ? 0 ? 0 0 ? ? 5 0 0 0 – 0 ? ? ? ? ? 1 ? 0 1 0 ? ? ? ? ? ? ? ? ?	0 ? ? ? – ? ? ? ? 0 0 ? 0 1 1 – 0 0 2 0 0 ? ? ? ? 0 – 0 ? 0 ? ? ? – – 0 0 0 0 0 1 ? ? 0 ? ? 0 ? ?	– 0 0 0 0 – ? ? ? 0 0 0 0 0 0 ? ? ? ? ? ? 0 – ? 0 3 1 0 – 0 ? ? ? 0 ? ? ? ? ? 0 – ? ? ? ? ? ? ? ?
Stylonurus*	0 0 0 0 0 – 0 ? 1 1 0 0 1 0 0 0 0 0 0 ? ? 1 ? 0 – ? 0 0 0 1 ? ? ? 0 1 – ? ? 0 ? ? 1 ? ? ? ? ? ? ? ? ? ?	0 0 0 ? ? 0 0 0 0 0 0 1 ? ? 0 0 0 ? 0 ? 0 0 ? ? 5 0 0 0 – 0 ? ? ? ? ? 1 ? 0 1 0 ? ? ? ? ? ? ? ? ?	? ? ? ? – ? ? ? ? ? 0 ? 0 1 1 – 0 0 ? 0 0 ? ? ? ? 0 – 0 ? ? ? ? ? ? 0 0 0 ? ? ? ? ? ? ? ? ? ? ? ?	– 0 ? 0 0 – ? ? ? 0 0 ? ? 0 0 ? ? ? ? ? ? 0 – ? 0 3 1 0 – 0 ? ? ? 0 ? ? ? ? ? ? ? ? ? ? ? ? ? ? ?
Plesiosiro*	0 0 1 1 0 – 0 ? 0 0 0 ? ? ? ? ? 0 0 0 ? 1 ? 1 0 ? 0 0 ? ? ? ? ? ? ? ? ? ? 0 ? ? 0 ? ? ? ? ? ? ? ? ? ?	0 0 ? ? ? ? ? ? ? ? 0 0 0 ? ? 0 ? ? ? ? 0 ? ? ? A ? 0 0 – 0 ? ? ? ? ? 1 ? ? ? ? ? ? ? ? ? ? ? ? ?	? ? ? ? – ? ? ? ? 0 ? ? 0 0 0 ? ? 0 ? ? 0 ? ? ? 0 1 ? 0 ? 0 ? ? ? ? ? 0 0 ? ? ? ? ? ? ? ? ? ? ? ? ?	– ? ? ? 0 – ? ? ? ? 0 ? ? ? ? ? ? ? ? ? ? 0 – – 0 0 ? 0 0 1 ? ? ? 0 ? ? ? ? ? ? ? ? ? ? ? ? ? ? ?
Neocarus	0 0 0 0 1 – 0 0 0 0 0 0 1 0 0 1 0 0 0 0 0 1 0 1 0 0 0 0 1 1 0 0 0 0 0 5 ? ? 0 ? ? 0 0 0 – – 0 1 0 0 0 – –	0 0 1 1 0 0 0 0 2 0 0 0 0 ? 0 0 0 ? 0 1 0 1 1 ? 4 0 0 0 – 0 ? ? ? ? 0 0 – 0 1 3 ? ? ? ? 0 1 1 1 0 1	0 0 0 0 – 0 0 0 0 1 0 0 0 1 1 ? 1 1 2 0 0 0 0 0 0 0 – 0 0 0 0 1 0 – – 0 0 0 1 0 0 0 – 0 1 0 0 0 0 0	1 0 1 0 0 – 0 ? 0 0 0 2 – – 0 ? ? 0 ? ? 0 0 – – 0 0 0 – – 1 1 0 0 1 1 1 ? ? ? 0 0 – 0 0 0 0 0 0 0 –
Siamacarus	0 0 0 0 1 – 0 0 0 0 0 0 1 0 0 1 0 0 0 0 ? 1 0 1 0 ? 0 0 1 1 0 0 0 0 0 5 ? ? 0 ? ? 0 ? 0 – – ? 1 ? 0 ? – –	0 0 1 1 0 0 0 0 2 0 0 0 0 ? 0 0 0 ? 0 ? 0 1 ? ? 4 0 0 0 – 0 ? ? ? ? 0 0 – 0 1 2 ? ? ? ? 0 1 ? 1 0 1	0 0 0 0 – 0 0 0 0 1 0 ? 0 1 1 ? 1 1 1 2 ? 0 0 0 0 0 0 – 0 0 0 ? 1 1 0 0 0 0 0 1 0 ? ? – 0 1 0 0 0 0 0	1 ? 1 0 0 – 0 ? 0 0 0 2 – – 0 ? ? 0 ? ? 0 0 – – 0 0 0 – – 1 1 ? 0 1 1 1 ? ? ? 0 0 – 0 ? ? ? ? ? ? ?
Caddo	0 0 0 0 1 0 0 1 0 0 0 0 1 0 0 0 0 0 0 1 0 1 0 1 0 1 0 0 0 1 0 0 0 0 0 1 ? 0 0 0 0 0 ? ? ? ? 0 0 0 0 0 – –	0 0 0 0 – 0 0 0 0 0 1 0 0 0 0 0 0 0 0 1 0 0 1 1 2 0 0 0 – 0 0 1 0 1 0 1 ? 0 0 – ? 0 ? ? 0 0 0 0 0 0	1 0 ? 0 – 0 0 0 0 0 0 0 0 0 0 0 0 0 1 0 0 0 0 0 0 0 – 0 0 0 – 1 0 – – 0 0 0 0 0 1 0 – 0 1 0 0 1 1 0	– 0 0 0 0 – ? 0 0 0 0 1 – – 0 1 2 0 1 1 0 0 – – 0 0 1 3 – 1 1 0 – 1 1 1 0 0 0 1 1 0 ? 0 0 1 0 0 0 –
Chileogovea	0 0 0 0 1 0 0 1 0 0 0 0 1 0 0 0 0 0 0 1 0 1 0 0 – 0 0 0 0 1 0 0 0 0 0 1 ? 0 0 0 0 0 ? ? ? ? 0 0 ? 0 ? – –	0 1 0 0 – 0 0 0 0 0 1 0 0 0 0 0 0 0 0 1 0 0 1 1 2 0 0 0 – 0 0 1 0 1 0 ? ? 0 ? ? ? 0 ? ? 0 0 0 0 0 0	1 0 1 0 – 0 0 0 0 0 0 0 0 0 0 0 0 0 2 0 0 0 0 0 0 0 – 0 0 0 ? 1 0 – – 0 0 0 0 0 1 0 – ? 1 0 0 1 1 0	– 0 0 0 0 – 1 0 0 0 0 1 – – 0 1 0 – 1 1 0 0 – – 0 0 1 3 – 1 1 0 0 1 1 1 0 0 0 1 0 – 0 0 0 1 0 0 0 –
Cyphophthamus	0 0 0 0 1 0 0 1 0 0 0 0 1 0 0 0 0 0 0 1 0 1 0 0 – 0 0 0 0 1 0 0 0 0 0 1 ? 0 0 0 0 0 0 1 1 0 0 0 1 0 ? – –	0 1 0 0 – 0 0 0 0 0 1 0 0 0 0 0 0 0 0 1 0 0 1 1 2 0 0 0 – 0 0 1 0 1 0 ? ? 0 ? ? ? 0 ? ? 0 0 0 0 0 0	1 0 ? 0 – 0 0 0 0 0 0 0 0 0 0 0 0 0 2 0 0 0 0 0 0 0 – 0 0 0 ? 1 0 – – 0 0 0 0 0 1 0 – ? 1 0 0 1 1 0	– 0 0 0 0 – 1 0 0 0 0 1 – – 0 1 0 – 1 1 0 0 – – 0 0 1 3 – 1 1 0 0 1 1 1 0 0 0 1 0 – 0 0 0 1 0 0 0 –
Gonyleptes	0 0 0 0 0 0 0 1 0 0 0 0 1 0 0 0 0 0 0 1 0 1 0 1 0 1 0 0 0 1 0 0 0 0 0 1 ? 0 0 0 0 0 1 0 – – 0 0 0 0 0 – –	0 0 0 0 – 0 0 0 0 0 1 0 0 0 0 0 0 0 0 1 0 0 1 1 2 0 0 0 – 0 0 1 0 0 0 1 C 0 0 – 1 0 0 0 0 0 0 0 0 ?	1 0 1 0 – 0 0 0 0 0 0 0 0 0 0 0 0 0 1 0 0 0 0 0 0 0 – 0 0 0 – 1 0 – – 0 0 0 0 0 1 0 – 0 1 0 0 1 1 0	– 0 0 0 1 – ? 0 0 0 0 1 – – 0 1 2 0 1 1 0 0 – – 0 0 1 3 – 1 1 0 0 1 1 1 0 0 0 1 1 0 ? 0 0 1 0 0 0 –
Leiobunum	0 0 0 0 1 0 0 1 0 0 0 0 1 0 0 0 0 0 0 1 0 1 0 1 0 1 0 0 0 1 0 0 0 0 0 1 ? 0 0 0 0 0 0 0 – – 0 0 0 0 0 – –	0 0 0 0 – 0 0 0 0 0 1 0 0 0 0 0 0 0 0 1 0 0 1 1 2 0 0 0 – 0 0 1 0 B 0 1 C 0 0 – 1 0 0 0 0 0 0 0 0 0	1 0 1 0 – 0 0 0 0 0 0 0 0 0 0 0 0 0 1 0 0 0 0 0 0 0 – 0 0 0 – 1 0 – – 0 0 0 0 0 1 0 – 0 1 0 0 1 1 0	– 0 0 0 0 – 0 0 0 0 0 1 – – 0 1 2 0 1 1 0 0 – – 0 0 1 3 – 1 1 0 0 1 1 1 0 0 0 1 1 0 1 0 0 1 0 0 0 –
Sclerobunus	0 0 0 0 0 0 0 1 0 0 0 0 1 0 0 0 0 0 0 1 0 1 0 1 0 1 0 0 0 1 0 0 0 0 0 1 ? 0 0 0 0 0 ? 0 – – 0 0 0 0 0 – –	0 0 0 0 – 0 0 0 0 0 1 0 0 0 0 0 0 0 0 1 0 0 1 1 2 0 0 0 – 0 0 1 0 0 0 1 C 0 0 – 1 0 0 0 0 0 0 0 0 0	1 0 ? 0 – 0 0 0 0 0 0 0 0 0 0 0 0 0 1 0 0 0 0 0 0 0 – 0 0 0 – 1 0 – – 0 0 0 0 0 1 0 – 0 1 0 0 1 1 0	– 0 0 0 1 – ? 0 0 0 0 1 – – 0 1 2 0 1 1 0 0 – – 0 0 1 3 – 1 1 0 0 1 1 1 0 0 0 1 1 0 ? 0 0 1 0 0 0 –

Taxon	Character coding			
E. spelaea	0 0 0|1 0 1 2|1 0 0 0 0 0 0 1 0 0 ?|1 0 0 0 0 0 1 0|? 1 0 0 0 0 0 1 0 0 0 0 0 0 1 ?|0 ?|1 0 0|1 0 0|? 0|? -|? -|? 0|? 0|1 0 ? ? – –	0 0 1 0 – 0 0 0 0 0 0 0 0 0 0 0 0|? 0 0 1 0 0 1 0 4 0 0 0 – 0 1|2 1|0 0 3 1 0 – 0 0 – ? ? ? ? ? ? ? 0 0|1 0 1	0 0 0 0 0 0 0 0 0 0 0 0 0 0 0 0 0 0|? 2|0 0 0 0 0 0 0 1|0 – 0 1 0 – 0 1 0 0 0 0 1 0 0 0 0 0 1 1 0 0 0 0 0	– 0|2 0 0 0 – 0 0 0 0 0 0|2 0|– 0|– 0 ? |1 1 0 1 1 0 0 – – 0 2|3 1 2 0 1 1 0 0 1 0 0 ? ? ? 0 1 0 1 1|0 0 0 0 1|2 1|0 –
Eukoenenia	0 0 0|1 0 1 1 0 0 0 0 0 0 1 0 0 ?|1 0 0 0 0 0 1 0 1 0 0 0 0 0 1 0 0 0 0 0 0 1 ?|? 0 0 0 0 0 – – 0 0 0 ? ? – –	0 0 1 0 – 0 0 0 0 0 0 0 0 0 0 0 0 0 0 1 0 0 1 0 4 0 0 0 – 0 1 1 0 3 1 0 – 0 0 – ? ? ? ? ? ? ? 0 0 1	0 0 0 0 0 0 0 0 0 0 1 0 0 0 0 0 0 0 2 0 0 0 0 0 0 1 – 0 1 0 – 0 1 0 0 0 0 1 0 0 0 0 0 1 1 0 0 0 0 0	– 0|2 0 0 0 – 0 0 0 0 0 0 0 0 0 ? 1 0 1 1 0 0 – – 0 2|3 1 2 0 1 1 0 0 1 0 0 ? ? ? 0 1 0 1 1 0 0 0 1 0 –
Prokoenenia	0 0 0|1 0 1 1 0 0 0 0 0 0 1 0 0 ?|1 0 0 0 0 0 1 0 1 0 0 0 0 0 1 0 0 0 0 0 0 1 ?|? 0 ? 0 0 0 – – 0 0 0 ? ? 0 0	0 0 1 0 – 0 0 0 0 0 0 0 0 0 0 0 0 ? 0 1 0 0 1 ? 4 0 0 0 – 0 ? 1 0 3 1 0 – 0 0 – ? ? ? ? ? ? ? 0 0 1	0 0 0 0 ? 0 0 0 0 0 1 0 0 0 0 0 0 0 2 0 0 0 0 0 0 1 – 0 1 0 – 0 1 0 0 0 0 1 0 0 0 0 0 1 1 0 0 0 0 0	– 0|2 0 0 0 – ? ? 0 0 0 0 0 0 0 1 1 0 ? ? 1 0 – ? 0 2|3 1 2 0 1 1 0 0 1 0 0 ? ? ? 0 1 0 1 1 0 0 0 1 1|0 1
Allothyrus	0 1 0 0 0 – 0 1 0 0 0 0 1 1 0 0 0 0 0 0 0 ? 1 0 – 0 0 0 1 1 0 0 0 0 0 3 ? ? 0 ? ? 0 ? 0 – – ? 1 ? 0 ? – –	0 0 1 1 0 0 0 0 2 0 0 0 0 ? 0 0 0 ? 0 ? 0 1 ? ? ? 0 0 0 – 0 ? ? ? ? 0 0 – 0 0 – ? ? ? ? 0 ? ? 1 0 1	0 0 0 0 – 0 0 0 0 1 0 ? 0 0 0 ? 1 0 2 0 0 0 0 0 0 0 – 1 0 0 – 1 0 – – 0 0 0 1 0 0 0 – 1 1 0 0 0 0 0	1 0 1 0 0 – 0 ? 0 0 0 2 – – 0 ? ? 0 ? ? 1 1 – – 0 0 0 – – 1 1 ? 0 1 1 0 ? ? ? 0 0 – 0 ? ? ? ? ? ? ?
Amblyomma	0 0 0 0 0 – 0 0 0 0 0 0 0 – – 0 0 0 0 0 0 ? 1 0 – 0 0 0 1 1 0 0 0 0 0 3 ? ? 0 0 0 0 ? 0 – – ? 1 ? 0 ? – –	0 0 0 0 – 0 0 0 2 0 0 0 0 ? 0 0 0 0 0 1 0 1 1 0 0 0 0 0 – 0 ? 1 ? ? 0 0 – 0 1 4 0 0 0 0 0 1 0 1 0 1	0 0 0 0 – 0 0 0 0 1 0 0 0 0 0 0 1 0 2 0 0 0 0 0 0 0 – 0 0 0 0 1 0 – – 0 0 0 1 0 0 0 – 1 1 0 0 0 0 0	1 0 0 0 0 – 0 ? 0 0 0 2 – – 0 1 1 0 1 1 0 0 – – 0 0 0 – – 1 1 ? 0 1 1 0 0 0 0 0 0 – 0 ? ? 0 0 0 0 –
Argas	0 0 0 0 0 – 0 0 0 0 0 0 0 – – 0 0 0 0 0 0 ? 1 0 – 0 0 0 1 1 0 0 0 0 0 3 ? ? 0 0 0 0 ? 0 – – ? 1 ? 0 ? – –	0 0 0 0 – 0 0 0 2 0 0 0 0 ? 0 0 0 0 0 1 0 0 1 0 0 0 0 0 – 0 ? 1 ? ? 0 0 – 0 1 4 0 0 0 0 0 1 0 1 0 1	0 0 0 0 – 0 0 0 0 1 0 0 0 0 0 0 1 0 2 0 0 0 0 0 0 0 – 0 0 0 0 1 0 – – 0 0 0 1 0 0 0 – 1 1 0 0 0 0 0	1 0 0 0 0 – 0 ? 0 0 0 2 – – 0 1 1 0 1 1 0 0 – – 0 0 0 – – 1 1 ? 0 1 1 0 0 0 0 0 0 – 0 ? ? 0 0 0 0 –
Australothyrus	0 1 0 0 0 – 0 1 0 0 0 0 1 1 0 0 0 0 0 0 0 ? 1 0 – 0 0 0 1 1 0 0 0 0 0 3 ? ? 0 ? ? 0 0 0 – – 0 1 0 0 0 – –	0 0 0 1 0 0 0 0 2 0 0 0 0 ? 0 0 0 ? 0 ? 0 1 ? ? ? 0 0 0 – 0 ? ? ? ? 0 0 – 0 1 4 ? ? ? ? 0 ? ? 1 0 1	0 0 0 0 – 0 0 0 0 1 0 ? 0 0 0 ? 1 0 2 0 0 0 0 0 0 0 – 1 0 0 ? 1 0 – – 0 0 0 1 0 0 0 – 1 1 0 0 0 0 0	1 0 1 0 0 – 0 ? 0 0 0 2 – – 0 ? ? 0 ? ? 0 0 – – 0 0 0 – – 1 1 0 0 1 1 0 ? ? ? 0 0 – 0 0 0 ? ? ? ?
Glyptholaspis	0 1 0 0 0 – 0 0 0 0 0 0 1 1 0 0 0 0 0 0 0 ? 1 0 – 0 0 0 1 1 0 0 0 0 0 3 ? ? 0 0 0 0 0 0 – – 0 1 0 0 0 – –	0 0 1 1 0 0 0 0 2 0 0 0 0 ? 0 0 0 0 0 1 0 1 1 0 ? 0 0 0 – 0 ? ? ? ? 0 0 – 0 0 – ? 0 0 0 0 1 0 1 0 1	0 0 ? 0 – 0 0 0 0 1 0 0 0 0 0 0 1 0 2 0 0 0 0 0 0 0 – 0 0 0 – 1 0 – – 0 0 0 0 0 0 0 – 1 1 0 0 0 0 0	1 0 1 0 0 – 0 ? 0 0 0 2 – – 0 1 1 0 1 1 0 0 – – 0 0 0 – – 1 1 0 0 1 1 0 0 0 0 0 0 – 0 0 0 0 0 0 0 –
Chelifer	0 0 0 0 1 0 0 0 0 0 1 0 0 – – 0 0 1 0 0 0 0 0 – – 0 0 0 0 1 0 0 0 0 0 2 1 0 0 0 0 0 0 1 1 2 0 0 0 1 1 – –	0 3 1 0 – 0 0 1 2 1 0 0 0 0 0 0 0 0 0 1 0 1 1 1 5 0 0 0 – 0 0 1 ? 7 0 0 – 0 1 4 1 1 0 0 0 0 0 0 0 0	0 0 0 0 – 1 0 1 0 0 0 0 0 0 0 1 0 0 1 0 0 0 0 0 0 0 – 0 0 0 0 1 1 0 0 0 0 0 0 0 1 0 – 1 1 0 0 0 0 0	– 1 0 0 0 – 0 0 1 0 0 1 – – 0 1 2 1 0 0 0 0 – – 0 0 0 – – 1 1 0 0 1 0 0 1 0 0 0 0 – 0 0 0 0 0 0 0 –
Chthonius	0 0 0 0 1 0 0 0 0 0 1 0 0 – – 0 0 1 0 0 0 E 0 0 – 0 0 0 0 1 0 0 0 0 0 2 1 0 0 0 0 0 0 1 1 2 0 0 0 1 1 – –	0 3 1 0 – 0 0 1 2 0 0 0 0 0 0 0 0 0 0 1 0 1 1 1 5 0 0 0 – 0 0 1 ? 7 0 0 – 0 1 3 1 1 0 0 0 0 0 0 0 0	0 0 0 0 – 1 0 1 0 0 0 0 0 0 0 1 0 0 1 0 0 0 0 0 0 0 – 0 0 0 0 1 1 0 0 0 0 0 0 0 1 0 – 1 1 0 0 0 0 0	– 1 0 0 0 – 0 0 0 0 0 1 – – 0 1 2 1 0 0 0 0 – – 0 0 0 – – 1 1 0 0 1 0 0 1 0 0 0 0 – 0 0 0 0 0 0 0 –
Feaella	0 0 0 0 1 0 0 0 0 0 1 0 0 – – 0 0 1 0 0 0 0 0 – – 0 0 0 0 1 0 0 0 0 0 2 1 0 0 0 0 0 0 1 1 2 0 0 0 1 1 – –	0 3 1 0 – 0 0 1 2 0 0 0 0 0 0 0 0 0 0 1 0 1 1 1 5 0 0 0 – 0 0 1 ? 7 0 0 – 0 1 3 1 1 0 0 0 0 0 0 0 0	0 0 0 0 – 1 0 1 0 0 0 0 0 0 0 1 0 0 1 0 0 0 0 0 0 0 – 0 0 0 0 1 1 0 0 0 0 0 0 0 1 0 – 1 1 0 0 0 0 0	– 1 0 0 0 – 0 0 0 0 0 1 – – 0 1 2 1 0 0 0 0 – – 0 0 0 – – 1 1 0 0 1 0 0 1 0 0 0 0 – 0 0 0 0 0 0 0 –
Neobisium	0 0 0 0 1 0 0 0 0 0 1 0 0 – – 0 0 1 0 0 0 1 0 0 – 0 0 0 0 1 0 0 0 0 0 2 1 0 0 0 0 0 0 1 1 2 0 0 0 1 1 – –	0 3 1 0 – 0 0 1 2 1 0 0 0 0 0 0 0 0 0 1 0 1 1 1 5 0 0 0 – 0 0 1 ? 7 0 0 – 0 1 3 1 1 0 0 0 0 0 0 0 0	0 0 0 0 – 1 0 1 0 0 0 0 0 0 0 1 0 0 1 0 0 0 0 0 0 0 – 0 0 0 0 1 1 0 0 0 0 0 0 0 1 0 – 1 1 0 0 0 0 0	– 1 0 0 0 – 0 0 1 0 0 1 – – 0 1 2 1 0 0 0 0 – – 0 0 0 – – 1 1 0 0 1 0 0 1 0 0 0 0 – 0 0 0 0 0 0 0 –

Taxon	Character coding			
Cryptocellus	00000-0000 0010001000 0101000001 000003??0?? 01112000?0 --	1211000100 000?000001 00105120-0 ?1?500-014 ?0??010101	0??0-00001 0001100020 100000-000 ?10-000011 00-1100000	?0000-0?00 02--000-11 00--120--1 1001000??0 0-0000000-
*Poliochera**	00000-0?00 0????0?000 ???????0?? ??0??????0?? 0????????? ??	1??????0??? 000??0???? 0???51?0-0 ???5?0-?13 ?????????	????-?????1 ??01??0?? 1???00-??? ?????00??? ?????????	?????0-???? ?????????? ??--120--1 ?????????? ??????????
Ricinoides	00000-0000 0010001000 0101000001 000003??0?? 01112000?0 --	1211000100 000?000001 00105120-0 ?1?500-014 ?0??010101	0??0-00001 0001100020 100000-000 ?10-000011 00-1100000	?0000-0?00 02--000-11 00--120--1 1001000??0 0-0000000-
*Terpsicroton**	00000-0?00 0????0?000 ???????0?? ??0??????0?? 0????????? ??	1??????0??? 000??0???? 0???51?0-0 ???5?0-?13 ?????????	????-????? ??01??0?? 1???00-??? ?????00??? ?????????	?????0-???? ?????????? ??--120--1 ?????????? ??????????
Protoschizomus	001011|20000 0010010000 0101100000 10000010?00? 0111310000 00	0211000110 000?00??11 001?25000-0 ?0?5?0-00- 11?0000101	0000?00001 0000?00123 0100010000 -111000000 00-1100000	000011??00 000000????? 00--021211 11?1001110 1??0001020
Stenochrus	001011|20000 0010010000 0101100000 10000010001 0111310000 00	0211000110 0000001?11 00115000-0 ?01410-014 11?0000101	0000?00001 0000010123 0100010000 ?111000000 00-1100000	0000110100 0000001011 00--021211 1111001110 11100010?0
Centruroides	0000100000 100--00001 0100-10001 00110010?000 0010110100 00	0100-10000 1000000001 00116000-0 0005110011 0000100100	0111-00000 0000010010 001000-000 1110001011 10-1100111	-0000-1000 01--012110 00--0311-1 1101101000 0-10010011
Hadrurus	0000100000 100--00001 0100-10001 00110010?000 0010110111 00	0100-10000 1000000001 00116000-0 0005110011 0000100100	0111-00000 0000010010 001000-000 1110001011 10-1100111	-0000-1000 01--012110 00--0311-1 1101101000 0-10010011
Heterometrus	0000100000 100--00001 0100-10001 00110010?000 00102?0111 00	0100-10000 1000000001 00116000-0 0005110011 0000100100	0111-00000 0000010010 001000-000 1110001011 10-1100111	-0000-1000 01--012110 00--0311-1 1101101000 0-10010011
*Palaeoscorpius**	0000?00?00 100--0000? ?1?0-?0001 ????????0?? 0????????? ??	0D????0??? 0?????0??? 0???6000-0 ?????1???? ?????????	????-?????0 ??000?00?? 0??00-0?0 ?????01??? ?????????	-0?00-???? 0????????? ??--0311-? ????0????? ?????????
*Prearcturus**	0000100?00 100--00??1 ?????????? ????????0?? 0????????? ??	01?????0??? 000?????? ?????000-0 ?????????? ?????????	????-?????0 ????????? 0??00-??? ?????0???? ?????????	-0?00-???? ?????????? ??--0311-? ?????????? ?????????
*Proscorpius**	0000?00?00 100--0000? ?1?0-?0001 ????????0?? 1????????? ??	00????000? 01??0????? 0???6000-0 ??????1?10 ?????????	????-?????0 ??000?00?? 0??00-0?0 ?????01??? ?????????	-0?00-???? 0????????? ??--0311-? ????1????? ?????????

Taxon	Character coding			
*Stoermeroscorpio**	0 0 0 0 ? 0 0 ? 0 0 1 0 0 − − 0 0 0 0 ? ? 2 ? 1 − ? 0 0 0 1 ? ? ? ? ? ? ? ? 0 ? ? 0 ? ? ? ? ? ? ? ? ? ? ?	0 0 ? ? ? ? 0 0 0 ? 0 0 ? ? ? 1 ? ? ? ? 1 ? ? ? 6 0 0 0 − 0 ? ? ? ? ? 2 ? ? 1 0 ? ? ? ? ? ? ? ? ? ?	? ? ? ? − ? ? ? ? 1 ? ? 0 0 0 ? 0 0 ? ? 0 ? ? ? 0 0 − 1 ? 1 ? ? ? ? ? 0 1 ? ? ? ? ? ? ? ? ? ? ? ? ?	− 1 ? 0 0 − ? ? ? ? 1 ? ? ? ? ? ? ? ? ? ? ? − − 0 3 1 1 − ? ? ? ? ? 2 ? ? ? ? ? ? ? ? ? ? ? ? ? ? ?
Eremocosta	0 0 0 0 1 1|2 0 0 0 0 0 0 1 0 1 ? 0 1 0 0 1 1 0 1 0 1 0 0 0 1 0 0 0 0 0 2 ? 0 0 ? 0 0 0 − − 0 0 1 0 0 0 0	0 3 1 0 − 0 0 1 2 1 0 0 0 0 0 0 0 0 0 1 0 1 1 1 4 0 0 0 − 0 ? 1 ? 3 1 1 1 0 1 3 1 0 1 0 0 0 0 1 0 0	0 0 0 0 − 0 0 0 1 0 0 0 0 1 1 − 0 0 0 0 0 0 0 0 0 0 − 0 0 0 0 1 0 − − 1 0 0 0 0 0 1 − 1 1 0 0 0 0 1	− 1 0 0 0 − 0 0 0 0 0 2 − − 0 1 0 − 1 0 0 0 − − 0 0 0 − − 1 1 0 0 1 0 0 0 0 0 0 0 − 0 0 0 0 0 1 1 0
Galeodes	0 0 0 0 1 1|2 0 0 0 0 0 0 1 0 1 ? 0 1 0 0 1 1 0 1 0 1 0 0 0 1 0 0 0 0 0 2 ? 0 0 ? 0 0 0 − − 0 0 1 0 0 0 0	0 3 1 0 − 0 0 1 2 1 0 0 0 0 0 0 0 0 0 1 0 1 1 1 4 0 0 0 − 0 ? 1 ? 3 1 1 1 0 1 3 1 0 1 0 0 0 0 1 0 0	0 0 0 0 − 0 0 0 1 0 0 0 0 1 1 − 0 0 0 0 0 0 0 0 0 0 − 0 0 0 0 1 0 − − 1 0 0 0 0 0 1 ? 1 1 0 0 0 0 1	− 1 0 0 0 − 0 0 0 0 0 2 − − 0 1 0 − 1 0 0 0 − − 0 0 0 − − 1 1 0 0 1 0 0 0 0 0 0 0 − 0 0 0 0 0 1 1 0
Mastigoproctus	0 0 1 1 0 − 0 0 0 0 0 0 0 − − 1 0 0 0 0 0 1 0 1 1 0 0 0 0 0 1 1 0 0 0 0 1 0 0 0 1 0 1 1 1 3 1 0 0 0 0 0 0	0 2 1 1 0 0 0 1 1 0 0 0 0 1 0 0 1 1 1 1 0 0 1 1 5 0 0 0 − 0 1 0 1 5 1 1 0 0 1 B 1 1 1 0 0 0 0 1 0 1	0 0 0 0 1 0 0 0 0 1 0 0|1 0 0 0 1 0 1 2|1 3 0 1 0 0 0 1 0 0 0 0 0 1 1 1 0 0 0 0 0 0 0 0 − 1 1 0 0 0 0 0	0 0 0 0 1 0 0 1 0 0 0 0 0 0 0 0 1 0 1 1 0 0 − − 0 2 1 2 0 1 1 1 1 1 0 0 1 1 1 0 1 1 1 0 1 0 1 0 1 0
*Proschizomus**	0 0 1 0 0 − 0 ? 0 0 0 0 ? ? 1 0 0 0 0 0 ? ? ? 1 ? ? 0 0 ? ? ? ? 0 ? ? ? ? ? 0 ? ? 0 ? ? ? ? ? ? ? ? ? ? ?	0 2 ? ? ? 0 0 1 ? ? 0 0 0 ? ? 0 ? ? ? ? 0 ? ? ? 5 0 0 0 − 0 ?	? ? ? ? ? ? ? ? ? 1 ? ? ? ? ? ? ? ? ? ? 0 ? ? ? 0 1 0 0 ? 0 ? ? ? ? ? 0 0 ? ? ? ? ? ? ? ? ? ? ? ? ?	0 0 ? ? 1 ? ? ? ? 0 ? ? ? ? ? ? ? ? ? ? ? 0 − − 0 2 1 2 ? 1 ? ? ? 0 ? ? ? ? ? ? ? ? ? ? ? ? ? ? ? ?
*Gilboarachne**	0 0 0 0 0 − 0 0 0 0 0 0 ? ? 0 ? 0 0 0 ? 1 0 0 − ? 0 0 0 1 1 1 0 0 0 0 ? ? 0 ? ? 0 ? ? ? ? ? ? ? ? ? ? ?	0 0 ? ? 0 0 1 1 0 0 0 0 ? 0 0 0 ? 0 ? 0 ? ? ? 4 1 0 0 − 1 ? ? ? ? ? 1 ? 0 1 B ? ? ? ? ? ? ? ? ? ?	? ? ? ? ? ? ? 0 0 0 0 ? ? ? ? ? ? 0 0 2 ? 0 ? ? ? 0 1 0 0 ? 0 ? 1 ? ? ? 0 0 0 ? ? ? ? ? ? ? ? ? ? ? ?	− 0 ? 0 0 − ? ? 0 0 0 2 − − 0 ? ? ? ? ? ? 0 − − 1 1 0 − − 1 ? ? ? 0 ? ? ? ? ? ? ? ? ? ? ? ? ? ? ? ?
*Palaeocharinus**	0 0 0 0 0 − 0 0 0 0 0 0 1 ?|0 0 0 ? 0 0 0 ? 1 0 0 − ? 0 0 0 1 1 1 0 0 0 0 ? ? 0 ? ? 0 ? ? ? ? ? ? ? ? ? ? ?	0 0 1 ? ? 0 0 1 1 0 0 0 0 ? 0 0 0 ? 0 ? 0 ? ? ? 4 1 0 0 − 1 ? ? ? ? ? 1 ? 0 1 B ? ? ? ? ? ? ? ? ? ?	0 ? ? ? ? ? ? 0 0 0 0 ? 0 0 0 ? 0 0 2 ? 0 ? ? ? 0 1 0 0 ? 0 ? 1 ? ? ? 0 0 0 ? ? ? ? ? ? 1 ? 0 ? ? ?	− 0 ? 0 0 − ? ? 0 0 0 2 − − 0 ? ? ? ? ? 1 0 − − 1 1 0 − − 1 ? ? ? 0 ? ? ? ? ? ? 1 1 ? ? ? ? ? ? ? ?
*Euproops**	0 0 0 1 0 − 0 ? 1 1 ? − ? ? 0 ? ? ? ? ? ? ? ? ? ? ? ? ? ?	0 ? ? ? ? ? 1 ? ? ? ? ? ? ? ? ? ? ? ? ? ? ? ? ? 2 0 0 0 1 0 ? ? ? ? ? ? ? 1 ? ? ? ? ? ? ? ? ? ? ? ? ?	? ? ? ? − ? ? ? ? ? ? ? ? ? ? ? ? ? ? ? 0 ? ? ? ? ? − ?	? ? ? ? ? − ? ? ? ? ? ? ? ? ? ? ? ? ? ? ? ? − ? 1 0 1 0 − 0 ?
*Limuloides**	0 0 0 1 0 − 0 ? 1 1 ? − ? ? 0 ? ? ? ? ? ? ? ? ? ? ? ? ? ?	0 ? ? ? ? ? 1 ? ? ? ? ? ? ? ? ? ? ? ? ? ? ? ? ? 3 0 0 0 0 0 ?	? ? ? ? − ? ? ? ? ? ? ? ? ? ? ? ? ? ? ? 0 ? ? ? ? ? − ?	? ? ? ? ? − ? ? ? ? ? ? ? ? ? ? ? ? ? ? ? ? − ? 1 2 1 0 − 0 ?
Limulus	1 0 0 1 0 − 0 0 1 1 0 0 1 0 0 0 0 0 0 0 0 0 0 − − 0 1 1 0 1 0 1 1 1 0 − 0 1 0 1 0 0 0 1 0 2 0 0 0 0 0 0 1	0 0 0 0 − 0 1 0 0 0 0 1 1 ? 1 1 0 0 0 1 1 0 0 0 2 0 0 0 1 0 0 1 0 6 1 1 2 1 1 0 0 0 0 1 0 0 0 0 0 0	0 0 0 0 − 0 0 0 0 0 0 1 0 0 0 1 0 0 2 1 0 0 0 1 1 0 − 0 0 0 1 0 0 − − 0 0 0 0 0 1 0 − 0 0 1 0 0 0 0	− 0 0 1 0 − 0 0 0 0 0 0 0 1 0 1 1 0 1 1 0 0 − ? 0 0 1 0 − 0 0 0 0 0 0 0 0 0 0 0 0 − 0 0 0 0 0 1 1 1
Tachypleus	1 0 0 1 0 − 0 0 1 1 0 0 1 0 0 0 0 0 0 0 0 0 0 − − 0 1 1 0 1 0 1 1 1 0 − 0 1 0 1 0 0 0 1 0 0 0 0 0 0 0 0 1	0 0 0 0 − 0 1 0 0 0 0 1 1 ? 1 1 0 0 0 1 1 0 0 0 2 0 0 0 1 0 0 1 0 6 1 1 2 1 1 0 0 0 0 1 0 0 0 0 0 0	0 0 0 0 − 0 0 0 0 0 0 1 0 0 0 1 0 0 2 1 0 0 0 1 1 0 − 0 0 0 1 0 0 − − 0 0 0 0 0 1 0 − 0 0 1 0 0 0 0	− 0 0 1 0 − 0 0 0 0 0 0 0 1 0 1 1 0 1 1 0 0 − ? 0 0 1 0 − 0 0 0 0 0 0 0 0 0 0 0 0 − 0 0 0 0 0 1 1 1
*Weinbergina**	0 0 0 1 0 − 0 ? 1 1 ? ? ? ? ? 0 ? 0 0 ? ? 1 ? 0 − ? 0 0 0 1 ? ? ? ? ? − ? ? 0 ? ? ? ? ? ? ? ? ? ? ? ? ? ?	0 ? ? ? ? ? 0 ? ? ? ? ? ? ? ? ? ? ? ? ? 0 ? ? ? 3 0 0 0 0 0 ?	? ? ? ? − ? ? ? ? ? ? ? ? ? ? ? ? ? ? ? 0 ? ? ? ? ? − ?	? ? ? ? ? − ? ? ? ? ? ? ? ? ? ? ? ? ? ? ? ? − ? 1 2 1 0 − 0 ?
*Chimerarachne yingi**	0 0 ? 0 0 − ? ? ? 0 0 ? 0 − − 0 0 0 0 ? ? 1 ? 0 − ? ? ? ? 1 ? ? ? ? 0 ? ? ? ? ? ? ? ? ? ? ? ? ? ? ? ? ? ?	0 0 ? ? ? ? 0 1 ? ? ? ? ? ? ? ? ? ? ? ? 0 ? ? ? 4 0 1 0 − 0 ? ? ? ? ? 1 ? 0 1 ? ? ? ? ? ? ? ? ? ? ?	? ? ? ? ? 0 ? 0 0 ? ? ? ? ? ? ? 0 ? ? 0 ? ? ? 1 ? ? ? 0 ? ? 1 0 ? ? ? ? ? ? ? ? ? ? ? ? ? ? ?	? ? ? ? ? − ? ? ? 0 0 ? ? ? ? ? ? ? ? ? ? 1 0 1 0 3 1 2 0 1 ?

7.2 Relevant poster

Franz-Guess S., Starck J.M., International Congress on Invertebrate Morphology, Moscow, Russia (18.08.–23.08.2017)

7.3   Relevant talks

Franz-Guess S., Starck J.M., Life Science Munich Graduate School retreat, Wessobrunn, Germany (19.06.–22.06.2017): "Microscopic anatomy of sensory organs in *Eukoenenia spelaea* (Chelicerata: Palpigradi)"

Franz-Guess S., Starck J.M., International Congress on Invertebrate Morphology, Moscow, Russia (18.08.–23.08.2017): "Microscopic anatomy of sensory organs in *Eukoenenia spelaea* (Chelicerata: Palpigradi)"

Franz-Guess S., Starck J.M., Rosa Luxemburg Stiftung - MINT-Doktorand_innenseminar, Berlin, Germany (16.11. –17.11.2018): "Mikroskopische Anatomie eines miniaturisierten Eucheliceraten, *Eukoenenia spelaea* (Palpigradi)"